visual comfort l(AI)outs

A framework for daylight and view guidance during the early layout design process

MASTER THESIS

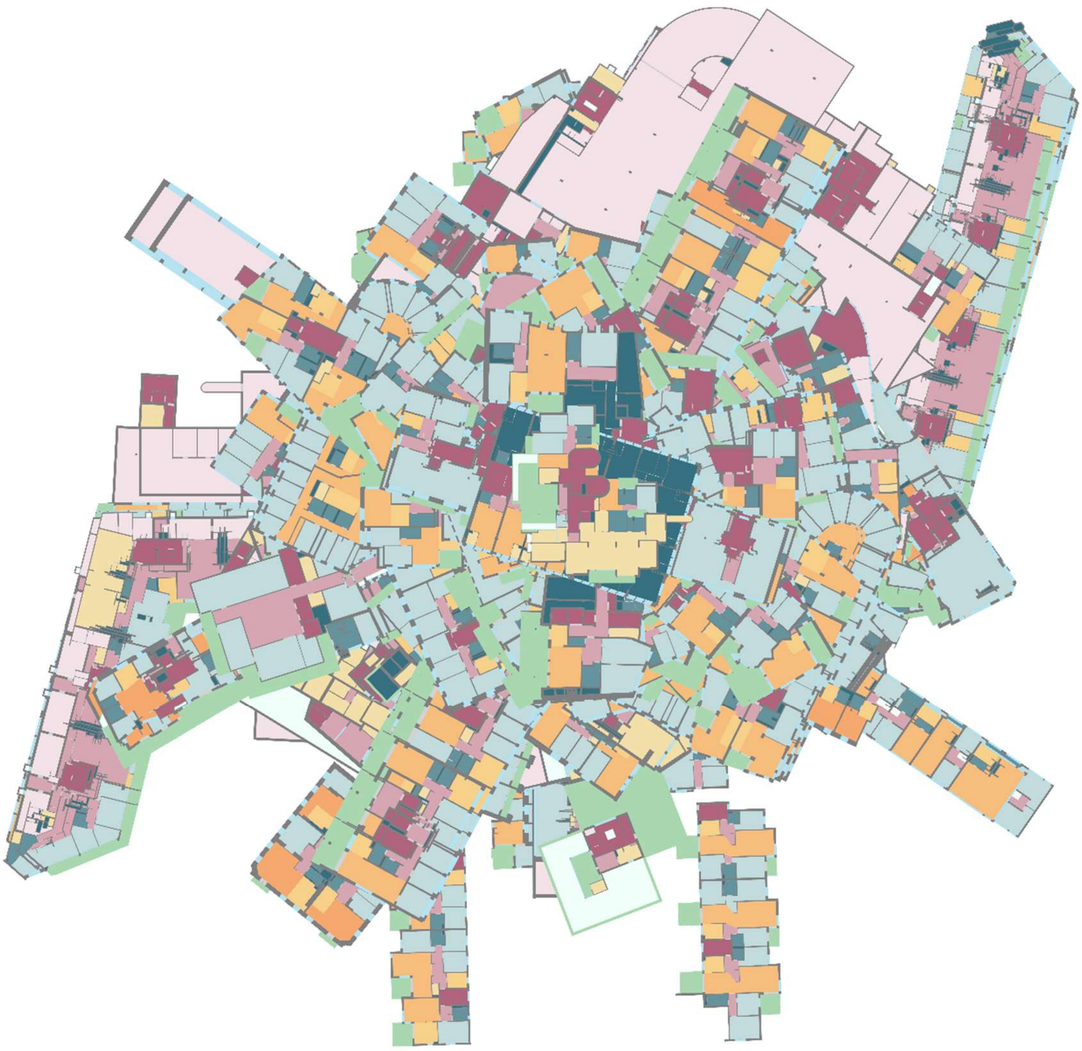

Charlotte Jeline Kat

Class of 2023

MSc in architecture, Urbanism and Building Sciences (Building Technology)

Technical University of Delft (TU Delft)

visual comfort l(AI)outs

visual comfort l(AI)outs

A framework for daylight and view guidance during the early layout design process

Building Technology Graduation Project
MSc in architecture, Urbanism and Building Sciences

[Author]
Charlotte Jeline Kat
5487528
November 10, 2023

[1st mentor]
Michela Turrin
Design Informatics
TU Delft

[2nd mentor]
Eleonora Brembilla
Climate Design
TU Delft

[Collaboration]
Fatemeh Mostafavi
AiDAPT lab
TU Delft

Acknowledgement

Over the past year, I have devoted myself to writing my master's thesis, which proved to be the most challenging and exciting experience of my academic experience. As this thesis marks the end of an intense, extremely enriching years of the Building Technology track at TU Delft, I can conclude that this journey widened my horizon as I now stand at the intersection between the architecture and engineering field. The Building Technology track gave me the opportunity to develop a unique set of skills, which I was able to apply extensively as I dove into the world of computational and look at a broader perspective on what it means for design in the built environment. I had the chance to be the chairperson of the Building Technology study association BouT, which gave me the opportunity to gain valuable insights into different perspectives on the built environment and how to collaborate effectively with people from different backgrounds to achieve shared goals. I am grateful for the connections I made with inspiring and knowledgeable individuals who helped me achieve a project I am deeply proud of.

I received extensive help, guidance, and support from many people during my master's thesis work. First and foremost, I would like to express my immense gratitude to my supervisors, Michela Turrin and Eleonora Brembilla, for their invaluable guidance and feedback throughout the research process. Their encouragement and expertise helped me complete my research and ensured that I learned and enjoyed the process along the way.

I would like to extend my sincere appreciation to Fatemeh Mostafavi, for her patience, expertise, and belief in me as I navigated the machine-learning field. Her assistance was indispensable in the success of my machine learning setup. Thank you for your encouragement and reminders of the significance and enjoyment of my research. Our discussions have been genuinely motivating. Thank you also, Martin Tenpierik, for supporting me during the final part of my thesis project in the absence of Eleonora. Your expertise was of great help in parts of the research, which allowed me to progress more efficiently.

This journey, however, would not have been the same without the support of my family. My parents, Marcel and Niesje, gave me invaluable trust in me as a person and in my competence. Never doubting me and effortlessly supporting me in every decision along the way. They provided me with a positive mindset and a determination to work hard for what I believe in.

Finally, I would like to extend a heartfelt thank you to all my friends. To the circle of close friends who came into my life during the chapter of the Building Technology track, you all have become my '2nd family', making this chapter of my life truly unforgettable. The challenges we faced together during the Building Technology track made our bond stronger, and together, we were able to make even the most difficult moments joyful. I am grateful to have had the opportunity to learn from so many talented individuals, both personally and professionally. So, thank you for being in my life as part of my BT family and, making all the challenges effortless while being by my side. I am lucky to have you all in my life. Despite being apart, I still feel connected to my friends back home in the North of the Netherlands. Sharing thoughts and supporting each other from a distance has given me different, valuable perspectives.

Thank you all,

Lotte

ABSTRACT

The interior layout of apartments is made in the early design stage of an architectural project when the decisions can significantly impact the building's performance. During the early design phase, the ability to impact an architectural project is the most important, and this phase serves as the foundation of subsequent design phases. Proper daylighting improves visual comfort and minimises the dependency on artificial lighting. Combining good natural (day)lighting with a greenery view substantially affects the health and well-being of the building occupants. Optimising the layout of apartments based on daylight and view in the early stage of the building is crucial to ensure visual comfort. In this regard, artificial intelligence presents the potential to provide valuable support for performance-based decision-making in interior zoning based on daylight and view. However, there is currently a lack of machine learning methods to support designers in making informed decisions regarding early interior design decisions that affect daylight and view quality.

The performance of daylight and view quality significantly impacts the overall quality of residential spaces. The EN17037 guideline ensures the quality of indoor spaces by providing specific requirements for residential spaces regarding the view and daylight quality. The national annexe of the UK for daylight in dwellings should be included to ensure that daylight requirements align with the specific purposes of different rooms in dwellings. Incorporating adequate daylight exposure and good views in residential spaces promotes a connection to the natural environment, contributing to overall satisfaction and a higher quality of life for occupants, and leads to lower energy consumption and a smaller carbon footprint in buildings. Significant design parameters that impact the performance of daylight and view in residential spaces include the building orientation, window fenestration and the interior layout arrangement, specifically the room type orientation. Optimising the layout for optimal use of daylight and views is crucial for creating well-designed residential spaces that promote well-being, energy efficiency, and sustainability.

A novel ML design process workflow has been proposed to integrate ML models seamlessly into the architectural design process. Designers upload their layout designs into a dedicated tool, where the layout designs are pre-processed for compatibility with the ML model. Subsequently, the ML model predicts daylight and view values, which are then translated into practical visual representations during an after-processing step. A multimodal machine learning model utilising a ResNet and fully connected network is the most effective for predicting daylight and view quality in residential spaces. An ML model is trained using one image feature and five numerical features to predict the median daylight illuminance on the 21st of March, July and December and the p80 for ground and sky view inside a room. The trained model achieved a test loss MSE of 0.0047 and a test MAE of 0.0440 for the prediction of the three daylight labels, a test loss MSE of 0.0057 and a test MAE of 0.0478 for the prediction of the two view labels. An optimisation step identifies the optimal apartment layout based on a layout evaluation method guided by EN17037 requirements. A multifaceted approach is suggested for evaluating and improving residential layouts for visual comfort, incorporating a novel assessment system that evaluates daylight, view, and room orientation quality in each room to assess the overall apartment layout's visual comfort comprehensively. Overall, this framework represents a significant advancement in integrating ML models into architectural workflows by systematically evaluating daylight, view quality, and room orientation, providing visual feedback, and offering optimisation suggestions that align with contemporary design standards and requirements.

KEYWORDS:
Residential apartments, daylight performance, view quality, multimodal learning, ResNet

Contents

~ empty page ~

Introduction

This master's thesis explores the utilisation of a machine learning (ML) model in the design process of residential apartments. In order to comprehensively understand the various research domains, a literature study offers some background knowledge on the different domains.

The literature study discusses subjects such as visual comfort, machine learning techniques and state-of-the-art of the use of deep learning within the field. These topics lay the foundation for the subsequent design framework, ML model setup and ML model evaluation.

Chapter 4 introduces a framework that enables using an ML model in the current design process of apartments. The design framework proposes a way to implement visual comfort predictions into the design loop of apartment layouts. Additionally, this chapter delves into a layout evaluation system that quantifies the visual comfort of apartment layouts.

Following that, chapters 5 and 6 scrutinise the dataset "Swiss dwellings", which is used for the ML model. The data within the dataset is analysed and cleansed. The proposed labels are generated from the cleaned dataset, and a search for proper features is conducted, leading to the proposed features.

Chapter 7 addresses the training of the proposed ML model and the performance of the trained ML models. Initially, three ML models, with and without pre-trained weights, are trained and compared. From this starting point, ablation studies are conducted to fine-tune the model. The best-performing model is further evaluated with specific examples from the dataset.

Chapter 8 illustrates the usage of the proposed framework with a case study. With a case study, a detailed explanation of each stage of the framework is provided, including examples. Lastly, the case study showcases how designers can evaluate and analyse the performance of different design options, and the optimiser demonstrates the best layout design option.

The thesis concludes with a discussion of the various aspects of the study, followed by an answer to the research questions and the provision of limitations and recommendations for future research. Overall, the study provides a thorough examination of the use of ML models for visual comfort performance evaluation in the design process of residential apartment layouts.

~ empty page ~

1 ResearCH FRAMEWORK

1.1 Background

Daylight and view assessments have become crucial to sustainable building design in recent years. This is due to their significant impact on occupant well-being and energy savings (Figueiro et al., 2017). Sustainable design aims to reduce negative environmental impacts while enhancing occupant health and comfort. The use of natural light plays a vital role in achieving these goals, as it influences energy use (Aries et al., 2015; Reinhart, 2014). The connection between the outdoors and indoors through views and daylight provides numerous psychological and physiological benefits to people. Good natural lighting is now widely expected as a crucial requirement for residential and non-residential structures. Natural light not only enhances the visual appeal of a space, but it also serves the functional purpose of providing light for work or reading. The presence of daylight in a building improves energy efficiency by lowering reliance on electric lighting. Moreover, natural lighting creates a connection to the outside that electrical lighting cannot replicate (Corrodi et al., 2008). Effective daylighting can partially meet a building's heating needs during winter by harnessing solar heat.

The quality and amount of natural light within a building are influenced by two main factors (Littlefair et al., 2022). The interior design of the space, including window dimensions and placement, room shape, and the colours used on internal surfaces, plays a crucial role. Additionally, the façade's fenestration can provide valuable information about orientation, weather changes, and the time of day (Nourkojouri et al., 2021). Secondly, the external environment's design plays a major role, particularly when tall obstructing buildings hinder adequate daylighting or block sunlight for extended periods of time. Thus, good visual comfort, categorised as sufficient access to daylight, glare control, and access to quality view, is essential for a sustainable and healthy project. However, despite the importance of providing good outside views, previous research mainly focused on daylighting effects and the outside view is rarely considered in fenestration (Ko et al., 2022).

Performance-based architecture is a design approach that considers building performance as a guiding criterion (Kolarevic, 2003). In this approach, designers gather building performance data to support decisions. They integrate the evaluation of engineering criteria into the early design phase and use simulated building performances to compare design options to make deliberate decisions. Performance-based design decisions based on visual comfort analyses are impacted by design decisions such as building form, fenestration, material properties, geological location, and local climate. However, daylight analysis is a repetitive, time-consuming, and challenging process when working with numerous design alternatives. Unfortunately, most designers do not integrate building performance analysis, such as daylight evaluation, during the early design process, despite the vital decisions made during this phase due to time constraints and the simulation's complexity. The process of daylight simulation calculation creates a divide between daylight performance evaluation and early design decision-making by being time consuming and laborious. While analysing view quality in spaces alongside daylight could be helpful in the early design phase.

Furthermore, including performance assessment from the start of a project reduces the effort and cost of changes. MacLeamy (2004) emphasises that the ability to impact the project decreases over time, with the first two phases being the most critical. As shown in Figure 1-1, early-stage decisions impact an architectural project most (MacLeamy, 2004). The first two phases serve as the foundation of subsequent design phases. In the preliminary phase, the designer defines the project's program, which outlines all the required rooms and spaces. The second phase is the schematic design phase, which precedes the design development phase. During the schematic design phase, one of the major decisions and first step is translating the program into an efficient building design. This involves creating a bubble diagram or space connections to shape the interior zoning arrangement. Designers consider key drivers of building performance, such as (day)light conditions, acoustical performance, and thermal conditions. McGregor et al. (2013) also stress that items with substantial impact should be studied early in a project. The curve of McGregor et al. (2013) emphasises the importance of studying design aspects with substantial impact early in a project, with daylight being the most critical factor in the curve, as shown in Figure 1-2.

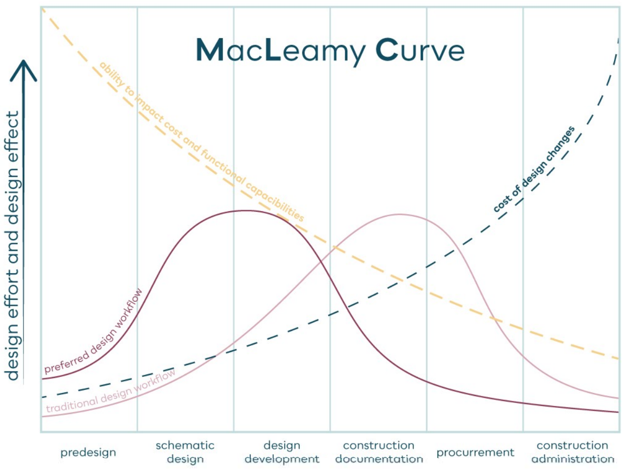

Figure 1-1: MacLeamy Curve (adapted from: MacLeamy, 2004)

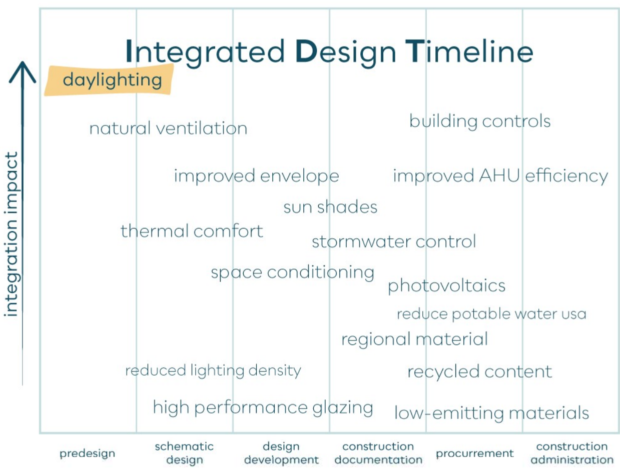

Figure 1-2: Design integration (adapted from: McGregor et al., 2013)

Hasenmaile et al. (2019) conducted a study on the Swiss real-estate market, showing that floor plans are a neglected aspect that leads to quality-of-life issues. The floor plan is the fourth most crucial factor for evaluating a home, following rent, apartment size, and brightness. (Hasenmaile et al., 2019). With technological advances, floor plans can now be analysed in detail, making it essential to include building performances in early design decisions. A well-planned floor plan can significantly enhance the quality of an apartment, and performance-based decisions can be made using simulations that enable quantitative measurement of layout quality.

While simulation-based methods accurately predict building performances, they hinder quick initial approximations during the early design phase. Simulation programs require a complex set of inputs unknown at the project's beginning, making it challenging to integrate performance-based data into the early phases (Nourkojouri et al., 2021). Therefore, a fast, accurate, and simple method to support decisions is desirable during the early design phase.

Artificial intelligence and machine learning are revolutionising many fields. By learning mathematical relationships between a dataset's indicators, machine learning methods can extract performance data without requiring time-consuming simulations or calculations (Nourkojouri et al., 2021). Machine learning-based algorithms can predict daylight performances based on correlated variables, enhancing the efficiency of building design decisions during the early stage. Artificial intelligence could predict visual comfort aspects based on supervised learning from real-life designs with daylight and view performance simulations. This thesis investigates to which extent computer vision models can be trained to predict visual comfort aspects such as daylight performance and view quality within a given floor plan and to which extend this machine learning model can be incorporated withing the early design phase.

1.2 Problem statement

The interior layout of apartments is made in the early design stage of an architectural project when the decisions can significantly impact the building's performance. The quality of daylight and view is crucial to the well-being of occupants, making it an essential factor in building design. In this regard, artificial intelligence has the potential to provide valuable support for performance-based decision-making in interior zoning based on daylight and view. However, there is currently a lack of machine learning methods to support designers in making informed decisions regarding early interior design decisions that affect daylight and view quality.

1.3 Research questions

1.3.1 Main research question

The objective of this study is to develop a tool that assists designers in making informed decisions based on daylight and view performance when designing floorplans for residential buildings. To achieve this goal, this research addresses the following research question:

HOW CAN A MACHINE LEARNING PROCESS SUPPORT DESIGNERS WITH EVALUATING AND OPTIMISING RESIDENTIAL LAYOUTS FOR DAYLIGHT AND VIEW PERFORMANCE DURING THE EARLY DESIGN PHASE?

1.3.2 Sub-research questions

In order to answer the main research question, this research addresses the following sub-questions:

1. What are the guideline requirements for daylight and view quality in residential spaces?
2. How do daylight and view quality affect the overall quality of residential spaces?
3. What design parameters impact the performance of daylight and view in residential spaces?
4. What is the most appropriate machine learning model for predicting daylight and view quality in residential spaces?
5. How can a machine learning model be incorporated into the layout design process to assist designers?
6. What quantitative metrics can be utilised in the design process to evaluate and optimise residential layouts for visual comfort performance?

1.4 Objective & boundary conditions

The purpose of this thesis is to assess the potential of artificial intelligence vision models to utilise a deep learning process to accelerate interior zoning design decisions. This research aims to develop a system that can present building performances of different design options to support designers in their decision-making. The main focus of this research is the intersection between two different building performances metrices, namely, daylight and view quality. The study will prove if combining the two performances metrices is possible with one machine learning method. This research focuses on the intersection between two building performances, daylight and view quality, and tests if one machine learning model can predict them. To simplify the study, three indicators for daylight and two view quality indicators will be used as a demonstrator.

By considering both performance factors in the same decision-making process, the methodology mimics real-world scenarios where multicriteria assessment must find a balance between many domains. Although the two used performance indicators may not provide the most reliable results in accurately quantifying the daylight and view quality, the research focuses on the method that allows for the combination of two different domains for an evaluation and optimisation process during the predesign phase. Even though making performance-based judgments with only two indicators is uncommon, these demonstrators are intended to show how the methodology works. If the study proves successful, the method can be expanded to include a more overall performance assessment for daylight and view. This next step is primarily a computational time issue and might result in layouts with reliable performance outcomes.

The goal is to explore how AI can support designers in assessing daylight and view quality based on the EN17037 guidelines in the early stages of an architectural design process rather than solely in post-design assessments. A dwelling dataset is utilised to showcase and test the proposed approach in supporting designers in assessing these two distinct performance indicators during the design process.

1.5 Methodology

This thesis utilises a mixed-methods study to answer research questions and achieve the main objectives. The methodology consists of three phases guiding the research: discovery, development, and evaluation. Figure 1-3 provides a diagrammatic representation of the research outline, which is explained below.

1.5.1 Discovery phase

During the discovery phase, relevant literature is collected and analysed to understand the current state of research comprehensively. Key concepts, theories, and methodologies related to research questions are identified. The literature study uses various search, screening, and selection methods for publications related to daylight, view quality and AI. This study selects six keywords: natural (day)light, view quality, visual comfort, dwelling, residential floorplan, and machine learning (ML) process. These keywords are searched in databases such as Google Scholar, Scopus, Science Direct, and Web of Science. Titles and abstracts are screened to find relevant papers.

The literature research is divided into four parts to answer the sub-questions discussed in Chapter 1.3.2. The first part defines the requirements of residential spaces for daylight and view quality according to guidelines. The second part examines the influence of daylight and view quality on the interior layout of apartments and the influence that design parameters have on daylight and view quality. The third part reviews machine learning methods to predict and validate daylight and view quality. The review on AI will also ensure that getting more familiar with these tools and models. This review gives a direction for an applicable machine learning model and creates the basis for developing the machine learning process framework in which a layout validation method is used to quantify layouts based on daylight and view quality.

1.5.2 Development phase

During the development phase, the research study implemented, including developing a machine learning model and analysing and pre-processing the dataset for training. The dataset is analysed, and features and labels suitable for the machine learning task are defined. The Swiss Dwellings dataset is cleaned to create a data frame for training and evaluation of the machine learning model. The data framework will be divided into three parts: the training and test samples and a part that can be used for evaluations and case studies. The knowledge from the discovery phase and the input and output of the data frame will define the proper machine learning model that might alter slightly during the training process. Subsequently, the training samples are used to train the machine learning model. Different machine learning models are trained and compared. After an iterative process of fine-tuning the ML model, the model should be able to predict the daylight performance and the view quality within apartment spaces. The machine learning model will provide spaces' daylight and view performance, which designers can utilise during their decision-making process with the use of the designed ML process framework.

1.5.3 Evaluation phase

During the evaluation phase, the machine learning model is thoroughly assessed to identify areas of strength and weakness and objectively pinpoint potential improvements. The evaluation involves testing the model with various samples to gain insight into the ML model's loss function. Furthermore, the ML model is evaluated with unseen sites to explore design parameters which may affect the performance of the ML model. To test the ML design process framework thoroughly, a case study is conducted. The evaluation findings are then reflected upon and summarized in the report, leading to a discussion and final conclusion of the main research question. Finally, the research limitations are discussed, and future research proposals are made.

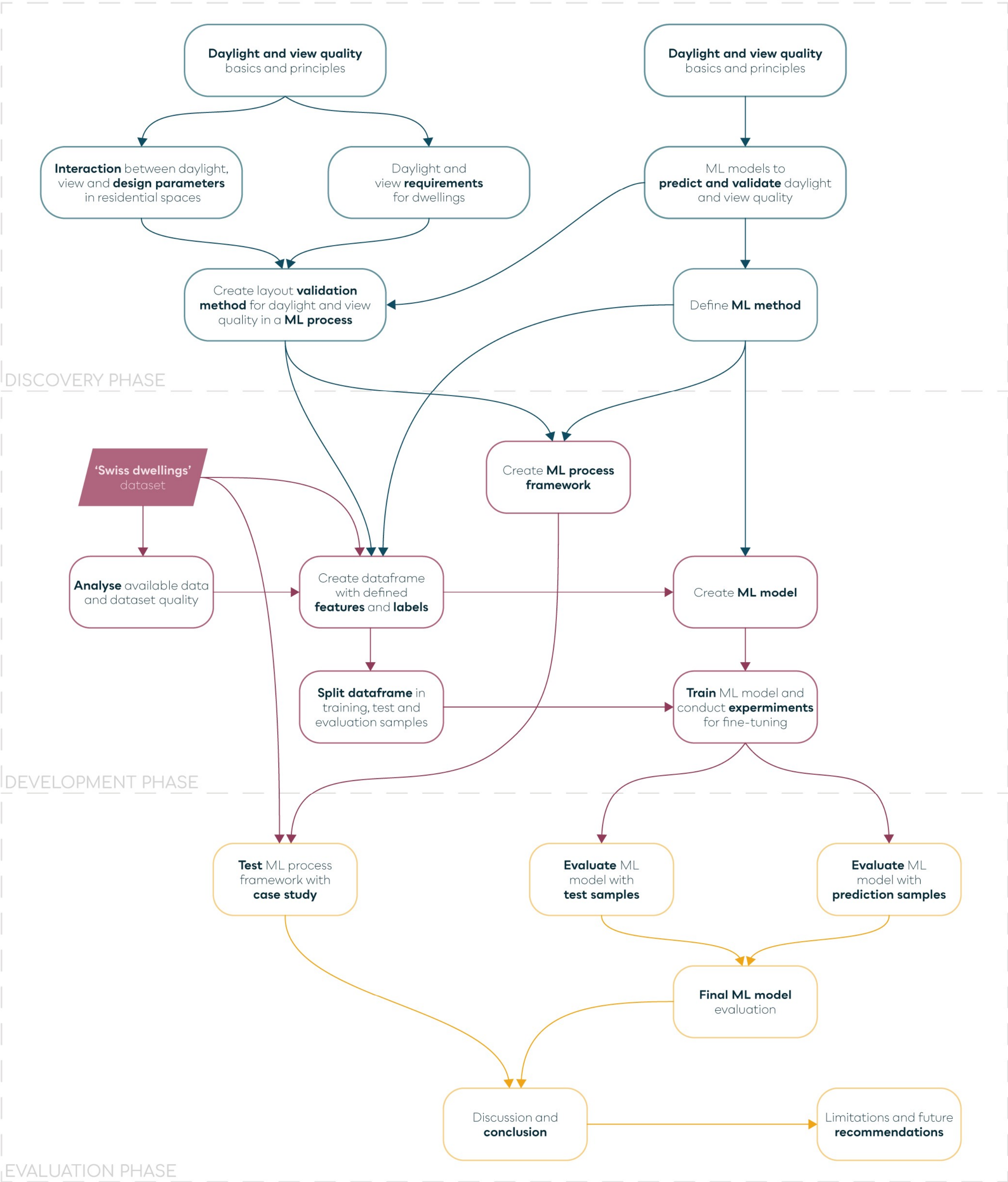

Figure 1-3: Research outline (Source: author)

Sunshine lifts the spirits – SLL, 2013

2 VISUAL COMFORT

Windows can significantly enhance a comfortable and healthy indoor environment. Providing access to daylight and a view of the outside are the two most important functions of windows (Boyce, 2003). Occupants appreciate a window's view for providing information about the outside world, and daylight is perceived as more comfortable and appealing than artificial lighting (Corrodi et al., 2008). Furthermore, by reducing the need for artificial lighting, daylight can lower the energy consumption of buildings. However, controlling daylight and view is a complex task requiring thoughtful consideration of multiple factors and a balance between competing objectives. To encourage building designers to assess adequate daylit spaces, the European Committee for Standardization (2018) created the standard norm EN17037. The standard norm EN17037 (2018) aims to ensure that all occupants can access adequate daylight levels and good views. The standard outlines a verification approach for assessing daylight in buildings and recommends four visual comfort criteria: indoor daylight provision, view-out, exposure to sunlight, and protection from glare. Each visual comfort area of assessment has three levels of recommendation. This thesis, focuses on the requirements for indoor daylight provision and view-out given by the EN17037.

This chapter covers some of the elements contributing to this challenge and describes the effects of daylight and view on human health and well-being. The first subchapter investigates the relationship between a building's occupants' comfort, productivity, and daylight quality and views. After that the sub-chapters cover the requirements, for daylight and view quality in buildings and the variables that impact them.

2.1 Occupants' well-being

Many studies confirm that the quality of light affects individuals' physical and psychological well-being. All these studies show that moderate sunlight exposure benefits human health. There are three ways that light can affect what individuals can accomplish and what they decide to do; through the visual system, via non-visual influences on physiology, and through perception (SLL, 2014). Everything that enters through our eyes influences our body and mind, affecting a person's biological clock (sleep and wakefulness), heart rate, functional organs, and state of mind. Daylight and view substantially affect natural human functions and are central to our well-being (Edwards et al., 2002; Ko et al., 2022). Lighting affects circadian rhythms, human performance, alertness, health, and safety (Boyce, 2003; Mardaljevic et al., 2011). Circadian rhythm impacts sleep quality, energy, alertness, mood, cognitive performance, and other natural functions of people (Mardaljevic et al., 2011).

A core principle of sustainable building design is ensuring sufficient daylight by a controlled admission of natural light, direct sun, and skylight. Lighting has a profound effect on the way occupants experience time and space, both consciously and unconsciously. Satisfactory daylight results in a better mood, less tiredness, reduces eyestrain, higher cognitive performance, and long-term memory consolidation (Edwards et al., 2002). In comparison, lack of natural light causes depression, eating disorders, cancer, heart disease, and other illnesses (Anderson, 2003). Furthermore, many studies show a direct link between the quality of a space and daylight (Edwards et al., 2002). During the design of a room, the designer should consider a space's variation of use during the different moments or days. The use of adequate daylight reduces the requirement for electric lighting, which reduces energy consumption and ultimately reduces the carbon impact of a building.

Considering the significant time humans spend indoors (Gifford, 1995; Klepeis et al., 2001), windows are an essential architectural element since they allow much-needed contact with the outdoors (Bell, 1973; Collins, 1976). A visual link to the environment is made possible by seeing the outdoors, which provides information on the local climate, changes in the weather, and the time of day (EN 17037, 2018; Heschong, 2021). Besides daylight, the view of the outdoors is also relevant to a person's well-being (Kaplan, 2001; Ko et al., 2022). Views through the window convey information about diurnal and seasonal changes in outdoor content with the added visual interest of people, birds, and other fleeting activities, providing cognitive stimulus and relief from the more controlled indoor environment (Heschong, 2021). A good view positively affects residents and influences the sale or rent (Hasenmaile et al., 2019). The view quality is directly linked to the state of mind since the influence of the view from a window connects to positive effects on discomfort, stress, and emotion (Ko et al., 2022). Views of the outdoors can provide information that alleviates the exhaustion brought on by prolonged times spent indoors and provides the chance for the refreshment and relaxation that a change of scenery brings (EN 17037, 2018). The view through a window contributes to the daily acquisition of natural information, ensuring the essential relationship of humans with nature. However, views can significantly impact the privacy of buildings and residences, including both residents' privacy and view-out quality. The converse to view-out is privacy, the ability to prevent people from seeing in (Tregenza & Wilson, 2011). Whereas view into a building can give information about its function, in the case of residential buildings the privacy of the occupants must take precedence (SLL, 2014). While a poorly constructed view can undermine privacy and cause discomfort, a well-crafted view can connect residents to the outside world. Collins (1976) expresses that a large window that provides a view-out of a building may need more privacy for its occupants. While Tregenza and Wilson (2011) mention that privacy requirements depend highly on culture, and the need for security typically implies maintaining awareness of specific external spaces. A window design involves a conflict of needs, as security and privacy frequently precede individual preferences for view.

View quality
The role of windows in building design extends beyond simply providing natural light and ventilation. A view through a window enhances the experience of a building for all occupants (SLL, 2014). 'View' is what a person can see from a particular place, and the view from inside a building occurs through visual information transmitted through windows when (day)light reflects off outdoor environment surfaces (Tregenza & Wilson, 2011). Windows also serve as a medium for visual information, allowing occupants to connect with the surrounding environment and experience the therapeutic benefits of attractive or interesting views (SLL, 2014; Tregenza & Wilson, 2011). However, as Collins (1976) notes, the acceptability of a view is also influenced by its informational and dynamic qualities, as well as the size, shape, and location of the window providing the view. While extensive windows may provide the "best" view, they can also lead to issues such as energy waste, overheating, and glare. Thus, a balance between view and (day)light is necessary for building designs.

2.1.1 View-out standard norm EN17037

The assessment for a view-out is one of four visual comfort criteria in the standard norm EN17037, which recommends three levels (rated as minimum, medium or high) through vertical, inclined, and horizontal apertures (EN 17037, 2018). The standard's 'view-out' evaluation relies solely on the geometric properties of the building and its immediate environment. The verification procedures recommended by the standard primarily involve geometric measurements on 2D plan and section views, with different alternatives for verifying via photographs, applicable only for existing structures or through rendered images (EN 17037, 2018). The norm recommends three view-out levels by three performance level indicators: horizontal viewing angle, distance to the view obstructions, and the number of visible view layers, see Table 1. The overall view-out performance level corresponds to the indicator's lowest level score of the three performance indicators.

Table 1: View-out recommended target values (EN 17037, 2018)

View-out recommendation level	*Horizontal sight angle*	*Outside distance of view*	*View layers**
Minimum	≥ 14°	≥ 6 m	1
Medium	≥ 28°	≥ 20 m	2
High	≥ 54°	≥ 50 m	3

** The number of layers seen from ≥ 75% of the utilized area and at least the landscape layer is included*

The horizontal sight angle describes the amount of available view to a space by the width of the view opening as seen from an observer's point of view. The recommended view widths are equal to or more than 14°, 28°, and 54°, respectively. The reference point for the view width is the farthest point of a utilized space; see Figure 2-1.

The outside distance of view describes the amount of visual information outside, the distance between the window's interior surface and major obstructions in front of the opening preventing direct view and/or part of the sky from entering the space, see Figure 2-2. The recommended view distance is greater than or equal to 6, 20 and 50 meters, respectively.

The view layers describe the quality of the view-out by considering the presence of distinct layers compromising a view. The three types of view-out layers are: a layer of ground, a layer of landscape (natural, architectural or horizon line), and a layer of sky, see Figure 2-2. The recommended levels are 1, 2, and 3 visible view layers. Additionally, the landscape layer must always be present in at least 75% of the utilized area. The reference point for view layers has no horizontal restrictions, as long as the point is inside the utilized area. However, the norm limits the point height sitting eye level (1.2 m) and standing eye level (1.7 m).

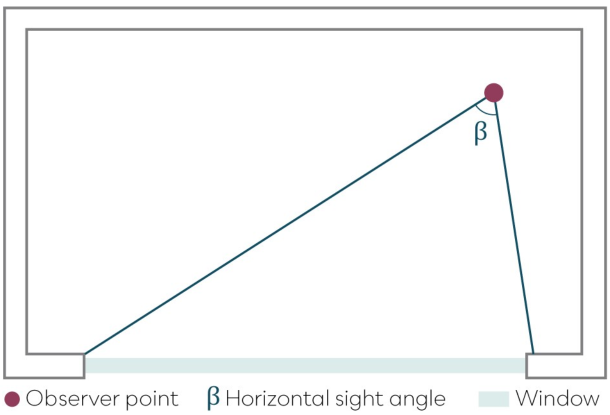

Figure 2-1: Assessment horizontal sight angle (adapted from: Kuhlenengel et al., 2019)

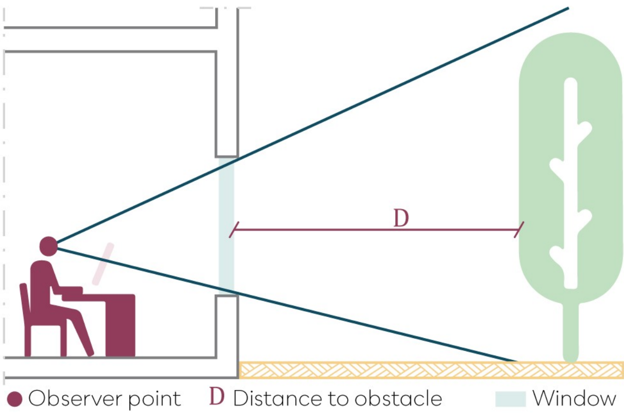

Figure 2-2: Assessment of outside distance of view and view layers (adapted from: Kuhlenengel et al., 2019)

2.1.2 Other view assessment guidelines

Building standards do not widely use three vertical layers to denote a view. However, some guidelines, that focus on human perception of views and their impact on well-being, describe view quality by layers. The United States Green Building Council's Leadership in Energy and Environmental Design (LEED) (2020) rating system includes requirements for view and daylight in its criteria for indoor environmental quality. One of the many objectives of the credit "Daylight and quality views" is to connect the building's residents with the outdoors. According to the LEED (2020), a view to the outside, referred to as a view of the sky or ground, must be present on at least a portion of the floor space.

The Building Research Established Environmental Assessment Method (BREEAM) gives credits for an adequate view when the landscape layer can be seen from a seated position (BREEM, 2021). BREEAM (2021) defines a adequate view as a view of landscape or buildings rather than only a view to sky. In the BREEAM guideline required opening size of a window is depending on the distance of a workspace to a window.

According to the Society of Light and Lighting (SLL)(2014), a window should provide a general picture of the surrounding scenery, and include the foreground and sky in the view. The guideline approaches the view-out quality of a room as a photograph, where the main surrounding scenery should be focussed in the middle of the view and the other view layers should form around it (SLL, 2014). They address that the foreground, classified as ground layer in the EN17037, is the area of interest in which occupants most often direct their glaze. Overall, the guideline in the Lighting Guide 10 of the SLL (2014) is nearly the same as in the norm EN17037.

2.1.3 View layers

Ko et al. (2022) describe a view qualification method (View Quality Index) that includes three primary indicators: view content, view access, and view clarity. View content is the sum of visual features from the window view, corresponding with view layers of EN17037. View Access measures the amount of view seen from the occupant's position, similar to the indicator horizontal sight angle of EN17037. View Clarity assesses how clearly the view content appears in the window view when seen by an occupant, which the standard norm EN17037 does not include.

In their research, Kuhlenengel et al. (2019) showed that the number of view layers significantly positively affects students' achievements in American classrooms. From their research, Kuhlenengel et al. (2019) discuss that the view metrics from the norm introduce some limitations. They address that a further distance to major obstructions leads to a more significant vertical view height, potentially leading to more layers within the view. Thus, the outside distance of view and view layers are inherently correlated. Kuhlenengel et al. (2019) also point out that outside distance of view is obsolete since view layers provide more information about the visual environment. They address that negative design aspects potentially affect the horizontal sight angle, such as increased window surface areas, which results in excessive sunlight penetration. Therefore, this thesis only covers the view-out performance indicator view layers.

The number of layers indicates how varied the outside view is. The three view layers of EN17037 are in line with Collins' (1976) suggestion that windows provide information through three layers: the sky (upward), the cityscape (horizontal), and the ground (downward). The ground layer includes information of activities. The standard considers landscape as any urban object, natural object, or the horizon line. The landscape layer provides information about the outside conditions, especially location, time and weather. The norm EN17037 (2018) suggests a fish-eye projection for complex window shapes or multiple openings to quantify the number of visible layers, as shown in Figure 2-3. A wide-angle projection technique called "fish-eye" mimics how people see their surroundings by capturing a large field of view.

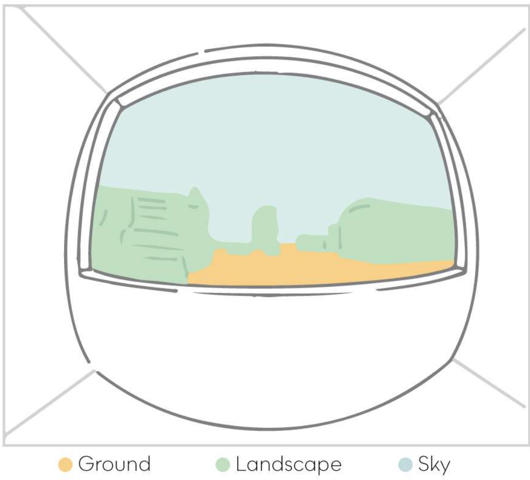

Figure 2-3: View layers in fisheye-view (adapted from: Brembilla et al., 2021)

Computationally assessing view layers

The EN17037 guideline's method for assessing the number of view layers using the fish-eye projection is not designed for computational evaluation. The guideline provides no recommendations regarding specific numerical values, such as steradian measurements (the unit of solid angle), to determine the presence of a view layer. Instead, the guideline relies on manual evaluation approaches. An examiner must subjectively determine the existence or absence of a layer based on their visual evaluation of the fish-eye projection. The downside of this method is that it results in subjectivity and inconsistencies in the evaluation process. To elaborate, various examiners may interpret an identical fish-eye projection differently, resulting in differences in view layer assessment.

In their study, Brembilla et al. (2021) researched the possibility of computationally assessing view-out, as described in the norm EN17037. They propose the concept of steradian thresholds to evaluate view layers computationally. Brembilla et al. (2021) argue that it is necessary to establish a predetermined visibility threshold (t) in terms of view layers measured in steradians to determine the visibility of a given layer accurately. They investigated different minimum visibility threshold (t) values across a grid of analysis points at 1.7 meters high to determine whether to count a layer as effectively part of a view, see Figure 2-4. However, Brembilla et al. (2021) do not provide a specific recommendation regarding the choice of threshold to quantify the number of layers in their study.

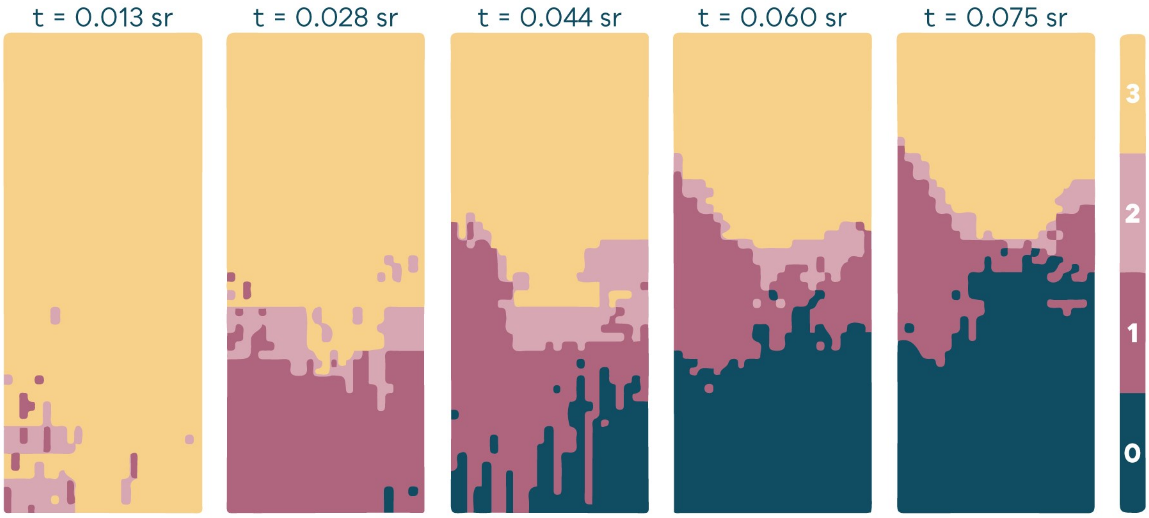

Figure 2-4: Investigation of visibility thresholds (Adapted from: Brembilla et al., 2021)

2.1.4 View to nature

Multiple studies show that nature views contribute to residents' satisfaction and quality of life and can enhance working (Kaplan, 2001; Tregenza & Wilson, 2011). Tregenza & Wilson (2011) address that occupants prefer views encompassing a wide distance scale over those with limited extent. The view given by a window creates a connection to the outside environment, and Tregenza & Wilson (2011) emphasise that especially scenes containing water are preferred. However, the norm EN17037 (2018) promotes distant views regardless of their visual content. The SLL (2014) addresses that a view that consists of elements at some distance allows occupants to take visual breaks from their task by glazing into the distance, which relaxes the eye muscles of the occupants (SLL, 2014).

On the contrary, in their research, Kent and Schiavon (2020) found that the preferred distance of obstacles by occupants depends on the type of visual content. Occupants do not mind having the natural landscape layer close by, whereas occupants prefer urban features to be further away (Kent & Schiavon, 2020). The research of Sepúlveda et al. (2022) addresses that the relation of low view-out quality with high levels of urban obstructions, despite the presence of multiple layers in the view. Additionally, the SLL (2014) also mention that natural views are more beneficial than urban views. However, they also address that any view is better than none. Kent and Schiavon (2020) developed Observer Landscape Distance (OLD), a calculation method to quantify the distance of the view layer landscape from the occupant.

2.2 Daylight quality

Daylight is an important qualitative component of a room that provides several advantages for the occupants. Well-lit rooms provide a significant quantity of light indoors that vary with the time of day and season. Daylight is the controlled use of natural light by reflecting, scattering, admitting and/or blocking direct sunlight and diffusing light to achieve a desired lighting effect (Reinhart, 2014). Most daylight performance indicators determine the daylight availability in the interior with illuminance, which measures the amount of light received on a surface and is typically expressed in lux (lm/m2).

2.2.1 Daylight evaluation metrics

To evaluate the quality of light daylight performance metrics are used. There are two daylight calculation methods types: static and dynamic (Ayoub, 2019). The daylight factor (DF) is one of the most widely used static metrics that provide quick feedback on daylight in worst-case conditions. The daylight factor (DF) is a percentage that expresses the ratio between the indoor illuminance (Ei) on a working plane and the amount of unobstructed exterior illuminance (Eo) under overcast sky conditions (EN 17037, 2018; Giblett et al., 1970), as seen from (2.1). The main consideration in calculating the daylight factor is the sky component, whereas other considerations include internal and external reflection components, and the light losses in the daylight aperture (Hellinga, 2013). In the literature, an average daylight factor of 1% is defined as the minimal amount at which occupants will truly experience daylight, a daylight factor greater than 5% might cause glare problems, and a daylight factor greater than 10% could lead to heat concerns (Dietrich, 2006; Dubois, 2001). The daylight factor simulation is fast, but the results have poor reliability since this metric does not consider climate conditions or orientations (Dogan & Park, 2019; Reinhart, 2014).

$$DF = \left(\frac{E_i}{E_o}\right) \cdot 100 \tag{2.1}$$

Since the availability of natural light outside at a specific location and the properties of building spaces and surroundings influence the amount of daylight in a space, the evaluation of daylight performance should also consider the availability of daylight at a site. As an alternative to the daylight factor, climate-based daylight metrics are being developed, which investigates daylight access in a model under actual conditions specific to the site and building. Dynamic and climate-based metrics include climatic data (exterior diffuse illuminance), which incorporates the change in sky conditions at a specific geographical location into the metrics (Le-Thanh et al., 2022). Two most commonly utilized climate-based daylight evaluation metrics are Daylight Autonomy (DA) and Useful Daylight Illuminance (UDI) (Nabil & Mardaljevic, 2005; Reinhart, 2014).

Daylight autonomy (DA) measures the percentage of occupancy hours throughout a year in which an occupant can perform a viewing task with only daylight (Hopkinson, 1963; IES, 2012). The daylight autonomy percentage shows how often the minimum illuminance threshold of, e.g., 500 lux is met or exceeded during occupied hours (Hellinga, 2013; IES, 2012).

The useful daylight illuminance (UDI) uses hourly sun and sky conditions from a location-specific weather dataset to measure the percentage of the occupied time that falls within a specific target range of illuminances (Le-Thanh et al., 2022; Nabil & Mardaljevic, 2005). The UDI metrics typically range from 100 to 3000 lux (Dogan & Park, 2019; Le-Thanh et al., 2022).

2.2.2 Task-dependent illuminance level

The required illuminance levels for a certain task depend on the visual acuity required for the task and, to a lesser extent, the specific characteristics of the immediate environment in which the task at hand takes place. Occupants cannot use lighting effectively when the illuminance is below 100 lux (SLL, 2014). Illuminance that exceeds the maximum of 3000 lux may cause glare or energy-wasting (Dogan & Park, 2019; Le-Thanh et al., 2022). The task illuminance requirements for both daylight and electric lighting are the same. However, Dogan and Park (2019) emphasize that the influence of glare in residential buildings is less significant since occupants have better control over their environment and can mitigate glare by modifying furniture layout. Furthermore, occupants can mitigate the oversupply of daylight and glare at façade level with simple measurements (Dogan & Park, 2019). Table 2 shows the recommend illuminance levels per task type and or setting from the SLL lighting guide 9 and 10.

Table 2: Recommended illuminance levels per task and/or setting (SLL, 2013; SLL, 2014)

Illuminance	*Task*	*Residential room type*
100 lx	Movement task and casual seeing without perception of detail	Corridor, stairs, storage, lift lobbies, lounge, toilets, bedrooms
150 lx	-	Bathrooms, study room, dining area
200 lx	No perception of detail required	Kitchen, laundry rooms, office, entrance
300lx	Moderately easy task	Recreation spaces
500 lx	Moderately difficult task, colour judgement required	Desk area
1000 lx	Very difficult task, perception of small detail required	-

2.2.3 Daylight provision standard norm EN17037

In order to guarantee that people have access to sufficient natural light in their houses, the guideline EN 17037 (2018) specifies a minimum daylight level for buildings. However, the standard does not adapt the minimal requirements depending on the building type or cultural context.

The guideline provides two standard calculation methods for daylight provision assessment in buildings. The first method is the daylight factor (DF) calculation. The second method is a spatial daylight autonomy (sDA) calculation that is more detailed since it computes for a typical year the hourly sky and sun conditions derived from the climate data of the site. The second method uses a simulation model that includes the building with the actual orientation, window area, obstructions and shading devices. Simulation models such as Radiance or Daysim simulate the daylight levels for different times and days of a representative year. The simulation considers the variations in weather and sunlight conditions throughout the year.

The EN 17037 (2018) standard states that a space with openings in the façade, is considered to provide adequate daylight if an illuminance level (ET) across 50% of the area and the minimum illuminance level (ETM) across 95% of the area is achieved. The specific regulations from EN 17037 (2018) for rooms with vertical openings is shown below in Table 3 on a reference plane 0.85 meters above the floor. For the target illuminance, the required illuminance needs to be reached over at least 50% of the space for at least half of the daylight hours.

Table 3: Recommendations of daylight provision by daylight openings in vertical and inclined surface (EN 17037, 2022)

Daylight provision recommendation level	*Target illuminance**	*Min. target illuminance***	*Fraction of daylight hours*
Minimum	300 lx	100 lx	50%
Medium	500 lx	300 lx	50%
High	750 lx	500 lx	50%

** For 50% of the space, ** For 95% of the space*

2.2.4 Other daylight assessment guidelines

The British Standards Institution (BSI) (2019) added a national annexe for the UK to the EN17037 norm. The annexe is added to create achievable recommendations for different room types in dwellings. The UK committee comments that for dwellings the EN17037 recommendations are not always achievable because of i.e., significant external obstructions.

The BSI recommends the illuminance targets as given in Table 4. The annexe includes daylight targets recommendations for three different room types. The recommendations are lower than the minimum target illuminance given in the EN17037. For multiple use spaces, the BSI recommends the highest target illuminance of the room types in that space. The BSI (2019) stresses that they do not see an additional value on testing the minimum target illuminance (for 95% of the space) for dwellings, only recommendation for 50% of the space is given. The BSI (2019) notes that rooms that exclude an illuminance of 500 lux should be checked for overheating, since those rooms are likely to be at risk of overheating in summer.

Table 4: Recommendations of target illuminance per room type in UK dwellings (BSI, 2019)

Room type	*Target illuminance**	*Fraction of daylight hours*
Bedroom	100 lx	50%
Living room	150 lx	50%
Kitchen	200 lx	50%

2.3 Influencing design aspects

Design elements are essential in defining daylighting quality and view inside building spaces. The early stages of the design process allow affecting daylight availability and aesthetic relations with outside surroundings. Building orientation, room arrangement, and window placement all have a considerable influence on the distribution and intensity of daylight within interior spaces. Experts in the industry have extensive knowledge regarding design concepts and general rules of thumb for optimizing daylighting accessibility. However, transferring this knowledge into practical applications might be challenging for non-experts. Understanding the underlying concepts of how the sun's movement influences a building's illumination and the rules of thumb for daylight accessibility are required for making educated design decisions.

2.3.1 Building orientation

The orientation of the building and its windows is critical when assessing the amount of sunlight received and the views from within. The orientation of a building has a significant effect on how much sun a building receives during the day, Figure 2-5. While optimal orientation may not always be possible due to constraints such as street networks or nearby buildings, it is essential to consider orientation in order to reach the most effective approach (SLL, 2014). Obstructions, such as large buildings, can impact the amount and distribution of light that reaches windows and rooms. The degree of obstruction on the site should be considered to construct effective passive solar design that maximizes winter solar gains. The orientation of windows in relation to the sun, as well as the level of sunlight penetration, have a considerable impact on solar gain (SLL, 2014).

The degree of obstruction on the site should be considered to construct effective passive solar design that maximizes winter solar gains. The orientation of windows in relation to the sun, as well as the level of sunlight penetration, have a considerable impact on solar gain. For places that require sunlight, south-facing windows within 90 degrees of due south are suggested, whereas main window walls for passive solar heating should face within 30 degrees of due south (Littlefair et al., 2022). North and south-facing structures with a long east-west axis are easier to shade, whereas east or west-facing facades require more care because the sun is lower opposite the windows (Littlefair et al., 2022). In cold and moderate climates, sunlight is often appreciated in homes at practically any time of the day, providing there is enough thermal mass and natural ventilation to prevent overheating (SLL, 2014).

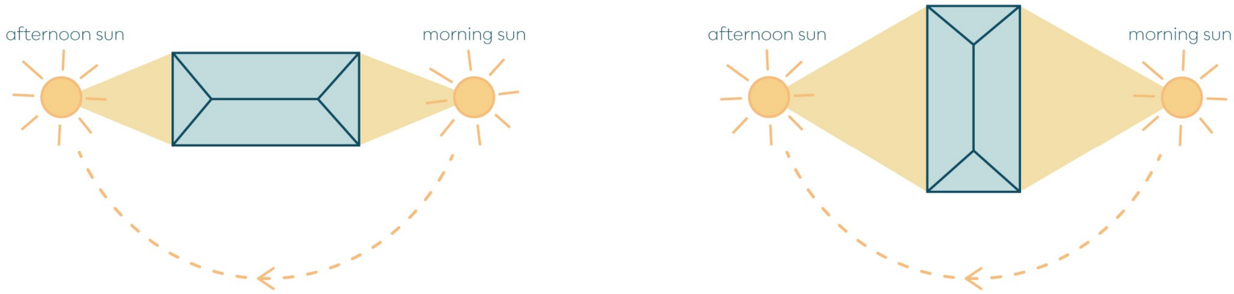

Figure 2-5: Influence of building orientation on sun access (Source: author)

2.3.2 Residential space layout design

The presence of daylight in different areas is determined by their distinct purposes and needs. Some spaces value daylight, while others may need to reduce or eliminate it depending on their intended use. As a result, space design should be adapted to accommodate daylight in a way that is consistent with their intended activities (SLL, 2014). The significance of a view in a given location is determined by the occupancy pattern, the use of the space, the duration of the occupants' presence, as well as the furniture layout and whether people will be standing or seated (SLL, 2014). Littlefair et al. (2022) stresses that the most important factor that affects the duration of sunlight inside the building is the interior layout, and two key factors mainly affect this, orientation and overshadowing. In addition Littlefair et al. (2022) stress that the amount of daylight that is required in a room depends on what the room usage. For instance, kitchens and living rooms need more daylight than bedrooms, thus should be placed further away from obstructions (Littlefair et al., 2022). Littlefair et al. (2022) describe that at predesign phase of floorplan designs, the positions of windows may not have been decided, which makes the orientation of different room times more important. Additionally, Littlefair et al. (2022) suggest to assess the overall sun lighting potential on floor level of a dwelling by counting how many apartments have the main living room facing South, East or West. They stress that the aim should be to minimise the number of apartments having the main living room solely facing North, Northeast or Northwest, unless those living rooms have some compensation factor such as an appealing view to the outdoors.

As a result, the process of space planning and interior layout is critical in improving daylight design techniques. However, it is crucial to remember that when designing an interior layout for apartments, different individuals have different expectations of their living space (Hasenmaile et al., 2019). Thus, a person's lifestyle, gender, age, cultural background, social ethics and economic conditions reflect in a person's house and priorities when considering a home layout.

Following the sun

The planning of the interior layout includes various design principles, such as aspect, prospect, orientation, privacy, circulation and grouping. The layout's orientation means the room arrangement with respect to the north direction. For occupants to perceive changes in weather and day in time in residential buildings, it is desirable to have a variation of daylight during the day. However, spaces should avoid drastic seasonal daylight changes (Dogan & Park, 2019). Several studies have discussed the placement of dwellings' rooms concerning the sun's path. Schwagenscheidt (1930), Pearson (1998), and Neufert et al. (2012) suggested domestic programs and room types for each cardinal direction for buildings on the Northern Hemisphere. All four studies based the optimal room placement on different objectives. Schwagenscheidt based the room placement mostly on the direct sun and optimising the usage of solar-heat gain. While Pearson based the roomplacement on natural lighting and Neufert et al. based the room placement on the timeframe a room is used.

In 1930 Schwagenscheidt conducted comparative sun studies to determine the “scientific” optimum arrangement of rooms according to the sun's course, see Figure 2-6. Schwagenscheidt (1930) established a correlation between cardinal directions and specific residential rooms. However, Schwagenscheidt never aimed for an inflexible application of a scheme for arrangement orientation. Schwagenscheidt included the minimum and maximum sun courses in the graphic to provide information about which rooms are lighted in the summer but not winter. Considering the intensity of sunshine and its effect on heating and cooling loads, the diagram suggests an east-west-oriented building for solar heat-control since mechanical cooling was not the standard then.

In 1998 Pearson addressed the variation in the amount and quality of light according to the needs of a space. Pearson (1998) made a diagram to express the importance of the room's location when designing with natural light, see Figure 2-7. Pearson’s (1998) diagram aims for homes that become more ‘daylight healthy’ and less reliant on artificial lighting. Pearson (1998) stresses that bright light is essential in kitchens, offices and workrooms, so direct light should penetrate those spaces.

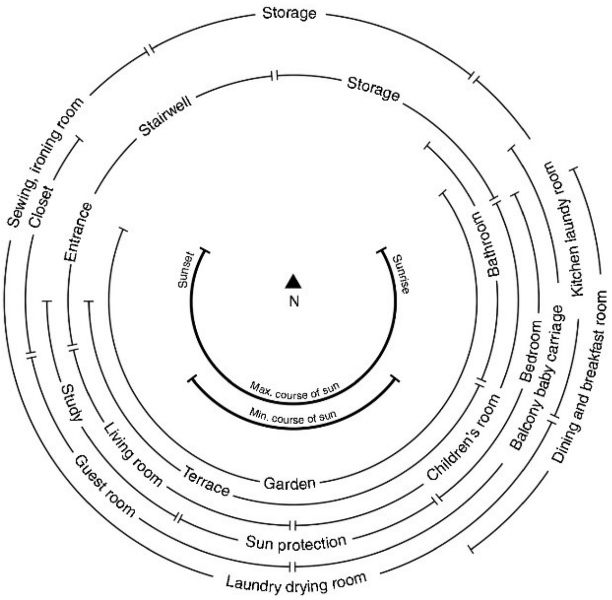

Figure 2-6: Room arrangement for solar heat-control (Source: Schwagenscheidt, 1930)

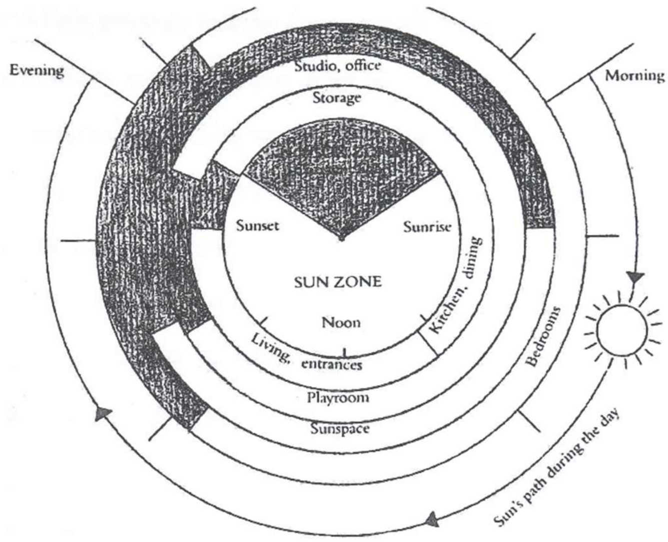

Figure 2-7: Room arrangement for optimal natural light gain (Source: Pearson, 1998)

In 2012 Neufert et al. address the close link between a floor plan and the sun's movement, which connects to the space's orientation. Neufert et al. (2012) suggest that designers should place certain room types in a specific cardinal direction in such a way that natural light is most acvcessible during the frequently used timeframe of a space, see Figure 2-9. Additionally, they describe the periods of occupations of different residential room types and their placement for desired sunlight. Neufert et al. (2012) considered both access to direct light and diffuse northern-light.

In 2013 the SLL address geometric constraints for passive solar design on an open site. They mention that their recommendations are less relevant in closely built-up areas, where the winter sun is highly obstructed. The SLL (2013) suggest that heat-generating spaces should face towards North, together with corridors and intermittently used spaces such as bathrooms and storerooms. Additionally the SLL (2013) recommends to place bedrooms in such a way that sunlight can enter throughout the year.

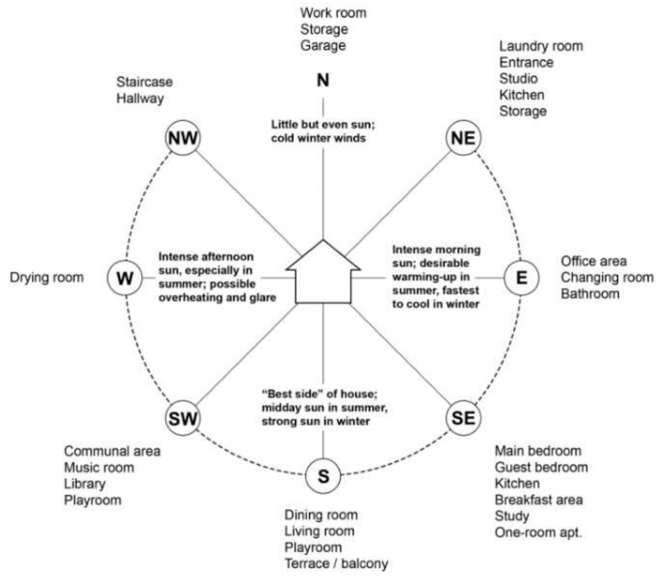

Figure 2-8: Room arrangement following usage timeframes (Source: Dogan & Park, 2019, adopted from: Neufert et al.2012)

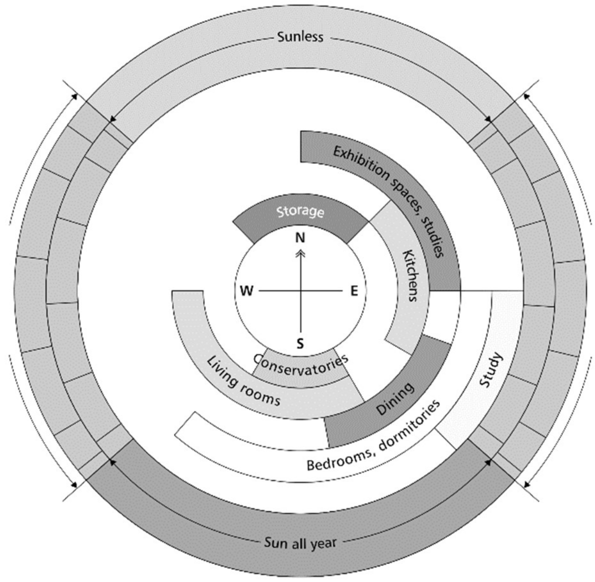

Figure 2-9: Sunlight availability (Source: SLL, 2013)

Optimal room arrangements

The previous four studies have similarities and differences, but all have their strength. From the comparison below, a new combined diagram is conducted for the Northern Hemisphere, see Figure 2-10. It is essential to mention that each location has a different sun path and a slightly different diagram based on the exact sun path at each latitude.

Neufert et al., Pearson and the SLL position the working room on the North side. In contrast, Schwagenscheidt placed non-functional rooms on the North side, including storage spaces and stairwells. Schwagenscheidt places the study room towards the Southwest side. Therefore, based on heating and cooling demand and lighting electricity demand, a study room or office space is best placed between the West to summer sunrise. Based on the four previous studies, room types where occupants do not spend much time, such as storage rooms, can benefit from the no-sun side, and circulation areas are best placed between summer sunset and Northeast. Outdoor spaces such as gardens, balconies and loggias are best placed during the sun hours. Schwagenscheidt, Neufert et al. place the bathroom on the East side, while the SLL places the bathroom around the North side. Therefore, positioning the bathroom between North and East.

According to the first two studies, the bedroom should face the morning sun. Early morning sunlight benefits interior spaces without becoming excessively warm (Corrodi et al., 2008). The morning sun is the most effective regulation of sleep patterns and helps occupants to wake up (Anderson, 2003; Dogan & Park, 2019). Dogan and Park (2019) express that a bedroom that receives abundant morning light in the summer months but remains completely dark during winter mornings can promote sleep grogginess or sleep disorders, as well as seasonal affective disorder. To optimize the occupant's exposure to natural light, designers should consider placing rooms where people spend less time awake on the North side and rooms where people spend most of their time on the South and Southwest side (Anderson, 2003). Meanwhile the last two previous mentioned studies place bedrooms around the Southeast side, ensuring sunlight throughout the year. Hence, positioning the bedroom between summer sunrise and the South, so occupants gain morning sun benefits in both summer and winter while waking up.

According to the four previous studies, the dining room is best placed between the kitchen and living room. Schwagenscheidt and Pearson position the kitchen and dining room around the East side, whereas Neuert et al. place the dining room on the South and the SLL places the dining room around Southeast. Littlefair et al. (2022) mention that living rooms mainly require sunlight, and occupants especially value sunlight in the afternoon. Littlefair et al. (2022) advise placing the living room towards the South or West and the kitchen towards the North or East. Furthermore, Littlefair et al. (2022) argue that sunlight is less crucial in bedrooms and kitchens, and occupants mostly prefer the morning sun over the afternoon sun in these rooms. Since most people spend their time in the living room, especially in the afternoon, the living room is best placed between the South and the summer sunset. The kitchen is best placed on the East side, between Northeast and Southeast. Based on the four previous studies, the dining room is best placed between East and Southwest.

Figure 2-10: Optimal room orientation, Northen Hemisphere (Source: author)

2.3.3 Window size and positioning

The shape, size, and position of windows influence how daylight distributes inside the interior space (Loe et al., 1999), see Figure 2-11. The SLL (2014) recommends that during the conceptual design process, designers should not only discuss views but also consider potential obstructions, such as shading devices that may partially or totally hinder views. However, the benefits of high-level glazing should be evaluated against the possibility of increased sky glare, which may interfere with occupants' work (SLL, 2014).

Window area is an important consideration because it affects both the amount of daylight and heat gain and loss. The daylight and thermal conditions are frequently at disagreement, i.e., the larger the window area, the more daylight, but also the higher the heat loss and gain unless other features are added into the design to counteract these effects (SLL, 2014).

High windows are more effective at allowing natural light to enter, particularly into the deeper areas of a floor plan, because they are less obscured by other structures, trees, or the ground. When compared to regular windows, taller windows can let in more light or be kept smaller to save energy. Nonetheless, some lower windows are often necessary to allow occupants to enjoy outdoor views.

When windows are limited to one wall only, deep in the room the view is limited (SLL, 2014). Aside from aesthetics, the placement of windows on a building's facade can have a significant impact on the view, glare, and distribution of daylight (SLL, 2014). While window patterns are frequently believed to be part of the facade's rhythm, each window provides a unique perspective to the outdoors.

The positioning of windows within a wall is crucial for achieving the appropriate distribution of daylight in a space (SLL, 2014). Incorporating windows on multiple walls provides benefits such as increased daylight uniformity by increasing the no-sky line area in deprived locations (SLL, 2014). In addition, it decreases glare by increasing the luminance of surrounding surfaces while maintaining the brightness of the visible sky (SLL, 2014). Furthermore, many windows in naturally ventilated buildings boost ventilation rates on hot days, minimizing the influence of solar gain (SLL, 2014).

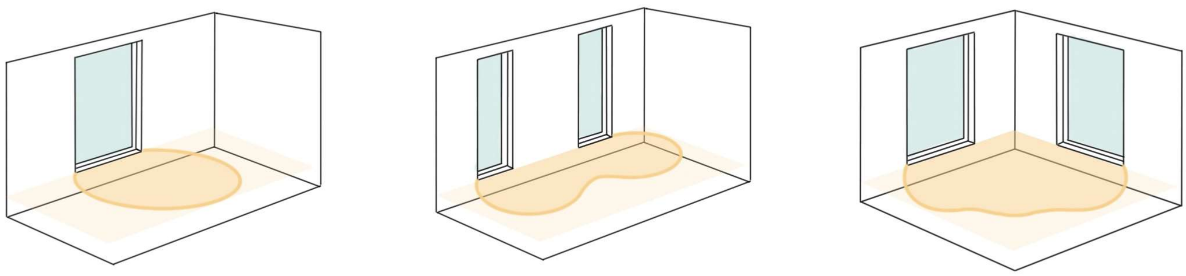

Figure 2-11: Window patterns (SLL, 2014)

2.4 Conclusion

Research has shown that the presence of daylight in indoor spaces directly affects indoor spaces' quality. Lighting significantly influences human well-being, affecting sleep, energy, mood, and cognitive performance. Besides, lack of natural light has negative health consequences, including depression and eating disorders. Incorporating enough daylight into a space reduces the need for electric lighting, leading to lower energy consumption and a smaller carbon footprint for buildings. Therefore, architects and designers must carefully consider the availability of natural light during the design process, considering its variability throughout different times and days.

Since people spend most of their time indoors, windows become a crucial architectural element that connects them with the outdoor environment. The quality of the view from a window directly impacts a person's mental state, reducing discomfort, stress, and negative emotions. Natural views, in particular, enhance the overall satisfaction of a space.

Guidelines like EN17037 ensure the quality of indoor spaces. The EN17037 guidelines specify requirements for residential spaces regarding the view and daylight quality. View quality is evaluated based on three key aspects: the horizontal sight angle, the distance to the outside view, and the number of view layers. It is worth noting that some studies have identified limitations in the view metrics outlined in the norm. The number of layers provides the most comprehensive information about the visual environment's quality.

Achieving a target illuminance level across at least 50% of the space determines the daylight quality of a space. The EN17037 guideline sets a minimal target illuminance level of 300 lux. However, a national annexe recognizes that this threshold is not always met in dwellings while the space still provides sufficient daylight for the room's intended use. Different spaces have varying daylight needs, with some requiring ample daylight and others necessitating controlled or reduced light based on their intended activities. Therefore, the additional levels outlined in the national annexe should be included in the quantification of daylight quality, so the requirements of different spaces adapt to accommodate daylight in alignment with the room's specific purposes.

Building orientation and window placement are critical factors influencing the sunlight and views received within a building. The size, shape, and position of windows significantly impact the distribution of daylight within interior spaces. Interior layout, particularly the orientation and potential overshadowing, is vital in optimizing the duration of sunlight penetration. An optimal room type orientation, such as bedrooms facing southeast, kitchens facing east, and living rooms facing southwest, enhances solar-heat control, natural lighting gain, and aligns with usage timeframes and sunlight availability. All of these factors contribute to overall well-designed residential spaces. In conclusion, careful consideration and integration of daylight and view and thoughtful architectural and interior design decisions are essential for creating indoor environments that promote well-being, energy efficiency, and sustainability.

~ empty page ~

3 Neural networks

Machine learning algorithms can predict daylight performance by leveraging interrelated variables. Integrating artificial intelligence can enhance the efficacy of architectural decisions during the preliminary phases of a building design. The building industry most commonly uses neural networks when predicting visual comfort aspects of a building with machine learning.

The initial section of this chapter provides a short overview of machine learning. Following that, the chapter introduces the principles of neural networks and the current usage of neural networks to predict visual comfort aspects in the field. The subsequent section delves deeper into the principles of convolutional neural networks and the current applications in the field. Lastly, this chapter explores multimodal learning and the usage of multimodal learning in the field.

3.1 Machine learning overview

Artificial intelligence (AI) refers to the ability of machines to perform tasks that typically require human intelligence and require solutions that can learn from their own experience. "AI is a collection of concepts, problems and methods for solving problems" (Elements of AI, n.d.). There are two types of AI: strong AI and weak AI. Artificial General Intelligence (AGI) and Artificial Super Intelligence are the two levels of a strong artificial intelligence system with consciousness and sentience. Artificial Narrow Intelligence is a weak AI, meaning systems designed to perform a single task. As a subset of Artificial Narrow Intelligence and a therefore weak AI, machine learning (ML) refers to computer models and algorithms used by machines to perform a particular operation (Roy, 2020). Deep learning is a machine learning method that incorporates learning from examples and is inspired by how the brain functions, namely the interconnection of neurons (Costa, 2019; Roy, 2020). Deep learning reproduces how the human brain functions. Deep learning performs tasks that humans frequently perform, and the computer model helps filter the input data through layers to predict and categorize information (Roy, 2020). The relationship between the three aspects is visualised in Figure 3-1.

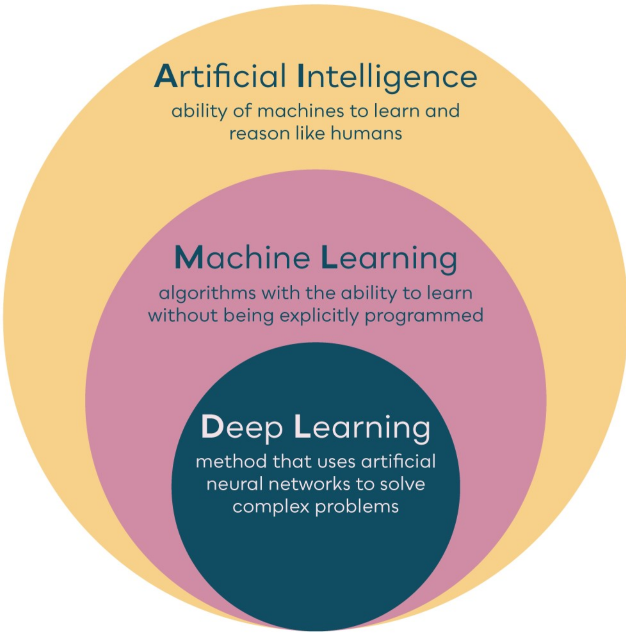

Figure 3-1: Difference between AI, ML, and DL (Source: author)

3.1.1 Machine learning

Without explicit programming, machine learning enables computer systems to learn from data using algorithms to analyse and make predictions or decisions (Fedak, 2018; Han et al., 2012; Mitchell, 1997). Machine learning examines sample training data to build a mathematically correct model that illustrates complicated relationships between several independent inputs and target outputs. ML algorithms identify patterns in historical data, and the trained ML model follows these patterns to predict insightful conclusions in new data (Fedak, 2018). Most artificial intelligence techniques focus on creating specific algorithms to enhance modelling speed and result accuracy (Arbab et al., 2021). Additionally, if properly taught, these tools can decrease processing time by altering some building parameters throughout the design phase. Artificial intelligence techniques generally speed up optimization and raise the likelihood of discovering the optimum solution by reducing the search space (Su & Yan, 2015).

3.1.2 Machine learning concepts

There are four primary divisions for categorizing different machine learning techniques: supervised learning, unsupervised learning, semi-supervised learning, and reinforcement learning (Bishop, 2006; Mohammed et al., 2016). The different types of machine learning techniques are shown in Figure 3-2. Each machine learning approach has advantages and limitations that might play a significant role, depending on its learning capacity, the characteristics of the data, and the desired result (Bishop, 2006; Sarker, 2021). The common problem tasks of supervised and unsupervised learning are classification, regression and clustering (Han et al., 2012; Sarker, 2021). These problem types are not exclusive; sometimes, a problem might have a combination.

Based on a training dataset with numerous input-output pairs, supervised learning analyses a labelled dataset to construct a model that connects input variables to output variables (Han et al., 2012; Mohammed et al., 2016). Supervised learning is a task-driven approach used when a particular set of inputs leads to identifying a specific goal (Sarker, 2021). Classification and regression are the two main subfields of supervised learning (Mohammed et al., 2016; Sarker, 2021). Classification and regression are a type of supervised learning, see Figure 3-2. Classification problems aim to predict a discrete label or class for a given input data (Han et al., 2012; Muhammad & Yan, 2015). There are many classification algorithms, such as Naïve Bayes, K-nearest neighbours, support vector machine, decision-tree and neutral networks (Han et al., 2012). Regression problems aim to predict a continuous numeric value for a given input (Sarker, 2021). Regression models predict missing or unavailable numerical data values and identify the distribution trends based on available data (Han et al., 2012). Some familiar types are regression algorithms are linear, polynomial, lasso and ridge regression (Sarker, 2021).

Unsupervised learning exhibits a self-organization to identifies patterns and relationships in the input data to recognize target variables without output data, and thus without the need for humans (Han et al., 2012; Mohammed et al., 2016). Unsupervised learning is frequently used for exploratory purposes, finding important patterns and structures, groupings of data, and extracting generative characteristics (Sarker, 2021). The most common task within unsupervised learning is clustering. Clustering problems aim to group similar data points without using labelled data (Han et al., 2012). Objects are clustered based on the principle of maximizing the intraclass similarity and minimizing the interclass similarity (Han et al., 2012). Common clustering algorithms include k-means, hierarchical, and density-based clustering (Han et al., 2012).

Semi-supervised learning combines supervised and unsupervised learning, as it trains a model with labelled and unlabelled data (Han et al., 2012; Mohammed et al., 2016). Semi-supervised learning is valuable when many unlabelled data sets and few labelled data sets are available (Mohammed et al., 2016). A semi-supervised learning model aims to provide more accurate predictions than a model generated using only labelled data (Mohammed et al., 2016; Sarker, 2021).

Reinforcement learning interacting with its environment and receiving feedback in the form of rewards or penalties (Bishop, 2006). The model learns to take actions that maximize its rewards over time (Mohammed et al., 2016)

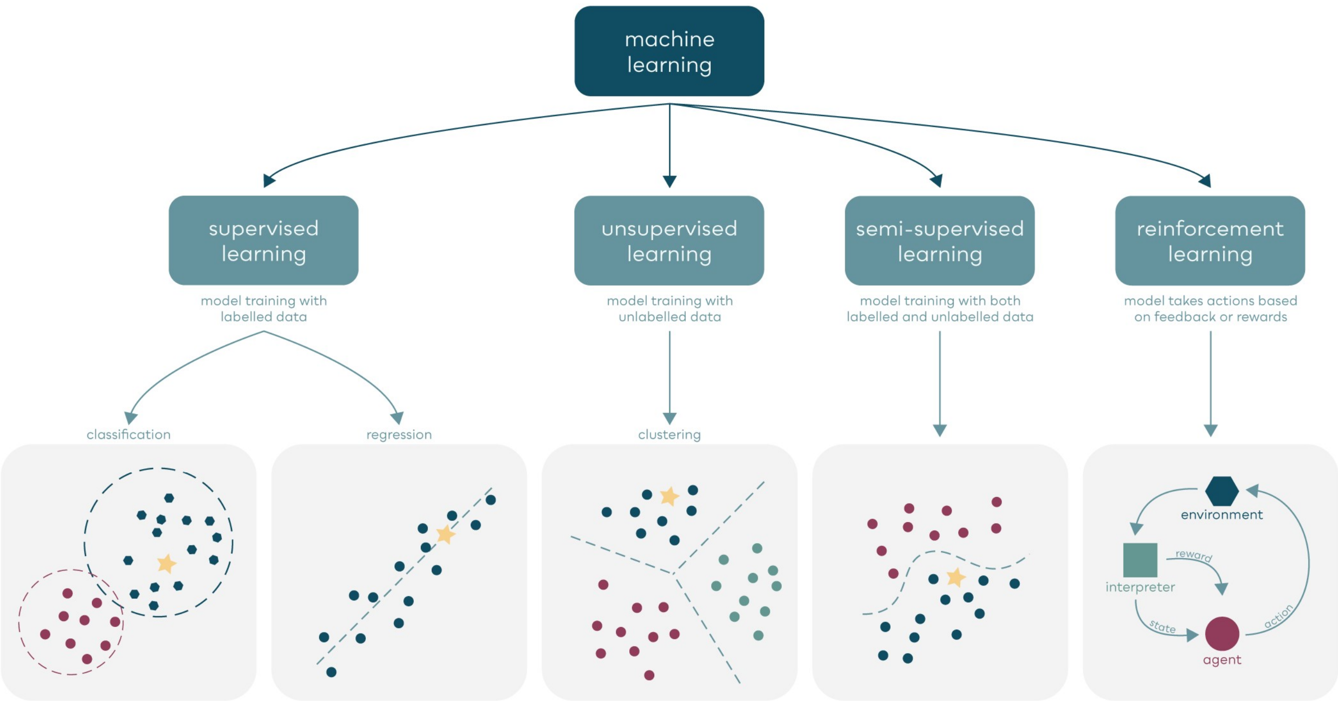

Figure 3-2: Types of machine learning techniques and problem types (Source: author)

3.1.3 Machine learning process

The different steps of creating a machine learning model can vary depending on the specific task and type of ML algorithm. However generally the process can be broken down into seven steps: data collection, data preparation, data splitting, model selection, model training, model evaluation, and model refinement, see Figure 3-3.

Understanding the issue that needs to be resolved and identifying the required data are both part of the first step, data collection. It is crucial to gather relevant historical, experimental, observational, or simulation-derived data since the quality of the data directly influences the predictive model's accuracy (Ayoub, 2020). The following stage, data preparation, results in a data frame. Data preparation includes cleaning, organizing, and randomizing the data for the ML model. The functioning of the ML algorithm differs depending on the ranges of the data variables; hence standardization, scaling, and randomization of the data are necessary (Ayoub, 2020). Data splitting separates the data frame into several subsets for model training once the data has been prepared (Ayoub, 2020). This stage divides the data frame into training, test, and validation samples. The next step is model selection, which entails picking the best machine learning (ML) method and model architecture for the task. Model training is the following phase, which involves using the training samples to train the model. An optimization algorithm adjusts the model's parameters to ensure that the model can make accurate predictions on the training data. The training process is iterative, which involves updating the model's parameters until the model performs to a satisfactory level. Then, during the model evaluation, test samples to determine how well the model performs on data that has not yet been seen and to identify any errors or potential improvement areas (Ayoub, 2020). An evaluation metric evaluates the model's performance (Ayoub, 2020). To enhance the model's performance on the task, the model refinement process comprises adjusting the hyperparameters, applying different architectures, or employing various training strategies (Ayoub, 2020).

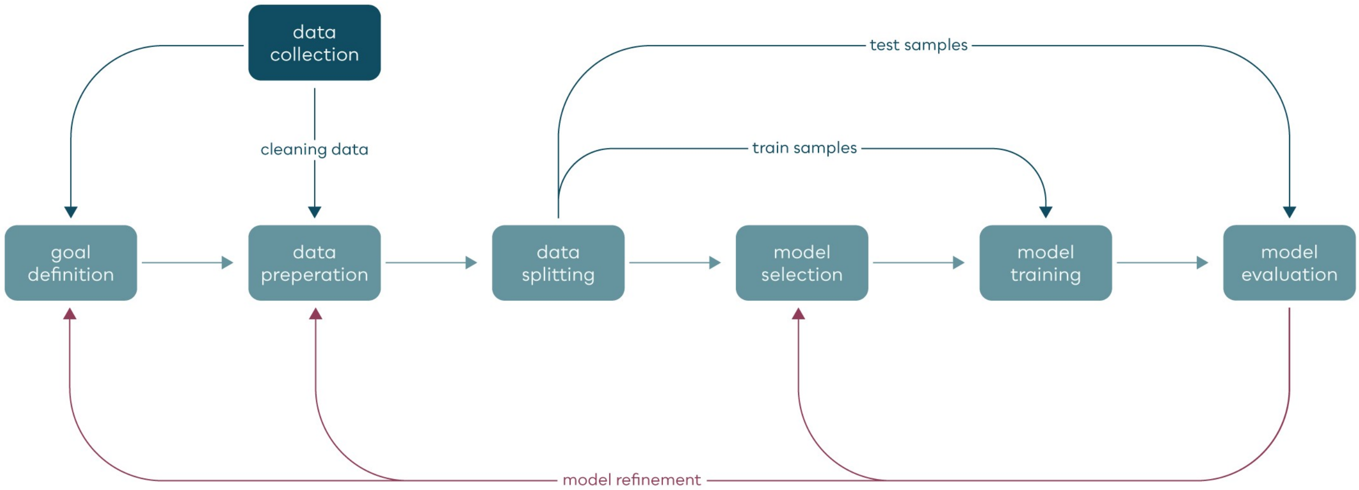

Figure 3-3: Machine learning process (Source: author)

Variables

A machine learning algorithm utilizes features and labels to generate predictions or decisions. Other terms for features and labels are predicators and response variables, independent and dependent variables, respectively. Features are input variables that are the data's characteristics pertinent to the issue at hand. Features identify the relationships between the input and the output. Features could be continuous, categorical, or binary in nature (Muhammad & Yan, 2015). Labels are variables that represent the values or predictions that the model generates as output (Muhammad & Yan, 2015). Labels evaluate the model's performance.

Parameter types

A machine learning model has two parameter types: model parameters and hyperparameters. While hyperparameters are predetermined before training, model parameters are learned from data. In order to reduce the cost function or loss function of the model, the optimization algorithm learns its parameters. The weights and biases of a neural network, the coefficients of a linear regression model, etc. are examples of model parameters. The practitioner sets the hyperparameters, which are the parameters that regulate the model's overall capability and behaviour. Hyperparameters include the learning rate, the number of hidden layers, the number of neurons per layer, the regularization strength, etc. Hyperparameters' ideal values are often discovered by trial and error, grid search, random search, or more sophisticated optimization approaches.

3.1.4 Deep learning

Deep learning is a branch of machine learning that entails developing deep neural networks, which in most cases are artificial neural networks (ANN) with several layers (Muhammad & Yan, 2015). These networks develop representations of the incoming data that become increasingly complex. A deep neural network can learn very complex, non-linear correlations between inputs and outputs as its layers extract data and representations at many levels of abstraction (Muhammad & Yan, 2015). Deep learning models are incredibly accurate at tasks like speech recognition, image identification, and natural language processing (Muhammad & Yan, 2015). Deep learning uses a lot of data to estimate complex functions when the inputs and outputs are far apart (Stevens et al., 2020).

3.2 Neural networks

The core of deep learning algorithms are neural networks (NN) (Stevens et al., 2020). The term and structure of neural networks are derived from the biological neural networks in the brain (Stevens et al., 2020). Neural networks execute the time evolution of physical phenomena regulated by differential equations, construct lower dimensional representations, and learn non-linear relationships. Neural networks can be classified into several categories, each with unique characteristics and applications. The specific task and data will determine the type of neural network architecture to be used. The most common neural networks are Transformer, Autoencoder, Generative Adversarial Networks (GANs), Recurrent Neural Networks (RNNs), Feedforward Neural Networks (RNNs), and Convolutional Neural Networks (CNNs).

The building blocks of neural networks are artificial neurons, or nodes. In 1958 Rosenblatt introduced perceptrons as a simplified model of a biological neuron (Bishop, 2006). A simplified notation of a perceptron model or step function is:

$$f_{(x)} = \begin{cases} 0, & w \cdot x + b < 0 \\ 1, & w \cdot x + b \geq 0 \end{cases} \tag{3.1}$$

where w is the weight, x is the input and b is the bias. Weights are applied to the input data to indicate their relative importance. The summation function combines the inputs and their associated weights to determine their sum (Bishop, 2006). The sum is shifted left or right using bias. The weights determine the contribution of the input to the output (Mitchell, 1997).

A perceptron has n binary inputs, x, that represents the incoming signal from the neighbouring neurons, and the output of the perceptron, $f_{(x)}$, is a single binary value indicating if the perceptron is 'fired' (Yehoshua, 2023), see Figure 3-4. The perceptron node consists of a binary step activation function.

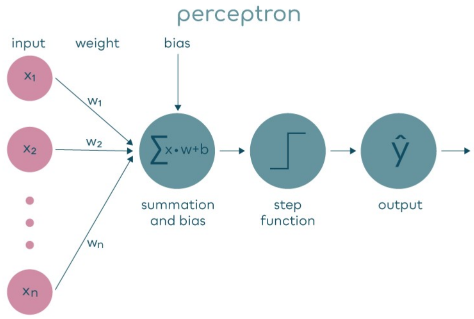

Figure 3-4: Perceptron model (Source: author)

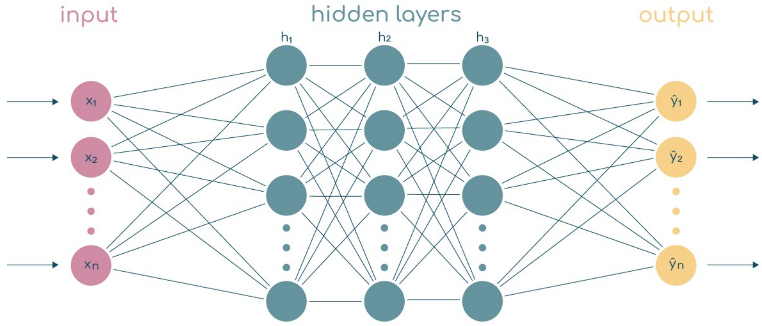

Figure 3-5: Feed forward neural network structure (Source: author)

Multilayer perceptrons (MLP) consists of perceptrons fully connected together into a network. A network consists of three levels: an input layer, one or more hidden layers, and an output layer (Bishop, 2006), see Figure 3-5. When the network consists of two or more hidden layers, the network is an artificial neural network (ANN). A basic form of an ANN is a feed forward network where each neuron is connected to every neuron in the previous layer, and data moves in a single direction from input to output without looping back, see Figure 3-5.

The node's output is transformed by an activation function, determining whether the neuron may be triggered. The output signal of a neuron, or set of neurons, is determined by the activation function of a neural network, a mathematical function applied to the output (Bishop, 2006). ANNs consists of nodes, or also called activation functions, that return an output typically between 0 and 1 or -1 and 1. An activation function adds non-linearity to a neuron network, which enables the neural network to learn more intricate and subtle correlations between the inputs and outputs (Bishop, 2006). Changing the node to a non-linear activation function allows for backpropagation and the stacking of multiple layers of neurons (Baheti, 2021). The most common used activation functions are sigmond, Tanh function, ReLU, Leaky ReLU and ELU (Baheti, 2021), see Figure 3-6. At each of the three levels of an ANN a different activation function is used. The hidden layer mostly uses a ReLU, and all layers within the hidden layer have the same activation function.

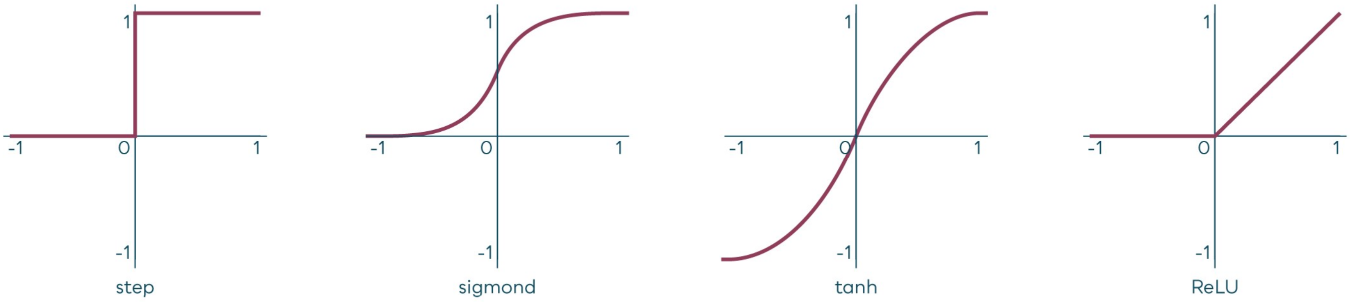

Figure 3-6: Activation functions (Source: author)

3.2.1 ANN for visual comfort in spaces

Using machine learning (ML) methods to forecast daylight availability in varied contexts has recently gained more attention.

This chapter overviews various studies conducted in the field and highlights several ML techniques that forecast daylight performance. The studies discussed in this chapter have various applications, from estimating the quantity of daylight in specific buildings to forecasting daylight availability in metropolitan settings.

Ayoub (2020) evaluated recent studies that used machine learning algorithms to forecast the daylighting of spaces and assessed features of the studied buildings, the employed algorithms, the types of problems, input and output parameters, , and the used error metrics in those studies. Ayoub (2020) noted that half of the experiments used the Artificial Neural Network (ANN) model. The remaining investigations used Multiple Linear Regression (MLR), Support Vector Machine (SVM), and Decision Tree models. In 2021, Arbab et al. (2021) concluded that ANNs were the most effective model for indoor illuminance determination after evaluating various ML models such as Linear regression, Support vector machines, decision tree, random forests and ANN.

In 2022 Ngarambe et al. made an overview of the current usage of machine learning tools for daylight design and control. Out of the 25 studies that used machine learning techniques to optimize daylight in the early building design phase, 20 studies generated data using simulation tools and 5 studies generated data with field measurements, simplified physical models or other less traditional systems (Ngarambe et al., 2022). Ngarambe et al. (2022) state that the most fundamental reason behind the use of simulation data is the possibility to consider various design schemes for longer time periods and the possibility to consider different building geometries, orientations, materials, and window geometries. The most used daylight simulation tools for data generation were Energy Plus, DIVA, and Daysim (Ngarambe et al., 2022). The model input parameters that are used in most studies can be classified to four main elements: outdoor climate conditions, building geometry, window properties, and time factors. The most used output parameters of the model can be classified in three main groups: daylight (e.g., DF, DA, sDA, UDI, etc.), glare (e.g., ASE, DGI, DGP, spatial Visual Discomfort (sVD)), and quality of view (view factor, view depth, view range, etc.) (Ngarambe et al., 2022). From the reviewed literature eighteen studies only used an ANN, showing that most studies mainly employed supervised ANN algorithms (Ngarambe et al., 2022). Ngarambe et al. (2022) conclude that the limitations of the current use of ML techniques to estimate daylight performances in the early building design phase mainly come from the constrains that come with the use of simulation tools to generate the used data. Furthermore, greater diversity in the use of algorithms, particularly hybrid models, should be promoted (Ngarambe et al., 2022).

Nourkojouri et al. (2021) proposed a machine learning model that predicts visual comfort parameters at the early phases of design using an Artificial Neural Network (ANN) algorithm. The study used a dataset with 2,880 design options for a shoebox space with a one-side window, Figure 3-7. The design alternatives emerged from ten physical room features, including room and window fenestration, room orientation, shading state and interior surface reflectance. The study used eight labels in total, three daylight labels, two glare labels and three view quality labels. The dataset consisted solely out of simulation data conducted by Radiance for daylight and glare and geometrical calculations for view. The authors tested multiple architectures and the best performing architecture of the ANN consist of a single hidden layer with 40 neurons. In their study the regression problem reached an overall accuracy of 91.7%. However, the authors mention that their actual error might be problematic since it could cause the predicted value to fall above or below thresholds that are defined by building standards or certifications. For their space, parameters that affect the window to wall ratio and room dimensions are the most influential parameters.

In a different study, Le-thanh et al. (2022) created a machine learning framework to predict daylight performance classification building layouts. The dataset consisted of 400 layout options with in total 79,559 sensor points. The rooms layout options consisted of parametrically generated layout designs based on four squares, see Figure 3-8. The study used four labels for useful daylight illuminance ranges (UDI). The dataset consisted solely out of simulation data conducted by DIVA. The study tested multiple architectures and the results of this study showed an ANN architecture consisting of three hidden layers with 120 hidden nodes as the most suitable architecture. The most impactful input parameter was the position and size of windows on the ANN's accuracy.

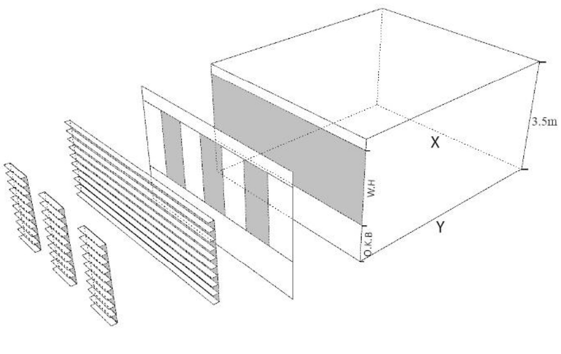

Figure 3-7: Shoebox space (Source: Nourkojouri et al. 2021)

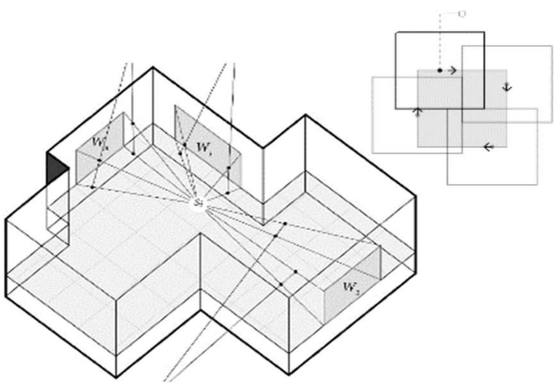

Figure 3-8: Space set-up (Source: Le-thanh et al. 2022)

3.3 Convolutional Neural Network

A form of an ANN is a convolutional neural network (CNN), where each neuron is only connected to the neighbouring neurons from the previous layer. A CNN processes and analyse images and other types of multidimensional data (Géron, 2019), the matrix multiplication is replaced by a convolutional operation (Murphy, 2022). The basic idea of a CNN is to divide the input into overlapping 2D image patches, and comparing each patch with a set of small weight matrices (Murphy, 2022). A CNN consist of an input layer, convolutional layer, pooling layer, and fully connected layers (Géron, 2019), see Figure 3-9. As the image gets progresses through the network the image gets smaller and smaller, while it also gets deeper and deeper thanks to convolutional layers (Géron, 2019).

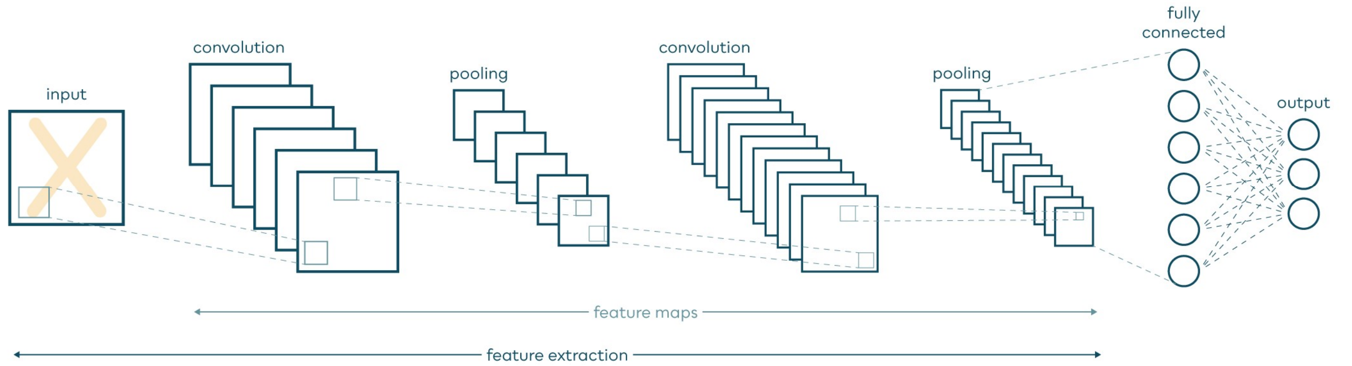

Figure 3-9: Typical CNN architecture (Source: author)

The convolutional layer is the most important building block of a CNN that extract input features and through multiple convolutional layers outputs the corresponding feature map (Zhang et al., 2023). A convolutional layer contains a set of kernels, and an input image. A kernel is a small matrix with weights, and is smaller than the image. The feature detected by performing the convolution, the dot product of the input patch with the kernel (Murphy, 2022), see Figure 3-10. The kernel systematically moves across the input image to detect a feature map anywhere in the image.

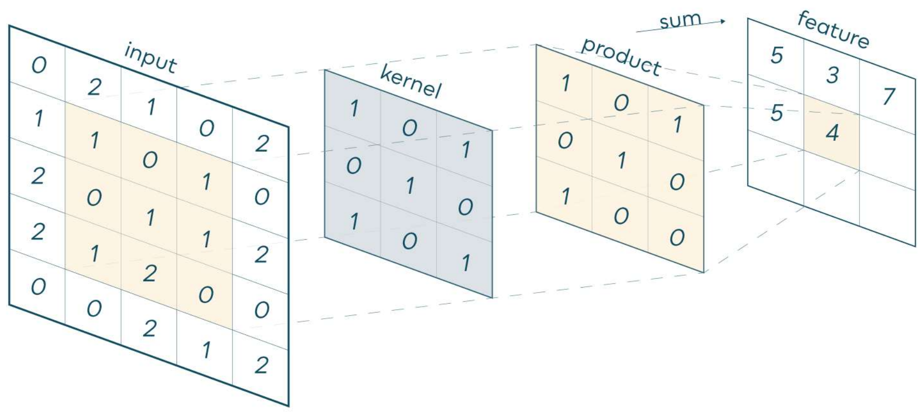

Figure 3-10: Convolutional layer principle (Source: author)

A pooling layer downsamples (i.e. shrinks) the image, this reduces the computational load, memory usage and the number of parameters (Géron, 2019). Reducing the number of parameters limits the risk of overfitting. Therefore, it not only retains the main feature, but also prevents overfitting (Zhang et al., 2023). Commonly used pooling layers are max pooling and average pooling (Murphy, 2022), Figure 3-11. Max pooling returns the maximum input value to the next layer and average pooling return the main of the input values.

The last element of a CNN is a fully connected layer. The fully connected layer learns non-linear combinations of high-level features and works the same as multilayer perceptrons (Saha, 2018). The model extracts and recombines the features maps, in such a way that complex features can be learned (Zhang et al., 2023).

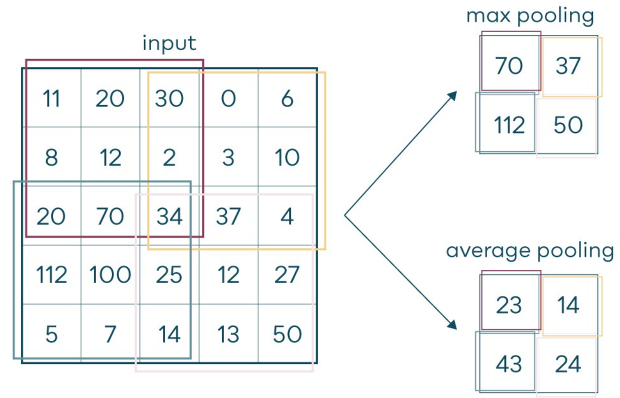

Figure 3-11: Pooling layer principle (Source: author)

3.3.1 Residual Network

The depth of a network is critical to the performance of a model and deep networks often have the problem of degradation, the training and test error rate increases as the number of layers increases (Zhang et al., 2023).

In 2015, He Kaiming introduced the concept called Residual Blocks in a new neural network architecture called ResNet to solve the problem of degradation and makes deep networks easier to optimize (Géron, 2019). He et al. (2015) used the 'ImageNet 2012' dataset to train their model. The data for the ImageNet dataset is collected from search engines and manually labelled by humans to one of the 1,000 object classes (ImageNet, 2021). The images of the ImageNet dataset consist of pictures taken in the real world varying from small to big objects. They presented several experiments on ImageNet to show the degradation problem and evaluate their method that now is known as ResNet, Figure 3-12. The trained model by He et al. (2015) is designed to process pictures to extract critical characteristics and patterns from the data.

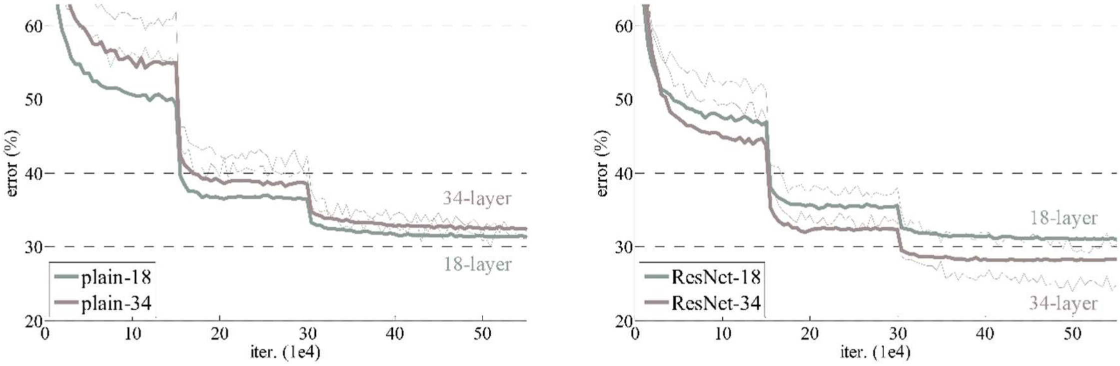

Figure 3-12: ImageNet example images (K. He et al., 2015)

In situations where deep neural networks are needed, a ResNet proved to perform, for example for feature extraction, semantic segmentations, and for various Generative Adversarial Network architectures (Sharma, 2021). A ResNet uses 'skip connections' to connect activations of a layer to further layers by skipping layers in between. Thus, a residual connection provides another path for data to reach further parts of the neural network by skipping some layers, see Figure 3-13.

In the traditional feedforward network the input will simply go through the layers one by one, resulting in the output of layer $i+n$ shown in Formula 3.2.2. In a residual block the identity mapping is applied on current input is the previous layer, resulting in x, then it performs element wise addition resulting in the output for layer $i+n$ (Sharma, 2021).

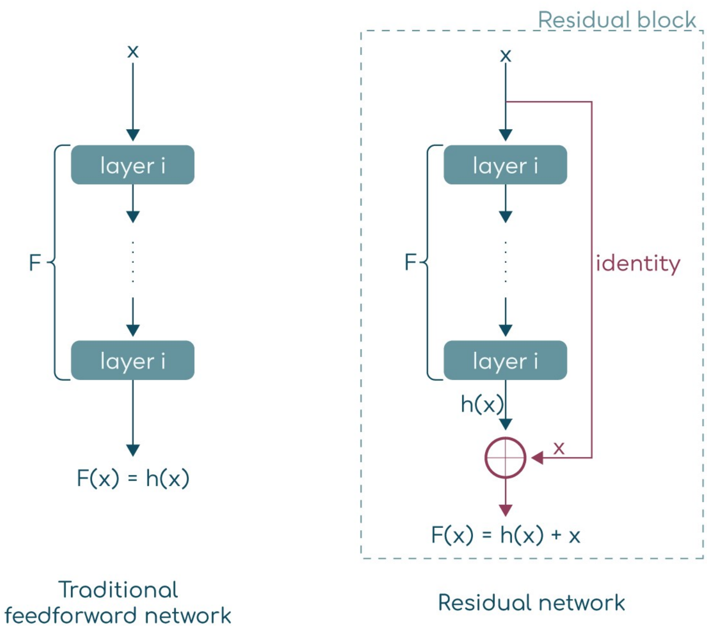

Figure 3-13: Residual block (Adapted from: Sharma, 2021)

3.3.2 CNN for visual comfort in spaces

The limitations of machine learning models that use ANNs lie in the dataset and building descriptions (Q. He et al., 2021). The input variables are limited since the building geometries are simplified in most studies and described based on room width, length, height, elevation, and window position (Q. He et al., 2021). Thus, with the use of ANNs the free design space of an architect in the early-design phase is not well represented due to the constrains that numerical values give to datasets.

In contrast, He et al. (2021) used ResNet (CNN) and pix2pix (GAN) to predict the overall daylight performance metrics and visualize the illuminances, respectively, see Figure 3-14. The dataset consisted of 575 parametrically generated shoe-box rooms and 575 real-case room designs. An image representing geometrical information of the room is the input of the model and the output is the predicted daylight performance including mean lux, UDI and sDA. With their study He et al. (2021) show that the trained ResNet-50 model is able to predict daylight performance for general building forms instead of earlier shown show-box cases with forms controlled by specific parameters. Visualizing the results with the pix2pix model showed the efficiency and effectiveness in predicting the illuminance distribution (Q. He et al., 2021).

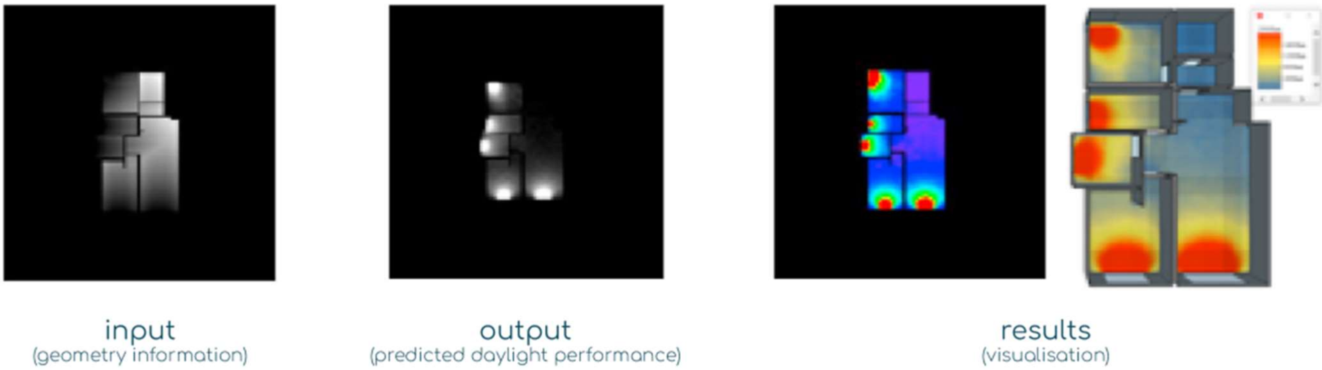

Figure 3-14: Input & output (Adapted from: Q. He et al. 2021)

He et al. (2021) trained two models, one for real case layouts and one for parametrically created layouts. Both models convered a low and stable error rate after 200 epochs. Figure 3-15 shows the real case training loss curve and the comparison between the predicted and ground truth values.

He et al. (2021) used the coefficient of determination (R^2) and the mean square error (MSE) to measure the prediction performance of the model. For the mean lux prediction of the real case the model reached an MSE of 0.010 on the training and 0.036 on the test set. The parametric box predictions for mean lux reached an MSE of 0.020 on the training and 0.038 on the test set.

In their study He et al. (2021) mention that with the below 1 second time-cost, their model can fulfil real-time intuitive feedback for human designers to optimize the daylight performance. However, their model generalized on climates, building orientation, grid size, and façade, which are limitations that need further investigation before the model could be used for design cases.

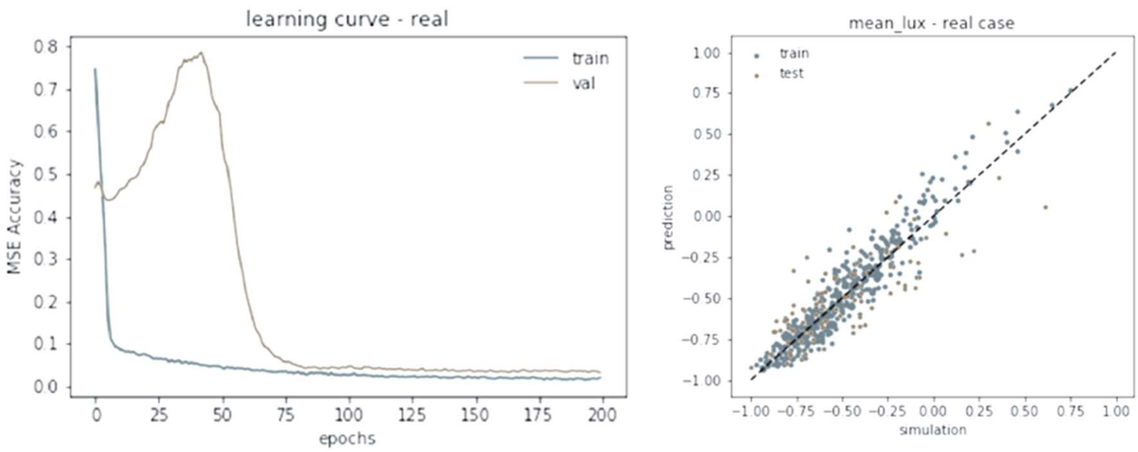

Figure 3-15: Real case training loss curve & mean lux prediction comparison (Source: Q. He et al. 2021)

3.4 Multimodal learning

Multimodal models are capable of understanding and processing information from one or more streams of data (also known as modalities) (Bayoudh et al., 2022). Typically, modalities can include text, images, video, voice, sounds, and music (Poulinakis, 2022). A deep learning model can better understand its surroundings by combining several modalities, given that certain clues are only accessible in specific modalities (Poulinakis, 2022). Multimodal learning is widely applied within affectively computing, robotics, human-computer interaction and healthcare (Bayoudh et al., 2022).

Fusion is the task of combining data from two or more modalities in order perform a to prediction. There are three general approaches of multimodal data fusion: early fusion, late fusion and hybrid fusion (Poulinakis, 2022). Early fusion includes the integrating features immediately after feature extraction, see Figure 3-16.

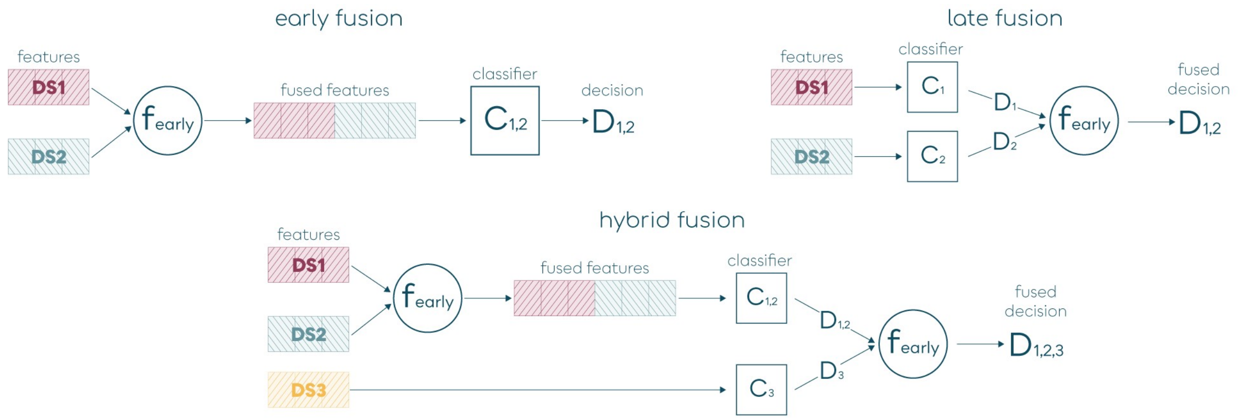

Figure 3-16: Multimodal learning, fusion types (Source: author)

3.4.1 Relevant work

Multimodal learning is not widely used within the field of the built environment. However, in 2022 Sheng et al. studied the application of deep multimodal learning for energy prediction in residential buildings, see Figure 3-17. In their study, Sheng et al. (2022) combined the structure of multilayer perceptron (MPL) and a CNN algorithm to input both textual and visual data. The visual data consisted of Google Street View images and the textual input consisted of building specifications that could not easily be determined by the appearance (Sheng et al., 2022). Sheng et al. (2022) mention that the multimodal deep learning network further decreased the prediction error over single network performances.

In a different field, Peña et al. (2020) used multimodal learning to showcase how gender and ethnicity biases can be harmful in recruitment tool. Peña et al. (2020) used a multimodal learning architecture composed by a ResNet50 and a fully connected network, see Figure 3-18. In their study Peña et al. (2020) showed that the usage of multimodal learning can prevent undesired effects of biases and therefore improve the fairness in the AI-based recruitment field.

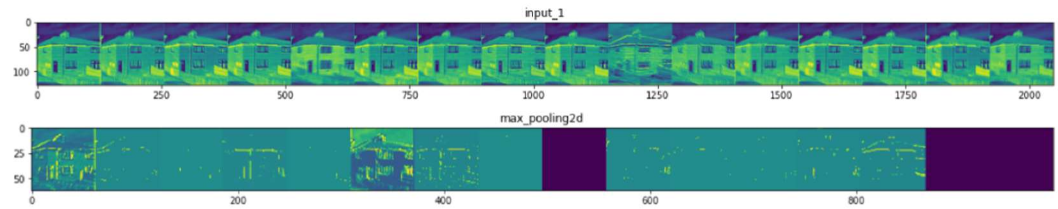

Figure 3-17: Energy prediction feature maps (Source: Sheng et al., 2022)

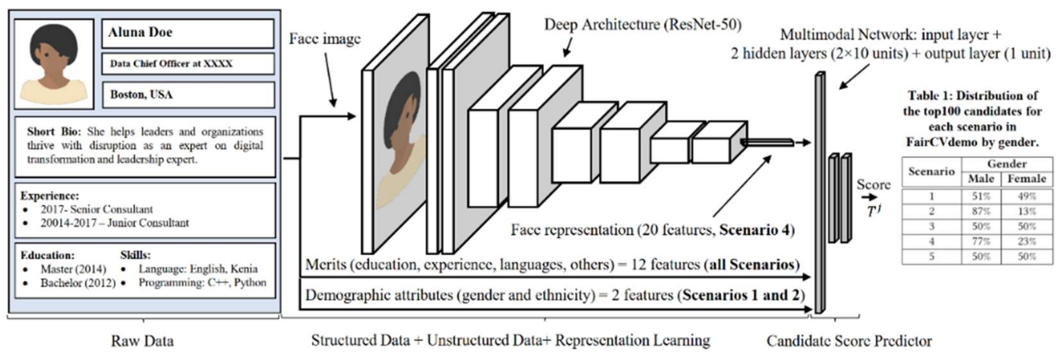

Figure 3-18: Multimodal learning architecture composed of ResNet-50 and a fully connected network (Source: Peña, 2020)

3.5 Conclusion

As discussed in the review of related research above, most studies on deep learning for assessing internal visual comfort have focused on daylight performance. While some work has been done on view quality, its applications have been limited. Artificial neural networks are commonly employed to evaluate visual comfort performance in a space by converting geometrical data into numerical values. However, during the early stages of architectural design, 2D drawings and rough estimates are common, making it difficult to translate them into numerical data. One study attempted to use a grayscale image incorporating all geometrical data for training a CNN to predict daylight performance. This approach is closer to real-world design situations but lacks additional numerical values, requiring a translation process. Combining both approaches can address the shortcomings of AI in assessing visual comfort performance during the early phases of architectural design. Multimodal learning, which uses different data types, can fill the research gap. Research indicates that combining ResNets and numerical data can enhance machine learning predictions. Therefore, a multimodal model combining ResNet and a fully connected network for using both image and numerical data shows the potential to predict visual comfort in indoor spaces, see Figure 3-19.

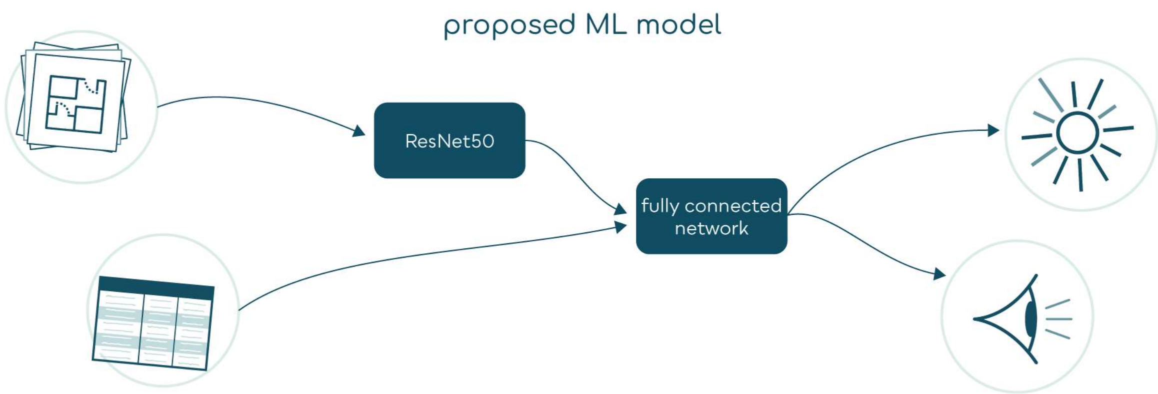

Figure 3-19: Proposed ML model for daylight and view prediction with a layout image and numerical features

~ empty page ~

4 ML DESIGN FRAMEWORK

This chapter presents an exploration of the designed machine-learning process framework. The first part describes the framework for that enables the usage of a machine learning model in the layout design process. After that, a thorough description of the layout evaluation system is given that that quantifies the visual comfort of apartment layouts.

4.1 Layout design framework

To use ML prediction in a design process, the traditional design workflow has to change to make space for the support of an AI tool. Figure 4-1 shows the overall ML process framework for layout design tasks with the support of an AI. In total, four main steps can be recognised.

Firstly, the designer selects their apartment layout options and uploads them into the tool. In the background, the apartment layouts are pre-processed, for each room of the apartment, an image will be created. Secondly, the machine learning model will use the room images with additional numerical features to predict a daylight and a sky view value.

After the prediction, the results are post-processed. The daylight and view values are translated into colours on the apartment layout to make the results easily usable and understandable for designers. A ranking system will quantify the apartment's daylight and view quality and investigate room placement's orientation quality. The designer receives performance-based feedback on each layout and gets insight into the quality of each layout. In this way, the designer can easily quantify the different layout designs against each other. Additionally, an optimiser will show the best option for each of the three aspects and the overall best performance.

With this feedback, the designer can decide to create more design alternatives based on the best-performing layout designs. In this case, the loop starts over again, where the designer creates new layout options and receives direct feedback on each layout design's performance. When the designer is desired with the performance of the layout of the design, they can make a performance-based design decision for the layout design choice, after which the standard design workflow continues.

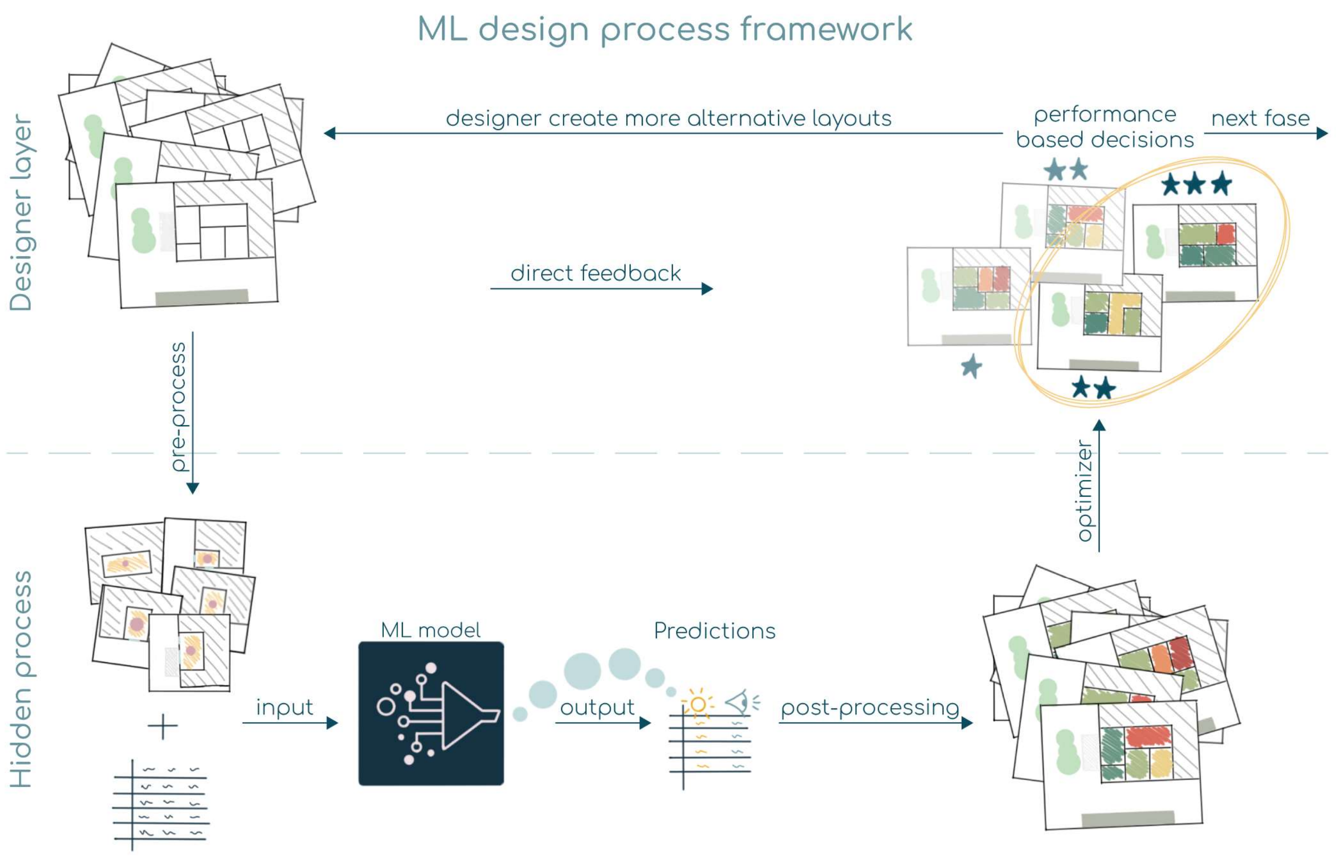

Figure 4-1: ML design process framework for layout design tasks

4.2 Layout evaluation system

In the ML framework post-processing, each apartment layout will be evaluated and quantified against a ranking system. The ranking system is done for daylight quality, view quality and the orientation quality of the apartment. Only living spaces such as bedrooms, living rooms, kitchens and dining rooms are considered to evaluate an apartment. Additionally, the placement of the outdoor space is considered to evaluate the orientation quality.

The evaluation of the performances is done one three different levels: room level, apartment lever per aspect and the overall apartment level. For room level, the requirements from the guideline are used for daylight and view quality. For the apartment level per aspect a 50% rule is used. Where 50% of the room in the apartment need to reach a certain level to reach a certain performance level for that apartment. The overall apartment performance is depending on the apartment performance per aspect and works with an average point system. The following chapter explains the layout evaluation system in detail.

4.2.1 Daylight evaluation

Based on the earlier discussed research into the daylight requirements, four daylight levels are given to define the daylight level of a room. The target illuminance needs to be reached over at least 50% of the space, which is in accordance with the median of each room. Additionally, the target illuminance needs to be reached during at least 50% of the sunlight hours. For this research three daylight hours are used, the median of those three daylight hours is used to test for the target illuminance.

The minimum level that a room can reach depends on the room type of the living space. For a bedroom to reach the minimum level, a lower illuminance is needed over 50% of the space than for a living room. Table 5 shows the target illuminance that needs to be reached for 50% of the space to reach a certain daylight level in a room.

Table 5: Room daylight level requirements

Daylight level	*Target illuminance**
Minimum	bedroom/room: 100 lx, living room: 150 lx, kitchen: 200 lx
Low	300 lx
Medium	500 lx
High	750 lx

** For 50% of the space*

To evaluate the overall daylight quality of an apartment, an additional ranking system with six labels is made based on the room daylight levels of Table 5. A room must reach the minimal threshold for a daylight level to meet the guideline requirements. Otherwise, the rooms will be labelled as insufficient. Table 6 shows the requirements for the living spaces of an apartment to reach a specific daylight label. All apartment daylight labels have a minimal requirement for the living space with the lowest daylight level. Additionally, labels D, C and B have a second requirement, which must be reached for at least 50% of the number of living spaces in that apartment. For example, an apartment with five living spaces needs at least three living spaces with daylight label 'medium', and the living space with the lowest daylight level cannot be lower than the 'low' daylight level to reach an overall daylight label of 'C'.

Table 6: Apartment daylight label requirements

Daylight label	*Room with the lowest daylight level*	*Daylight level for 50% of the living spaces*
F	Insufficient	-
E	Minimum	-
D	Minimum	Low
C	Low	Medium
B	Medium	High
A	High	-

4.2.2 View layers evaluation

Table 7 shows the requirements to evaluate the view quality of a room. As mentioned earlier, a layer is considered present if it reaches a 0.06 sr threshold, which is equal to a threshold of 0.477% of the total spherical view. To reach the minimum view level, the landscape layer must be present for at least 75% of the space.

Table 7: Room view quality level requirements

View level	*View layers present**
Minimum	Landscape layer
Medium	2 layers, incl. landscape layer
High	All layers

** For 75% of the space*

To evaluate the view quality of a full apartment, an additional raking system with five labels is made based on the room view levels of Table 7. A room must reach the minimum threshold for the view level to meet the guideline requirements for the room to be labelled with a sufficient label. Table 8 shows the requirements for the living spaces of an apartment to reach a particular view label. All apartment view labels have a minimal requirement for the living space with the lowest view level. Additionally, labels C and B have a second requirement, which must be reached for at least 50% of the number of living spaces in that apartment. For example, an apartment with six living spaces needs at least three living spaces with a view label 'high', and the living space with the lowest view level cannot be lower than the 'medium' view level to reach an overall daylight label of 'B'.

Table 8: Apartment view label requirements

View label	*Room with the lowest view level*	*View level for 50% of the living spaces*
E	Insufficient	-
D	Minimum	-
C	Minimum	Medium
B	Medium	High
A	High	-

4.2.3 Orientation evaluation

As mentioned in Chapter 2.3.2, each room type has an optimal orientation based on energy consumption, the usage of the room during the day and the access to natural lighting. Based on the earlier mentioned optimal placement, a ranking system per room is created to evaluate the orientation quality of the room. For the indoor living spaces to reach the highest level, the room's orientation has to live in between the optimal orientation of the room type, as shown in Figure 2-10. For each lower level, one of the eight intercardinal directions is added to one or two sides of the orientation range, see Table 9. Figure 4-2 visually represents the orientation levels per room type with the corresponding orientation range.

For rooms with windows on multiple sides the main direction is determined and used for the orientation assessment. The main direction is the side on which the most window area is located. For example, a room with three sides has a window area distribution of 20% East, 10% Southeast and 70% West, the main direction of the room is in this case West.

Table 9: Room orientation level requirements

	Orientation range		
Room type	Low	Medium	*High*
Living room	East to North	Southeast to Northwest	South to West
Dinning	Northeast to Northwest	Northeast to West	East to Southwest
Kitchen	Northwest to Southwest	Northeast to Southwest	Northeast to Southeast
Bedroom	North to West	North to Southwest	East to South
Outdoor space	Northeast to Northwest	East to West	Southeast to Southwest

To evaluate the orientation quality of a full apartment, an additional ranking system is created with five labels based on the room orientation levels of Table 9. For the orientation, there is no insufficient placement of rooms. Since there is no insufficient room level, no additional requirement is added for the room with the lowest orientation level. Thus, the apartment is only tested against one requirement for 50% of the number of spaces. Table 10 shows the requirements for the spaces of an apartment to reach a particular orientation label. In this case, the apartment is tested for the earlier mentioned living spaces and the outdoor space. For example, an apartment with four indoor living spaces and one outdoor space has to reach 'medium' level in at least three of the spaces to reach the overall orientation label 'C'.

Table 10: Apartment orientation label requirements

View label	*Room with the lowest orientation level*	*Orientation level for 50% of the spaces**
E	Minimum	-
D	Minimum	Low
C	Minimum	Medium
B	Minimum	High
A	High	-

** Space types including: bedroom, living room, dinning, kitchen and outdoor spaces*

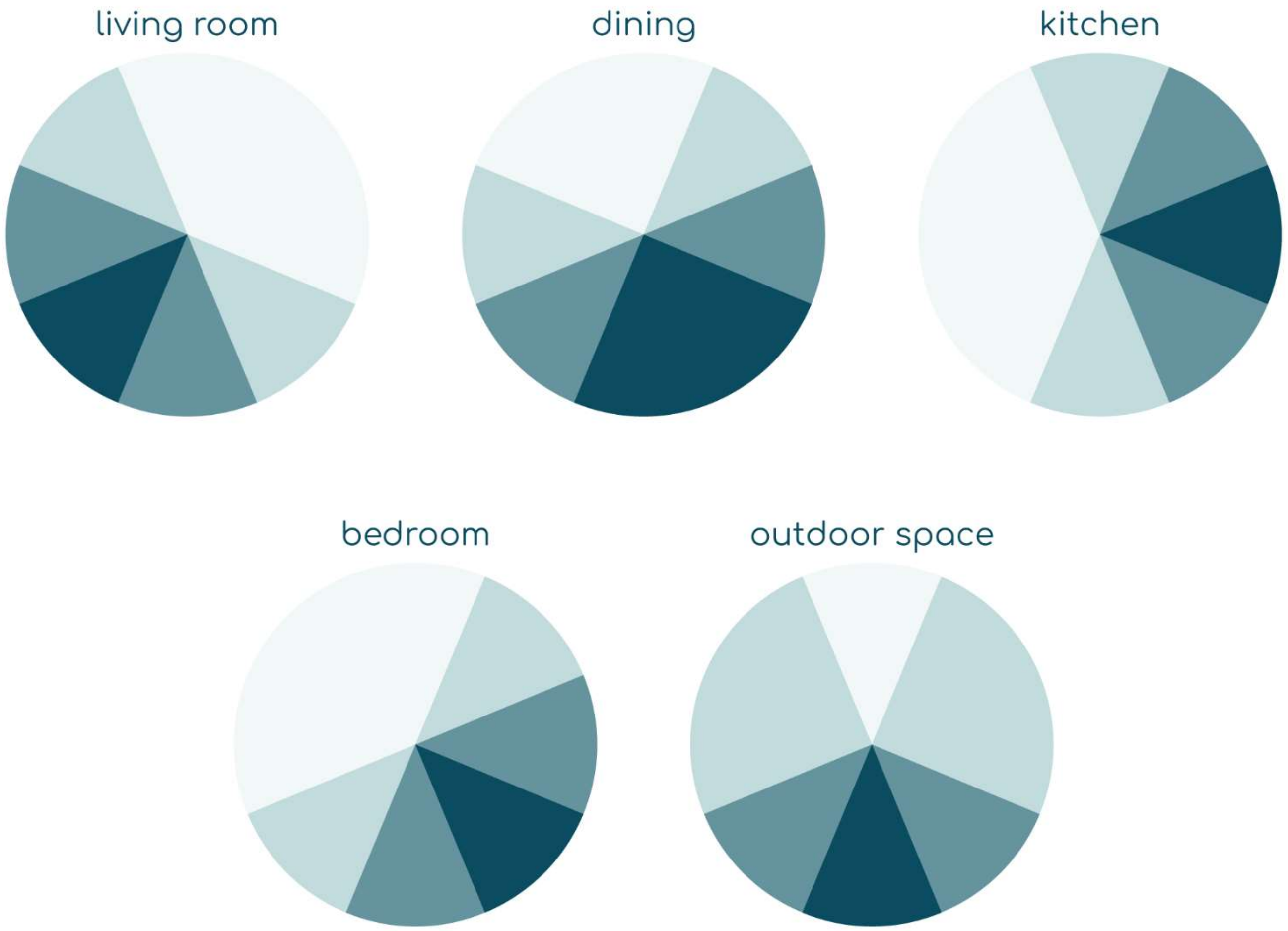

Figure 4-2: Visualization of orientation levels with their orientation ranges

4.2.4 Overall apartment evaluation

To quantify the overall apartment quality, a ranking system is created. The ranking system consists of six labels ranging from A to F. In the ranking system a penalty system is introduced; if the label or daylight or view reaches the lowest possible label, the apartment automatically reaches label F. The labels of the three categories are normalised from zero to one, see Table 11.

Table 11: Category label normalisation to category points

Category label	Daylight x_{day}	View x_{view}	Orientation x_{orient}
A	1	1	1
B	0.8	0.75	0.8
C	0.6	0.50	0.6
D	0.4	0.25	0.4
E	0.2	0	0.2
F	0	-	-

The penalty score ensures that all the overall labels above F ensure that an apartment meets the minimal requirements of the EN17037 guidelines. With the normalised category scores, an average equation is used to determine the overall category score:

$$y_{overall} = \frac{x_{day}+x_{view}+x_{orient}}{3} * pen \tag{4.1}$$

$$pen = \begin{cases} 1, & if\ x_{day} \neq 0\ and\ x_{view} \neq 0 \\ 0, & otherwise \end{cases} \tag{4.2}$$

where x_{day}, x_{view} and x_{orient} are the normalised category labels of the room, and pen is the penalty score. The penalty is set to zero when the daylight or view category equals the lowest possible category. In addition, a more parametric way of determining the overall score is also realised. With the parametric equation, the designer influences which of the three aspects they want to focus on or whether or not to include one aspect in the overall raking of the apartment. The parametric formula for the overall category score is:

$$y_{overall,par} = \frac{(x_{day}*w_{day})+(x_{view}*w_{view})+(x_{orient}*w_{orient})}{3} * pen \tag{4.3}$$

where w_{day}, w_{view} and w_{orient} are the weights of each category that add up to one. The category label can be determined based on the category score, where the category label will correspond with the range of the category score, Table 12.

Table 12: Category points with category label

Overall category label	A	B	C	D	E	F
Overall score $y_{overall}$	[1-0.86]	[0.85-0.71]	[0.70-0.56]	[0.55-0.36]	[0.35-0.01]	[0]

4.3 Conclusion

Integrating AI, particularly ML models, into traditional architectural design has been challenging. To address this, a new workflow has been proposed, including an additional step for integrating an ML model and assessing building performance indicators. The proposed approach involves designers uploading their layout designs into a dedicated tool, which preprocesses the design options into a format suitable for the ML model. The ML model uses this data to predict daylight and view values, followed by an after-processing step that evaluates the overall quality of rooms and apartments in terms of daylight and view quality.

To comprehensively assess layout quality, a new layout evaluation system has been introduced to quantify the visual comfort quality of entire apartments. This system systematically assesses daylight and view quality in each room, enabling the determination of the daylight and view quality of the entire apartment layout. Moreover, to optimise the layout design's visual comfort potential, an additional ranking system is introduced to evaluate the orientation of each room type in residential apartments. The orientation evaluation system systematically assesses room orientation quality for each room and subsequently evaluates overall layout quality based on these orientations. The three aspects of daylight, view, and room orientation are combined to provide an overall quality assessment of the layout.

The post-processing step translates the ML model's predictions and defined daylight and view qualities into a practical visual representation for designers to evaluate. An optimisation step is employed to identify the optimal apartment layout, guided by the requirements outlined in EN17037. During this optimisation process, designers can specify their focus for optimisation among the three aspects. This background optimisation step gives designers direct feedback on their design options, enabling them to investigate the performance indicators of different rooms and apartments. With the performance data and the insights from the optimiser, designers can make informed decisions that enhance the quality and performance of residential layouts as they progress through subsequent stages of the design process.

In summary, this proposed framework represents a significant advancement in the architectural design process, seamlessly integrating ML models into the workflow by guiding designers on performance indicators. By systematically assessing daylight, view quality, and room orientation and providing visual feedback and optimisation suggestions, this approach empowers designers to make informed decisions that enhance the quality and performance of residential layouts, aligning with modern design standards and requirements.

~ empty page ~

5 "Swiss dwellings" dataset

The "Swiss dwellings" dataset forms the cornerstone of this research. This chapter outlines different parts of the dataset, highlighting the comprehensive scope and representativeness. A crucial aspect before using a dataset is data preprocessing. To ensure the dataset's integrity and reliability, missing and erroneous entries are detected, and the simulation results are validated.

The first two sections of this chapter provide information on the dataset's contents. The following sections provide a verification of the daylight and view simulation from the dataset. The fourth section focuses on identifying missing information within the dataset, as well as removing unusable data and outliers. This step involves ensuring that all necessary information is included for the labels and features of ML model training. The resulting cleaned dataset is used for subsequent research, including data analysis and ML model training. Lastly, the limitations of the 'Swiss dwellings' dataset are discussed along with recommendations for improving this dataset and future datasets.

5.1 Dataset overview

The dataset used for this study is "Swiss Dwellings v3.0.0: A large dataset of apartment models including aggregated geolocation-based simulation results covering viewshed, natural light, traffic noise, centrality and geometric analysis" (Standfest et al., 2022). Archilys compiled the dataset based on the company's commercial projects on digitization and building analysis. The dataset of this study consists of over 45,000 apartment samples in approximately 3,100 apartment buildings located within Switzerland. The dataset includes room-level geometries, typology, visual, acoustical, topological, and daylight characteristics. On the building level, the dataset includes location-specific characteristics and a 10-minute walkshed from each building. This study only focuses on the geometry, view and daylight characteristics.

The dataset contains information on the geometrical values of each room. For each room, an apartment, site, building, floor, plan, unit and area ID to place the room correctly. Figure 5-1 shows a visual representation of the different scales within the dataset. The geometry dataset provides each room's unit usage, entity type and subtype, entity height, elevation and polygon geometry. The 2D geometries consist of an apartment's areas, walls, railings, columns, windows, doors, and features (for example, sinks and bathtubs). Since the dataset consists of existing building plans of clients, Archilyse converted the geometries from geo-referenced to geometries that do not represent the real-world location of the buildings.

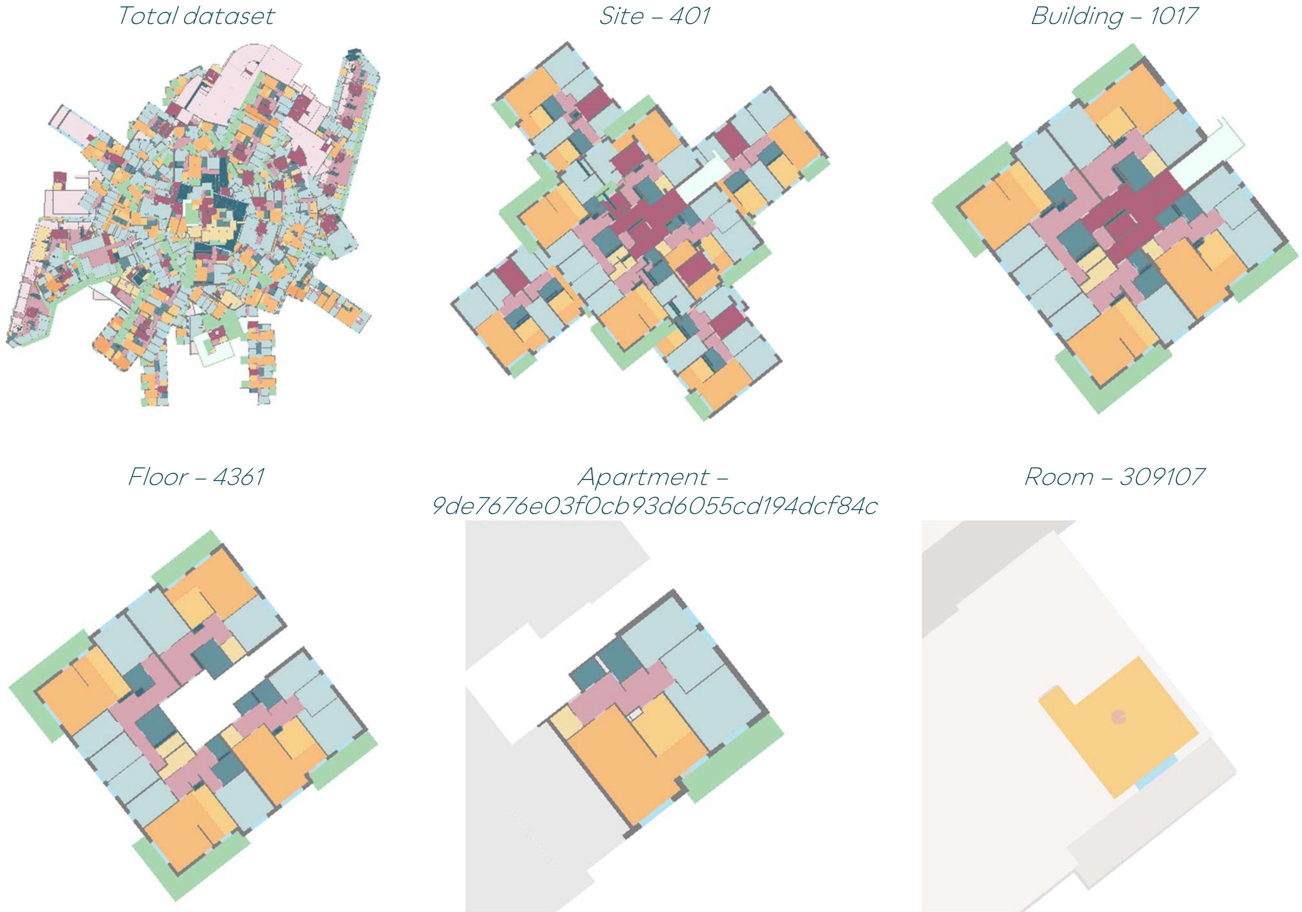

Figure 5-1: Visual representation of room 309107 within the dataset geometry (Source: author)

5.2 Environmental simulation

Besides the geometrical model, the simulation dataset provides data per room on the apartments' visual, acoustic, solar, layout, and connectivity-related characteristics. The total simulation dataset consists of 367 columns. The dataset provides the view and light simulation data using the room-wise aggregations' min, max, mean, std, median, p20, and p80. For instance, p20 describes the simulation value represents at least 20% of the positions in the room. The median describes the median simulation value of all the positions in the room, and the max describes the maximum simulation value of any position in the room.

The view and daylight simulations used environmental data from "SwissTopo". SwissTopo consists of a digital detailed 3D building model that covers the whole of Switzerland and consists of over 70 million 3Dobjects (SwissTopo, n.d.). The 3D model represents every building, bridges, cable cars, forests, and individual trees, see Figure 5-2.

Figure 5-2: SwissTopo, a digital 3D model of Switzerland (Source: SwissTopo, n.d.)

5.2.1 Daylight simulations

To help understand the impact of solar radiation, sun simulations are done on the object a grid from the analysed object for each room in the dataset. The goal of these simulations is to identify surfaces that have great solar potential. The amount of solar radiation defines the sun simulations on a grid from the analysed object. Included in the simulation is direct sun and scattered light. The simulations are performed for the 21st of March, 21st of June and the 21st of December. The simulation outcome is given for the room-wise aggregations min, max, mean, std, median, p20 and p80 in kilolux (klx). The simulation is performed for a spatially distributed grid in the interior floorplan at 0.1 m above the floor. The grid is a 25 cm hexagonal grid.

Archilyse uses their own software for the daylight simulations. The CIE Standard Clear Sky, polluted atmosphere, is used for the brightness of the sky. No materials are included and reflections are not considered. With these simulations the amount of direct sunlight from the sky is determined.

5.2.2 View simulation

The view simulations include calculations about the visual amount of buildings, greenery, water and mountains on a grid from the analyses object. The values are expressed as proportion of the total view of a sphere, which represents 4 π steradians (sr) and represent the amount a particular object category occupies in the spherical field of view. The simulation outcome is given for the room-wise aggregations min, max, mean, std, median, p20 and p80. Archilyse did simulations using their own software. The simulation were done by 3D rendering cubemaps, using Vulkan. The simulation is performed for a spatially distributed grid in the interior floorplan at standing eye-height at 1.55 m above the floor.

5.3 Dataset verification

The quality of a dataset determines the reliability of analytical results and plays an essential part in the credibility of any simulation-based analysis based on a model's prediction. This sub-chapter delves into the work of dataset verification for the simulated values of daylight and view to assess the quality of the dataset utilized in this study.

5.3.1 Room selection

Forty rooms are selected from the dataset for the verification process. A comprehensive set of criteria determined the selection process, assuring the representativeness and quality of the chosen rooms. The criteria included six categories: living spaces, windows on one side, absence of landscape view layer, minimum daylight and high sky view value, absence of site obstructions and diverse room orientations. The selected rooms included living spaces such as living rooms, bedrooms, kitchens and rooms. This restrain was chosen to maintain the relevance of the simulations within the context of the domestic environment. To simplify the simulation method, only rooms with windows on one side of the façade were selected. Since the environmental context of the buildings in the dataset is not given, only rooms without the landscape view layer were selected. This way, unknown obstacles, such as trees or buildings outside the building site, were ruled out. Exclusively, rooms with a landscape nature or urban view smaller than 0.1% were considered. A minimal daylight value was established as a criterion for room selection to ensure rooms with sufficient access to daylight. The minimum daylight value consisted of 50 lux for the 21st of March, June and December at 12 o'clock. Additionally, rooms with a sky layer more prominent than the view layer nature and urban were selected to ensure the presence of the view to the sky layer exclusively. The selected rooms were scrutinized to ensure the absence of significant obstructions from either the building itself or neighbouring buildings on the site. Lastly, the selection consists of rooms from each orientation to create a diverse set of rooms.

Applying these criteria ensured the chosen rooms' diversity and representativity, showcasing the entire dataset's integrity. In total 37 rooms are selected for the verification that all met the six criteria. For each cardinal direction four to five rooms are selected. Table 13 shows the ranges of the room characteristics. Appendix A shows an overview of how each room is located within their apartment layout. The rooms are all modelled in respect to a ground plane the rooms are elevated based on the elevation of the room. The rooms are modelled with the correct face types and boundary conditions of the room, see Figure 5-3.

Table 13: Room characteristics ranges

Room characteristic	Range
Room area	7.4 – 29 m^2
Total window area	1.9 – 6.4 m^2
Room elevation	0 – 20.3 m
Room height	2.6 m
Window to floor ratio	0.12 – 0.45
Room depth ratio	1 – 3.7
Orientations	North, Northeast, East, Southeast, South, Southwest, West, Northwest

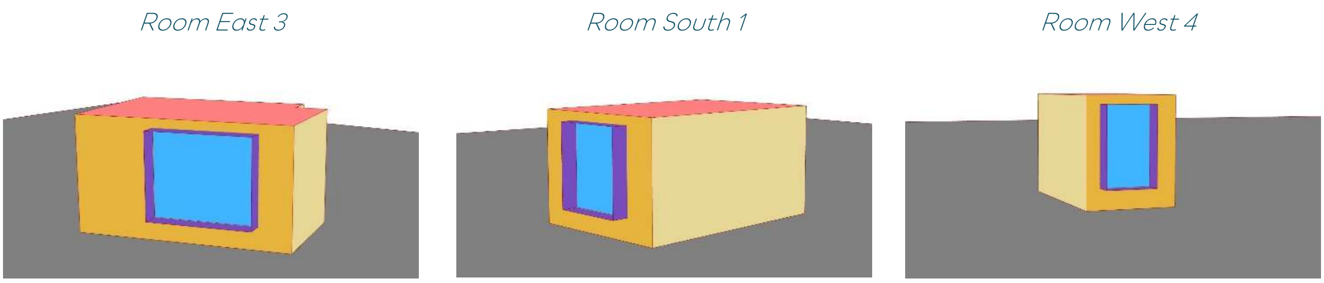

Figure 5-3: Examples of room modelling

5.3.2 Daylight simulations set-up

The daylight simulations conducted for this verification were executed using the Honeybee plugin, which uses Radiance (version 5.4a) and Dysim for daylight analysis. To provide an in-depth understanding of daylight dynamics, point-in-time simulations were performed on three days during the year: March 21st, June 21st, and December 21st , each at 12:00 locale time. The simulations used the standard CIE sky model, sunny sky with the sun, to ensure that the solar irradiance model corresponded with the lighting standards. A 25 by 25 cm grid was used, which corresponded with the grid size used for the simulations done in the dataset.

The weather information for the simulations was obtained from Geneva, Switzerland. Consequently, the exact location of the various rooms was standardised to a single location in Switzerland in the verification. It is critical to understand that access to sunshine is affected by the location of the building, as it influences climatic characteristics such as the amount of sunlight and the angle of sunlight. Switzerland's mountainous terrain can cause significant variations in local sunshine availability and climate. Unfortunately, the current dataset does not provide the exact location. Therefore, the verification's climate is normalised to one location, Genova.

Two different simulations were conducted. The first simulation aimed to fully replicate the conditions for the daylight simulation as given in the dataset. In this simulation, the two most crucial settings concluded the number of ambient bounces in combination with the material reflectance. The simulation ran with one ambient bounce and no material reflectance since the simulations in the dataset included the amount of direct sunlight and light from the sky without considering reflecting light. Because of this, both direct and sky light were considered with one bounce and the reflecting light is entirely absorbed by the materials. The second simulation followed the simulation parameters as given in the EN17037 guideline. The simulation parameters for both the daylight simulations are listed in Table 14.

Table 14: Daylight simulation parameter settings

Simulation parameter	*Simulation 1 - remake*	*Simulation 2 - guideline*
CIE sky type	Sunny with sun	Sunny with sun
Site location (latitude, longitude)	Geneva (46.25, 6.13)	Geneva (46.25, 6.13)
Plane height [m]	0.1	0.85
Grid size [m]	0.25x0.25	0.25x0.25
Material reflectance (floor, ground, walls, ceiling)	(0, 0, 0, 0)	(0.2, 0.2, 0.5, 0.7)
Window transmittance	0.91	0.67
Ambient combination (ab, aa, ar, ad, as)	(1, 0.4, 32, 512, 256)	(5, 0.4, 32, 512, 265)

5.3.3 View simulations set-up

The view simulations conducted for this verification were executed using the Ladybug (version 1.4.0) plugin for environmental analysis. Specifically, Ladybug's "View Percent" component was used to simulate the percentage of view to sky from an input geometry (the plane) compared to its surrounding context. This view evaluation approach determines the quality of a view from a specific indoor location. Two simulations ran to replicate the view simulation in the dataset as closely as possible.

The spherical view type was selected as it determines the sphere percentage unhindered by the contextual geometry for each point. This method gives equal weight to all portions of the sphere. We may conclude that the remaining unobstructed view only consists of a view of the sky, considering that the selected rooms do not have a substantial quantity of view of nature or urban present. A grid of 25 by 25 centimetres was adopted from the dataset simulations. A plane height of 1.55 meters was used throughout this simulation, corresponding to the provided value in the dataset. The EN17037 standard recommends plane heights of 1.2 or 1.7 meters. Given that the plane height used in this simulation lies in between the required range, changing the plane height will not change the outcomes too much. In the second simulation the plane height is set to 1.2 meters. The simulation parameters for the two sky view simulations are listed in Table 15.

Table 15: View to sky simulation parameter settings

Simulation parameter	*Simulation 1 - remake*	*Simulation 2 - guideline*
View type	Sky exposure	Sky exposure
Plane height [m]	0.1	1.2
Grid size [m]	0.25x0.25	0.25x0.25
Vector resolution	577 vectors	577 vectors

5.3.4 Simulation results

Figure 5-4 shows the results of the daylight and view simulations for three rooms. The detailed results of the simulations are shown in Appendix A. At all the different directions a big difference between the remake simulation and the simulation according to the guidelines shows. Three first reasons for the big difference in illuminance can be found in the settings of the second simulation. Firstly, the second simulation includes internal reflections, leading to more light inside the room. Secondly, the glass properties are taken into account, a lower transmittance leads however to less light passing through the window. Lastly, the higher plane height receives more light. Overall these three main difference lead to higher daylight values causing the big difference between the two simulations. Looking at the two sky view simulations no big difference is shown, as expected since only the plane height is changed.

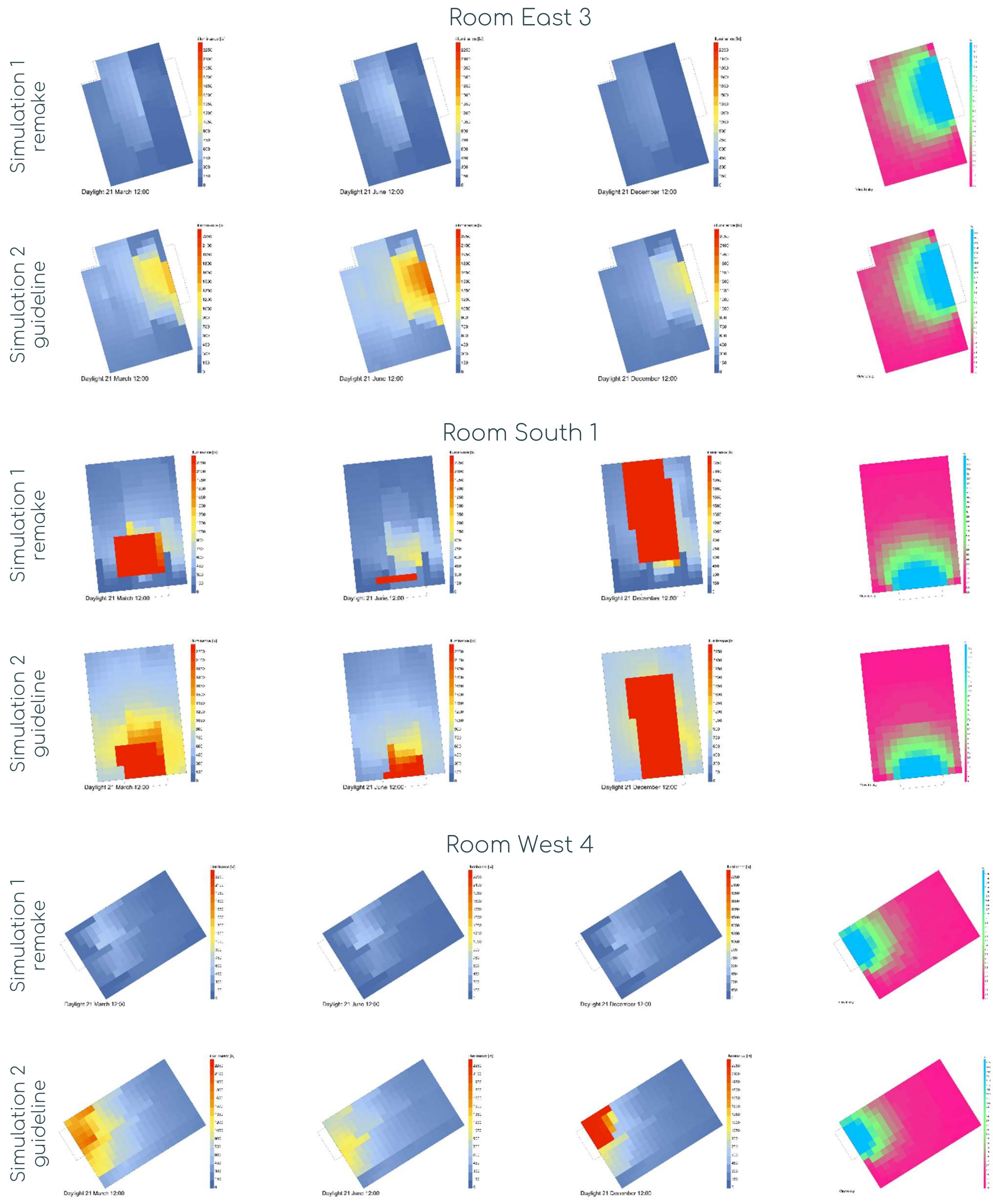

Figure 5-4: Dataset verification simulation results for 3 rooms

5.3.5 Simulation comparison

For the results comparison the median of the rooms is used, in this way extreme values in the results are ruled out. Figure 5-5 shows the simulation results of the two different simulations in comparison with the values in the dataset. For the daylight values an interesting observation can be made that the simulation results from the guideline simulation come closer than the simulation values of the remake simulation and the guideline simulation values are always higher than the remake simulation values. Additionally, for higher values from the dataset the simulations show lower values, while for lower values in the dataset the simulations show higher values. Different sources of discrepancy can be found between the simulations that are done and the simulations of the dataset.

Firstly, a different grid structure is used, as the simulations in the dataset used a hexagon grid, while the verification simulations are done with a square grid. Additionally, an accurate environment is not modelled for the verification simulations, the environment and the building itself are not modelled. This could explain some differences between the results even though the rooms are carefully selected in such a way that obstructions are minimal. Kharvari (2020) mention that the sky model plays an vital role in the daylight calculations. This could explain a difference in the values since the dataset simulation are done with the CIE sky model 'Standard Clear Sky, polluted atmosphere', while in the simulations a 'sunny with sun sky' of Honeybee is used. Additionally, the weather file of Geneva is used for all rooms instead of the exact weather location file, which could also lead to changes in the solar irradiance and thus the illuminance levels. Lastly, an important reason why the remake simulation values differ is the ambient parameter combination that is unknown from the dataset simulations.

A clear correlation between the verification simulations and the dataset values is not observed. However, it is important to mention that for a machine learning model patterns are relevant, not the exact values. Hence, a similar trend would be expected when the dataset simulations will change in accordance with the guideline as the correlation between the two verification simulations.

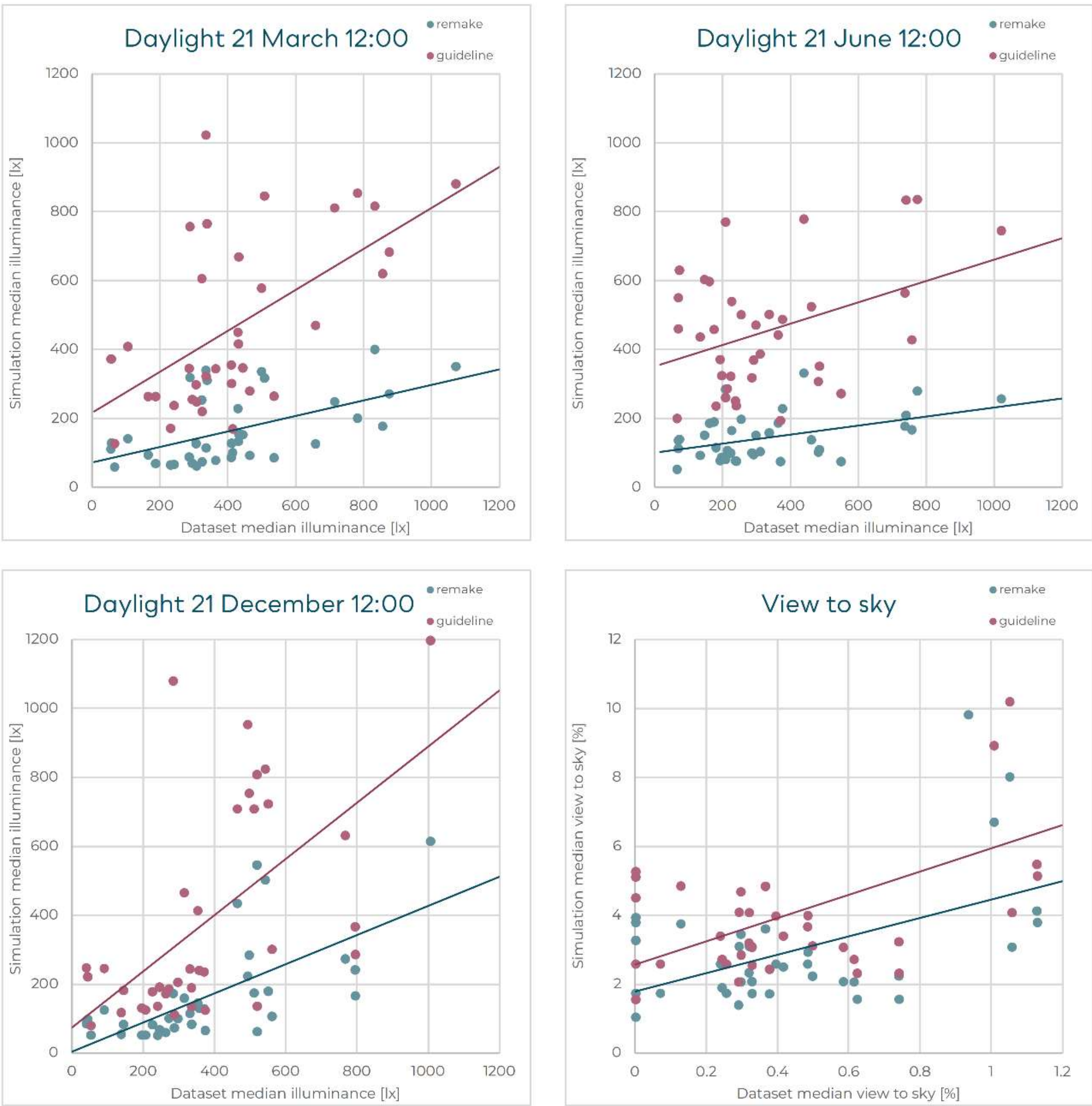

Figure 5-5: Simulation results comparison with dataset values

5.4 Apartment & room selection

Data cleaning is a pivotal step in data analysis to enhance the data's quality and usability. For the reliability and validity of the ML model, it is crucial to carefully select apartments and rooms that are appropriately defined and structured. Identifying and rectifying inconsistencies, errors, and missing information that could arise during data gathering is a critical element of data cleansing. The data cleaning process consisted of seven steps to select the proper apartments and rooms to be used for this research. The raw dataset comprised 45,175 apartment layouts, and the cleaned dataset comprised 42,022 apartment layouts. Firstly 119 duplicate rows are dropped, and all the features are removed from the dataset, which consisted of 317,930 rows. Table 16 shows a detailed overview of the data cleaning steps and the deducted number of apartments during the steps.

For the sake of this research from the dataset, only the following room types are selected: room, living room, kitchen, dining, bedroom, and studio. Since this research only covers the visual comfort aspects of indoor spaces, all the outdoor areas are removed from the dataset, for instance, balconies, loggias and winter gardens. Apartments with multiple stories are removed; those apartment layouts are outside the scope of this research. Secondly only the apartments that are inside the simulation dataset are selected. Apartments that have windows shared between rooms or apartments are removed and additionally apartments that had windows that were connected to a room are also removed. Next, rooms that have no daylight levels but have view to sky are removed. Rooms with nan values in the simulation value columns are removed, these are areas inside apartments such as voids or shafts. Lastly, apartments that consisted of outliers for the two machine learning labels for daylight or sky view are removed. Appendix D.Part II shows the code for the data preparation.

To have a useable dataset for the machine learning model a statistical approach is used to remove the outliers based on the mean and standard deviation. The outliers of the dataset are selected based on the median daylight value of March 21st, June 21st and December 21st at noon and the p80 view to ground and sky value. For each of the five performance aspects the outliers are individually selected based on three times the std. From this the apartments are selected that did not fall within any of the five outlier types.

Table 16: Data cleaning detailed overview

	Description	Apartments	Area ids
	Total number with redundant room types	*45,175*	*315,036*
	Total number without redundant room types	43,192	98,228
1	*Multiple story apartments*	1,735	25,724
2	*Apartments not in simulation dataset*	3	8
3	*Apartments with shared windows*	868	2,099
4	*Apartments with other geometrical difficulties*	248	843
5	*Rooms without daylight with view to sky*	27	55
6	*Rooms with nan label or featuture values*	2,468	6,267
7	*Daylight and view outliers*	4,821	10,677
	Total number of final apartments	34,757	78,278

5.4.1 Shared windows and geometrical difficulties

Within the dataset not all geometries of the apartments are drawn in the same way. There are apartments that have a window geometry that is shared between rooms, between areas or between apartments, see Figure 5-6. Apartments that include areas shared window geometries are removed from the dataset, since additional information about each window that belongs to an area is added into the ML model. Additionally, within the process of connecting windows to their area apartment layout with thick walls resulted in not connecting windows to their area. Manually connecting the windows with other geometrical difficulty such as thick walls would be possible, however for the sake of this research those apartments are eliminated from the dataset. Appendix D.Part I shows the code that was used to find missing information in the dataset and identify the shared windows and geometrical difficulties.

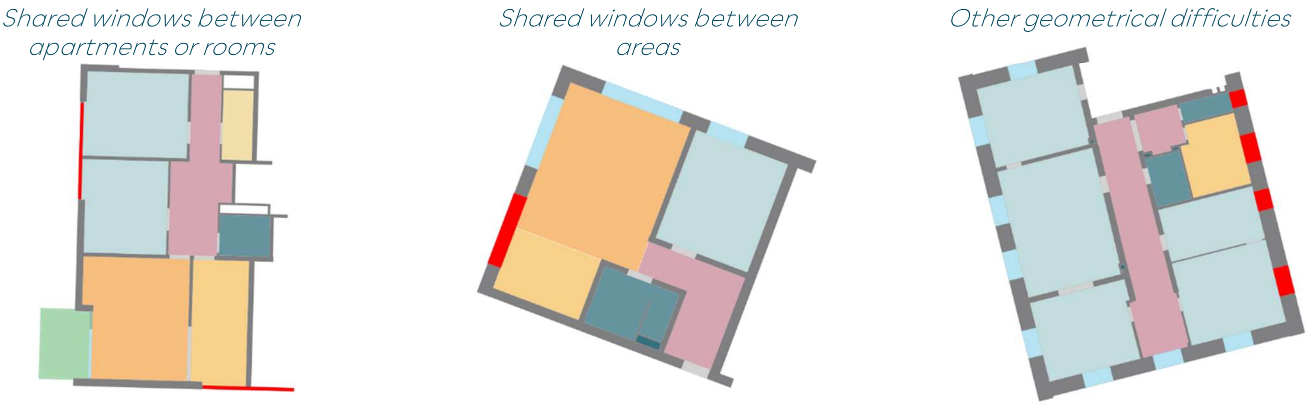

Figure 5-6: Apartments with shared window geometry or geometrical difficulties (Source: author)

5.4.2 Removing daylight and sky view outliers

The last step included the removal of the outliers for the two machine learning labels median daylight values on the 21st of March, June and December and p80 values for view to the ground and view to sky. Outliers are data points in a dataset that vary considerably from the mean values. Eliminating outliers is critical for various reasons. Outliers can have a significant influence on model training, causing the model to be skewed or biased toward these extreme values. Which could result in inaccurate predictions and poor generalization. Additionally, outliers introduce noise into the model, which could lead to reducing the overall predictive value of the model. The outliers are selected one by one for each of the five labels based on the full dataset based on the three times standard deviation method. The dataset is then cleaned by removing apartments that include rooms that fall in one of the five outlier categories.

Figure 5-7 visualizes the labels normalized data, the first two boxplots show the data with the outliers and the lower two boxplots show the data after removing the outliers. The boxplots with the outliers show a large number of datapoints that depart greatly from the rest of the data. Looking at the data with the outliers, 95% of the data for the daylight label is located within the lowest 10% of the values and for the view label 95% of the data is located within the lowest 20% of the values. The boxplots with the outliers highlight the potential skewing effect that the data could have on the machine learning model.

Looking at the lower two boxplots containing the data after the removal of the outliers, there is a huge shift in the data distribution. The data without the outliers show a better representation of the data with a wider and more equal distribution. After the outlier removal, 95% of the data for the daylight label is contained within the lowest 70% of the values and for the view label 95% of the data is located within the lowest 80% of the values. This data distribution guarantees a better concentration of the machine learning model on the patterns of a bult of the data.

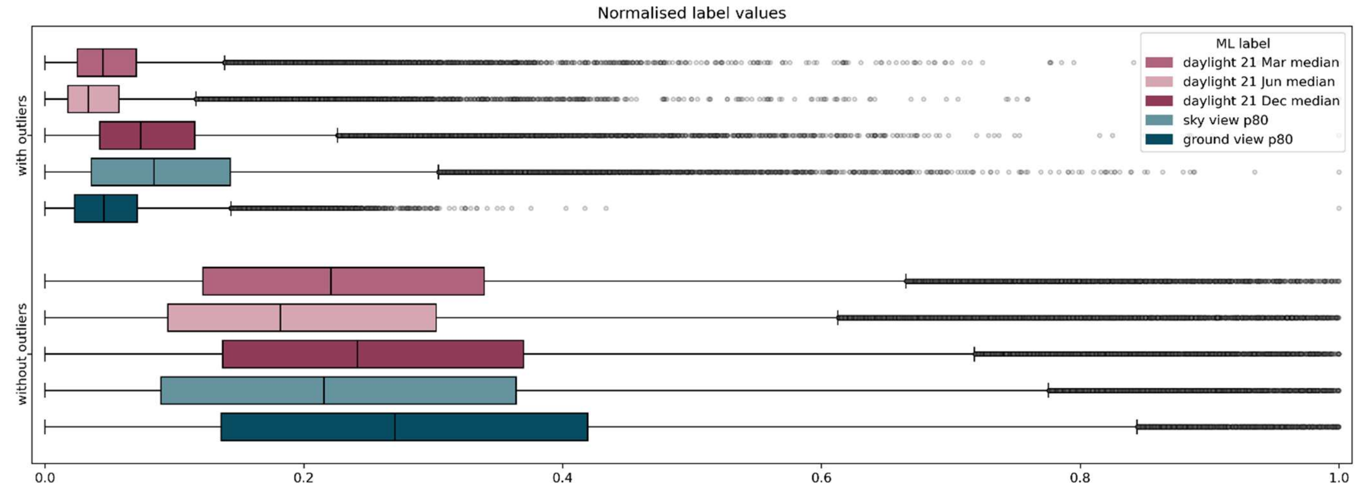

Figure 5-7: Boxplots of normalised ML labels with and without outliers

Figure 5-8 shows the distribution of the daylight and view to sky values with and without the outliers in two scatterplots. Removing the outliers made some adjustments in the ranges of the daylight and view values. The median daylight values for the 21st of March at noon with outliers range from 0 to 8,900 lux, while the values without the outliers range from 0 to 1,700 lux. The p80 view to sky values with the outliers range from 0 to 15.2% while the values without the outliers range from 0 to 5.5%.

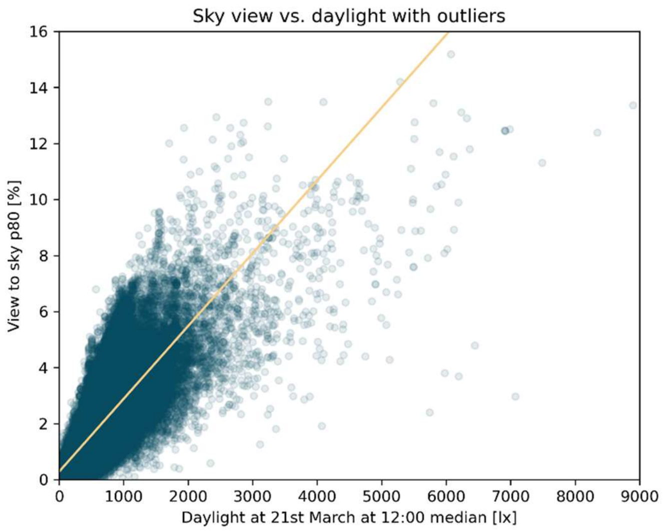

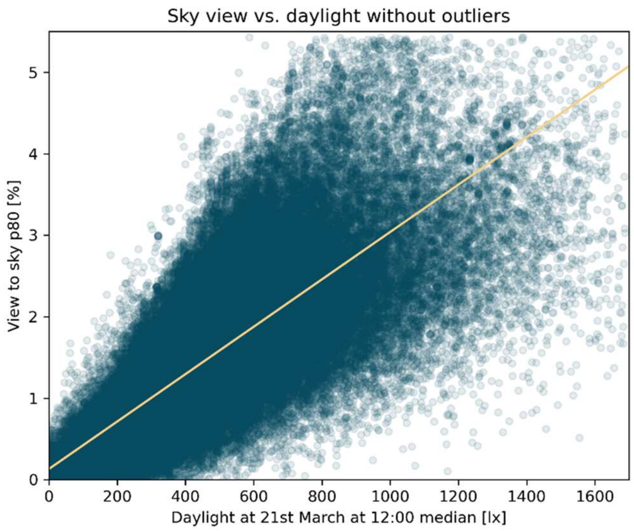

Figure 5-8: Scatterplots of normalised ML labels with and without outliers

5.5 ‘Siwss dwellings’ dataset limitations

While analysing the 'Swiss dwellings' dataset, three primary areas are detected where the dataset falls short. The dataset misses essential information for complete analysis and misses essential descriptions of the components in the dataset. Additionally, inconsistencies are discovered within the dataset. In the following part, each of the three areas is described.

5.5.1 Missing information

The first limitation of the dataset is missing information. Notably, the dataset in its current condition lacks critical features necessary for undertaking a thorough study of the dataset's simulation values concerning the rooms' characteristics. In the dataset, there is no difference between an inside door and a door that leads to a balcony. However, most often, doors that connect to a balcony contain glass, while inside doors that connect one indoor space to another do not. To get a complete understanding of how much glass a room contains, doors that are connected to outdoor spaces are changed from entity subtype 'DOOR' to 'OUTSIDE_DOOR'. Therefore, when addressing windows from now on, this is considered the entity subtypes' WINDOW' and 'OUTSIDE_DOOR'.

The absence of a clear relationship between windows and their corresponding rooms is a severe problem, limiting the capacity to correlate specific room parameters with matching simulation data. Therefore, the dataset must include information specifying which windows are connected to which room. Additionally, the data should include the window area per window and the total window area per room. This information gives a clear understanding of how much access a room has to the outdoors. Combining these two aspects allows a quick investigation of the total window area for each room, strengthening the dataset with essential information streams. In addition, window orientations should be included in the dataset to understand the influence of room orientation on simulation values fully.

5.5.2 Missing description

Another critical aspect of creating an ideal dataset is the addition of detailed explanations for all dataset components. The dataset currently needs more clarity in terms of column definitions and units of measurement, preventing complete understanding and application. Columns such as "height", for example, should be more specified. An additional note that includes the specific meaning of "height" is essential. For example, floor-to-floor height for rooms and total window height for windows. Similarly, "elevation" should be described as the height at which the top section of the floor is located and the height of the windowsill. Additionally, the dataset should clearly describe the geometric entities represented by polygons, whether the "window" category includes the frame and the glass or only the glass component.

To allow complete data interpretation, the dataset should clearly explain the simulation approach, indicating whether it matches a particular standard or takes a customised approach. For transparency and replicability, the dataset should include information on the boundary conditions used to produce the simulations, including simulation settings and boundary conditions. In this way, the simulations could be reconstructed using the provided description. Including these detailed descriptions is critical in converting a dataset with simulation values into a more useable resource for research and analysis.

5.5.3 Inconsistency

Another significant shortcoming of this dataset is inconsistency within the dataset. There are two main inconsistencies found within this dataset. Firstly, the placement of buildings on the site, with instances where different buildings located on one site are not regularly positioned relative to one another. Such variations could create confounding variables and complicate comparison studies, emphasising the importance of a uniform approach to building placement concerning sites in the dataset. Variations in how windows are drawn also stand out as a noteworthy inconsistency. As described in Chapter 5.4.1, in some situations, window geometries are shared between rooms or even between different apartments.

Lastly, the dataset contains inconsistency among the different files of the dataset. For example, the "entity_subtype" column in the "geometry" file should be in accordance with the "layout_area_type" column in the "simulations" file. However, the two different files have differences in the room type column when it comes to the usage of capital letters and the unique room types the two files contain, while the two columns describe the exact same data.

5.6 Optimal dataset recommendations

To enhance the quality of the "Swiss Dwellings" dataset, some key modifications need to be made. These changes can be categorised into three categories: guideline simulations, performance analysis data, and overall consistency. These categories apply to all dwelling datasets in Europe that contain simulation and geometrical data.

Datasets including simulation data for buildings in Europe, should conduct the simulations in accordance with the European guidelines. In this way, not only can a building be checked on requirements that are accepted across Europe, but datasets that consist of data from different countries could be merged together. By comparable conducted simulations, a single ML model can be trained using these different datasets since the correlations between simulation results and geometrical data will be similar.

Additionally, the given geometrical information in the dataset should consist of information that is essential for the type of simulation data which the dataset includes. Giving the geometrical data for each room in accordance with the simulation types in the dataset allows for easy performance analysis and a more thorough data analysis of the dataset.

Lastly, if the dataset is split into different files, there should be an overall consistency across all files. Additionally, the way the different sites are geometrically drawn within the dataset should be consistent.

~ empty page ~

6 Data analysis

This chapter provides a detailed analysis of the dataset's information. The first section focuses on the overall daylight and view data of the dataset. The second part of the chapter delves into the foundational components of a machine learning process, the labels and feature selection. In the second section, each possible feature is compared against the labels to understand patterns, relationships and correlations. The importance of each feature is discussed, leading to a final feature selection. Lastly, the distribution of the different visual comfort levels and labels within the dataset is analysed.

6.1 Daylight data

The dataset contains eighteen different daylight categories grouped within three days. For each day, the associated daylight hours are given, see Figure 6-1. The three days that are included in the dataset are the 21st of March, the 21st of June, and the 21st of December, also known as the equinoxes and solstices. On the 21st of March, the equinoxes, the sun is exactly above the equator, making the day and night of equal length. On the 21st of June and December, the solstices, the sun's path is the furthest away from the equator, making it the longest and shortest day of the year. Analysing the daylight for these three days provides a general understanding of the daylight quality throughout the year.

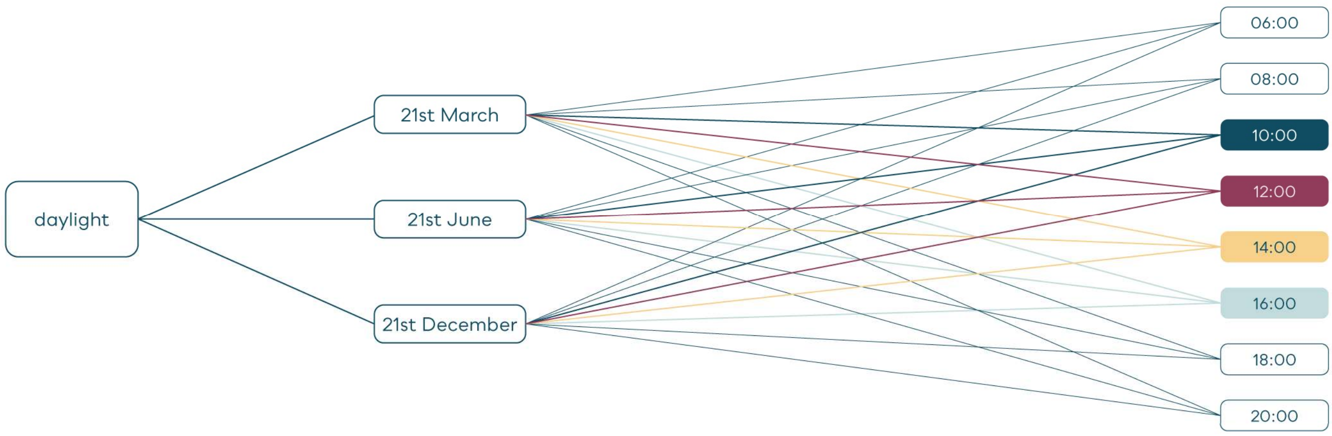

Figure 6-1: Daylight categories dataset

6.1.1 Daylight hours value distribution

Figure 6-2 illustrates the distribution of daylight levels at frequent daylight hours for each day. For each of the days and hours, nearly 95% of the data has daylight levels below 1250 lux. Outliers are removed from the dataset for all three days at noon. The highest illuminance values are found on the 21st of March at 16:00, while the lowest illuminance values are found on the 21st of December at 16:00. The median values on the 21st of March are almost equal for the four hours, while there is a clear difference between the median values of the hours on the 21st of June and December.

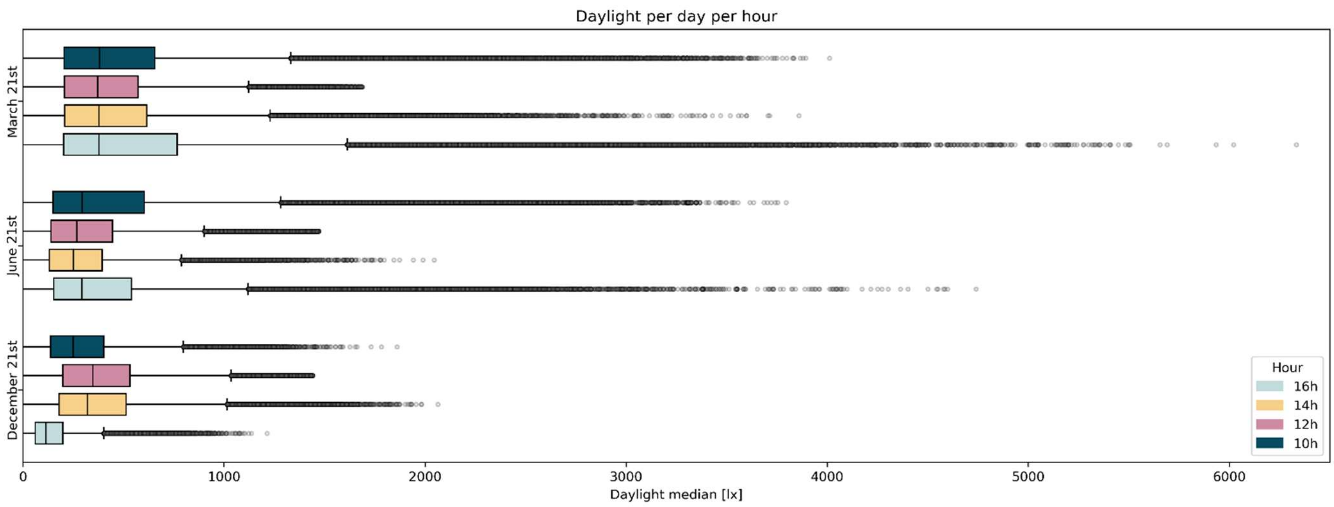

Figure 6-2: Daylight boxplot per day per hour

6.2 View data

In the dataset, various view categories are described that can be linked to the four view categories given by the EN17037, see Figure 6-3. The ground view category consists of the ground, railways and different street types such as tertiary streets, secondary streets, primary streets, and pedestrians. The sky layer contains the sky category from the dataset. The 'landscape nature' represents natural environment characteristics, such as parks, forests or waterfronts. Within the dataset, 'landscape nature' is depicted through three view types: greenery, mountains, and water. In contrast, the 'landscape urban' view category represents urban environmental characteristics such as city streets, surrounding buildings, plazas, and commercial areas. In the dataset, 'landscape urban' includes buildings that are not located on the site. An additional view category is included within the dataset, namely view site. The view site category contains buildings on the site itself, views of the same building and interior views such as walls, flooring and the ceiling from the room itself.

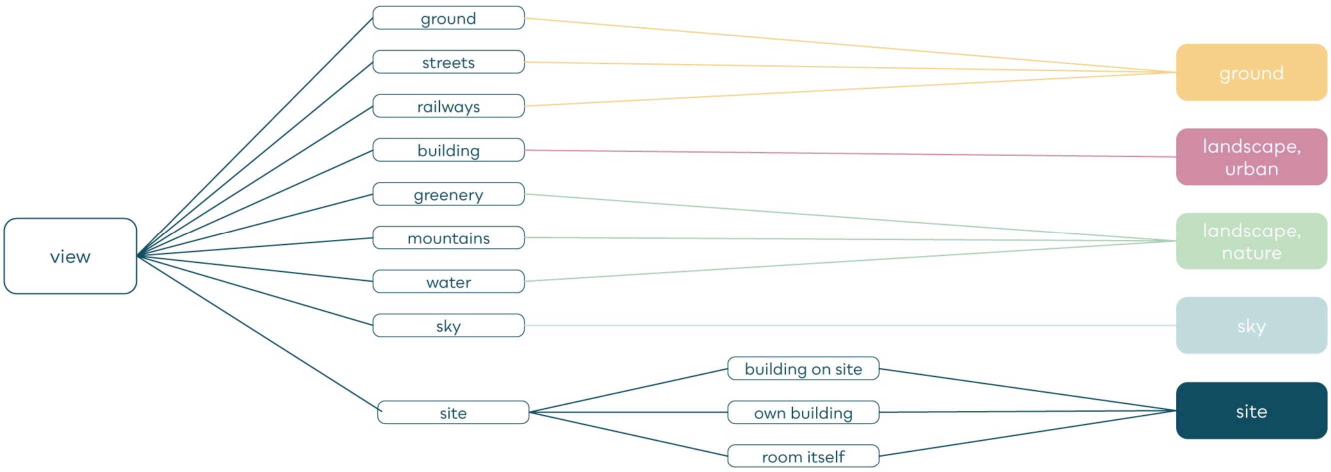

Figure 6-3: View categories dataset

6.2.1 View category value distribution

The dataset's view values are expressed as a proportion of the entire view and represent the amount a particular object category occupies in the spherical field of view. A 4π steradian image is a 2-dimensional representation of a 3-dimensional sphere shaped like an oval or a circle. It captures the entirety of the sphere, allowing the observer to see in all directions, from front to back and from up to down. Steradian is the internationally recognised unit for measuring solid angles, and a sphere contains 4π Steradians.

Within the dataset, the view values are normalised. The view results in Steradian are divided by 4π, indicating a proportion of the total view. Figure 6-4 shows the distribution of the different view categories in a proportion of the full view. The view to urban landscape category contains the highest view values, and the view to sky category contains the lowest outliers. The median value of the view of a natural landscape is the lowest.

According to the research of Brembilla et al. (2021) a layer is present in a view if a certain Steradian threshold is reached. For example, if the threshold of 0.06 sr would be used to determine whether a layer is present or not, it corresponds to 0.477% of the total view. For the sake of this research, a threshold of 0.477% is used to determine whether or not a view layer is present for the subsequent parts of this research.

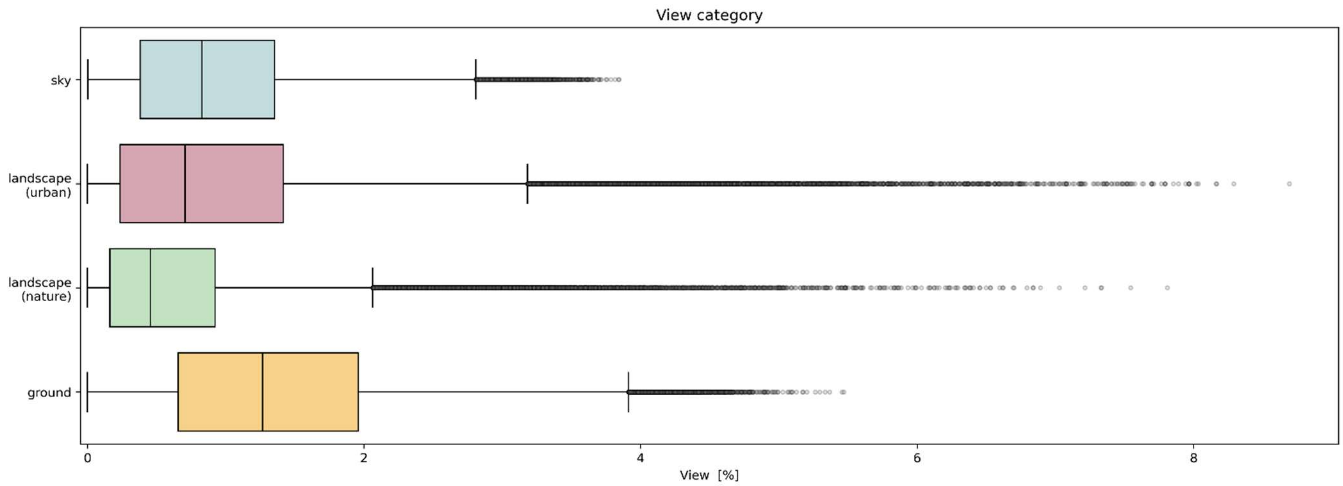

Figure 6-4: Distribution view per category

6.3 Labels

Labels represent the target variables that a machine learning model seeks to predict. For this research, three daylight labels and two view labels are selected. For the daylight labels, the 21st of March, June and December are chosen at 12:00, see Figure 6-5. For the daylight labels, the median value is chosen because the EN17037 guideline measures the target illuminance against 50% of the space.

For the view labels, view to ground and view to sky are chosen, see Figure 6-6. View to sky indicates an unobstructed visibility of the sky from within a space. For the view labels, the p80 (80th percentile) value is chosen because the EN17037 guideline measures the presence of a view layer against 75% of a space.

By selecting the median value for daylight and the p80 value for view, in the broader framework, the predicted daylight and view values can be tested against the EN17037 guideline to quantify the visual comfort quality of the space.

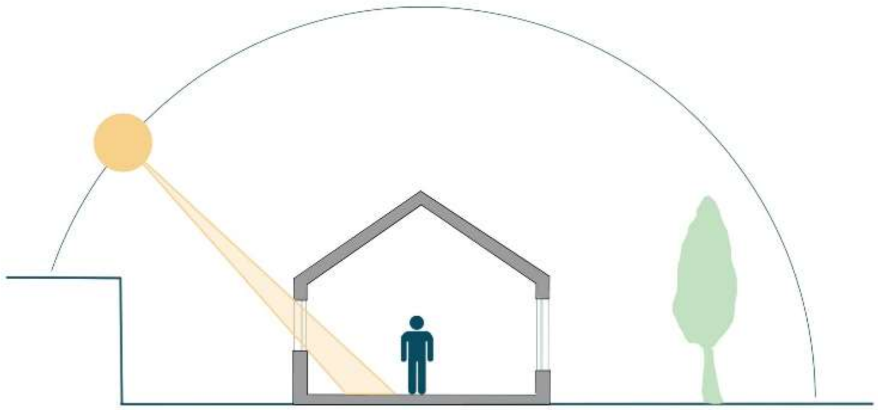

Figure 6-5: Label 1-3, daylight 21st of March, June, and December at 12:00 (Source: author)

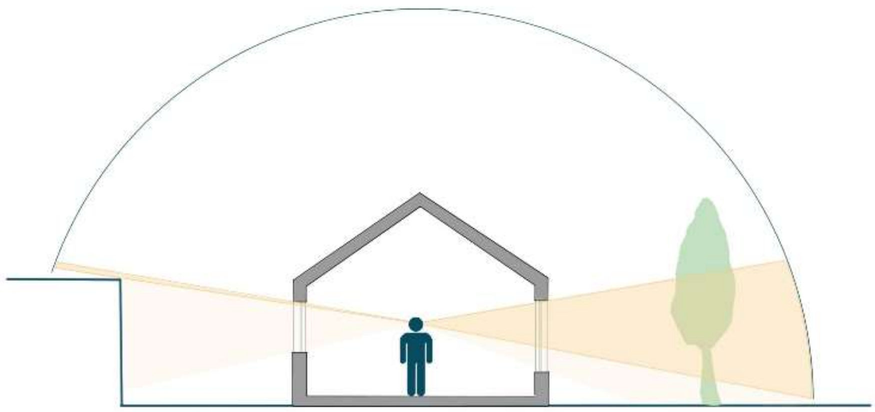

Figure 6-6: Labels 4 & 5, view to ground and view to sky (Source: author)

6.4 Features

To capture the essential aspects influencing the two labels ‘daylight’ and ‘view to the sky’ a feature study has been conducted. The features for this study consist of one image feature along with numerical features. An image feature is proposed, which contains six features embedded in the image with room characteristics.

Additionally, potential numerical features are discovered that contain essential information influencing the labels that cannot be shown on the image. A detailed examination of each feature’s relationship with the two labels and their correlation is provided. Based on the feature importance and the provided analysis, the numerical features will be selected.

Context visualization

For each apartment, an image is created for each of the living spaces within the apartment, see Figure 6-7. Each image consists of six embedded features the image contains, which are the room depth ratio, room area, room orientation, window distribution, and site and environmental obstructions, see Figure 6-8

The area of the room is highlighted in yellow on the image. A boundary box of 15x15 meters is created from the centre of the room. The full context around the room that falls within the 15-meter bounding box is given in the image. In the images, the rest of the floor that falls within the boundary box is added in light grey to give an understanding of the obstructions from the building itself. The balconies or loggias on the floor are highlighted in grey since these geometries only partly block lighting. Additionally, the floors in the building that are higher than the current floor of the apartment are added in a darker grey to give an understanding of overhangs.

Since there is no information in the dataset about the actual environmental obstructions, a circle is used to express the presence of the view landscape layer. The circle's radius depends on how much of the landscape layer is present in the room. The environmental circle is divided into two parts: a green part to express how much of the total view of landscape consists of nature and a pink part to express how much of the view is urban view. A threshold of 0.477% is used to determine if the landscape layer is present. The threshold of 0.477% corresponds with one of the view thresholds in the earlier mentioned studies. The circle only appears on the image if this threshold is reached.

Figure 6-7: Examples of image feature

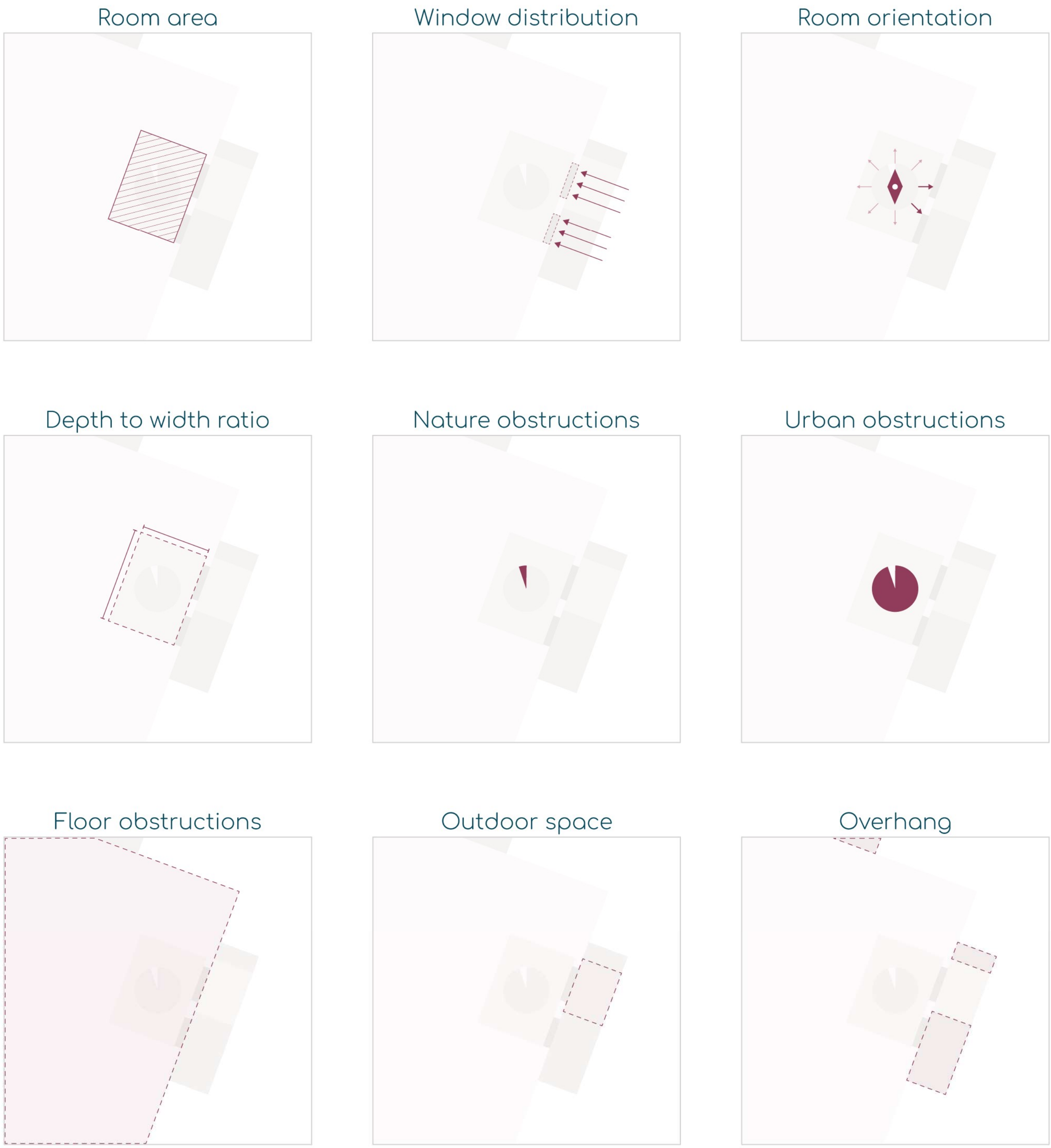

Figure 6-8: Overview hidden image features

Room area

The image feature shows information about the area of each room. The room area shows a slightly weak correlation between the daylight and view-to-sky availability. Figure 6-9 and Figure 6-10 show a subtle negative trend when the room area exceeds 20m^2, above this threshold a slight decrease in both the daylight and view to sky availability occurs when the room area increases. However, it is important to note that the size of the room must be considered in combination with the total window area of a room. A larger room may provide more access to the window area. However, the room could also have a higher room depth ratio, negatively affecting the total illumination and access to sky views. Thus, examining the window-to-floor ratio over the room area is more valuable. Most rooms fall within a room area range of 0 to 20m^2 and outliers can be found above a room area of 40 m^2.

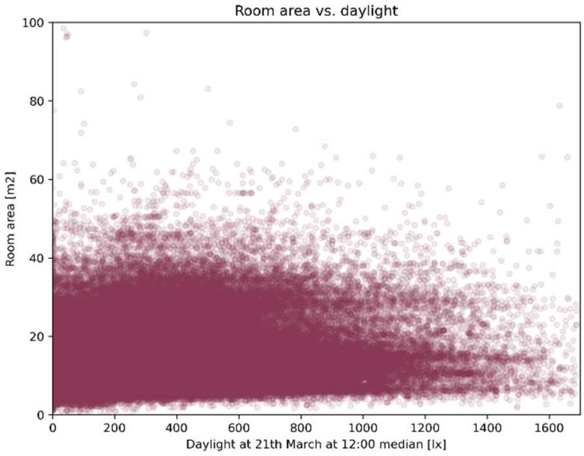

Figure 6-9: Room area vs daylight

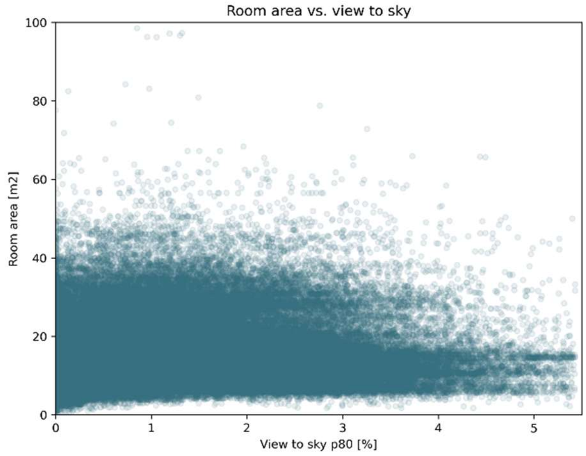

Figure 6-10: Room area vs view to sky

Room width to depth ratio

From the image a general understanding can be found about the relation between the room width and room depth. The width-to-depth ratio of a room impacts the availability of daylight and the view of the sky within a room. Figure 6-11 and Figure 6-12 show the relationship between the depth of a room and the availability of daylight and a view of the sky. Both plots show a clear trend: the daylight and view-to-sky values decrease as the room's depth increases. When the depth ratio surpasses three, a notable shift occurs, where the negative slope of the correlation becomes notably steeper compared to the slope for the depth ratio under three. As a result, when the room depth ratio exceeds three, the influence of the room's depth becomes much more evident. Most rooms have a room depth ratio between one and three.

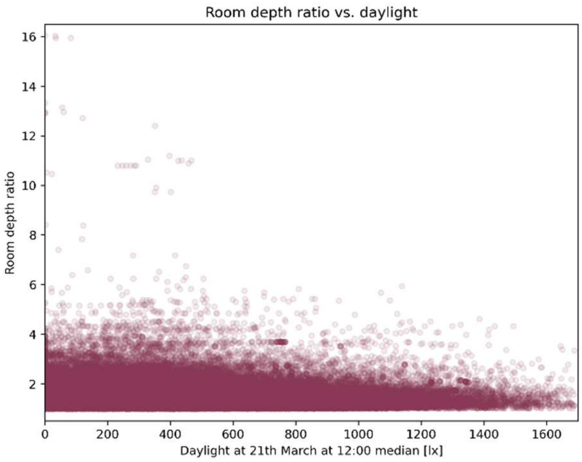

Figure 6-11: Room width to depth ratio vs daylight

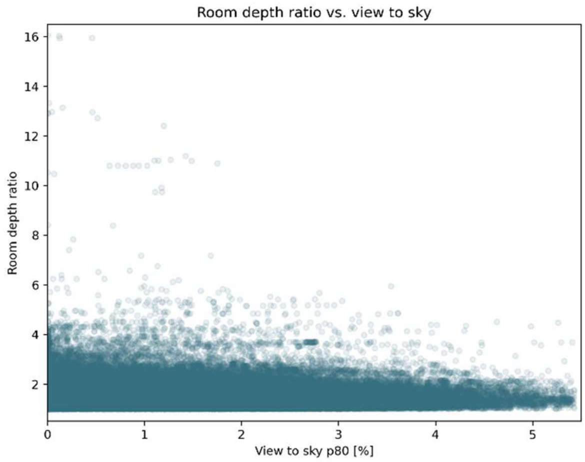

Figure 6-12: Room width to depth ratio vs view to sky

Window to floor ratio

The window-to-floor ratio in a space significantly impacts the availability of daylight and the view of the sky. Figure 6-13 and Figure 6-14 illustrates the relationship between the window-to-floor ratio and daylight and view-to-sky availability. A clear pattern emerges, showing that daylight and view availability improve as the window-to-floor ratio increases. On the other hand, a critical insight can be recognized by a definite hard end line at the bottom of the data points. This line emphasizes the need to preserve a minimum window-to-floor ratio to retain a certain amount of daylight and a view of the sky within a space. Looking at the data from the rooms with windows, the window-to-floorratio mostly ranges from zero to 0.5.

Rooms without any windows stand out in these scatterplots. Even though these rooms do not have any direct access to windows, they still have access to daylight and a sky view. Most of these rooms are areas within a room, for example, a kitchen area within a living room space. Even though those areas are not directly located at a window, the light still gets to that area. Rooms without windows do not reach high daylight and view-to-sky availability, corresponding with the hard-end line at the bottom data points. This can be explained by the fact that those areas often lay deeper into the building, and thus, daylight and view access is more challenging.

Since the image does not show the window area, the window-to-floor ratio can not be found in the image. Therefore, the window-to-floor ratio should be considered as a numerical feature of the machine learning model.

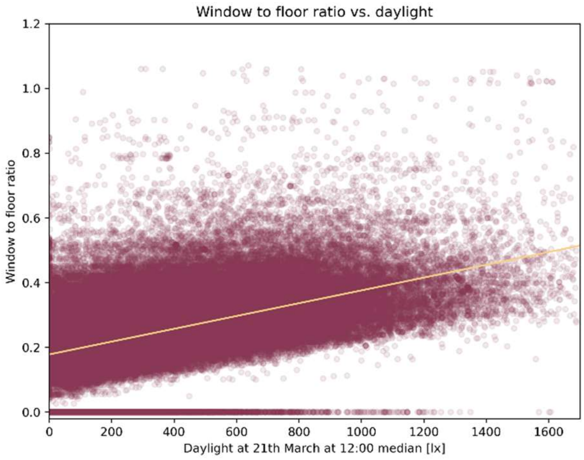

Figure 6-13: Window to floor ratio vs daylight

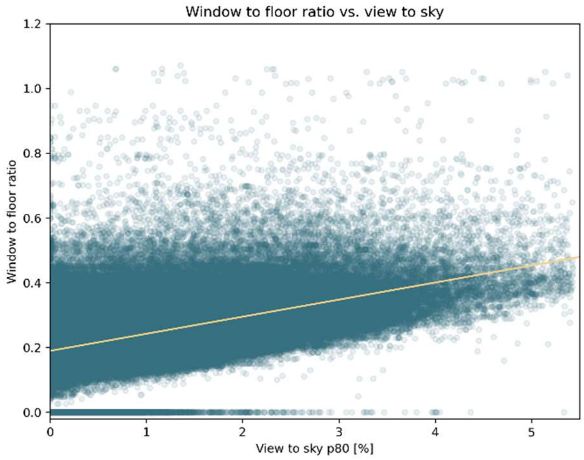

Figure 6-14: Window to floor ratio vs view to sky

Window distribution

In the image, the window distribution is showcased. Not only illustrates the image where the windows are placed on a horizontal plane, but also whether a room has windows that face one or more directions. The window distribution influences daylight and view. The window distribution influences daylight since it gives information about how light is distributed in the room and from which side light can enter the room. The window distribution influences view because it gives information about from how many directions obstacles could be in from of the window. When windows are spread over multiple sides, this could lead to having a big obstruction on one side of the room but not the other side of the room. Figure 6-15 and Figure 6-16 show the correlation between the number of walls with windows. The scatterplots do not show a high correlation based on the number of sides with windows in a room and the daylight and view-to-sky availability. Based on this analysis, the feature 'number walls with windows' is not a strong feature. Most of the rooms have one, two or three facades with windows.

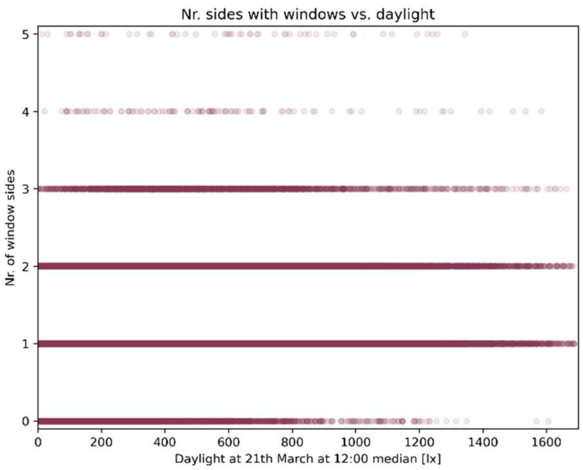

Figure 6-15: Window distribution vs daylight

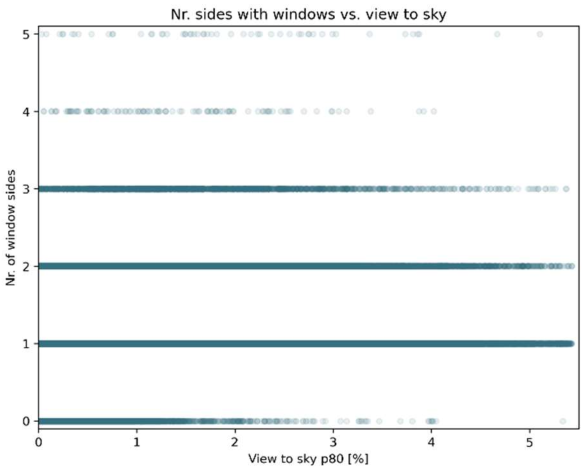

Figure 6-16: Window distribution vs view to sky

Room orientation

One embedded feature of the image is the orientation of the room. In the image, North is always facing upwards. The orientation influences daylight since the sun moves from East to West during the day on the Northern Hemisphere. This can also be seen in Figure 6-17, which showcases the daylight values of rooms with windows on one side of the room for different orientations on the 21st of March, the 21st of June and the 21st of December at 12:00. As expected, the lowest daylight values are found in rooms that face North, Northeast, West and Northwest for the sun position at 12:00.

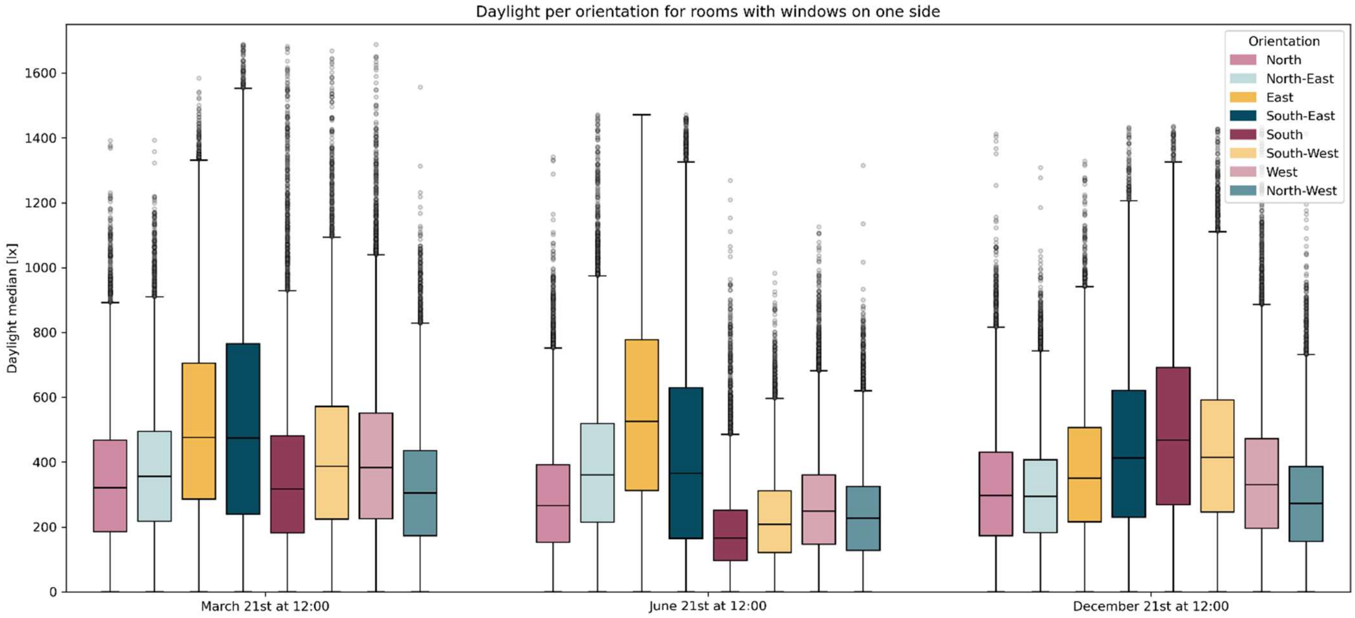

Figure 6-17: Daylight boxplot per orientation for one sided window rooms

The distribution of the windows across the different orientations can not easily be captured into one number and is, therefore, a strong image feature. However, in the image, the exact distribution of the windows can not be captured since the window area of each window can not be found in the image. Therefore, the main orientation of a room could be a possible numerical feature to go along side the image feature.

For each room, the main orientation is found, which is the orientation with the highest window area. Figure 6-18 and Figure 6-19 illustrate the relation between the main orientation of the room and the daylight and view-to-sky accessibility. The dataset shows a nice representation of all the different main directions. No clear relation between the main orientation of a room and the daylight and view-to-sky availability can be found.

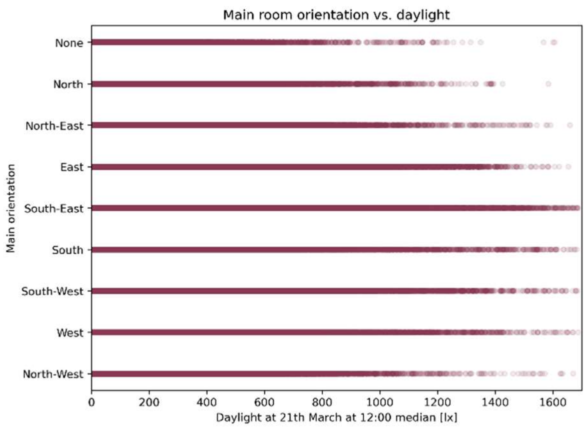

Figure 6-18: Main room orientation vs daylight

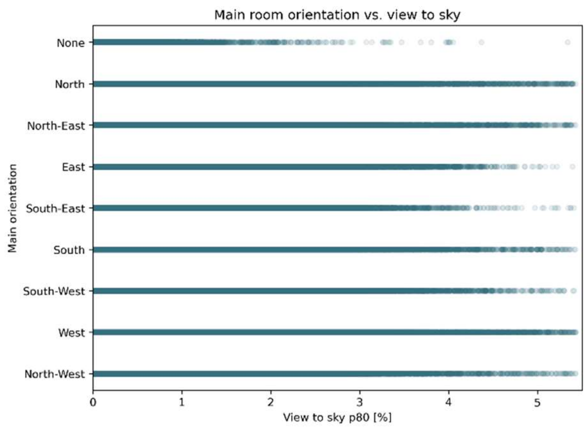

Figure 6-19: Main room orientation vs view to sky

Environmental obstructions

In the image, a circle is placed in the middle of the room to express the obstructions by nature or urban context. This is done because the view to landscape layer impacts how much light enters a room and how much of a view is blocked. However, within the dataset, the environment of a building is not given as geometries because of the privacy of the building's residences. When looking at the relation between view-to-nature and view-to-urban, the two categories of the landscape layer, a trade-off between the two views is observed. As one of the two landscape views increases, the other landscape view becomes more prominent, see Figure 6-23. The relation between view to landscape and the daylight and view to ground and sky availability does not show a strong correlation, see Figure 6-20, Figure 6-21 and Figure 6-22. However, it is important to mention that considering the surrounding environment and its obstructions is essential when analysing the daylight and view-to-sky availability.

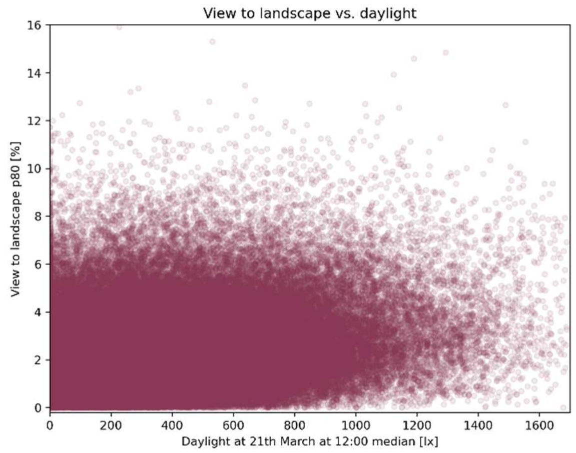

Figure 6-20: View to landscape ratio vs daylight

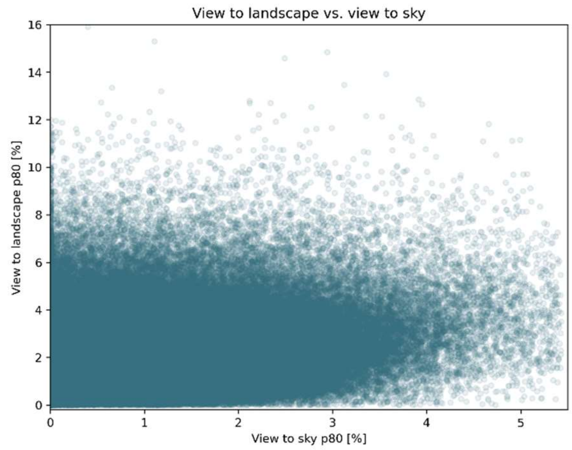

Figure 6-21: View to landscape vs view to sky

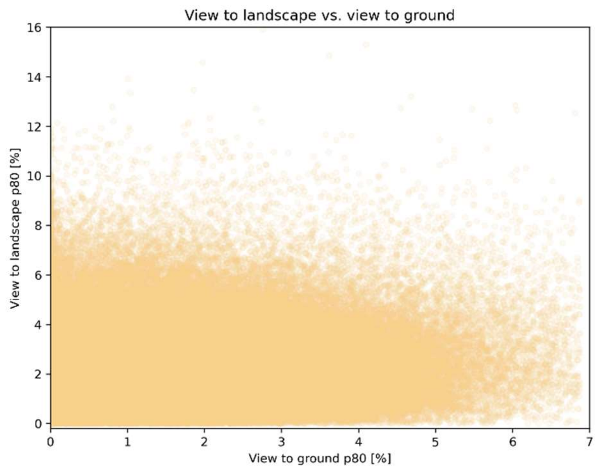

Figure 6-22: View to landscape vs view to ground

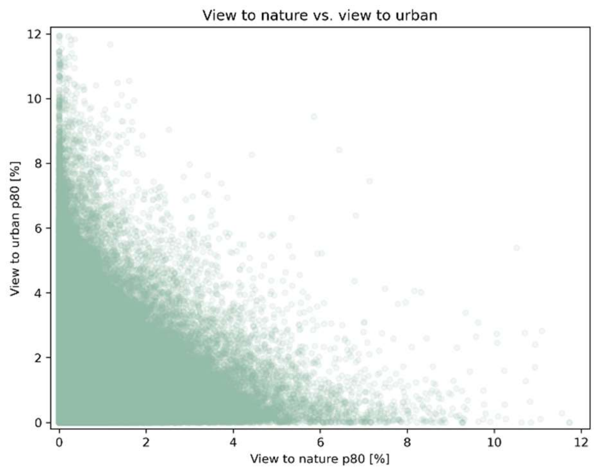

Figure 6-23: View to nature vs. view to urban

Site obstruction

In the image, three categories of site obstructions are shown, namely, outside areas, building geometries on the same floor, and building geometries on higher-placed floors. Outdoor spaces include balconies, loggias, winter gardens and terraces. A noticeable tendency emerges when looking at the scatterplots: a negative correlation, Figure 6-24. As the view-to-site value increases, the availability of daylight and view-to-sky inside the rooms decreases. Most rooms contain view-to-site values between 96% and 100%.

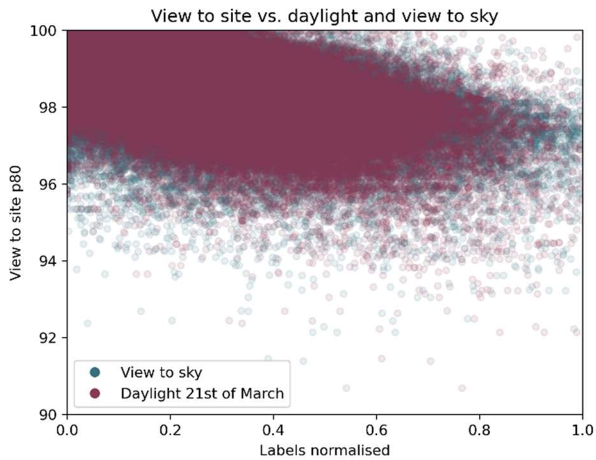

Figure 6-24: site obstruction vs. daylight and view to sky

Elevation / floor height

Another essential feature which is not shown in the image feature is the elevation of a room. Figure 6-25 and Figure 6-26 show the relationship between elevation and the availability of daylight and view-to-sky within a space. The scatterplots show a weak positive correlation between elevation and daylight and view-to-sky availability. The elevation ranges from -10 to 60 meters, with the largest number of rooms being between 0 and 20 meters above ground level. Notably, trends appear in the data, with rooms positioned below ground level and above 40 meters above ground level, indicating lower values for both daylight and view the lower or higher the rooms are located. Additionally, two comparisons are made between view to ground and view to landscape with elevation. Figure 6-27 shows an as expected negative correlation between view to ground and the elevation of a room. Figure 6-28 shows an as expected positive correlation between view to landscape and the elevation of a room.

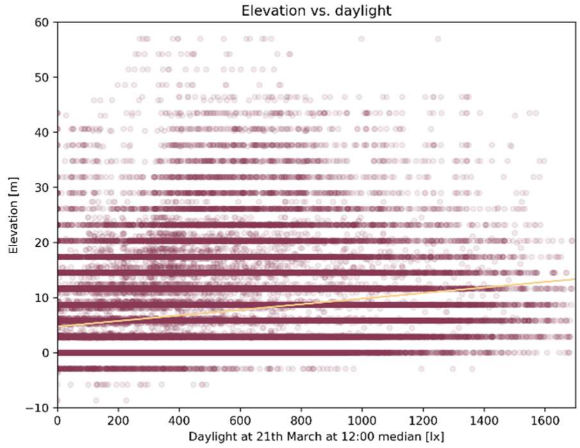

Figure 6-25: Elevation ratio vs daylight

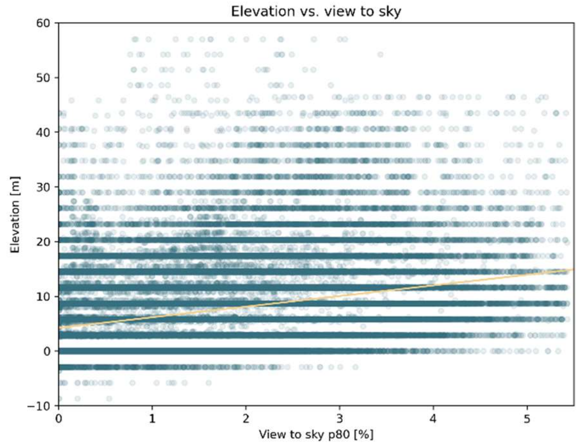

Figure 6-26: Elevation ratio vs view to sky

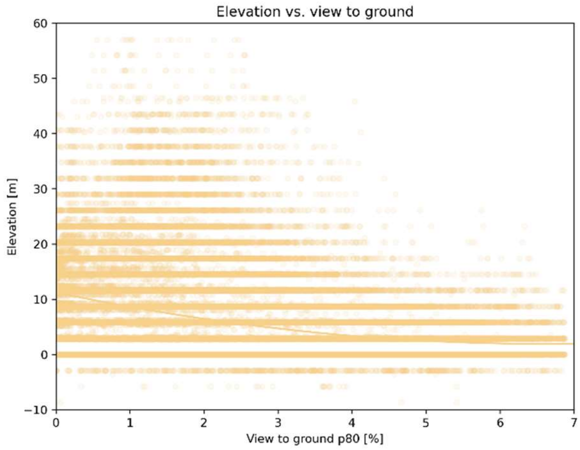

Figure 6-27: Elevation ratio vs view to ground

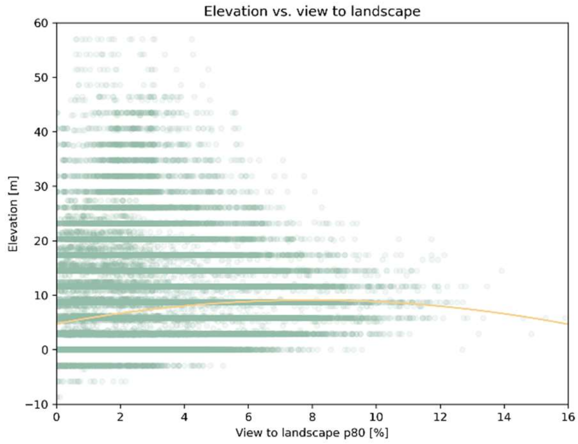

Figure 6-28: Elevation ratio vs view to landscape

Room height

Lastly, the image also does not show the height of a room. However, the height of a room influences the daylight and view-to-sky availability and thus should be considered. Figure 6-29 shows the relationship between the height of a room and the values of the two labels, showing a weak positive correlation. However, it is essential to note that not enough data points are located above 2.8 meters, which limits the ability to draw conclusions for this part of the graph. The dataset has a quite narrow height range, with most of the rooms having a room height ranging between 2.4 and 2.6 meters.

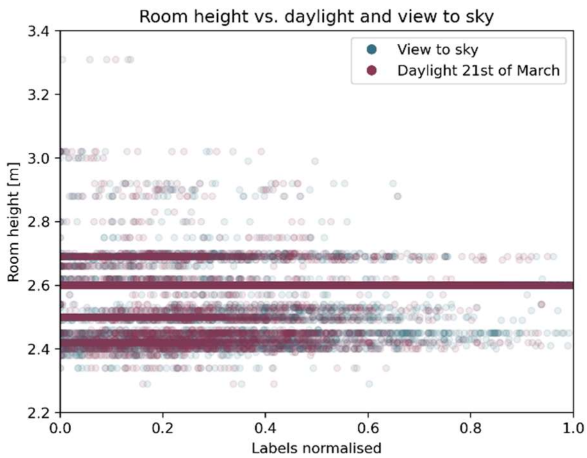

Figure 6-29: Room height vs. daylight and view to sky

6.4.1 Feature distribution

The distribution and importance of features play a crucial role in the performance of machine learning (ML) models. For a feature to be considered strong, it must be well-represented throughout the dataset, with few or no outliers, to ensure consistency and pattern recognition. Any outliers present can significantly impact the performance of an ML since outliers do not fit in the patterns that an ML model learns from.

Figure 6-30 illustrates the distribution of the analysed features. Two outstanding features that show a bad representation throughout the dataset are the window distribution and the room height. These two features show that 95% of the data is represented as one value in the dataset, meaning it would be a weak feature. However, the window distribution is fairly simplified for analysis purposes and represents the number of facades that a room has windows on, which means that the current dataset mainly represents rooms with windows on one side. The window-to-floor ratio and the main orientation are well-represented values in the dataset and show the least outliers among the features. The elevation feature shows many outliers on the higher side of the normalised values, meaning that rooms located on the higher floors of high buildings are underrepresented.

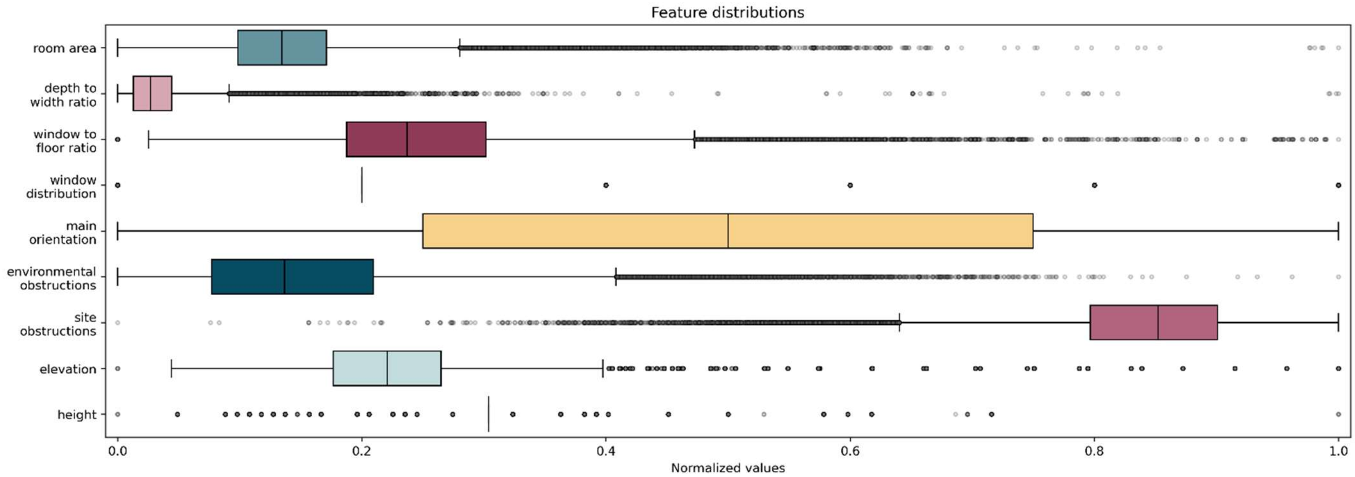

Figure 6-30: Feature distribution

6.4.2 Feature importance

The importance of different features is analysed concerning daylight and view performance, utilising Random Forest Regression to examine the relationship between the features and labels. Random Forest Regression identifies the features that have the greatest impact on the outcome of the labels. Before training the Random Forrest Regression, the features are normalised.

Figure 6-31 shows the feature importance of the discussed features on each of the five labels. As expected from the feature distribution, the room height and the window distribution do not have a high impact on the labels. The window distribution is shown on the image feature and says something about the dataset, it indicates that either more rooms with windows on multiple sides need to be added to the dataset or the dataset should be cleansed from the window distribution outliers to ensure better ML model performance. Additionally, based on the feature distribution and feature importance, room height is a weak numerical feature.

The feature site obstruction is illustrated on the feature image and shows the highest influence on the labels. The site obstruction mainly describes the relationship between the interior obstructions and the windows.

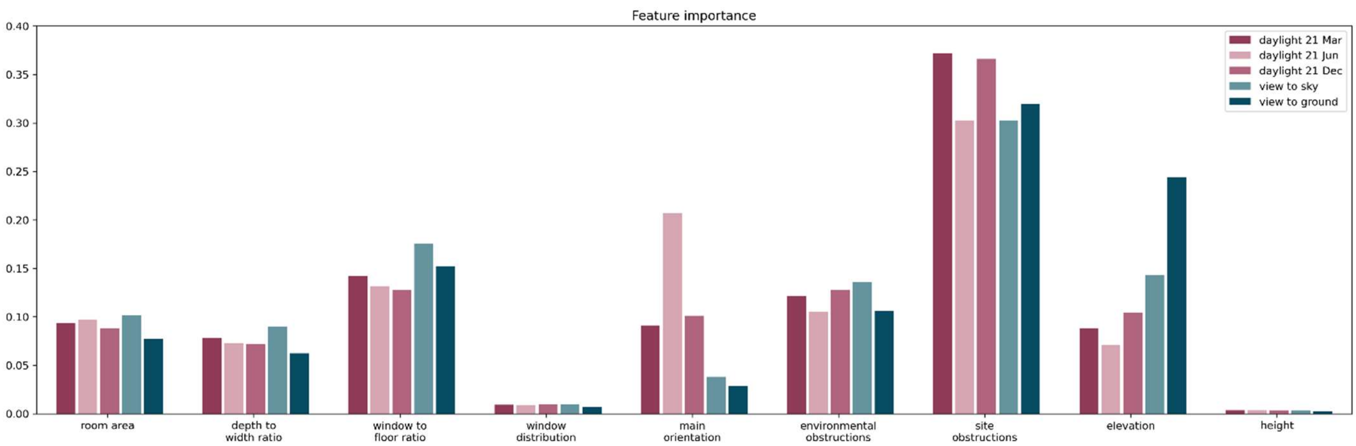

Figure 6-31: Feature importance

6.5 Visual comfort performance distribution

Based on the layout evaluation system proposed in Chapter 4.2, the visual comfort performance quality of each room and apartment within the dataset can be found. In the optimal situation, the dataset used for the training should have a good representation of all performance levels and labels. In this sub-chapter, for each room in the dataset, the visual comfort performance levels are found. Subsequently, for each apartment in the dataset, the performance label is found. This sub-chapter analyses the distribution of the performance levels and labels in the dataset.

6.5.1 Room performance levels

Figure 6-32 illustrates the distribution of the performance levels of each room over the dataset. The performance levels for daylight, view and orientation are found as described in Chapter 4.2. The daylight and orientation performance levels are well represented in the dataset. Note that the orientation performance level does not have an insufficient class. The view performance levels show a poor distribution over the performance level classes, as most rooms have a high view performance level. Note that the view performance class low does not exist.

Looking closer into the daylight performance levels in combination with the simulation verification, which is done in Chapter 5.3, one interesting observation can be made. From the simulation verification, it is known that the daylight illuminance values in the dataset are lower than expected when conducting the simulation based on the EN17037 requirements. Based on this, the same dataset would have a different and more skewed distribution if the daylight simulations had been conducted as per the guideline. The expected distribution would consist of fewer rooms with insufficient and minimum daylight levels and more rooms with a high daylight performance level.

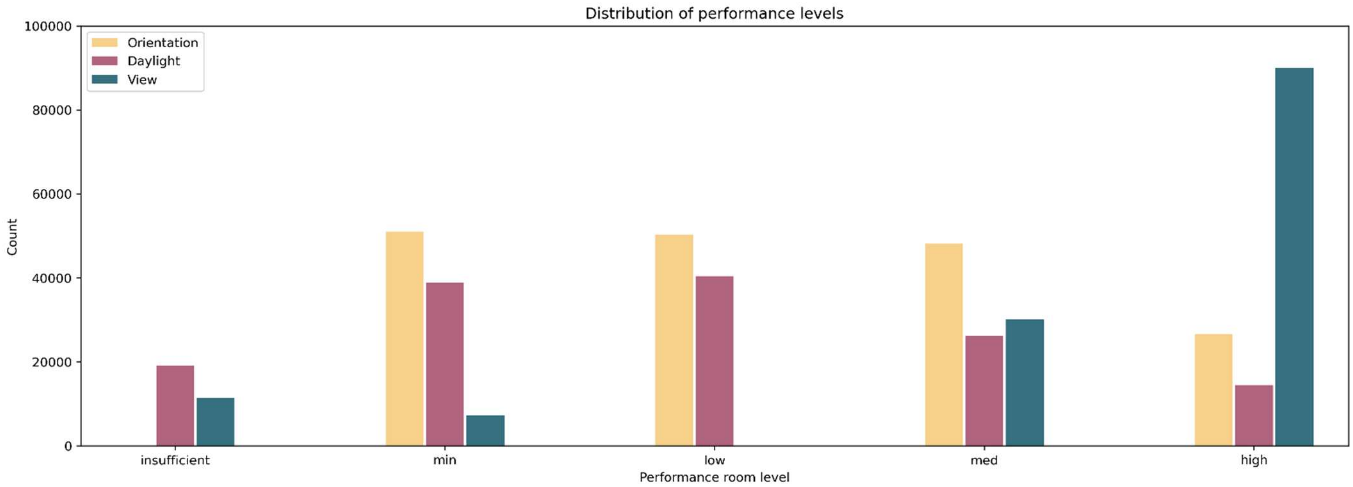

Figure 6-32: Room performance levels distribution

6.5.2 Performance levels relations

As shown in Figure 5-8, a clear relation between the view performance and daylight performance can be found. Where a higher sky view percentage results in a higher daylight illuminance value. Knowing this, it would be expected to see the same trend when comparing the daylight performance levels of rooms with the view performance levels of rooms. Figure 6-33 shows the relation n between the daylight performance level and the view performance level of each room. One interesting observation that can be made is that the majority of the rooms have a high view performance level but a low daylight performance level, which can be explained by the fact that the view level distribution is skewed towards the higher performance level. Knowing this, it is surprising to observe that quite some rooms with an insufficient view level still achieve medium and high daylight performance levels.

As known, the orientation of a room influences the sunlight availability of a space and, therefore, the daylight performance level of a room. Figure 6-34 shows the relation between the daylight performance level and the orientation performance level of a room. However, the orientation level of a room is based on the room type and the optimal placement, which indirectly says something about the relation between room usage and the optimal lighting conditions of a room. So, it is quite interesting to see a positive relation between the two performance levels.

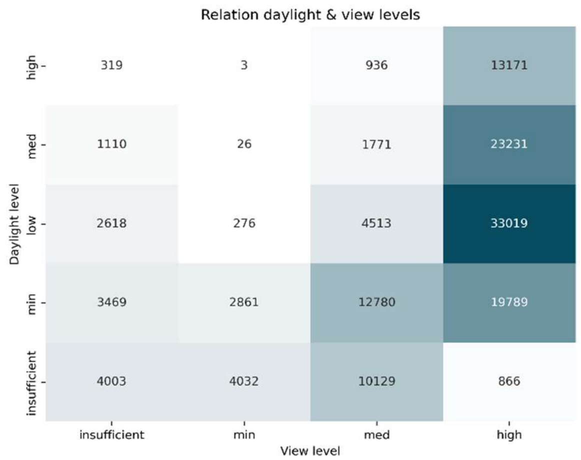

Figure 6-33: Daylight & view performance level relationship

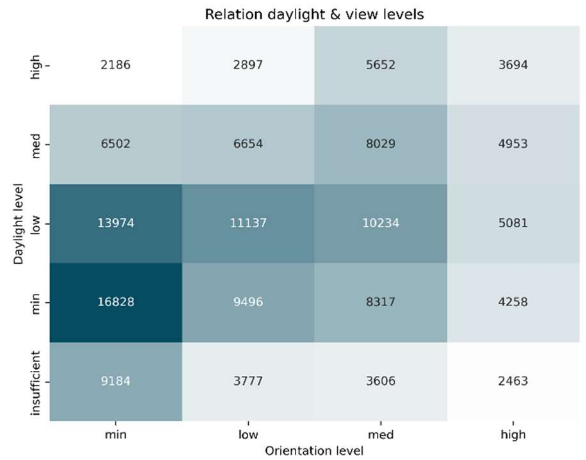

Figure 6-34: Daylight & orientation performance level relationship

6.5.3 Apartment performance labels

The distribution of the apartment performance labels is illustrated in Figure 6-35. While the room performance levels for daylight and orientation showed a good distribution, the apartment labels for daylight and orientation are skewed towards the lower side of the labels. Knowing that the daylight values in the dataset are most probably lower than they should be, more apartments than needed score an insufficient label F. On the other hand, the view performance labels of the apartments show a good representation of the labels. Note that for view and orientation, there is no performance label F.

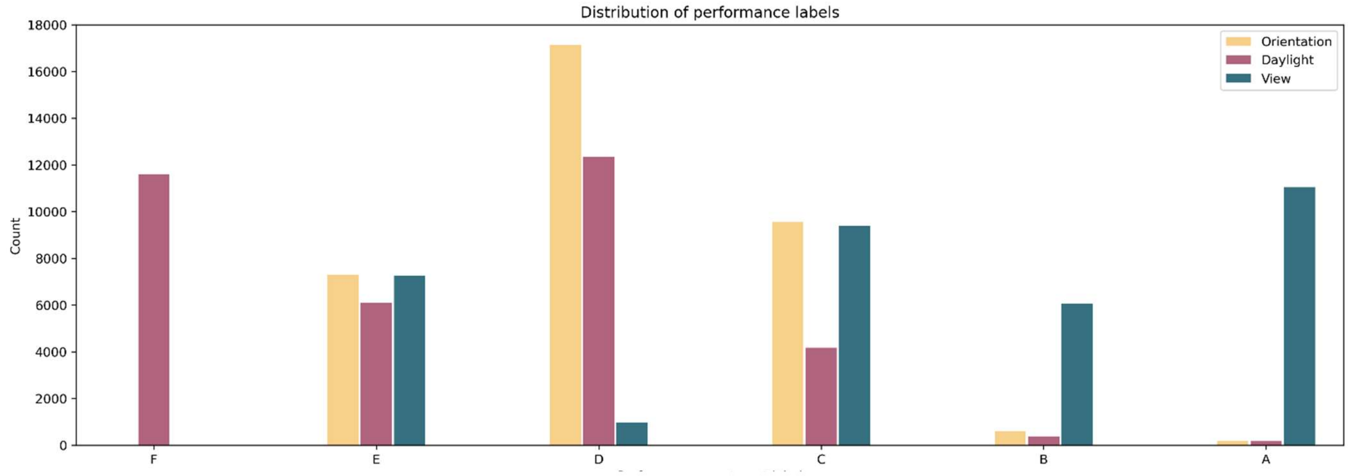

Figure 6-35: Performance labels distribution

6.5.4 Overall apartment performance labels

To fully understand the overall visual comfort quality of an apartment, a label system is proposed in Chapter 4.2.4. Based on this evaluation system, an overall performance label of each apartment in the dataset is found. Figure 6-36 shows the distribution of the overall visual comfort apartment performance labels in the dataset.

One first observation is that the overall performance label F is overrepresented in the dataset. Note that this label is given based on the penalty score. Thus, all these apartments consist of at least one room that has insufficient daylight or view quality and does not reach the minimal EN17037 requirements. The distribution shows that the higher labels are underrepresented in this dataset.

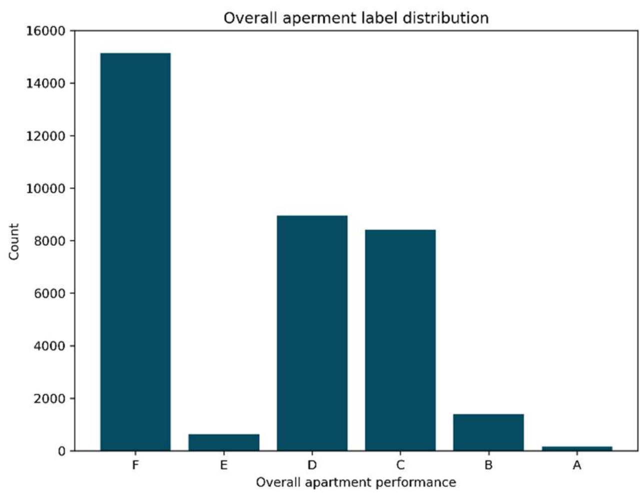

Figure 6-36: Performance labels distribution

6.6 Conclusion

For the ML model, five labels are selected, consisting of 3 daylight labels and two view labels. For the daylight labels the median value of the room is selected, and for the view labels the p80 value of the room is selected, which is in accordance with values used in the EN17037 guideline to test a room across requirements. For the features of the ML model, one image is proposed along with numerical features. The image feature represents one room in the dataset and contains embedded features with information about the room size and orientation, window distribution and environmental and site obstructions. The feature distribution and feature importance, in combination with the feature analysis, reveal that the elevation and window-to-floor ratio show the most significant relation with the labels. Therefore, the additional numerical features of the ML model will be elevation and window-to-floor ratio. Figure 6-37 illustrates the relation between the selected features and the embedded features in the image feature with the labels.

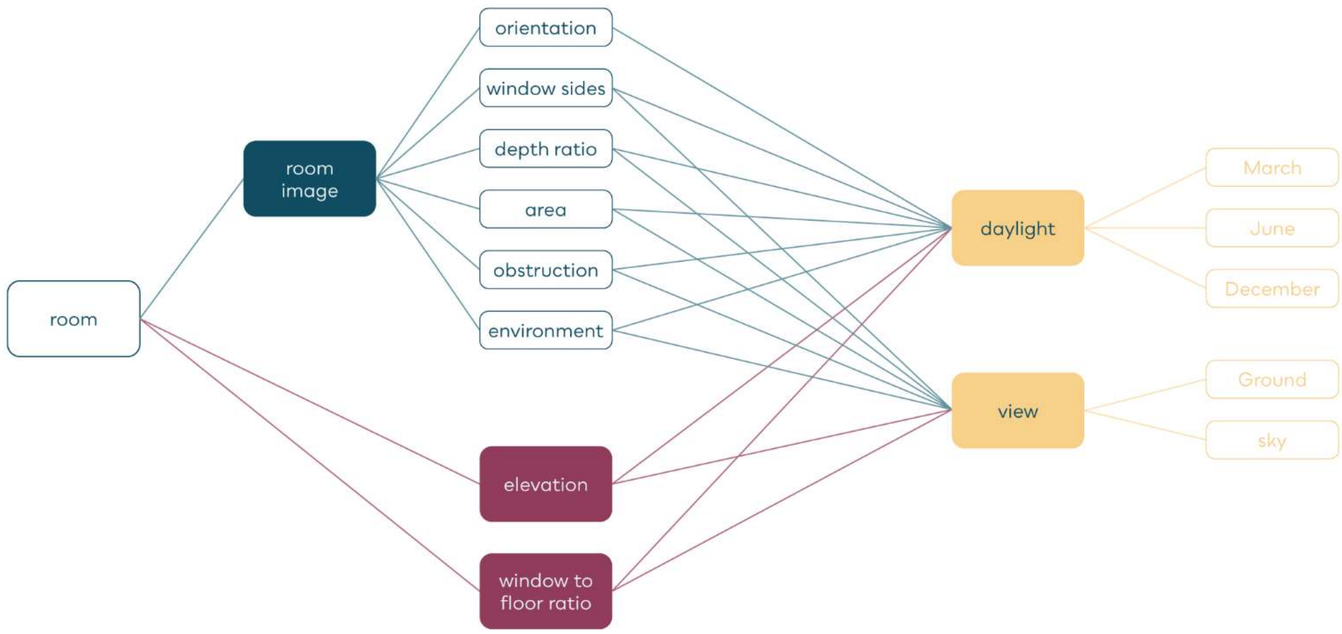

Figure 6-37: Overview features in relation to labels

~ empty page ~

7 ML MODEL PERFORMANCE

This chapter is divided into different sections, each essential for evaluating the machine learning model's performance for the given task. Firstly, the used dataset split is presented. Then, a baseline model is created, which makes predictions with only the image feature. Subsequently, the proposed ML model set-up is discussed, and this model is trained three times while changing the ResNet from pre-trained to not pre-trained.

Based on the baseline model and the findings during the first three ML model trainings, ablation studies are executed. From the ablation studies, the best ML model architecture and hyperparameters are selected as the final model. The last section concludes with a more in-depth evaluation of the best-performing model set-up, providing a broader perspective on the model's strengths and limitations.

7.1 Data splitting

For the training of the model, in total, fifty-five thousand rooms from almost fourteen thousand apartments are used, which is roughly 40% of the full dataset, see Table 17. To ensure that the full potential of the dataset is used within 40% of data usage, a randomiser is used to select the apartments for the training dataset. The randomiser ensured that all sites within the dataset were represented and that outliers of the dataset were selected. For the evaluation of the model, an additional prediction dataset is created with thirty tree sites consisting of standard apartment layouts and uncommon geometries. The prediction sites are excluded from the training dataset to ensure that the model has not seen the exact same apartment type during the training.

Table 17: Insights of total, training and prediction dataset

Dataset characteristics	*Total dataset*	*Training dataset*	*Predictions dataset*
Sites	1,287	1,254	33
Buildings	2,551	2,522	75
Apartments	34,757	13,905	538
Rooms	138,922	55,632	2,321

The features and labels are normalised based on the total cleaned dataset. Figure 7-1 shows how the features and labels are distributed within the total dataset. From the label distribution, we can conclude that the 40% of the total dataset data is a good representation of the total dataset. The training dataset is split into three parts: the training set, the validation set that is used during the training and the test set that is used to evaluate the trained model. From the training dataset, 80% of the data is used for the training, including the training and validation set, and 20% is used for the testing. This split of the dataset is used to train all the following models.

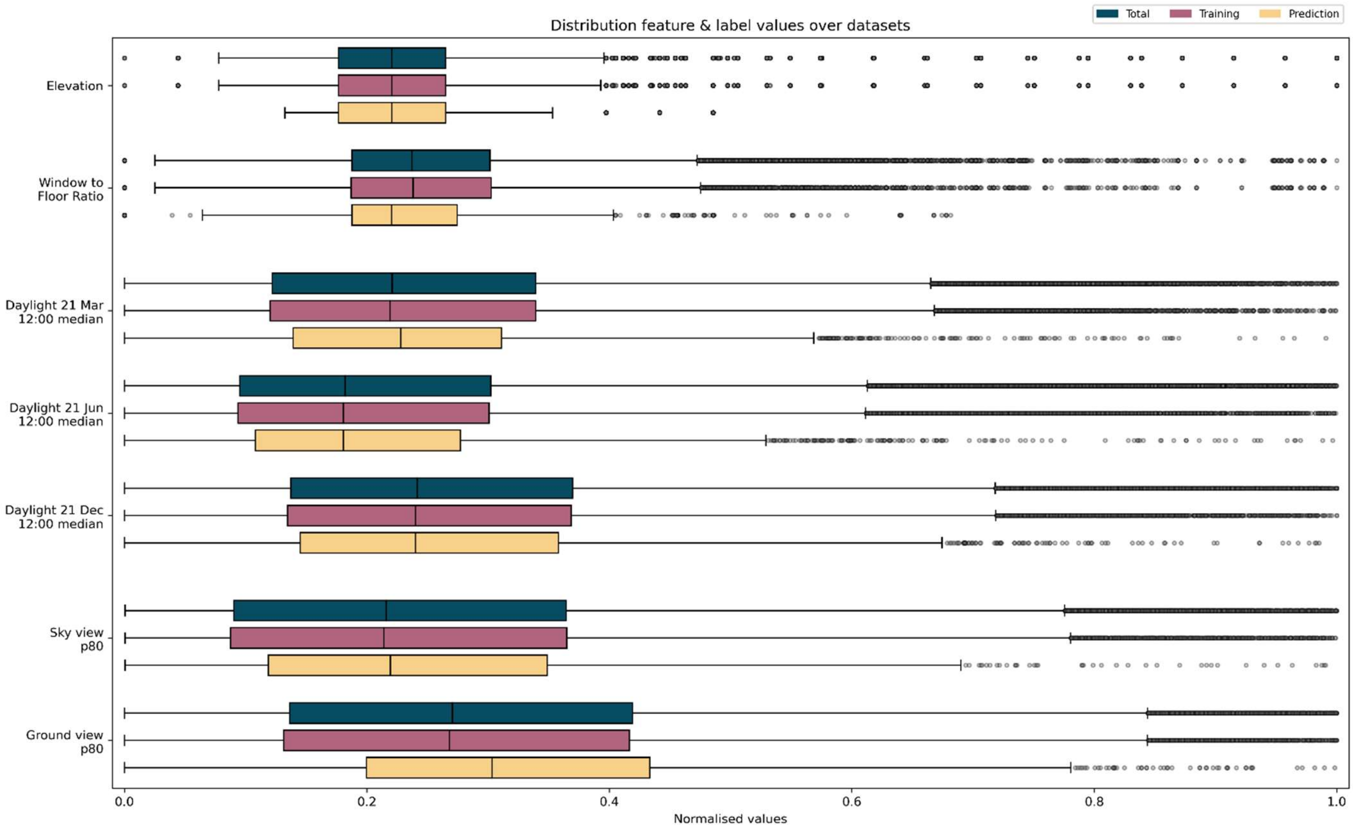

Figure 7-1: Training set distribution of features and labels

7.2 Model 0 – baseline

As per Chapter 3.5 a multimodal ML model would outperform a CNN model. To test whether or not a multimodal approach is suited for the problem at hand, first, a baseline model is created. In this case, the baseline model consists of ResNet50 model with the image feature as input, see Figure 7-2. After the image feature goes through the RestNet50, batch normalisation, leaky ReLu and global average pooling are applied before a fully connected network. Appendix E describes the detailed architecture of the baseline model and the training settings.

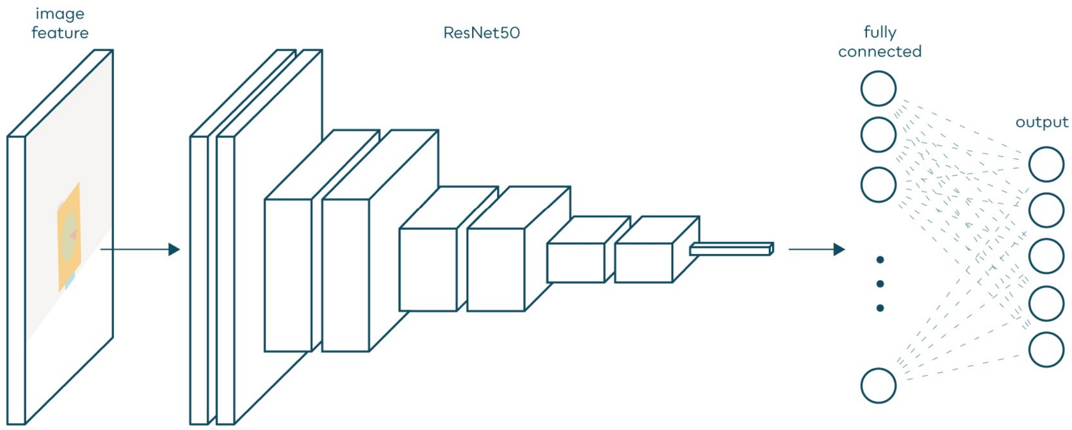

Figure 7-2: Overview baseline model architecture

The baseline model forms the foundation for comparing the performance of all the further trained models. The ResNet50 does not use any pre-trained weights, and all layers of the ResNet50 model are trainable. During training, early stopping of ten epochs is used to prevent overtraining and the learning rate was set at 0.0001. The training of the model is stopped early at epoch 20. The results of training the baseline model are illustrated in Figure 7-3.

The following findings can be found in the training results of the model:

- During the initial training (epoch 1-5), the training and validation loss significantly reduced, indicating that the model learns quickly and adapts to the training data. The training and validation MAE consistently decreases, indicating the improvement of the model's accuracy.
- A steady training progress can be recognised after epoch 5 when the training loss and MAE continue to decrease over time.
- There are fluctuations in the validation loss after epoch 8, which continues until the end of the training.
- After epoch 10, no improvements were made in the validation loss within the subsequent ten epochs, and the training was terminated at epoch 20. The 20th epoch has the following metrics: a training loss of 0.0101, a validation loss of 0.0251, a training MAE of 0.0742 and a validation MAE of 0.1138.
- In the test evaluation, the model achieved a test loss of 0.0226 and a test MAE of 0.1138.

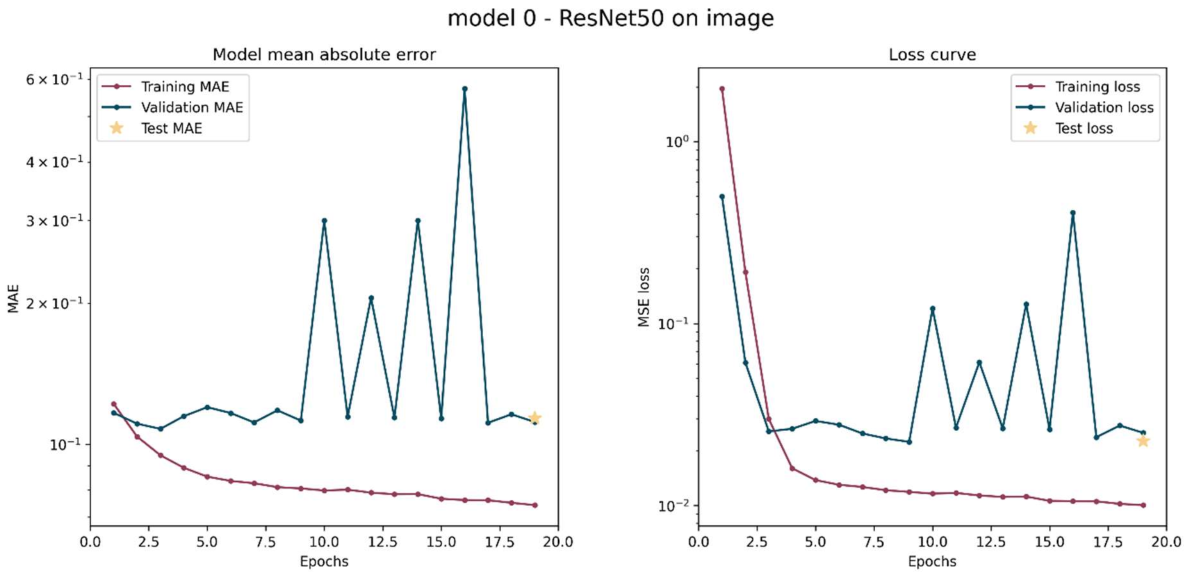

Figure 7-3: Model 0 training results

7.3 Pre-trained ImageNet model training

The fundamental part of the ML model set-up is using the ResNet50 architecture, which is well-known for its depth and efficiency in image classification tasks. For this part, three models are trained, all using the same architecture but differ in the base ResNet50 model. The first two models are built using a transfer learning approach using the pre-trained weights of a ResNet50 model. Transfer learning is an ML approach which involves building a new ML model on top of a prior ML model (Bhavsar, 2019). Transfer learning transfers knowledge gained by an ML model while learning one task to another model to learn a task. In this case, the pre-trained model of He et al. (2015) for image recognition is used.

The first model remains untrainable, keeping the knowledge embodied in its pre-trained weights. The second model allows for further fine-tuning to fit the purpose of the task at hand. The third model's strategy departs from the transfer learning approach. The third model contains an untrained ResNet50 architecture, staying free of any prior information. Comparing the results of these three separate models provides insight into the influence of a pre-trained ImageNet model for the task at hand.

7.3.1 ML model architecture

Figure 7-4 shows the main architecture parameters used in all the three models. A more detailed overview of the model's architecture can be found in Appendix E. The only difference between the first and the second models is the de-freezing of the layers to make them trainable. A standard image size of 224x224 pixels is used, which was also used in the earlier-mentioned study. After the image feature maps are extracted from the ResNet, a first completely connected layer is added to converge the spatial information into a one-dimensional feature vector. After the first fully connected layer, the numerical features are concatenated with the feature extracted from the first fully connected layer. The concatenated layer is put through batch normalisation and a leaky ReLu. Subsequently, a second fully connected layer is added. The final output layer is a dense layer with five output units and a linear activation function. The Adam optimiser with a mean squared error (MSE) loss function and a mean absolute error (MAE) metric is used to construct the model. During training, early stopping of 25 epochs is used to prevent overtraining. All three models could train for a maximum of 200 epochs with a batch size of 64. The learning rate is set at 0.001.

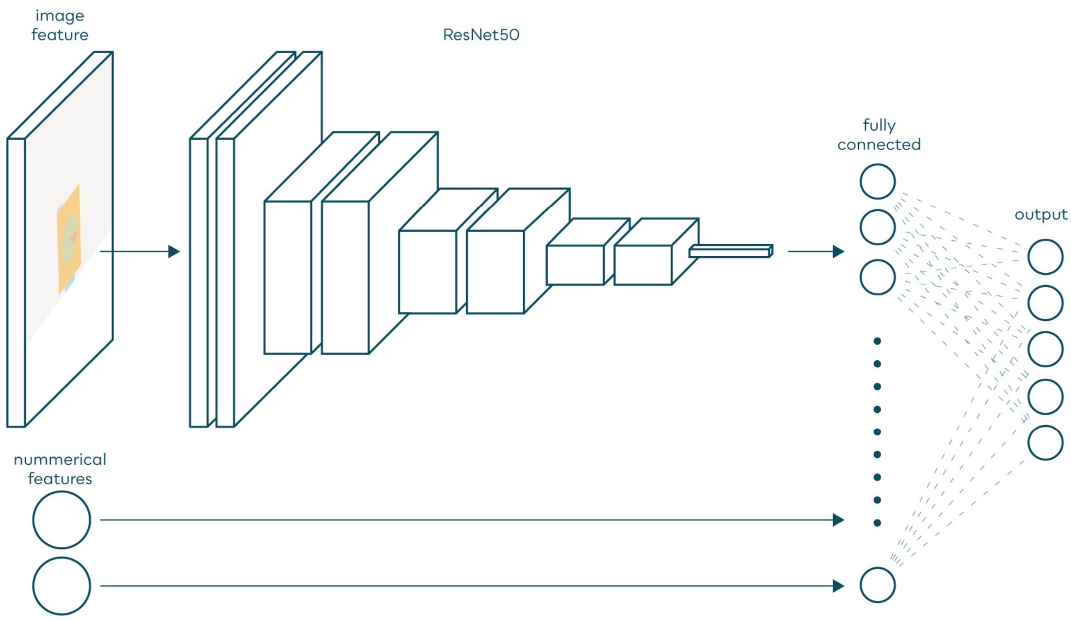

Figure 7-4: Overview ML architecture of models 1, 2 & 3

7.3.2 Model 1 – baseline ImageNet

The first model for the training is the baseline ImageNet model. The model uses a ResNet50 model that is pre-trained on ImageNet. The layers of this model are frozen, which means that the layers' weights will not be updated during the training. The training of the model is stopped early at epoch 188. Figure 7-5 shows the results of the first model training.

The following findings can be found in the training of the model:

- During the initial training (epoch 1-10), the training and validation loss significantly reduced, indicating that the model learns quickly and adapts to the training data. The training and validation MAE consistently decreases, indicating the improvement of the model's accuracy.
- A steady training progress can be recognised after epoch 10 when the training loss and MAE decrease consistently. The model stabilises after epoch 25 concerning the training loss and MAE.
- There are fluctuations in the validation MAE, which continues until the end of the training.
- After epoch 163, no improvements were made in the validation loss within the next 25 epoch and the training was terminated at epoch 188. The 188th epoch has the following metrics: a training loss of 0.0136, a validation loss of 0.0127, a training MAE of 0.0833 and a validation MAE of 0.0794.
- In the test evaluation, the model achieved a test loss of 0.0124 and a test MAE of 0.0793.

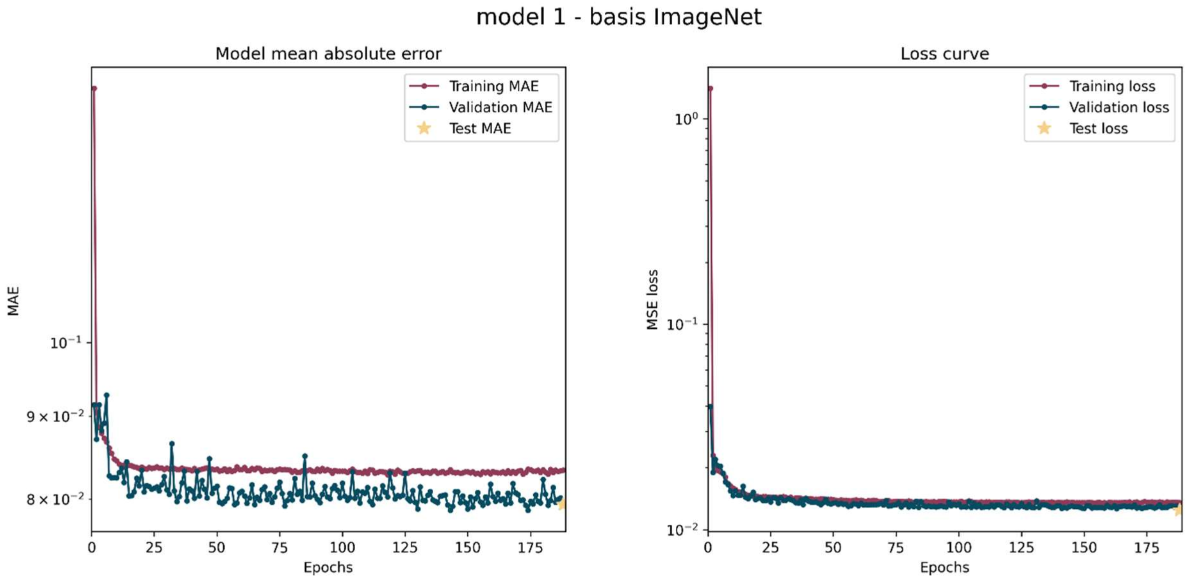

Figure 7-5: Model 1 training results

7.3.3 Model 2 – trainable layers

The second model for the training is the trainable model pre-trained with ImageNet. The model uses a ResNet50 model that is pre-trained on ImageNet. All the layers of this model are trainable, meaning that the layers' weights can be updated during the training. At epoch 158, the training of the modelled stopped. Figure 7-6 shows the results of the second model training.

The following findings can be found in the training of the model:

- During the initial training (epochs 1-6), the model starts with a relatively high training loss and MAE but quickly converges. The training and validation loss reduced significantly, indicating that the model learns quickly and adapts to the training data.
- The model stabilises and improves in terms of training loss and MAE during epochs 6-40. Signs of overfitting can be found from epoch 9 onwards. At this point, the training loss decreases steadily, while the validation loss increases.
- The validation loss and MAE fluctuated during the whole training, showing signs of overfitting. Significant fluctuation can be found in epochs 9 and 34 in the validation loss.
- After epoch 133, no improvements were made in the validation loss within the next 25 epoch and the training was terminated. The 158th epoch has the following metrics: a training loss of 0.0040, a validation loss of 0.0155, a training MAE of 0.0422 and a validation MAE of 0.0871.
- In the test evaluation, the model achieved a test loss of 0.0080 and a test MAE of 0.0612.

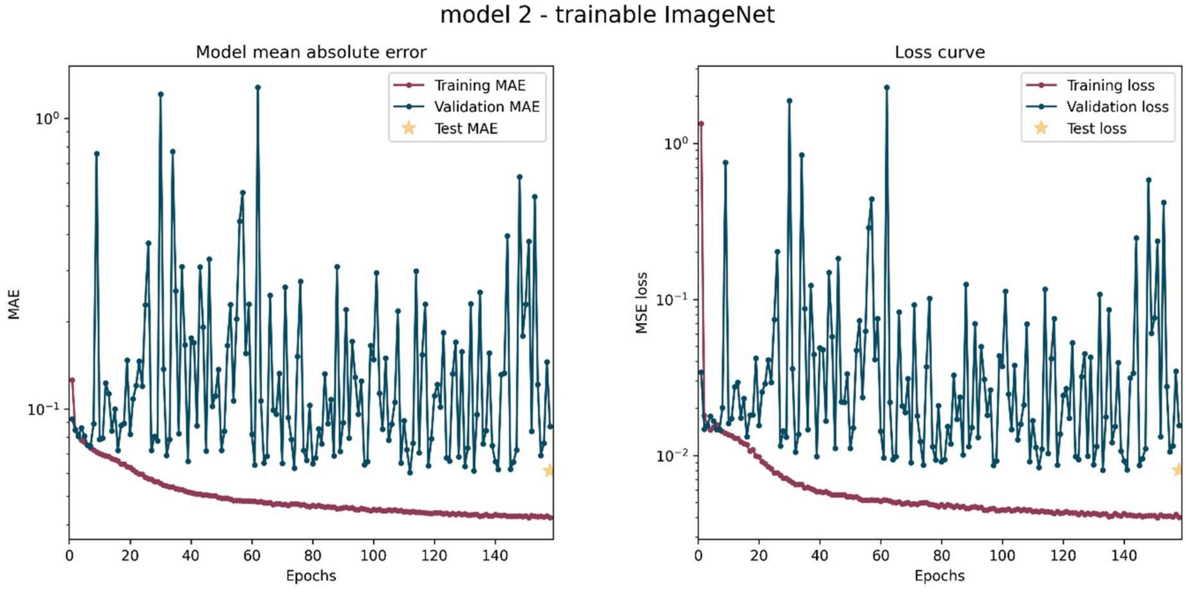

Figure 7-6: Model 2 training results

7.3.4 Model 3 – ResNet50 from scratch

The third model for the training is the proposed multimodal model without transfer learning. The model uses a ResNet50 without pre-trained weights, meaning the layers' weights will be defined during the training. The training of the model is stopped early at epoch 103. Figure 7-7 shows the results of the third model training.

The following findings can be found in the training of the model:

- During the initial training (epoch 1-14), the training loss and MSE significantly reduced and consistently decreased, indicating that the model learns quickly and adapts to the training data. The validation loss and MAE decrease substantially but show some fluctuations.
- The model stabilises and improves during epochs 14-60.
- The model training MAE stabilise after epoch 60 while the training loss decreases.
- The validation loss and MAE fluctuated during the whole training, showing signs of overfitting. Significant fluctuation can be found in epochs 14 and 24 in the validation loss.
- After epoch 78, no improvements were made in the validation loss within the next 25 epoch and the model was terminated at epoch 103. The 103rd epoch has the following metrics: a training loss of 0.0052, a validation loss of 0.0594, a training MAE of 0.0496 and a validation MAE of 0.1951.
- The model achieved a test loss of 0.0082 and a test MAE of 0.0612 in the test evaluation.

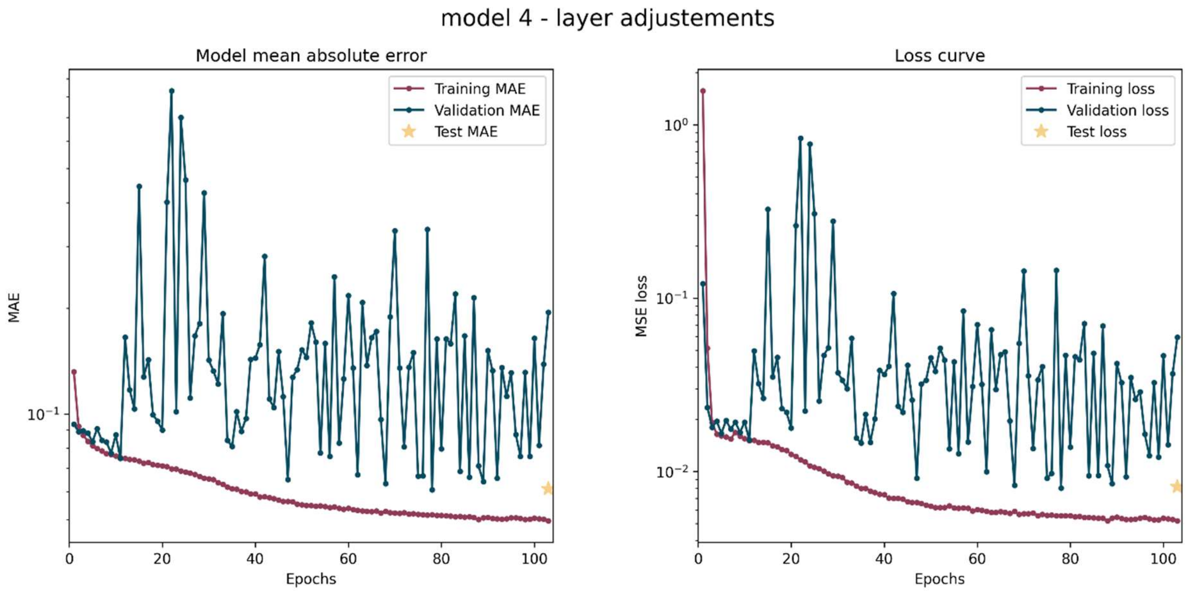

Figure 7-7: Model 3 training results

7.3.5 Evaluation of 3 trained models

Twelve apartments are selected from the prediction dataset to evaluate the performance of each of the three models. The selected apartments are general apartments from different sites and comprise 55 rooms.

Appendix F.Part I shows the twelve apartments used for this evaluation. The evaluation is done in different steps. First, the predictions for daylight and view are compared against the three models. Based on this evaluation, outliers and trends are selected and zoomed into in the second part of the evaluation. Part II and Part III of Appendix F show predictions for randomly selected rooms for daylight on the 21st of March and view to the sky.

Daylight predictions

Figure 7-8 shows the daylight predictions of the three models compared to the ground truth. Based on the predictions, the following findings were made:

- Model 1 has an MAE of 0.1168, model 2 has an MAE of 0.1122, and model 3 has an MAE of 0.1021.
- Model 1 has an MSE of 0.0245, model 2 has an MSE of 0.0225, and model 3 has an MSE of 0.0201.
- The distribution of the predictions for models 1 and 2, combined with the MAE and MSE, indicates that the model's predictions deviate from the ground truth and predict more significant average errors than model 3. All three models have the same specific outliers for both underprediction and overprediction.
- The predictions for the 21st of March are better for all three models compared to the other days.
- Both models 1 and 2 have an almost horizontal regression line for the 21st of June and December. The almost flat line indicates that the models the predictions have no strong correlation with the ground truth.

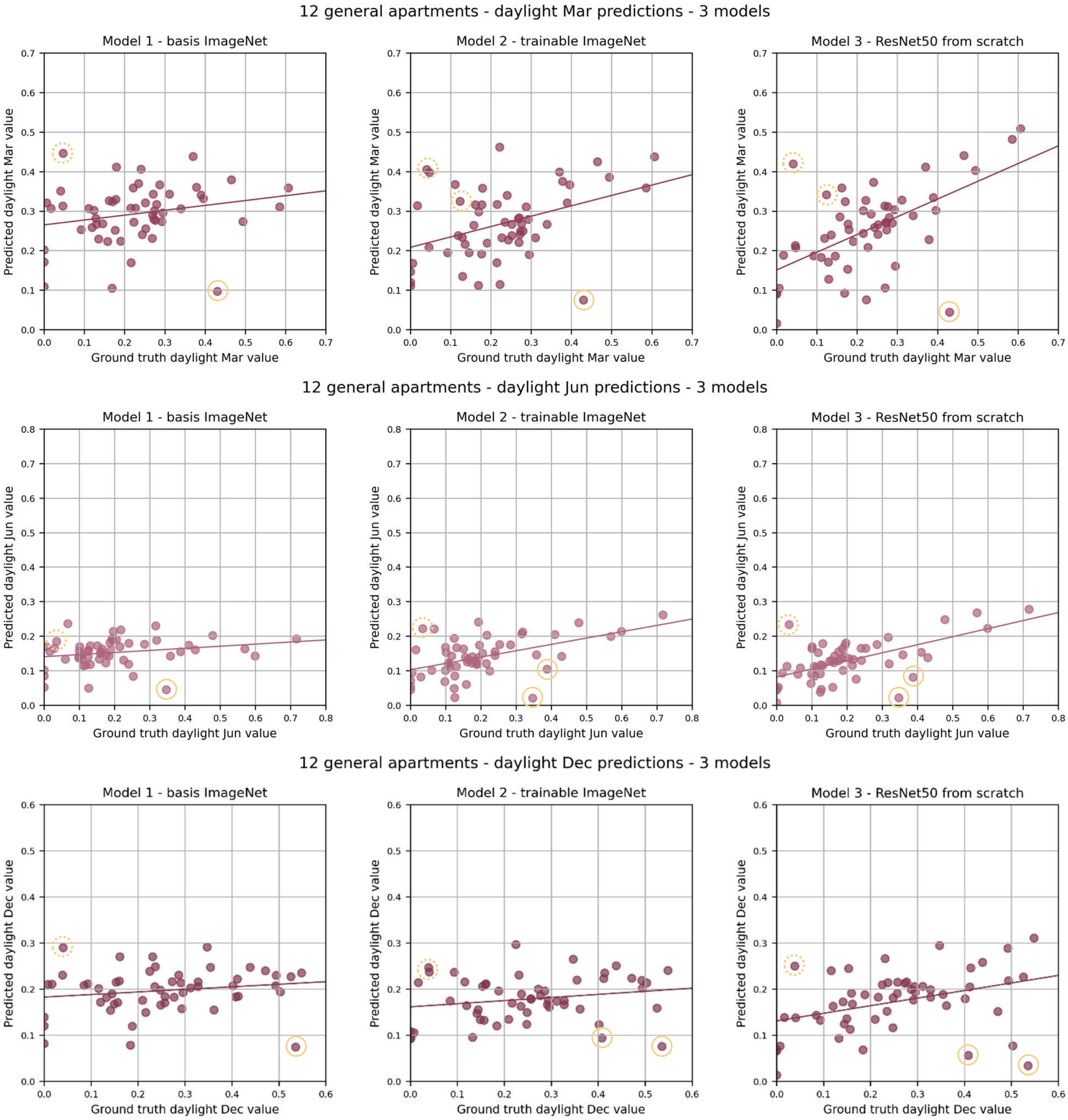

Figure 7-8: Trained models daylight prediction comparisons

View predictions

Figure 7-9 shows the three models' view-to-ground and view-to-sky predictions compared to the ground truth. Based on the predictions, the following findings were made:

- Model 1 has an MAE of 0.1465, model 2 has an MAE of 0.1556, and model 3 has an MAE of 0.1383.
- Model 1 has an MSE of 0.0318, model 2 has an MSE of 0.0345 and model 3 has an MSE of 0.0286.
- Based on the distribution of predictions for the three models, model 2 demonstrates less deviation from the ground truth and predicts minor average errors compared to models 1 and 2.
- Model 3 performs better on average than the first and second models regarding the MAE and MSE.
- All three models exhibit the same specific outliers for over- and under-prediction.
- The predictions for the sky view are better for all three models compared to the predictions for view to ground.

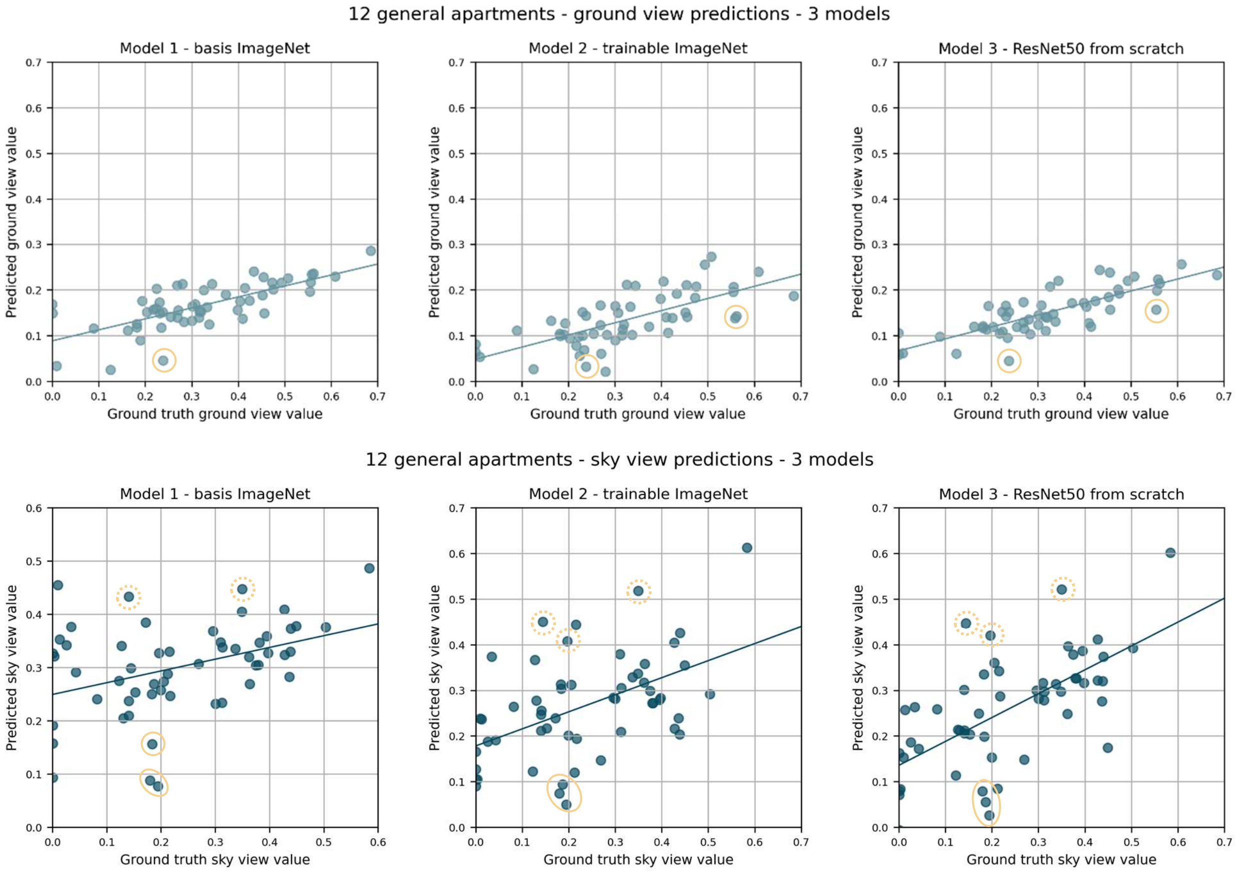

Figure 7-9: Trained models view prediction comparisons

Underprediction outliers

Three outliers underpredicted in all models are recognised when looking at the predicting graphs for daylight and view. The underprediction outliers are yellow in Figure 7-8 for daylight and Figure 7-9 for view. Figure 7-10 shows the three outlier rooms for daylight and the five outliers for view.

The second room, 'room 915172, is an outlier for the daylight on the 21st of March and the 21st of June and is an outlier for the view to the ground prediction. This room is not a room but an area in a space. The room has indirect access to a window. Because of this, the room's geometry does not include a window, making the prediction harder.

All the three outliers for view to sky, room ‘294881’, ‘908021’ and ‘282549’, have a window that is obstructed in front of it. This indicates a balcony or gallery in front of the window, blocking the daylight and view accessibility.

The fourth room, 'room 294881, is an outlier for view-to-sky prediction. Reasons for the underprediction can be found in the geometry of the room. The room geometry consists of two separate rooms adjacent to each other. The uncommon shape of the room can be a reason for the underprediction. Additionally, the room is quite extensive and deep compared to the others.

A pretty outstanding observation can be made when considering all six outlier rooms. Almost all rooms have no environmental obstructions since no circle exists in the feature image of four of the six rooms. Additionally, the environmental circle in the other two rooms is comparatively small.

Figure 7-10: Underpredicted rooms for daylight and view predictions

Overprediction outliers

The analysis of the three models reveals that two rooms are consistently overpredicted for the daylight label, as shown in Figure 7-8. Additionally, the analysis, as shown in Figure 7-9, indicates three rooms that are overpredicted for sky view by all three models. Figure 7-11 shows the geometries of the four rooms that are underpredicted for daylight and sky view by all three models.

The first room, 'room 989113', is overpredicted for daylight on the 21st of March and the view of the sky. Looking closer into the rooms that are overpredicted for sky view, a similarity can be found in the fact that all these rooms do not have any direct obstruction from a higher floor or balcony.

'Room 1602284' is an overpredicted outlier for predicting all three daylight days. Upon closer examination of the geometries of this room, it can be observed that it has a balcony space in front of the window and a quite present environmental obstruction circle.

Lastly, an interesting observation can be made by examining the similarities of the environmental circle in the image feature. All four rooms have the environmental circle present in the image feature. This is the opposite of the underpredicted rooms that mostly did not have the environmental circle present in the image feature. This similarity in design could explain why all three models overpredicted these rooms similarly.

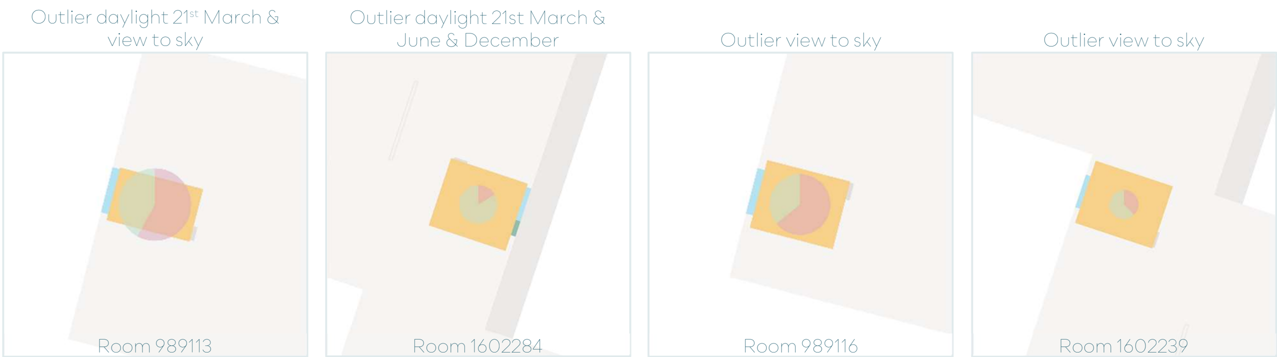

Figure 7-11: Overpredicted rooms for daylight and view predictions

Room performance level predictions

Looking at the broader application of the predictions, the main focus in the framework is giving designers feedback on the visual comfort quality of a space. This is directly linked to the different daylight and view performance levels that are translated from the predicted values. Therefore, the model should be able to predict accurately enough so the room is classified with the corresponding performance level.

Figure 7-12 illustrates the confusion matrixes of the daylight performance levels for all three models. Looking closer into how well the models' predictions are concerning the daylight performance levels of a space, it indicates that model 3 outperforms models 1 and 2. The earlier mentioned flat line of the daylight predictions by models 1 and 2 can also be seen in the confusion matrix. An interesting observation can be made, as the confusion matrixes indicate that neither of the models can predict medium and high daylight performance levels correctly.

Figure 7-13 illustrates the confusion matrixes of the view performance levels of all three models. As earlier mentioned, the distribution of the view level classes is skewed towards the higher end, and this is also indicated in the confusion matrixes as most room's ground truth is a high view label. Models 1 and 3 predict the room performance level quite well compared to the daylight performance levels, as less than 20% of the rooms are mispredicted. Notably, the degree of miscalculation in projecting the level of performance is never more than a single performance level away from the actual performance level.

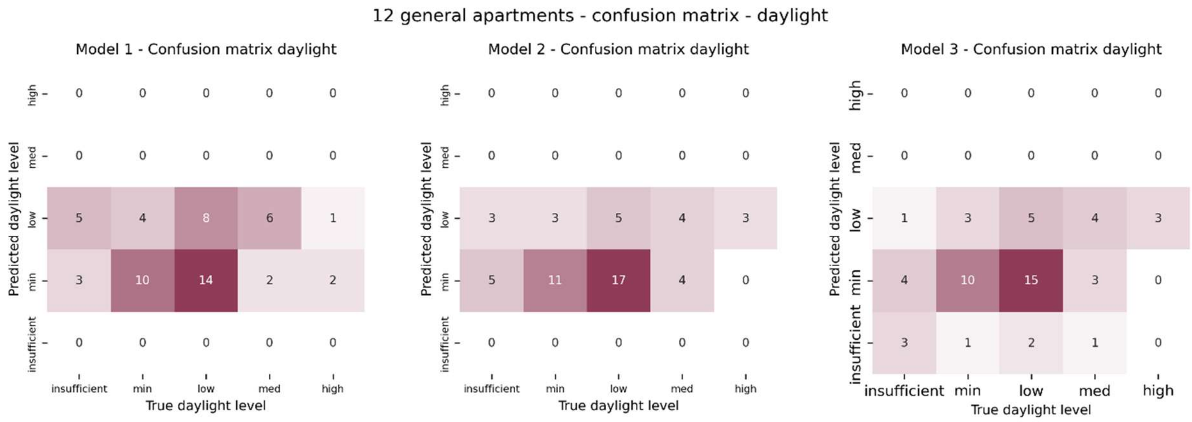

Figure 7-12: Trained models daylight performance level confusion matrix

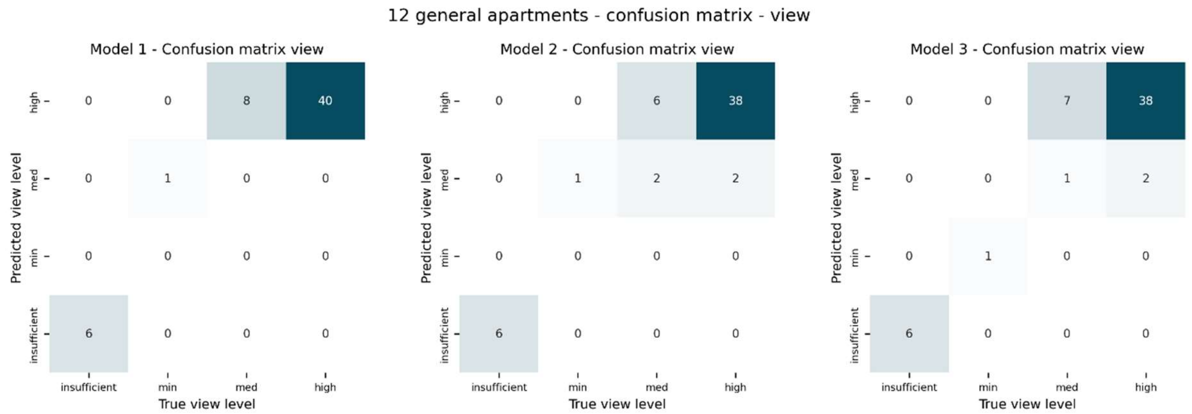

Figure 7-13: Trained models daylight performance level confusion matrix

Comparison of three trained models

The above findings provide valuable insights into these models' limitations and potential biases. One observation is that the view-to-sky prediction outperforms the prediction of all the other labels. The difference in the prediction quality between the daylight and view labels could indicate that the model needs to learn different things to predict daylight than when predicting for view.

Based on earlier observations made during the evaluation process, model 3 is the best overall performing model. Model 3 delivers the best predictions for the daylight and view labels. Furthermore, it does not generalise data erroneously for the latter. It can be deduced that this model exhibits the most potential out of all the models analysed. However, the objective of the ML model is to predict the daylight and view values accurately enough so that the predicted value will fall in the same guideline level as the ground truth. When looking closer into Figure 7-12 and Figure 7-13, the observation can be made that, at this moment, neither of the models reaches this requirement. Thus, further model training is needed to ensure a more accurate prediction of the daylight and view values to meet the model's objective.

7.4 Model ablation studies

Based on the earlier observation of the first three models' training process, an ablation study is done to fine-tune the ML model. The ablation studies are done with model 3 as a starting point. Firstly, the model is split up into two different models, one for daylight prediction and one for view predictions. Based on the results, experiments are done by adjusting the architectural layers. Additionally, experiments are done by adjusting the fusing moment of the image feature and the numerical features and experiments on different ResNet base models are conducted. Lastly, based on the findings of these three experiments, the hyperparameters of the best model are adjusted to fine-tune the model. Figure 7-14 provides an overview of the ablation studies conducted in this sub-chapter. The ablation studies will lead to a final fine-tuned model, which will be the final model of this research.

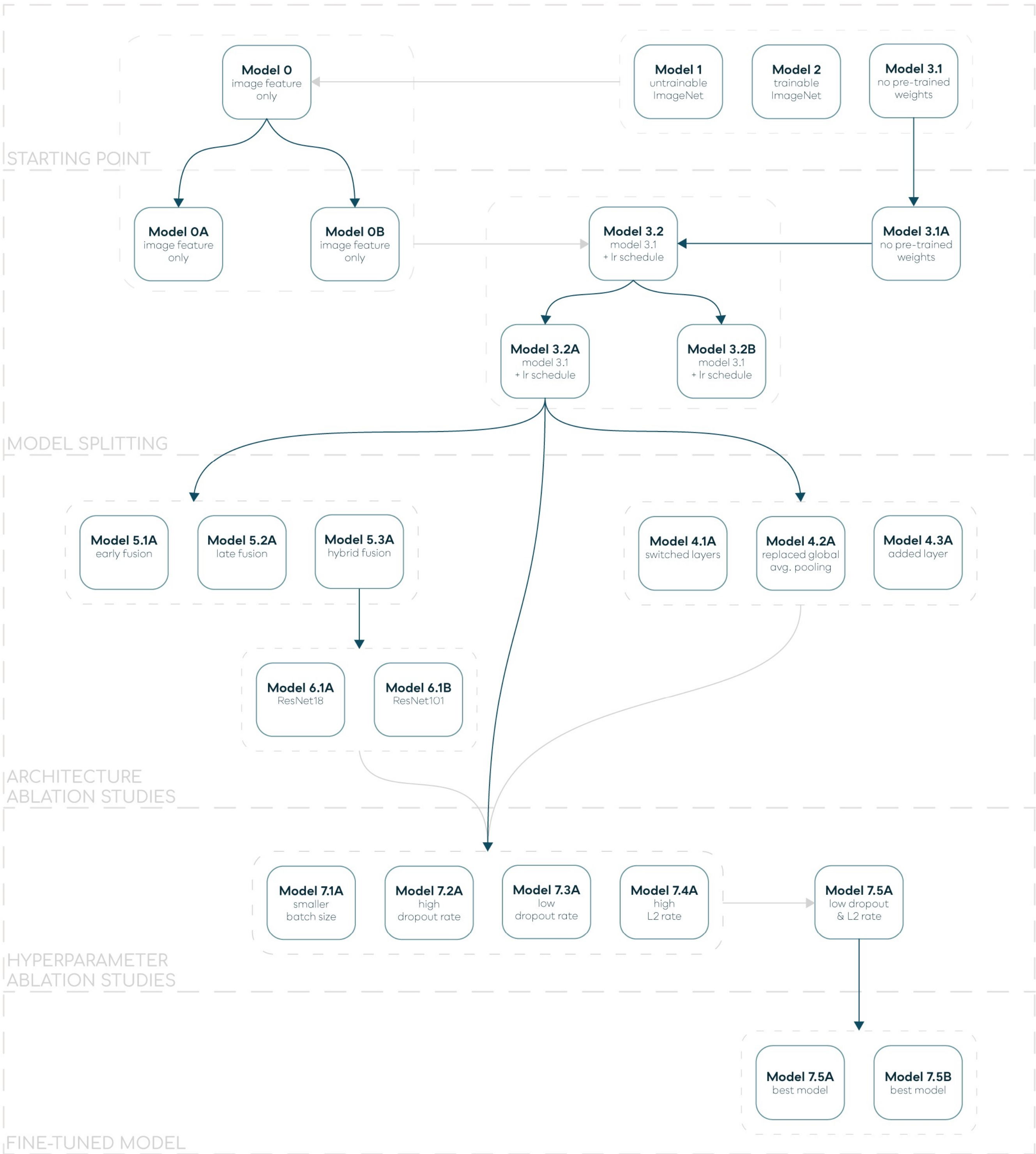

Figure 7-14: Overview ablation studies

7.4.1 Model splitting

As described while comparing the first three trained models, splitting up the model could improve the accuracy of the model's predictions. Table 18 shows the training results of splitting up the model into one model for daylight prediction and one model for view predictions. As of now, model A refers to the ML model trained for daylight predictions and model B for view predictions.

To start from the same baseline again, first, model 0 is split up into two models. Model 0 is only trained with the image feature as input. As shown in the table below, splitting up the model improves the performance of the model. The current baseline model for both metrics predictions has a test MSE of 0.0226. Splitting up the model improves the daylight predictions significantly, as the test MSE for daylight is reduced to 0.0183. This first experiment of splitting up the baseline model proves that creating two separate models results in more accurate predictions. As the first experiment showed promising results, the current model 3, now referred to as 3.1, is also split up into two parts. During the first training of this split-up model 3.1A, the model did not converge quickly enough. Therefore, a learning rate scheduler is added to the model, creating model 3.2. The learning schedule used during training gradually lowers the learning rate over time based on the number of iterations. The training of split-up model 3.2 resulted in promising performance. As the current model 3.1 reached a test MSE of 0.0082, the split-up model 3.2A for daylight prediction reached an MSE of 0.0057 and model 3.2B for view prediction reached an MSE of 0.0068. Thus, splitting up the model improved the accuracy of the model significantly. Both the daylight and view models showed a similar training process.

Table 18: Model performance comparison, splitting up model

	MSE			MAE		
ML model	Training	Validation	Test	Training	Validation	Test
Only image feature						
Model 0	0.0101	0.0251	0.0226	0.0742	0.1116	0.1138
Model 0A(daylight)	0.0075	0.0623	0.0183	0.0635	0.2163	0.0968
Model 0B(view)	0.0129	0.1725	0.0201	0.0865	0.3297	0.1030
Model 3.1						
Model 3.1	0.0052	0.0594	0.0082	0.0496	0.1951	0.0612
Model 3.1A(daylight)	0.0067	0.0840	0.0139	0.0536	0.2517	0.0705
Model 3.2						
Model 3.2	0.0086	0.0206	0.0121	0.0639	0.0974	0.0720
Model 3.2A(daylight)	0.0024	0.0058	0.0057	0.0332	0.0505	0.0503
Model 3.2B(view)	0.0026	0.0066	0.0068	0.0357	0.0534	0.0533

7.4.2 Architecture layers adjustments

Three experiments on layer adjustments are conducted based on model 3.2A. Table 19 shows the results of training the models. The first experiment, Model 4.1A, changed the order of one layer in the architecture. In the fully connected network of the image feature, the dropout layer and the dense layer are switched around. This model did not outperform model 3.2A.

The second experiment on the architectural layer also focussed on the image feature part. During this experiment, the global average pooling layer is replaced by a convolutional layer and latten. Although this model's architecture outperformed the first layer adjustment experiment, it did not outperform model 3.2A.

Lastly, an experiment to add more dense layers to the combined fully connected network is conducted. One extra dense layer and dropout are added at the end of the architecture. Furthermore, it is worth noting that the aforementioned architectural modification failed to surpass the performance of model 3.2A.

Table 19: Model performance comparison, architectural layer ablation studies

		MSE			MAE		
ML model		Training	Validation	Test	Training	Validation	Test
Model 3							
Model 3.2A(daylight)		0.0024	0.0058	0.0057	0.0332	0.0505	0.0503
Model 4							
Model 4.1A(daylight)	Swapped layer	0.0043	0.0116	0.0077	0.0471	0.0843	0.0627
Model 4.2A(daylight)	Replace global Avg.	0.0039	0.0062	0.0062	0.0434	0.543	0.539
Model 4.3A(daylight)	Added layers	0.0036	0.072	0.0071	0.0412	0.0584	0.0579

7.4.3 Different fusion moment

The current best model, model 3.2A, has a hybrid fusion moment. After the image feature goes through the ResNet50 layers, the output is connected to its own fully connected network. This fully connected layer is concatenated with the two numerical features input. Three experiments are conducted to investigate different fusing moments. Table 20 shows the outcome of these experiments.

The first experiment consisted of early fusion, where the output of the Resnet50 is directly concatenated with the numerical feature input. The second experiment consisted of late fusion, where the numerical features first go through a fully connected layer before concatenating with the fully connected network of the image feature. The third experiment consisted of hybrid fusion, where the numerical features go through a fully connected network, and the output of the ResNet50 layers is concatenated with the fully connected network of the image features. All the aforementioned fusing modifications failed to surpass the performance of model 3.2A.

Table 20: Model performance comparison, different fusing moment

ML model		MSE Training	MSE Validation	MSE Test	MAE Training	MAE Validation	MAE Test
Model 3							
Model 3.2A$_{(daylight)}$		0.0024	0.0058	0.0057	0.0332	0.0505	0.0503
Model 5							
Model 5.1A$_{(daylight)}$	Early fusion	0.0058	0.0550	0.0154	0.0525	0.1924	0.0864
Model 5.2A$_{(daylight)}$	Late fusion	0.0024	0.0064	0.0064	0.0325	0.0533	0.0531
Model 5.3A$_{(daylight)}$	Hybrid fusion	0.0050	0.0508	0.0097	0.0502	0.1815	0.0710

7.4.4 Different ResNet model

The currently used ResNet50 is a relatively deep and complex model, which could be an overkill. Therefore, experiments are conducted to test if changing the ResNet model to a lighter or heavier model influences the model's performance. The experiments are done on the basis of late fusing Model 5.2A, since this model showed potential in terms of the training MSE and MAE. Table 21 shows the results of the ResNet experiments.

The first experiment, model 7.1A, consists of a ResNet18 model, making the model significantly lighter and less complex. However, the test MSE of model 6.1A reaches as low as the test MSE of model 5.2A, model 6.1 plateaued way earlier than model 5.2A in terms of training MSE and MAE. The second experiment, model 7.2A, consists of a ResNet101 model, making the model significantly heavier and more complex. The results of model 7.2A indicate that this model has the weakest generalisation performance among the three models. All the ResNet modifications mentioned above failed to surpass the performance of model 5.2A.

Table 21: Model performance comparison, different ResNet model

ML model		MSE Training	MSE Validation	MSE Test	MAE Training	MAE Validation	MAE Test
Model 5.2							
Model 5.2A$_{(daylight)}$	Late fusion	0.0024	0.0064	0.0064	0.0325	0.0533	0.0531
Model 6							
Model 6.1A$_{(daylight)}$	ResNet18	0.0036	0.0065	0.0065	0.0426	0.548	0.0549
Model 6.2A$_{(daylight)}$	ResNet101	0.0067	0.0282	0.0156	0.0575	0.1180	0.0848

7.4.5 Hyperparameter adjustments

Based on the experiments on the architecture layers, fusing moment and ResNet model, model 3.2A is the best-performing model. This model is used to conduct experiments on the hyperparameter adjustments.

In the first experiment, the batch size was reduced to 32, which could act as a regularization and could help the overfitting problem of the model. The second experiment consist of a high dropout rate, which increases the random dropouts of the neurons during training and could reduce overfitting, especially in complex models or noisy datasets. The third experiment consists of a low dropout rate, which means that only a fraction of the neurons are deactivated. A low dropout rate prevents over-regularization and encourages the model to learn more from the data. The fourth experiment consists of a high L2 regularization rate, which sets a significant penalty on large weight and could prevent overfitting. The fifth experiment is a low dropout and L2 regularization rate, which allows the model to capture more complex patterns. However, a low L2 regularization rate could lead to overfitting.

Among all the hyperparameter modifications, as mentioned earlier, the best modification is a lower dropout and L2 regularization rate as used in model 7.5A, as shown in Table 22. Model 7.5A outperforms models 3.2A on both the MSE and MAE. Therefore, model 7.5A is selected as the best-performing model and further evaluated.

Table 22: Model performance comparison, hyperparameter adjustments

ML model		MSE Training	MSE Validation	MSE Test	MAE Training	MAE Validation	MAE Test
Model 3.2							
Model 3.2A$_{(daylight)}$		0.0024	0.0058	0.0057	0.0332	0.0505	0.0503
Model 7							
Model 7.1A$_{(daylight)}$	Batch size 32	0.0031	0.0060	0.0059	0.0386	0.0520	0.0515
Model 7.2A$_{(daylight)}$	High dropout rate	0.0062	0.0072	0.0072	0.0559	0.0611	0.0618
Model 7.3A$_{(daylight)}$	Low dropout rate	0.0013	0.0058	0.0055	0.0235	0.0490	0.0484
Model 7.4A$_{(daylight)}$	High L2 rate	0.0036	0.0068	0.0067	0.0417	0.0575	0.0571
Model 7.5A$_{(daylight)}$	Low dropout, L2 rate	0.0008	0.0051	0.0047	0.0185	0.0451	0.0440

7.5 Evaluation best-performing model

In order to assess the performance of the best-performing ML model in accurately learning correlations, two additional evaluations, in addition to the earlier conducted evaluation, are conducted, which ensures a thorough examination of the model's performance and its ability to recognize patterns and relationships within the data effectively. The earlier used 12 general apartments are again predicted with this model. Then, three standard apartment types are used for predictions, and the evaluation is done to see if the model is able to make similar predictions for the same room type. Lastly, three uncommon apartment geometries are used for predictions to see if the model can handle uncommon data.

The best-performing model, model 7.5A and model 7.5B, have the same architecture as shown in Figure 7-4, which means that the model uses an image feature and two numerical features to predict either the daylight performance or the view performance. The model uses a hybrid fusion method. After the image feature maps are extracted from the ResNet, a first completely connected layer is added to converge the spatial information into a one-dimensional feature vector. After the first fully connected layer, the numerical features are concatenated with the feature extracted from the first fully connected layer. Subsequently, a second fully connected layer is added. The final output layer is a dense layer with either two or three output units and a linear activation function. The hyperparameter of the model are fine-tuned resulting in a low dropout rate of 0.3 and a low L2 regularization rate of 0.0001. Appendix E gives a detailed overview of the model's architecture. The Python code of the final ML training is shown in Appendix D.Part III.

7.5.1 Model training

For the training of model 7.5, the Adam optimizer with a mean squared error (MSE) loss function and a mean absolute error (MAE) metric is used to construct the model. The model has a learning rate scheduler that starts at 0.001 and gradually decreases over time. During training, early stopping of 25 epochs is used to prevent overtraining, and the model could train for a maximum of 200 epochs with a batch size of 64.

The training of the daylight model is stopped early at epoch 81, and the view model stopped early at epoch 82. Figure 7-15 shows the results of the third model training. The following findings can be found in the training of the model:

- In initial training (epoch 1-10), both models start with a high initial training loss and MSE. However, both significantly reduced and consistently decreased, indicating that the model learns quickly and adapts to the training data. The validation loss and MAE decrease substantially but show fluctuations.
- The model's training loss and MAE stabilise and improve during epochs 10-50, with occasional plateaus in learning. These plateaus are addressed by reducing the learning rate, leading to an improvement in validation loss within four epochs after the learning rate reduction.
- The model validation loss and MAE stabilise after epoch 60 and start to plateau, while the training loss and MAE gradually decrease.
- After no improvements in validation loss the daylight model was early terminated at epochs 81. The 81st epochs achieved a training loss of 0.0008 and a training MAE of 0.0185. The view model stopped early at epoch 82. The 82nd epochs achieved a training loss of 0.0012 and a training MAE of 0.0236.
- The daylight model achieved a test loss of 0.0047 and a test MAE of 0.0440 in the test evaluation. The view model achieved a test loss of 0.0057 and a test MAE of 0.0478 in the test evaluation.

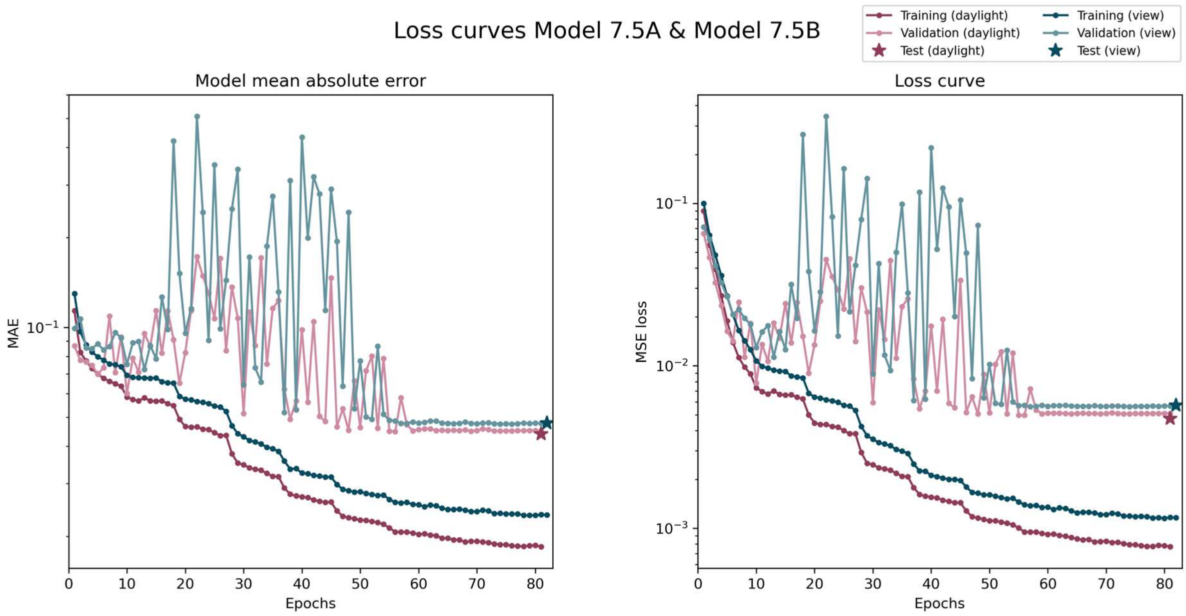

Figure 7-15: Model 7.5A & model 7.5B training results

7.5.2 General apartments

As mentioned above, twelve apartments are selected from the prediction dataset to evaluate the performance of the model on general apartments. Appendix F.Part I shows the twelve selected apartments.

Figure 7-16 illustrates the daylight predictions against the ground truth of model 3.2A. The predictions for the 21st of March are notably more accurate than those for June and December. The model underpredicts the values for the 21st of June and, the predictions for the 21st of December are quite generalised as the regression line does not show a substantial incline. Figure 7-17 illustrates the predictions by model 3.2B for the view values. The sky view predictions are way more accurate than the ground view predictions but show some outliers.

As this ML model will be implemented into the broader framework, the model must be able to predict the performance levels of a room correctly. Figure 7-18 illustrates the confusion matrixes of the daylight and view performance levels when translating the predictions of the best model to performance levels. Looking closer into how well the model's predictions are concerning the daylight performance levels of a space, a slight positive correlation is shown in the confusion matrix. One notable improvement is shown, as the model can now make slightly higher predictions and at least one medium daylight performance level was predicted. Looking into the prediction accuracy in terms of the view performance levels, Figure 7-18 indicates a quite good prediction.

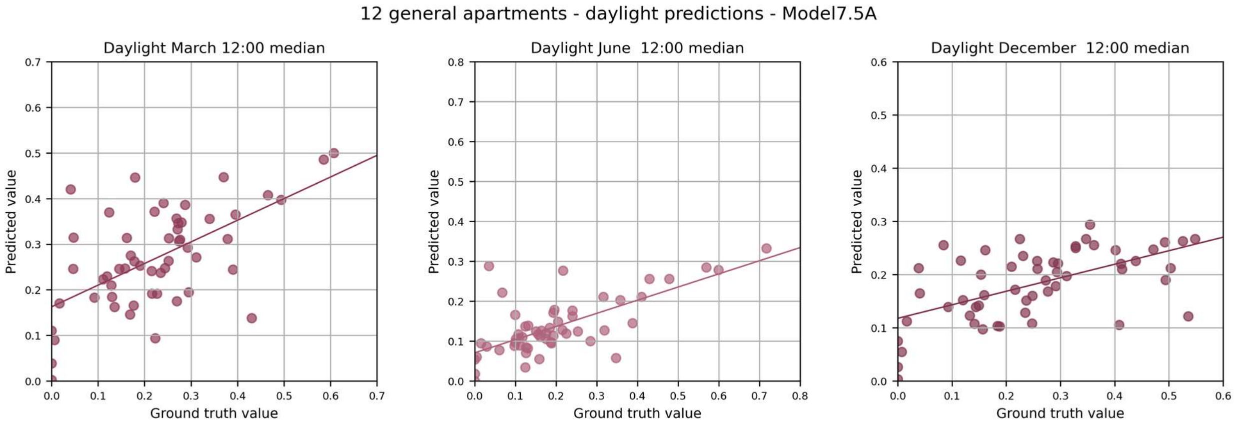

Figure 7-16: Best-model daylight predictions

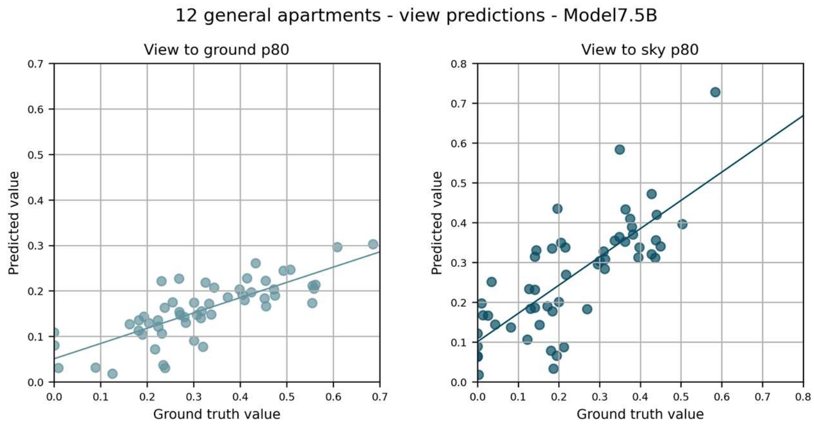

Figure 7-17: Best-model view predictions

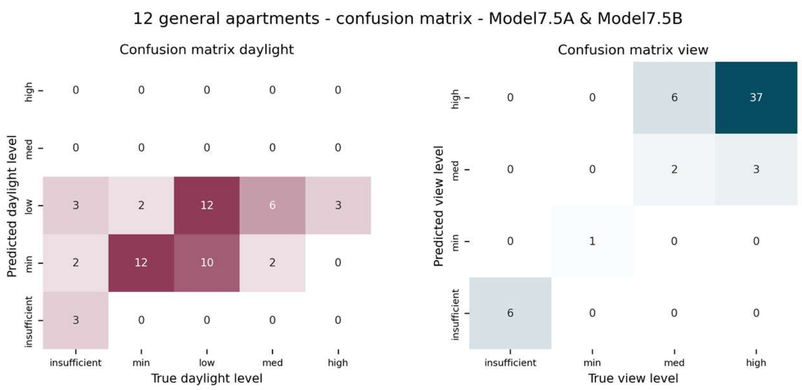

Figure 7-18: Best model performance levels prediction 12 general apartments

7.5.3 Standard apartment types

Figure 7-19 shows the three standard apartment types used for this evaluation. The first standard apartment type comprises a living room, a connected kitchen, and three bedrooms. This first standard apartment type is oriented towards the Northeast and Southwest. The second standard apartment type is oriented towards the South and consists of two bedrooms, and a connected living room and kitchen space. The third standard apartment type comprises two bedrooms and a separate kitchen and living room. The apartment type is oriented towards the Southeast and Northwest. To evaluate the performance of the model, the first standard apartment type was predicted sixteen times, the second apartment type twelve times, and the third apartment type was predicted eight times by the best model.

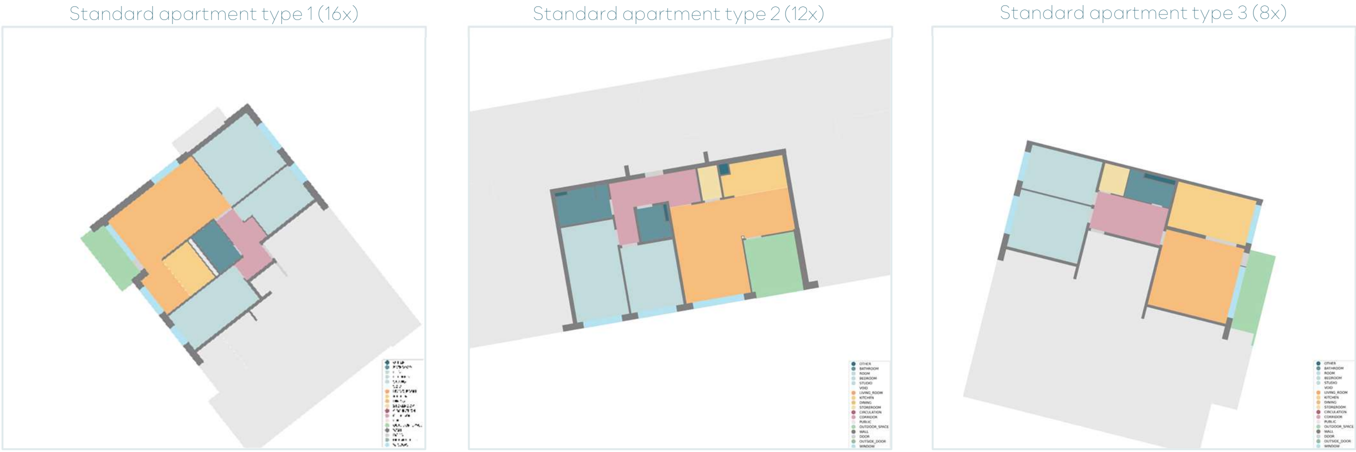

Figure 7-19: Standard apartment types

Performance level prediction

Figure 7-20 illustrates the confusion matrixes of the daylight and view performance levels predicted by the best model. Looking closer into how well the model's predictions are concerning the daylight performance levels of a space, it indicates that the model does not well predicts the daylight performance levels compared with the twelve general apartments. Additionally, in terms of the daylight performance levels, the model is underpredicting. The view prediction performance in terms of performance level is not good enough, as roughly 10% of the spaces have an incorrect view level.

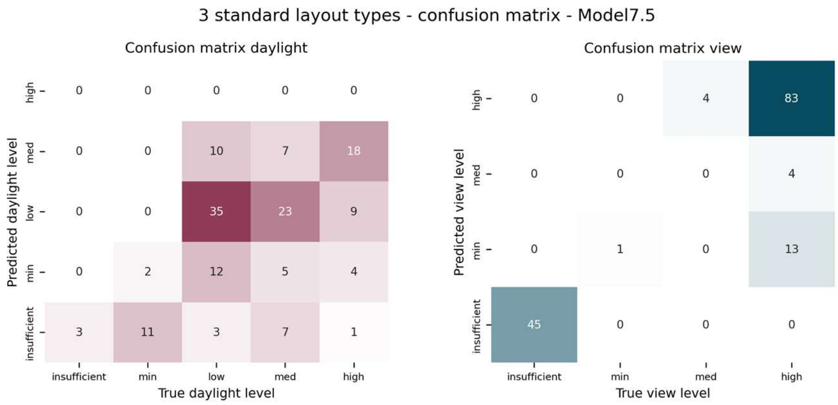

Figure 7-20: Best model performance levels prediction 3 standard apartment types

Daylight predictions

Figure 7-21 shows the daylight predictions made by the best model for the three standard apartment types mentioned. As expected, the daylight predictions for the 21st of March are more accurate than for the 21st of June and December. As expected, the model predicts the same room within the same range, indicating a positive linear correlation, especially for the second and third standard apartment types. However, there are some exceptions.

Firstly, standard apartment type one stands out more, as the daylight predictions per room type are more scattered. The predictions among different room types for standard apartment type one are more scattered than the other standard apartment types, which could be explained by the fact that the spaces of type one are less often a perfect square. Additionally, the kitchen (yellow) of standard type one seems to be harder to predict. This is in accordance with the earlier outlier analysis, where spaces that are areas within a space are mostly underpredicted. Nonetheless, the different rooms are still predicted within a clear group, suggesting that the model learned correlations between different room types to predict the daylight label.

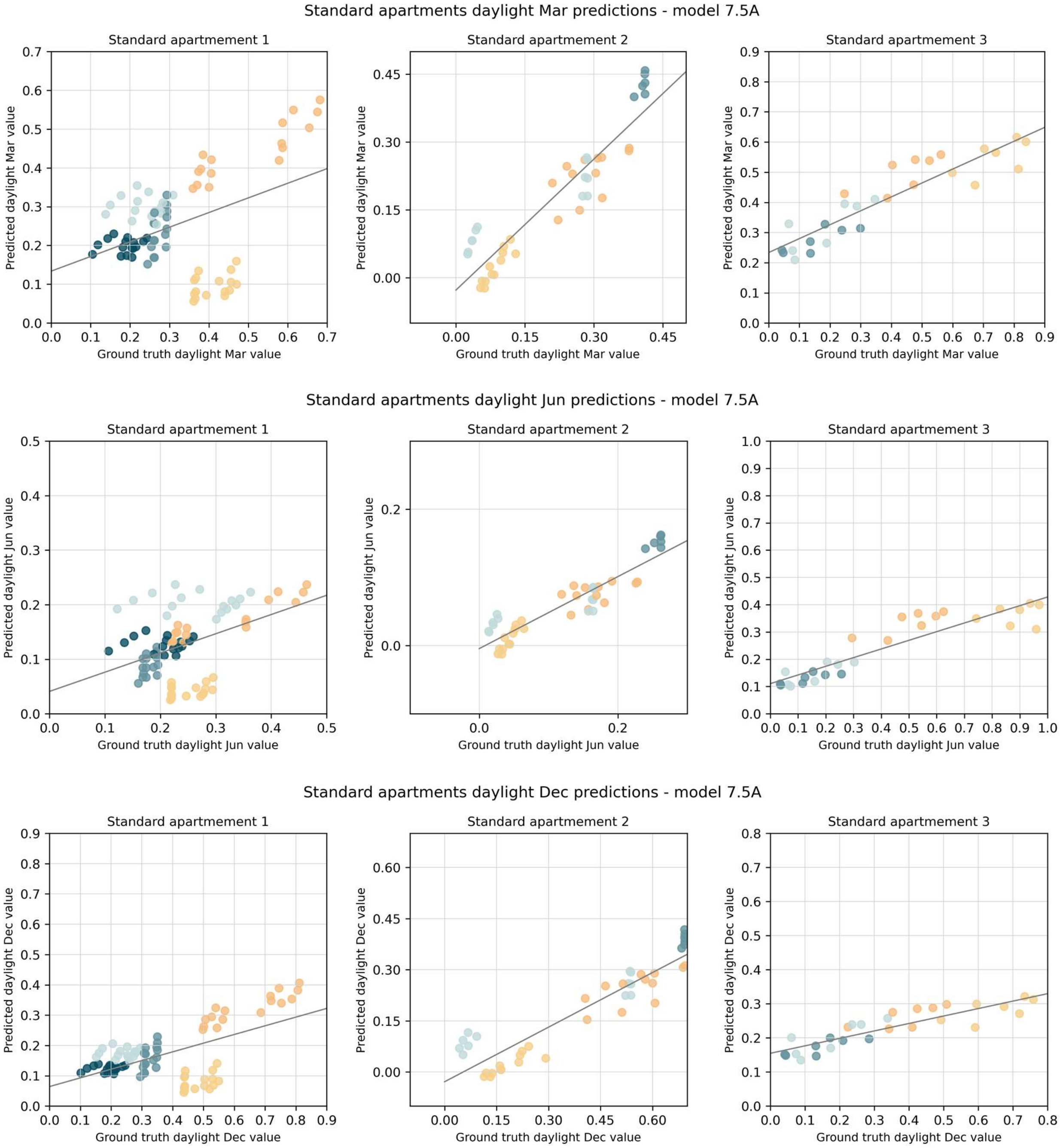

Figure 7-21: Standard apartments daylight predictions per room type

View predictions

Figure 7-22 shows the predictions made for the view labels for the three standard apartment types by the best model. All the different rooms of the standard apartment types are not always grouped together, indicating that the model did not learn correlations between a standard room type and view predictions. Especially looking into the sky view predictions, the predictions per room type are scattered around. For the ground view, the different room type predictions are grouped together, indicating that the predictions for each room per standard apartment type are comparable for the view-to-ground. Therefore, we can conclude that the model does not perform well for the view prediction of standard apartment types.

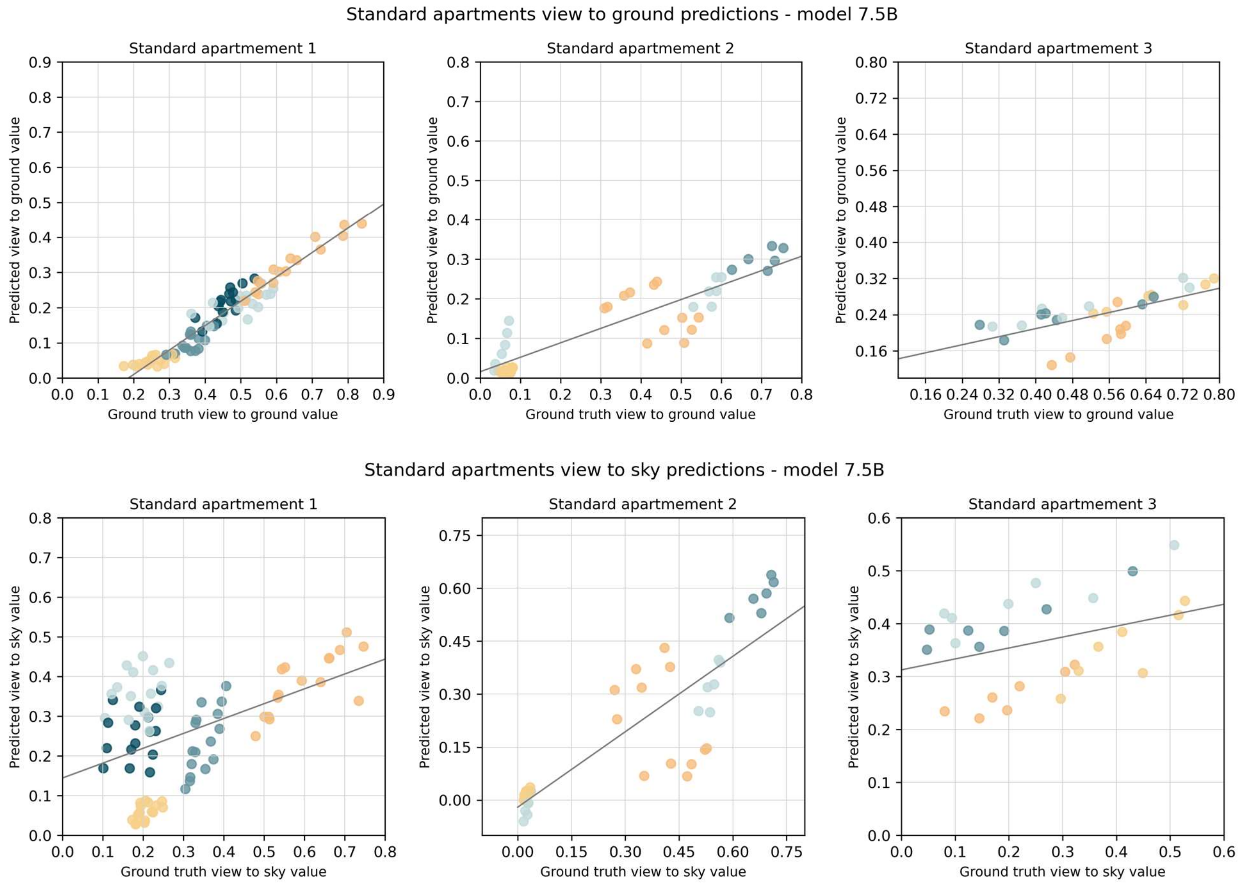

Figure 7-22: Standard apartments view predictions per room type

7.5.4 Uncommon geometries

In order to evaluate the model's performance, three uncommon geometry sites are selected for further evaluation, see Figure 7-23. The first uncommon site comprises apartments with sticking-out triangle shapes and windows on multiple facades. The second site consisted of apartments with angled edges and internal obstructions. From uncommon site 2, thirteen apartments are selected for the prediction that all are oriented towards North and South. The third uncommon site had apartments with windows that laid back and a partly curved façade. Four apartments were selected from the third site for prediction purposes.

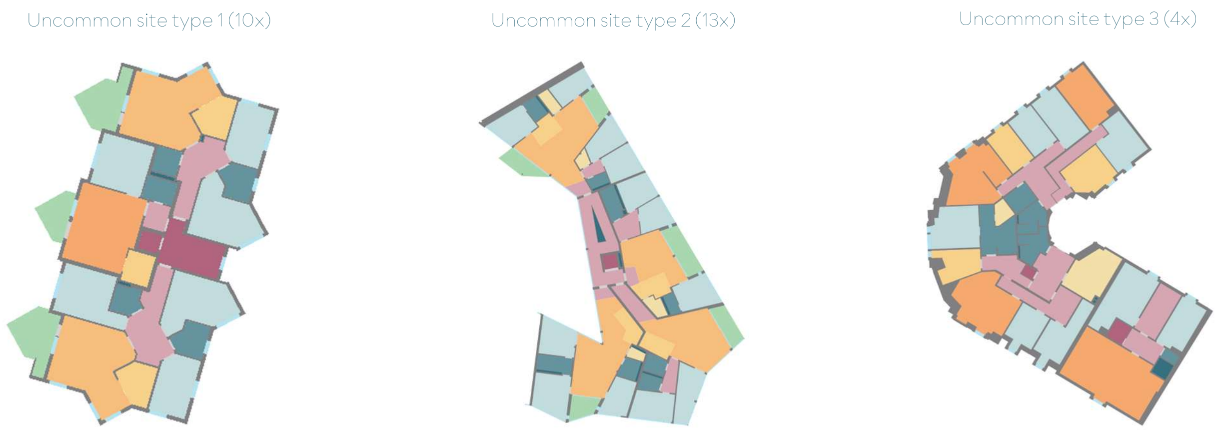

Figure 7-23: Uncommon geometry site types

Performance level prediction

The confusion matrixes of the daylight and view performance levels predicted by the best model are illustrated in Figure 7-24. Upon closer examination of the model's predictions for the daylight performance levels of a space, it is evident that the model performs relatively well in predicting the daylight and view levels compared to other evaluations. Generally, the model mispredicts up to two performance levels. However, the model tends to underpredict the daylight performance levels. Additionally, the view prediction performance in terms of performance level shows a clear positive regression. The model predicts reasonably well in terms of view, as only a fraction of the rooms is mispredicted with a maximum of one view performance class.

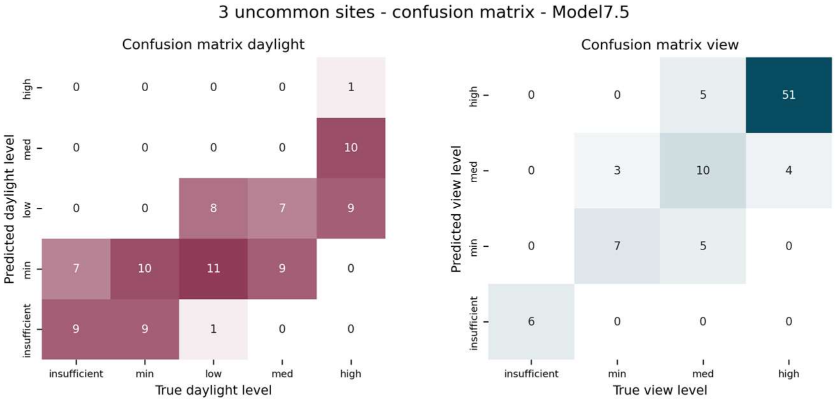

Figure 7-24: Best model performance levels prediction 3 uncommon sites

View predictions

Figure 7-26 show the view predictions by the best model for the three uncommon sites. Notably, the view-to-ground predictions for all three sites are underpredicted. Nonetheless, regarding ground view predictions of uncommon site 3, the results are relatively impressive compared to the other two sites. This is because site three predominantly comprises low view-to-ground values. The model excels in forecasting sky view labels for uncommon sites despite the presence of outlier predictions in all three sites. Notably, uncommon sites 1 and 3 appear to be well-predicted, with the regression line almost approaching a 45-degree angle.

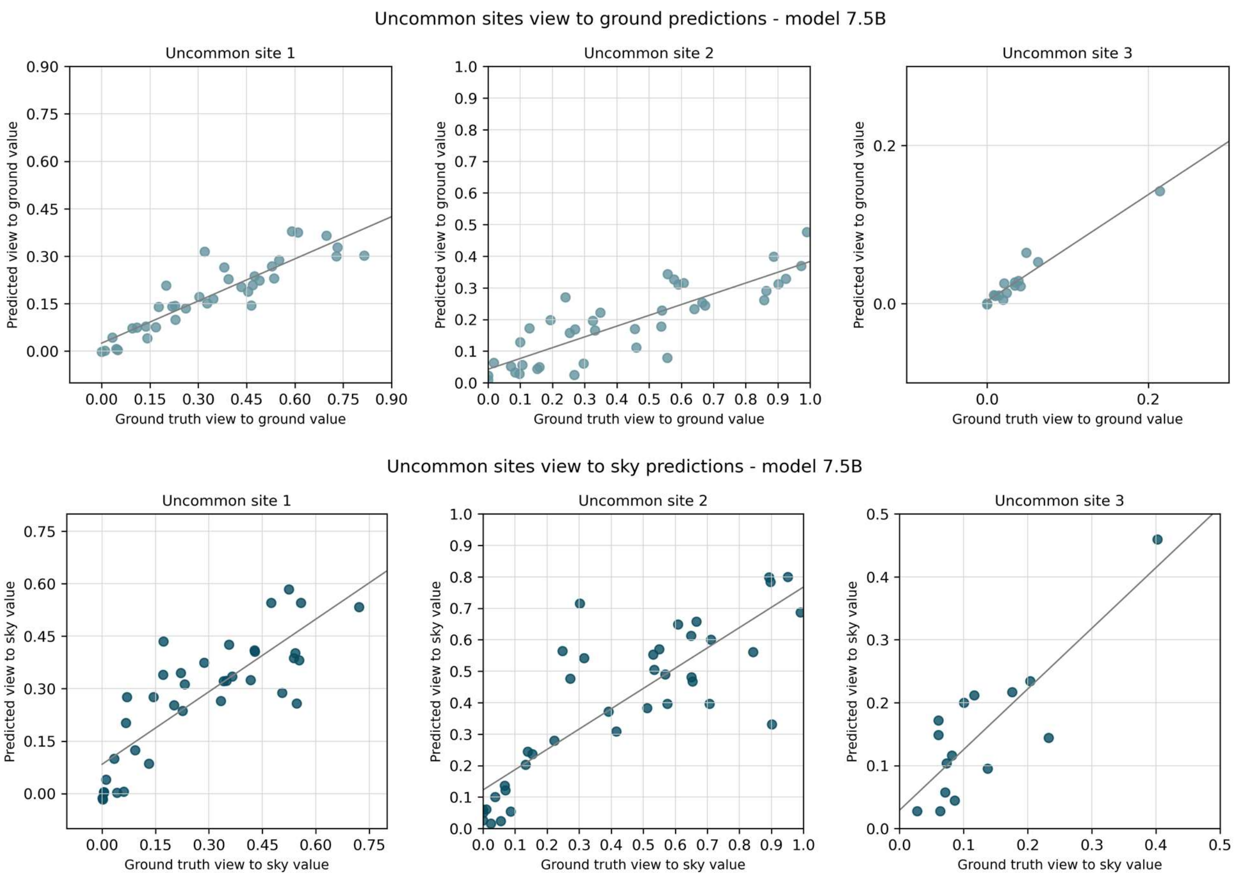

Figure 7-25: Uncommon sites sky view predictions

Daylight predictions

Figure 7-26 illustrates the best model's daylight prediction for the selected apartments in three uncommon sites. The daylight values for uncommon sites 1 and 2 are what we would expect, with the best-predicted value occurring on the 21st of March. Overall, the model tends to underpredict the daylight values for sites 1 and 2. Uncommon site 3, on the other hand, stands out from this trend with highly accurate predictions. In fact, on the 21st of March, the model overpredicts, which contrasts earlier daylight prediction evaluations. The predictions for the third uncommon site are more scattered compared to the first and second sites.

.

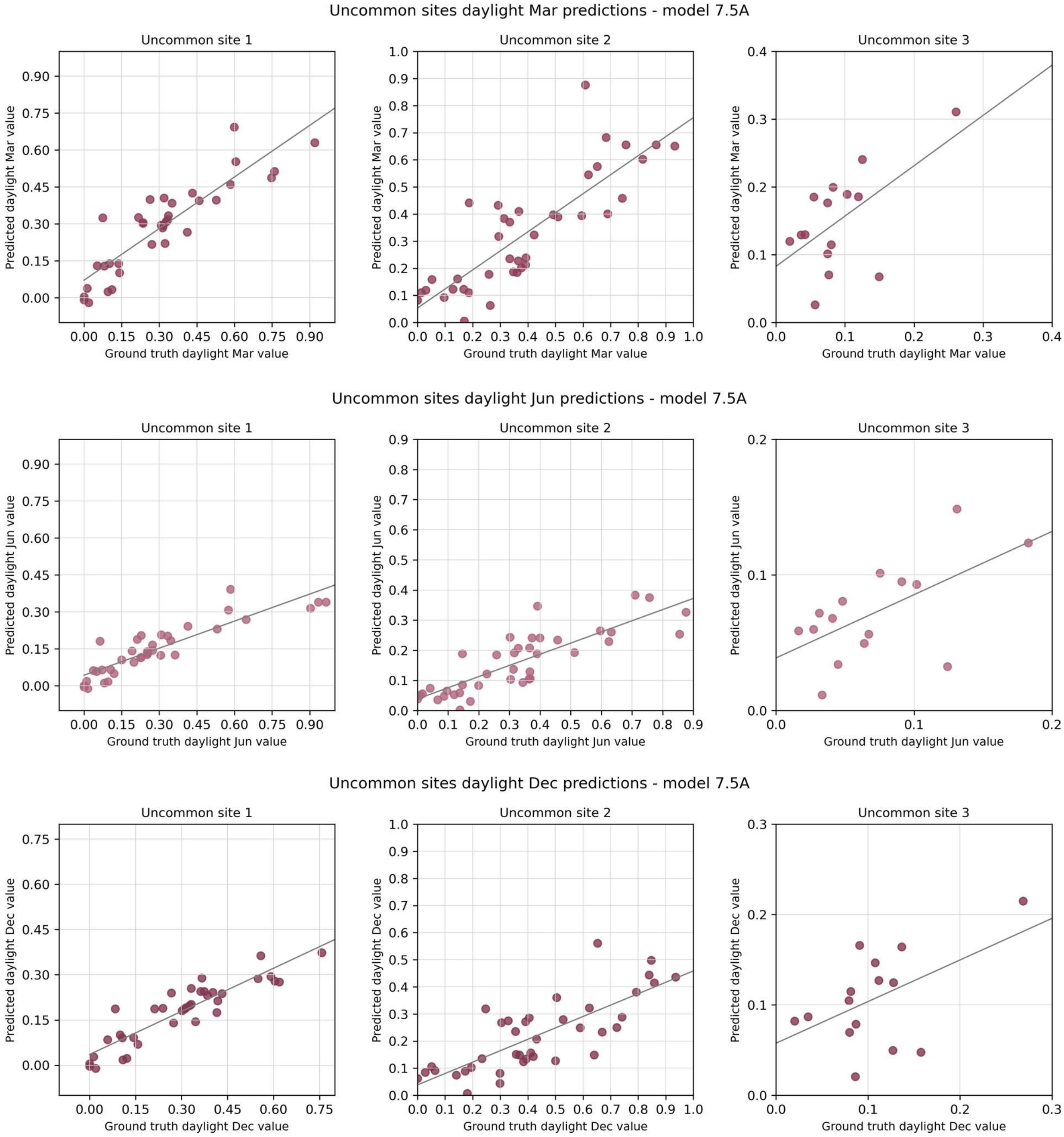

Figure 7-26: Uncommon sites daylight predictions

7.6 Conclusion

In this chapter, several experiments have been conducted to fine-tune the proposed ML model. From the experiments, it becomes evident that using a pre-trained ResNet50 model does not outperform training the same model from scratch. An experiment showed that the use of multimodal learning outperforms an ML model, which only learns from an image feature. Splitting the model into two distinct ML models, each trained to predict a single metric, proved to be an effective strategy. Ablation studies indicated that a late fusion model exhibits potential, and lower regularisation rates improve the performance of the ML model.

The optimal model identified in this study is model 7.5, which consists of a multimodal learning approach. Specifically, the model learns from one image feature and two numerical features, utilising hybrid fusion to concatenate the different feature types. The model architecture comprises a ResNet50 followed by a dense layer for the image feature. After concatenating the numerical features, another dense layer is added. The architecture uses low regularisation rates for dropout and L2 regularisation. The Adam optimiser with a mean squared error (MSE) loss function and a mean absolute error (MAE) metric is used to construct the model. During training, a learning rate scheduler and early stopping are applied. The model was trained with batch size 64.

After training the model, the best model achieved a training loss of 0.0008 and a training MAE of 0.0185 for the daylight metric, a training loss of 0.0012, and a training MAE of 0.0236 for the view metric. In the test evaluation, the model achieved a test loss of 0.0047 and a test MAE of 0.0440 for daylight predictions and a test loss of 0.0057 and a test MAE of 0.0478 for view predictions.

Nevertheless, while evaluating the best-trained model, it was evident that the current model does not meet the performance requirements. Therefore, further refinements are necessary to improve the ML model. The model underpredicts all the daylight labels on the 21st of June and December, as well as the view-to-ground label. Notably, the view-to-sky label is the best-predicted label across all evaluations. Regarding performance level accuracy, the model's predictions result in mispredictions of up to two daylight performance levels and up to one performance level for view.

~ empty page ~

8 Case study

To demonstrate the ML design process framework, a comprehensive case study has been conducted. The case study walks through every step of the ML design process framework, which showcases the usability of the framework for designers. The goal of the case study is to test if the ML framework is useable during the design process in the predesign phase.

8.1 Design problem

The design task at hand consists of the design of a layout for an apartment building located in Switzerland. The building consists of a conjunction of two squares that together form one building, see Figure 8-1. Each square contains three apartments per floor, with a central circulation space in the middle. The building balconies on one side of the building, either on the east side, as illustrated in Figure 8 1, or on the West side of the building. The design task centres around an apartment located at the intersection of the two squares, resulting in an apartment with obstructions from the building itself, see Figure 8-2.

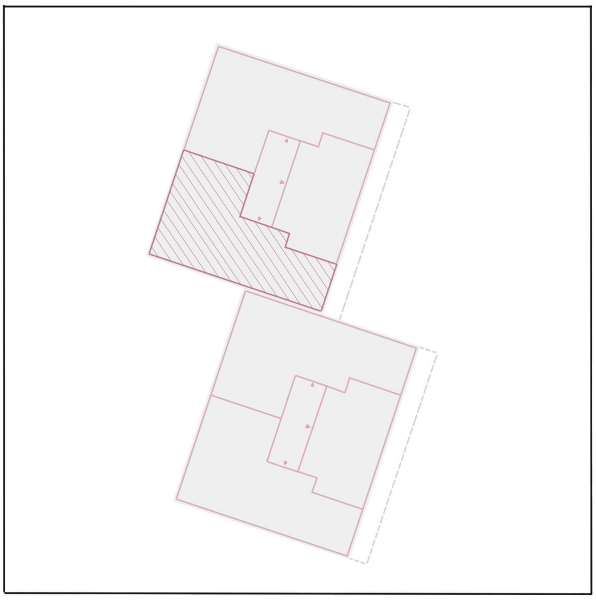

Figure 8-1: Case study building

Figure 8-2: Case study apartment boundary

The layout design for the apartment must meet specific requirements. The 73 m2 apartment should include three bedrooms, a living room, and a kitchen. The living room and kitchen can be combined into one space or consist of two separate rooms. Similarly, the bathroom and toilet can be a single room or two separate spaces. Table 23 shows the detailed requirements of the apartment.

Table 23: Apartment requirements case study

Characteristic	*Requirement*
Total m2 apartment	73 m^2
Balcony included	Yes, on East of West side
Nr of rooms	4 or 5 rooms
Living room & kitchen	±25 m^2
Bedroom	2x ±13 m^2 & 1x ±10 m^2
Bathroom & toilet	±5 m^2

8.2 Step 1 – pre-processing

8.2.1 Creating layout designs

For the case study, six alternative design layouts are created, see Figure 8-3. Designs 1, 3 and 5 have a balcony located on the East side of the building, while the other three designs have a balcony on the West side of the building. Designs 1 and 5 have the bedrooms grouped together, while the other designs have the bedrooms more spread out over different orientations. In designs 1, 3, 4 and 6, the kitchen faces South, while the kitchens faces towards East in designs 2 and towards West in design 5. The living room faces South in designs 2, 3, 4 and 6, while the living room faces East in design 1 and West in design 5.

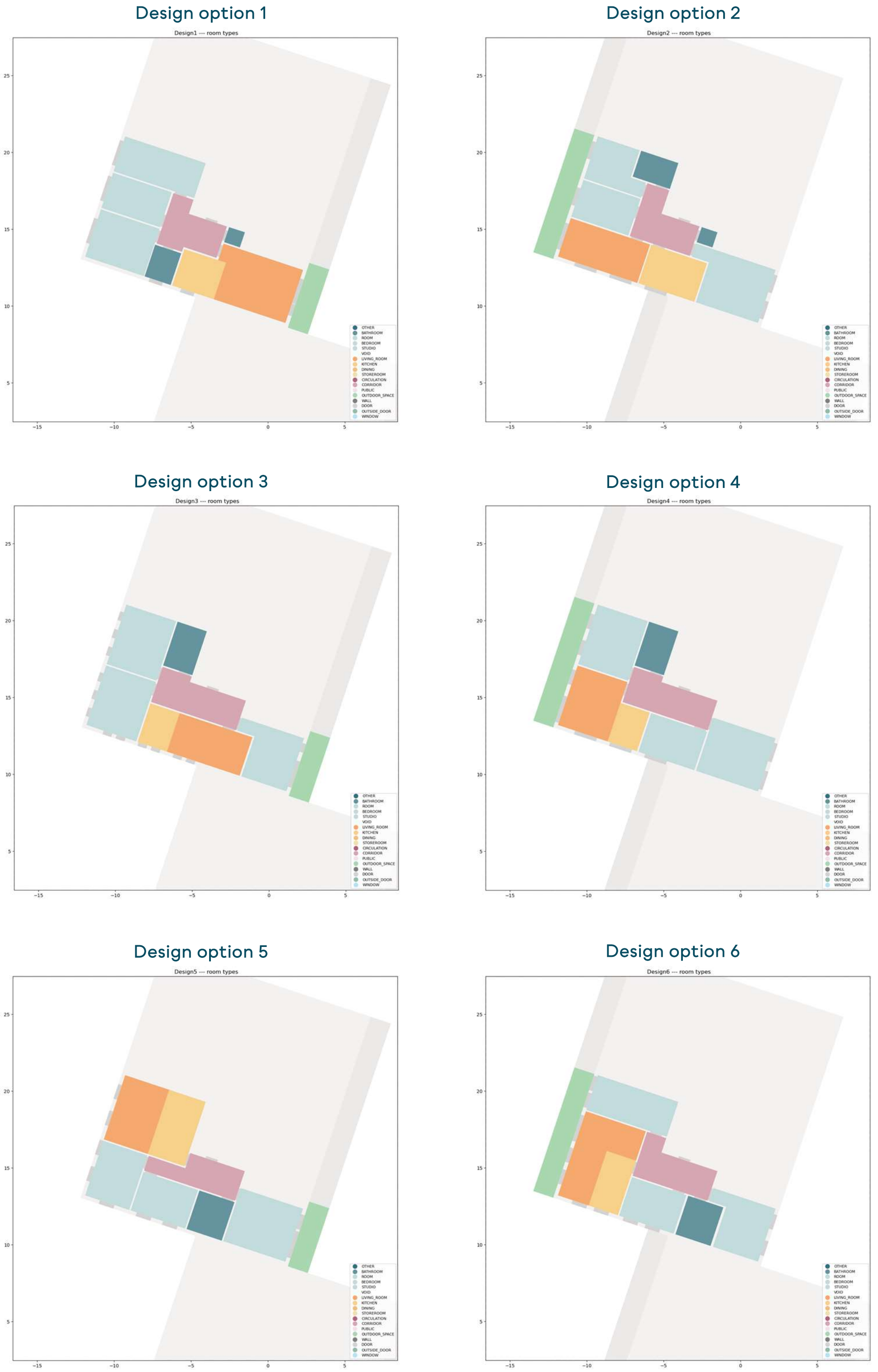

Figure 8-3: Layout design options for case study

8.2.2 Pre-processing designs

The first step is the pre-processing of the apartment layouts. Currently, this step is done based on a Rhino file with polylines. To begin, the designer must connect the Rhino file to the provided Grasshopper script and select the polylines of the designs. Then, using a Grasshopper Python component, the necessary data frame is created based on the polylines and additional information. Within the Grasshopper script, the designer must fill in the room type for each polyline and provide information on the room's elevation, height, and window height. The resulting CSV file is saved to a designated folder. Appendix G.Part I shows the Grasshopper script that connects to the Rhino design file and creates the CSV file.

The next step involves uploading the CSV file into the Python script that generates image features and numerical labels for each room. Within the framework, this step requires the most time, with sixteen seconds required to create all the image features for the six designs. Figure 8-4 shows the created image features for the design of one apartment. In this case, for design 1, a total of five images are created. Additionally, for each room, the elevation and the window-to-floor ratio are found and stored as a numerical feature in the Python script. The window-to-floor ratio is determined per room based on the designed windows, the given window height and the room size.

Figure 8-4: Image feature creation for case study design 1

8.3 Step 2 – ML predictions

The next step involves the background prediction of daylight and view values using the trained model, which takes both image and numerical features as input. This process takes approximately one second per apartment design, resulting in a total prediction time of under ten seconds for all six layout designs combined. It is important to note that the predicted labels are normalized values and must be unnormalized before they can be used in the subsequent steps. Table 24 displays the ML model's numerical output predictions for the median daylight on March 21st, p80 sky view, and unnormalized values.

Table 24: ML predictions for daylight on March 21st and sky view, case study design 1

Design nr.	Area ID	*Room name*	*Daylight Mar normalised*	*Daylight Mar [lx]*	*Sky view normalised*	*Sky view [%]*
1	100	Bedroom1	0.1337	226	0.2313	1.26
1	101	Bedroom2	0.1631	596	0.5462	2.97
1	102	Bedroom3	0.1036	365	0.2858	1.55
1	105	Kitchen	0.0779	302	0.1867	1.01
1	107	Livingroom	0.1159	303	0.0888	0.48

8.4 Step 3 – processing

Once the five labels have been predicted, the next step is to present the results in a way that is easy for designers to understand. This involves processing the predictions and overlaying them onto the layout design image. For each apartment design, twelve overviews of the results are generated, see Figure 8-5. Three levels of detail are shown for both the daylight and view predictions. Figure 8-6 illustrates the three levels of detail for one design option.

The first level of detail displays the absolute predicted value from the ML model. As discussed in Chapter 4.2, the daylight and view predictions are tested against the EN17037 guideline to determine the performance level of each room. Similarly, the performance of the placement of rooms is determined based on their main orientation. Each orientation of the room with the corresponding room type is tested against the layout evaluation method to determine the orientation performance levels.

The last level of detail is the overall performance of the apartment for each of the three aspects. The metric performance levels are tested per the layout evaluation system with the performance levels of each room. To provide an overall understanding of the apartment's quality, one overall performance label is given based on the three considered aspects: daylight, view and orientation.

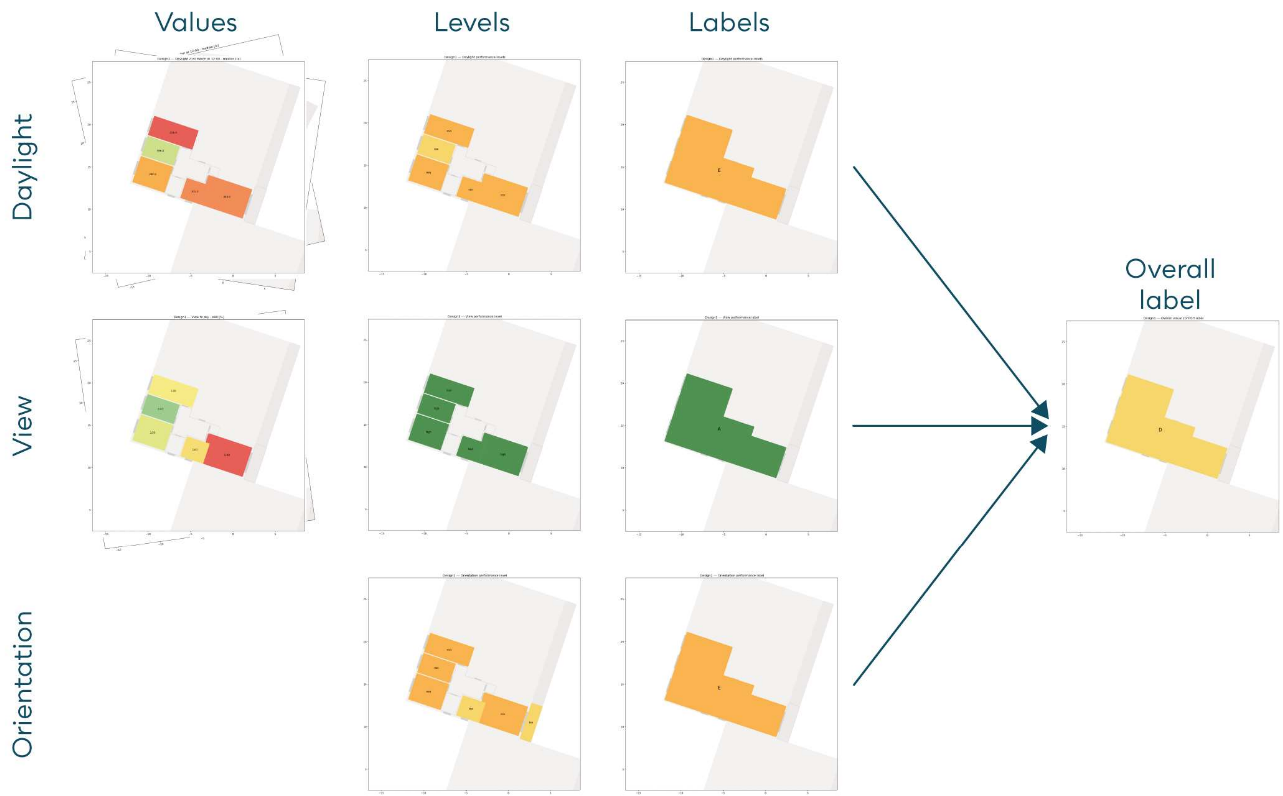

Figure 8-5: Overview processed predictions per detail level

8.4.1 Layout 1 – daylight detail levels

When zooming further into the first layout design, three levels of daylight quality can be accessed, see Figure 8-6. The first and most detailed level is the insight into the daylight illuminance values, providing insight into the predicted values for the median daylight of the room on March 21st at noon. The second level of detail showcases the daylight level of each room concerning the predicted daylight values. The daylight performance levels per room are derived from the median of the three daylight labels.

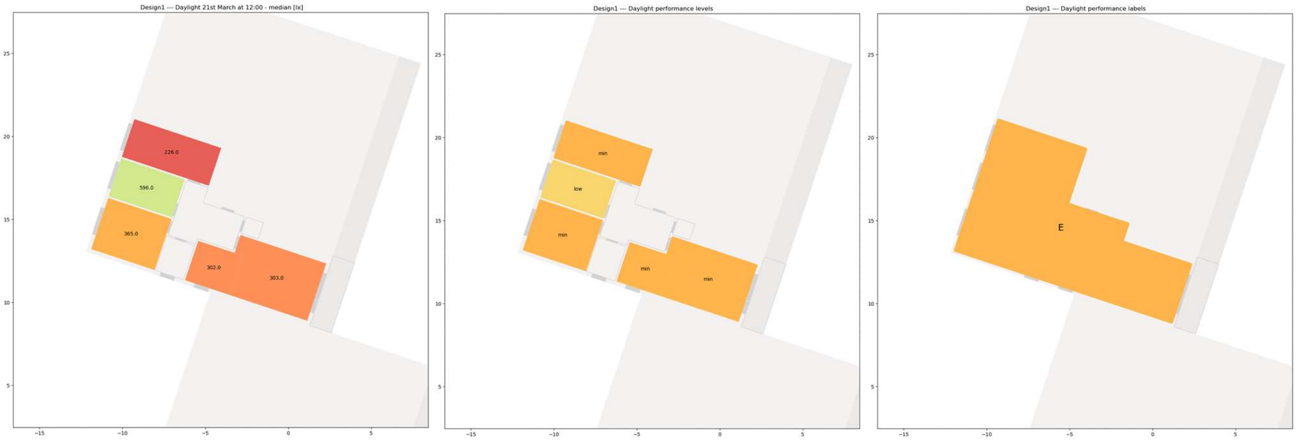

Figure 8-6: Daylight prediction results on different detail levels, design 1

The third level is the overall daylight label of the apartment. In this case, the apartment has four rooms with a minimum daylight level and one room with a low daylight level, as indicated in Table 25. The overall daylight level of the first design is E since 50% of the living spaces only meet the minimum performance level.

Table 25: Daylight performance level values and performance label, design 1

Room name	*Daylight median of 3 values [lx]*	*Daylight level*	*Overall daylight label*
Bedroom1	130	Minimum	
Bedroom2	310	Low	
Bedroom3	202	Minimum	E
Kitchen	170	Minimum	
Livingroom	171	Minimum	

8.4.2 Layout 1 – view layers detail levels

When looking into the view quality of the room, three levels of detail can be accessed, see Figure 8-7. The first and most detailed level provides insight into the view percentage for both view-to-ground and view-to-sky. This detail level showcases the predicted values for the p80 view percentage of the room. The second level of detail highlights the view performance level of each room in relation to the predicted view values and the known information about the presence of the view-to-landscape layer.

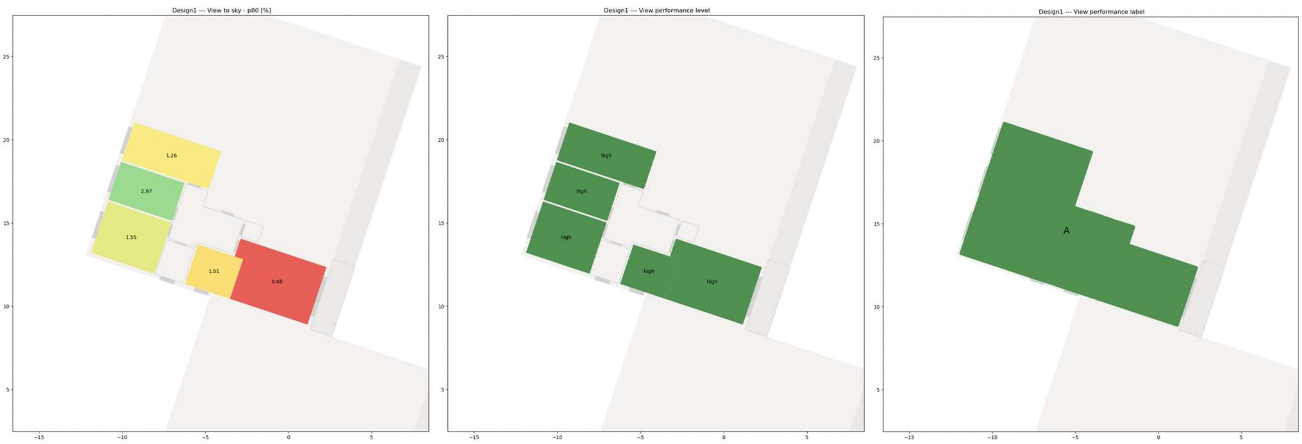

Figure 8-7: View prediction results on different detail levels, design 1

The third level is the overall view performance label of the apartment. In this case, the apartment only contains living spaces with a high view performance level, as indicated in Table 26. The overall view quality label of the first design is A since all the living spaces have a high view performance level.

Table 26: View performance level values and performance label, design 1

Room name	Ground view [%]	Sky view [%]	Landscape layer visible	Nr visible layers	View layers level	Overall view layer level
Bedroom1	0.96	1.26	Yes	3	3	A
Bedroom2	1.55	2.97	Yes	3	3	
Bedroom3	1.08	1.55	Yes	3	3	
Kitchen	0.70	1.01	Yes	3	3	
Livingroom	0.81	0.48	Yes	3	3	

8.4.3 Layout 1 – orientation detail levels

Regarding the orientation evaluation of the apartment design, two detail levels are provided, as illustrated in Figure 8-8. The first level aligns with the second level of detail in the daylight and view performance categories. The primary orientation of a room determines the orientation performance level. The corresponding orientation performance level per room is showcased in the layout design. The first level aligns with the second level of detail in the daylight and view performance categories. The primary orientation of a room and the room type determines the orientation performance level. The corresponding orientation performance level per room is showcased in the layout design.

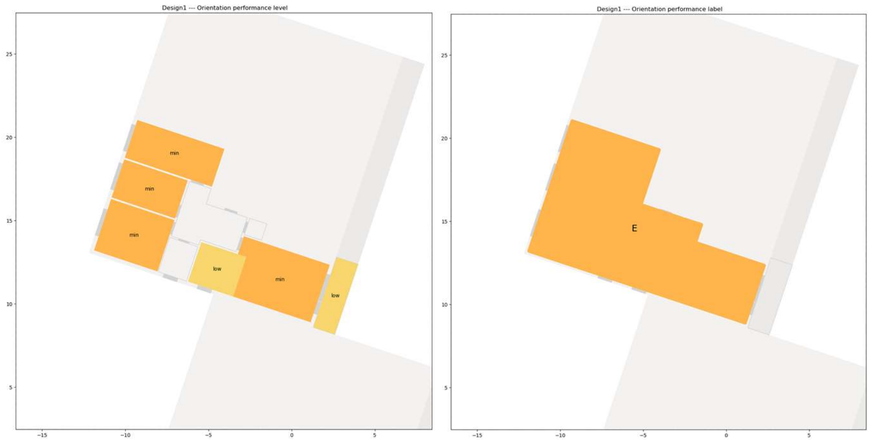

Figure 8-8: Orientation performance results on different detail levels, design 1

The second detail level is the overall orientation performance label of the apartment design. In this instance, the apartment has six spaces to test against in total since the apartment consists of five living spaces and one outdoor space. The apartment has four spaces with a minimum orientation level and two with a low orientation level, as indicated in Table 27. This results in an orientation label of E for the apartment design since four of the six spaces have a minimal orientation level.

Table 27: View performance level values and performance label, design 1

Room name	Room orientation	Orientation level	Overall daylight label
Bedroom1	West	Minimum	E
Bedroom2	West	Minimum	
Bedroom3	West	Minimum	
Kitchen	South	Low	
Livingroom	East	Minimum	
Outdoor space	East	Low	

8.5 Step 4 – optimizer

The visual comfort optimiser determines the top-performing apartment based on its overall visual comfort quality. Using the performance labels with the layout evaluation system, the overall visual comfort of each apartment can be classified. Design 1, for example, received an E performance label for daylight performance, an A performance label for view performance, and another E performance label for orientation performance. This results in the following overall performance label calculation for design 1:

$$y_{overall} = \frac{x_{day}+x_{view}+x_{orient}}{3} * pen \quad (8.1)$$

$$y_{overall,design2} = \frac{0.2+1+0.2}{3} * 1 = 0.47 \quad (8.2)$$

For the first design option, the daylight and view levels in the rooms meet the minimum requirement, so the penalty function is set to one. This, combined with the points for each performance label of the three metrics, gives an overall performance label of D for design 1. Table 28 provides a breakdown of the performance labels for the three aspects and the overall performance labels for the various layout design options.

Based on the overall performance label of each apartment, the optimiser determines the best-performing design. Figure 8-9 illustrates how the optimiser works, for example, with designs 3, 4, and 6. Out of the six provided design options, design 6 performs the best in terms of three visual comfort metrics.

Table 28: Overall performance labels per design option

Layout design nr	*Daylight label*	*View label*	*Orientation label*	*Overall label*
Layout 1	E *0.2*	A *1*	E *0.2*	D *0.47*
Layout 2	E *0.2*	A *1*	D *0.4*	D *0.53*
Layout 3	F *0*	C *0.5*	D *0.4*	F *0*
Layout 4	D *0.4*	B *0.75*	D *0.4*	D *0.52*
Layout 5	F *0*	E *0.25*	D *0.4*	F *0*
Layout 6	D *0.4*	A *1*	D *0.4*	C *0.6*

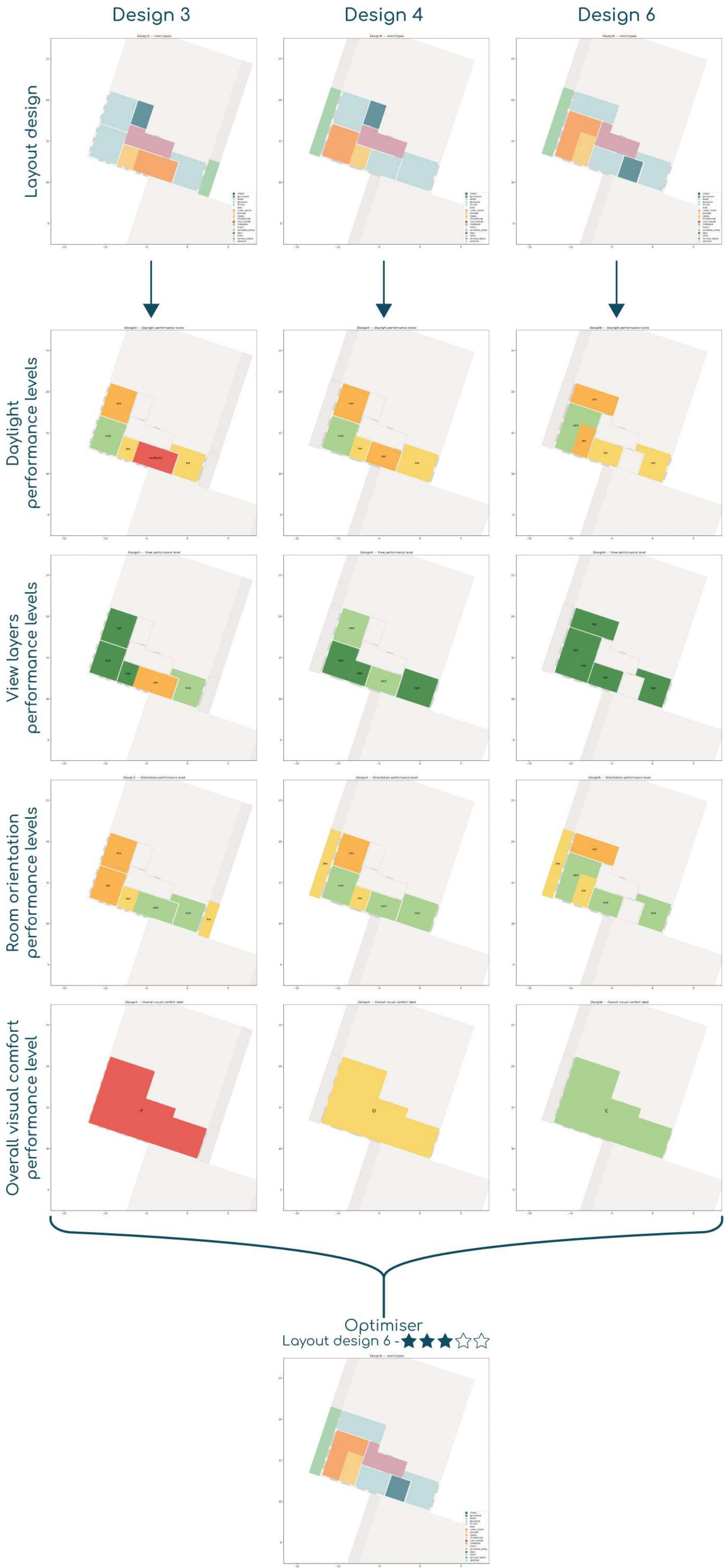

Figure 8-9: Optimiser example with design 3, 4 and 6

8.6 Step 5 – design analysis & selection

After the background process is completed, the designer is provided with direct feedback regarding the performance of each design, which facilitates comparisons between designs. Figure 8-10 compares the different room-wise daylight performance levels for all six layout designs.

Based on the performance comparison and overall apartment score for each design, the designer is able to make a performance-based decision. It is worth noting that two of the proposed designs do not reach the minimum requirements for daylight performance as per the EN17037 guideline and, therefore, could easily be excluded for further evaluation by the designer.

The feedback provided to the designer by the ML post-processor can be used in different ways. One option is for the designer to utilise the best-performing layout designs to create alternative designs based on the performance indicators if the designer is unsatisfied with the current layout designs. In this scenario, the loop of the ML design process framework is started once again from the beginning. The designer has to provide different layout options, from which an ML model makes predictions after the pre-processing step. After the ML predictions, the post-processing and optimiser will supply the designer with the tools for design evaluation once again.

Alternatively, suppose the designer is content with a layout design. In that case, the designer can select the optimal layout option based on the design problem and performance indicators, allowing the design process to progress to the next stage. According to the evaluation conducted by the designer and their expertise in the broader design task at hand, design 4 could be more suitable even though the overall best-performing apartment layout design is layout design 6. The primary difference between the performance of layout designs 4 and 6 is the level of view performance. However, design 4 reaches medium and high view performance levels in all rooms, which may suffice for the task at hand. It is crucial to mention that the ML design process framework, including the performance labels of the three metrics, is designed to support the designer. As the designs should be evaluated in the broader design context, the optimiser is not implemented in the framework to make decisions on behalf of the designer but provides a tool for the designer to make performance-based decisions.

Figure 8-10: Daylight performance levels for the different layout design options

8.7 Conclusion

The ML design framework was put to the test with a task to create a layout for a three-bedroom apartment with a living room and kitchen. To test the framework, six different layout options were created, each with varying balcony placement and room types.

With a Grasshopper component, a connection between the design process and the ML process is established. With the created CVS file from the Grasshopper component, the pre-processing step created the image and numerical features for each room. The best-performing ML model was used to predict daylight and view values for each of the six designs. Post-processing involved unnormalising the ML predictions and determining performance levels and labels using a layout evaluation system. Additionally, the visualisation step of the post-processing provides designers with hands-on tools to evaluate and compare different design options. The optimiser highlights the best-performing design based on overall visual comfort performance.

In the final step of the ML design process, the designer can make performance-based decisions based on the support from the ML model. In this step, the designer can decide on different further steps. Either the designer is satisfied and chooses the best option for the design task at hand, or the designer is not satisfied and produces new design options based on the provided feedback. In the ML design process framework, the ML predictions and optimiser provide tools for designers to make performance-based decisions without deciding for them. As the designs should be evaluated in the broader design context, the optimiser does not decide for the designer. However, the optimiser helps identify good design options and further support the designer in making performance-based decisions.

~ empty page ~

9 Conclusion

This final chapter concludes the methodology followed within the research to implement a machine learning process in the early stages of residential layout design to support designers. The chapter discusses the results of the different parts of the research, consisting of the dataset verification and analysis, machine learning evaluation and the ML process framework, respectively. Subsequently, conclusions are drawn from the results and discussion, and the research questions are answered. Lastly, the unforeseen limitations are expressed, and final recommendations are presented for any work on future work within the topic.

9.1 Discussion

This research addresses a framework to support designers during the early floorplan design process based on three performance indicators based on predictions from an ML model. In order to discuss the individual aspects, the discussion is broken into three subsections: the dataset quality, the performance of the ML model and the design process framework.

Dataset quality

The quality of the dataset utilised in the ML models played a vital role in the model's performance and evaluation of the model's predictive capabilities. A poorly constructed dataset can significantly hinder a model's ability to make precise predictions. The model's outcome could also be biased if the dataset contains inaccurate or biased information. Moreover, the methods should align with the guidelines used to classify the predictions when using a dataset with simulation results. Otherwise, the model's outcome may not align with the guidelines or be comparable with the needed requirements for performance evaluations. Therefore, it is crucial to ensure the dataset's quality and adherence to applicable guidelines to improve the reliability and usefulness of machine learning models across various applications. However, the used dataset used in this research did not follow the standard procedures of the EN17037 guidelines. This makes it hard to compare the outcome of the ML model with the requirements for the daylight and view quality assessment given by the EN17037 guideline.

ML model performance

In this research, the training direction of the ML model mainly deviated from the work of He et al., they used an image to predict daylight performance with a ResNet50 model. He et al. achieved a training loss MSE of 0.010 and a test loss MSE of 0.036 when predicting the mean illuminance with their real-case dataset. The best trained model in this research achieved a training loss MSE of 0.0012 and test loss MSE of 0.0057 for the two view labels. When only looking into the performance of the daylight median value prediction, the best-performing model in our study achieved a training loss MSE of 0.0008 and test loss MSE of 0.0047. This comparison highlights that the best trained model in this research failed to exhibit the superior predictive performance of the test loss MSE of 0.0036 from He et al. However, best trained model outperform the model of He et al. in terms of the training loss of the daylight model, this indicates that with further finetuning the model could be able to improve its accuracy and outperform the model of He et al. These findings emphasise the improved predictive capabilities of our model, especially in the context of daylight illuminance prediction.

Upon closer examination of the performance metrics, it is apparent that predicting daylight is more complicated than predicting view. The models consistently underpredict the three daylight days, resulting in feedback that skews the performance levels towards lower classes in the broader ML design process framework. This aligns with the simulation method of both metrics, where daylight simulation requires more input, computational power, and time. Looking closer into the view metrics, predicting view-to-ground values proves more challenging than predicting sky view. The evaluation shows that the sky view predictions sometimes reach an accuracy close to the desired 45-degree regression line, while the ground view values are repeatedly underpredicted.

The research delved into the impact of training an ML model using solely image features versus a combination of image and numerical features. Both the model that predicts five labels at once and the split-up models showed significant improvement when the numerical features were incorporated into the ML model. For example, model 0A, predicting only daylight values based on an image feature, achieved a test loss MSE of 0.0183. In contrast, model 3.2A, predicting only daylight values based on both an image feature and numerical features, achieved a test loss MSE of 0.0058. These findings emphasise that training an ML model with both an image feature and numerical features improved the predictive capabilities of a model significantly. However, model 0 was not fine-tuned, and early stopping was applied after ten epochs, as opposed to twenty-five epochs for model 3.2, which could account for the inferior performance of model 0.

Additionally, the research delved into the impact of using a pre-trained model for the ResNet50 model. The success of machine learning models that use pre-trained weights heavily relies on the compatibility between the pre-trained data and the task at hand. Pretrained models may not perform as well when applied to tasks that differ significantly from their training data. In this case, a pre-trained ResNet is used as a base model for the first two ML models that were trained with ImageNet, a dataset consisting of natural images. Using this pre-trained model for tasks that involve specialised or non-natural images may result in suboptimal performance. This could explain why the first two models were not performing that well and especially the second model did not stabilise during training. This indicates that using a pre-trained model that did not align with the task at hand was not beneficial.

During this research, several ablation studies were conducted regarding the architecture of the ML model. The ablation studies encompassed the splitting up of the model, testing different architectures, fusing moments, ResNet base models, and hyperparameter adjustments. The results of the ablation studies revealed a more accurate ML model, and the findings indicate a direction towards further investigation for better model improvement. The following section discusses the different experiments and proposes a final improvement direction.

The results of the experiments indicated that splitting up the model significantly improved its performance. Splitting up the multimodal ML model 3.2 resulted in a test loss MSE reducing from 0.0082 to a test loss MSE of 0.0057 for daylight and a test loss MSE of 0.0068 for view. This observation aligns with the difference in learning tasks when comparing the patterns that need to be learned for daylight predictions with those for view predictions. Nonetheless, it is worth mentioning that for future investigation, splitting up the ML model requires a critical eye since it substantially elevates the computational demands of the ML model training. Therefore, a finetuned model should be checked to determine whether the finetuned model architecture would perform as well on one ML model for predicting both performance metrics.

Upon closer examination of the experiments conducted on the different architecture layers and fusing moments, one experiment stood out. The late fusion experiment of model 5.2A achieved a lower training MAE of 0.0325 than the training MAE of 0.0332 of model 3.2A. Additionally, in terms of validation loss MSE, model 5.2A converged earlier, achieving a test loss MSE of 0.0064, while model 3.2A achieved a test loss MSE of 0.0057. These observations suggest that the late fusion model was able to learn more during training but did not outperform in terms of test performance. However, this indicates that late fusing model 5.2A shows potential, but further architecture layer and hyperparameter adjustments are necessary to make the model perform better.

The hyperparameter adjustments demonstrated interesting results and provided a clear direction for future investigation. Lowering the batch size to 32 or increasing the dropout or L2 regularization rate did not improve the training. However, lowering the dropout rate significantly improved the test loss MSE from 0.0057 to 0.0055 and the test MAE from 0.0503 to 0,0484. Lowering both the dropout rate and L2 regularization rate resulted in an improved test loss MSE of 0.0047 and test MAE of 0.0440.

Based on all these observations, the future direction of training the ML model should focus on investigating late fusion further. Additionally, a fine balance between a lower dropout rate and L2 regularization should be further examined to optimize the hyperparameters for better model performance.

In contrast to He et al.'s research, this study employed a coloured image feature, which could drastically influence the ML model's performance. To comprehensively assess this impact, it is advisable to examine variations of colour usage in the image features. In addition to examining the variance in colour, it is critical to investigate all the elements present in the image. This approach could result in an optimal image feature that is customized to the specific objective at hand.

Lastly, the cleansing of the dataset played a crucial role in this procedure. The dataset cleaning played an essential role in this study because the study utilized an available dataset that contained a substantial amount of extraneous information. It was essential to explore the dataset's full potential and eliminate subpar data. Nevertheless, it is imperative to consider the data cleansing process since it is plausible that valuable information may have been inadvertently discarded or that the data may have been altered unfavourably, resulting in unintended outcomes. Therefore, the data cleaning of the dataset might have affected the model's performance.

ML design process framework

When analysing the usability of the created framework for assessing the overall apartment quality, it is essential to critically evaluate how this method distributes the data among the classes. One crucial factor to consider is whether all labels tend to cluster in either the lowest or highest class, this would indicate that the created layout assessment framework is ineffective. The success of the layout assessment framework depends on its ability to effectively distribute data across all classes, as an imbalanced distribution can skew results and make the assessment less informative. Therefore, it is crucial to carefully examine the data distribution within the framework to determine its effectiveness and relevance.

Based on the current dataset, it appears that the performance level view from EN17037 is skewed towards the high-performance class. This is likely due to the mountainous terrain in Switzerland, which falls under the landscape view class, as well as the prevalence of greenery in rural areas. Since Switzerland consists of more rural areas with plenty of greenery instead of densely populated urban environments, this could explain the high presence of all three layers in numerous rooms.

As for the performance level daylight, the dataset shows a good distribution. However, it should be noted that the daylight values are lower than if they had followed the EN17037 guideline, resulting in more rooms with insufficient performance levels. This is reflected in the skewed distribution towards the lower side for daylight performance labels per apartment per the proposed layout evaluation system. Nevertheless, it is important to note that this does not necessarily indicate that the given class distribution method by the layout evaluation system needs correction, as the dataset itself contains lower daylight values than expected.

9.2 Conclusion

This research aims to answer the question: "How can a machine learning process support designers with evaluating and optimising residential layouts for daylight and view performance during the early design phase?". To conclude the main research question, the part below presents the findings on the raised sub-questions.

What are the guideline requirements for daylight and view quality in residential spaces?

The EN17037 guideline ensures the quality of indoor spaces by providing specific requirements for residential spaces regarding the view and daylight quality. To ensure adequate daylight quality, the guidelines set a minimum target illuminance level of 300 lux across at least 50% of the space. However, it is important to note that the UK national annexe recognises that this threshold may not always be achievable in dwellings while the spaces themselves still provide sufficient daylight for the intended use. Therefore, the UK national annexe introduces additional levels that should be considered to ensure that daylight requirements align with the specific purposes of different rooms. As for view quality, the EN17037 guidelines evaluate it based on three key aspects: the horizontal sight angle, the distance to the outside view, and the number of view layers providing comprehensive criteria to assess the quality of the visual environment.

How do daylight and view quality affect the overall quality of residential spaces?

The performance of daylight and view quality significantly impacts the overall quality of residential spaces. Adequate daylight exposure has been linked to several aspects of human well-being, including improved sleep patterns, increased energy levels, enhanced mood, and better cognitive performance. Furthermore, a good view from a window can reduce discomfort, stress, and negative emotions, contributing to overall mental well-being. Properly utilising natural daylight reduces the need for artificial lighting, leading to lower energy consumption and a smaller carbon footprint for buildings, enhancing energy efficiency and reducing energy costs for residents. Moreover, incorporating daylight and views in residential spaces promotes a connection to the natural environment, contributing to overall satisfaction and a higher quality of life for occupants.

What design parameters impact the performance of daylight and view in residential spaces?

Several design parameters significantly impact the performance of daylight and view in residential spaces. The building orientation is crucial, as it determines the amount and duration of sunlight and views received within interior spaces. Window size, shape, and placement are also critical, as they influence the distribution of daylight within interior spaces. Well-placed and appropriately sized windows can maximise natural light penetration and enhance view quality. Additionally, interior layout plays a vital role, as the arrangement of rooms and furniture can affect the accessibility and enjoyment of views and daylight. Proper orientation of room types can optimise solar heat-control natural lighting gain and align with usage timeframes and sunlight availability. Optimising the layout for optimal use of daylight and views is crucial for creating well-designed residential spaces that promote well-being, energy efficiency, and sustainability.

What is the most appropriate machine learning model for predicting daylight and view quality in residential spaces?

A multimodal machine learning model utilising a ResNet and fully connected network is the most effective for predicting daylight and view quality in residential spaces. While previous research has primarily focused on artificial neural networks for assessing daylight performance, they struggle with translating rough sketches and 2D drawings into numerical data during the early stages of architectural design. One study used a grayscale image with geometrical data to train a Convolutional Neural Network (CNN) to predict daylight performance, aligning more closely with real-world design scenarios. However, it lacks additional numerical values, necessitating a translation process. The proposed multimodal model overcomes these challenges by combining image and numerical data, demonstrating its potential for predicting visual comfort in indoor spaces and filling the research gap in assessing view quality during the early phases of architectural design.

How can a machine learning model be incorporated into the layout design process to assist designers?

A novel workflow has been developed to integrate ML models seamlessly into the architectural design process. Designers upload their layout designs into a dedicated tool, where the layout designs are pre-processed for compatibility with the ML model. Subsequently, the ML model predicts daylight and view values, which are then translated into practical visual representations during a post-processing step. Based on a layout assessment method guided by EN17037 requirements, an optimisation step identifies the optimal apartment layout. At the same time, it gives designers the space to specify their optimisation focus. This approach gives designers direct feedback on different layout options, enabling informed decisions that enhance residential layout quality and performance throughout the design process. Overall, this framework represents a significant advancement in integrating ML models into architectural workflows by systematically evaluating daylight, view quality, and room orientation, providing visual feedback, and offering optimisation suggestions that align with contemporary design standards and requirements.

What quantitative metrics can be utilised in the design process to evaluate and optimise residential layouts for daylight view performance?

A multifaceted approach is proposed to assess and optimise residential layouts for visual comfort, which includes a novel layout evaluation system that systematically evaluates daylight, view and orientation quality in each room. Furthermore, the layout assessment provides a comprehensive understanding of the entire apartment layout's visual comfort quality. An orientation evaluation system is introduced to assess room orientations, which is critical for optimising visual comfort potential in residential apartments. This orientation assessment is integrated with daylight and view quality evaluations, resulting in a holistic assessment of layout quality that considers the interplay of these three critical factors: daylight, view, and room orientation.

How can a machine learning process support designers with evaluating and optimising residential layouts for daylight and view performance during the early design phase?

Based on the findings of the sub-research questions, the main research question can now be addressed. In order to effectively incorporate an ML model for daylight and view predictions into the early phase layout design process, an additional background process is required. This process comprises three main components: pre-processing, predictions, and post-processing. Post-processing is particularly crucial, as it enables the implementation of the ML predictions into the design process by displaying the predictions on the layout designs.

To support designers in evaluating and optimising layout designs regarding daylight and view performance, a layout evaluation system based on guidelines should be integrated into the framework to measure the quality of the designs objectively. The integrated layout evaluation system provides a thorough assessment of the visual comfort quality of an entire apartment layout design, enabling designers to evaluate the provided design options. Furthermore, the layout evaluation system allows for the utilisation of an optimiser to achieve the optimal design solution regarding the visual comfort performance of an apartment layout.

9.3 Limitations

The research that was carried out could have been more extensive due to several factors. Three main limitations can be recognised in this study, namely the limitations of the utilised dataset, the limitations of the training process of the ML model and the limitations of the evaluation framework.

Dataset

Firstly, the "Swiss dwellings" dataset brought about several restrictions. The dataset utilised did not contain simulation results that were in accordance with European standards. Therefore, the proposed layout evaluation system does not correspond to the dataset simulation outcomes. The layout evaluation system tests each apartment against the given EN17037 guideline requirements, which are based on simulation results following the required method.

Due to the limitations of the dataset, several key design aspects were not incorporated into the research. For instance, due to privacy reasons, the actual environmental obstructions of the different sites were not included in the dataset but were encoded into the various view categories. In this research, the encoded environmental obstructions were used to incorporate the environmental obstructions; however, optimally, the placement of the different obstructions should be incorporated into the image feature.

ML training process

The main objective of this research was to evaluate the possibility of utilising an AI tool in the predesign process, which limited the research of training the ML model. Furthermore, due to time limitations, intensive training of the ML models and fine-tuning hyperparameters could not be extensively researched. This includes different ML model setups, fine-tuning the layer density, using different regularisation methods, and investigating other hyperparameter combinations.

Due to time constraints, a set of features was decided from the start of the model training. However, an opportunity lies here to research the optimal image feature by evaluating which aspects to include in the image and which features perform better as numerical features. The choice of numerical features could be further investigated by testing out more or less numerical features and different combinations of numerical features.

Additionally, during the training of the ML model, only 40% of the complete dataset was utilised due to the available computation power and time constraints, which limited the investigation in the use of the complete dataset to improve the ML model's performance.

Evaluation framework

In terms of the layout evaluation system, time constraints resulted in only five labels being predicted by the machine learning model. Consequently, this leads to an incomplete daylight and view analysis to evaluate the quality of an apartment based on the EN17037 guideline. Moreover, the layout evaluation system provides a general overview of apartment performance indicators, but a more comprehensive evaluation method requires further investigation. Thus, it is essential to conduct more extensive research to address these limitations and improve the study's findings.

9.4 Future development

Integrating an ML model into an architecture predesign process presents promising possibilities for assisting designers in making performance-based judgements for residential layout designs based on daylight and view quality. Several areas of future development arise in this field. This chapter describes five future development directions, including ML model optimisation, feature exploration, dataset relevance, and translations, including more building physics performance indicators and the broader application of the ML process framework.

ML model optimisation

Research could be carried out to investigate which ML architectures yield the highest performance for predicting daylight and view values based on room-wise layout designs. Additionally, a more thorough review of the impact of fine-tuning the ML model could be carried out to evaluate which hyperparameters could improve the performance of the ML model.

Feature exploration

Environmental characteristics, layout geometry, and contextual data could all be investigated as valuable elements to add to the ML model. Research could also determine the best layout of image features, evaluating the usage of colour coding on the image. Additionally, the differentiation between image and numerical features and selecting the best option for each feature could be explored. Another opportunity lies in further investigating outliers of the predictions and addressing these outliers differently on the image feature. For example, one of the earlier discussed outlier room types is an area that is located in a bigger space, such as a kitchen in a living room. Colour coding such a space with indirect access to windows differently from traditional room types could improve the performance of the ML model.

Another research direction is investigating the effect of environmental obstacles on image features. The research should be carried out with a dataset that includes environmental context placement, so the image feature includes the actual placement of trees and neighbouring buildings. This research will result in a better representation of how designers work during the predesign process.

Dataset relevance and translations

Research could be done to investigate the use of different datasets. Different dataset types could be investigated, such as datasets, including offices or public buildings. With this, the layout evaluation system must be reevaluated to adjust to the dataset. Additionally, methods could be explored to transform existing datasets with simulations that do not follow guideline principles to dataset formats aligning with the simulation assessment of guidelines. With this research, the existing datasets could be utilised in the ML process framework. Furthermore, research should be done toward merging different datasets with buildings in different countries for a more diverse dataset, which allows the application of the ML model to more situations.

Additional building physics performance indicators

To incorporate the ML process framework to a multi-performance assessment, the scope of the performance indicators has to be broadened. Research has to be done to encompass additional building physics aspects such as thermal comfort, acoustics and energy performance.

Alternatively, the model could also be extended to predicting different daylight labels on different days and times of the year, and the model could be broadened by including different view category labels. This way, a more comprehensive analysis of the entire layout performance could be done. Besides the daylight and view performance metrics, other performance indicators could be added to the ML design process framework.

Broader framework application

The application of the ML process framework could be broadened by implementing the framework on different scales. The current framework goes until the apartment level scale. However, opportunities lie in adjusting the framework to an entire floor and, subsequently, an entire building. With this implementation, the internal layout of individual apartments will be optimised, and the division of apartments on floors and the best placements of different apartment types on a floor will be addressed. In addition to predicting daylight and view values, the ML model could generate new layout alternatives optimised for daylight and view qualities. This would result in a process where the designer does not only receive direct feedback on the performance of a layout design but also receives alternative design options to move on within the design process.

Furthermore, investigating implementing more design decisions into the framework could broaden the framework application. For example, adding design decisions that are not easily translated into numerical values. However, to implement such design performances, an investigation towards a suitable quantification method is needed to quantify those design aspects and utilise an optimiser. The integration of ML models into the architectural predesign process has the potential to revolutionise the field and provide designers with data-driven insights that can enhance the performance of their designs.

~ empty page ~

10 Reflection

REFLECTION

The goal of this master's thesis was to explore the applicability of an ML process within an architectural design process. The resulting ML process framework came from researching the available dataset and testing how it could be used in a design process. Through this process, I developed my own ML process framework and evaluation system to support designers in the early design phases when making performance-based decisions. The final goal was to take the first step to apply an ML tool into the predesign phase while testing the visual comfort performance indicators against guidelines. This chapter covers a reflection on the master thesis process in two parts: the graduation process and the social impact of the master thesis.

GRADUATION PROCESS

How is your graduation topic positioned in the master track building technology?

The Building Technology Master track is part of the Master Architecture, Urbanism and Building Sciences (MSc AUBS). It covers topics that cover the bridge between architectural design and engineering and focuses on innovation within these two fields. The master tracks consist of five chairs that relate to different parts of the environment design field. The master's program has an interdisciplinary focus with freedom for students to explore other directions and topics within the Building Technology field. Building Technology focuses on multidisciplinary problems that require innovative solutions by integrating design and technical disciplines.

This thesis, "visual comfort l(AI)outs", relates to two chairs within Building Technology. Firstly, the Design Informatics direction focuses on generating a machine learning tool to find the interior layout parameters that affect the daylight and view and to find the optimal layouts based on this. Secondly, Climate Design is integrated to create visually comfortable residential layouts. Combining the two fields allows me to explore a design topic through fundamental and new arising topics within the built environment. Additionally, connecting these two fields broadens the possibilities of optimising everyday design tasks through Artificial Intelligence. With this workflow, AI can contribute to efficiently assisting designers and engineers in the early decision-making stage of residential layout exploration.

How are research and design related?

The complicated relationship between research and design has been essential to this graduation process. Where I tried to push the decision-making process during a design towards based on knowledge within the field and earlier done research. The moment when the performance indicator evaluation happens in a design process is a critical difference between a typical design approach and my study's approach. Traditional design processes often analyse the performance indications at the end of the design process, leading to decisions that are only possible within the limited boundaries left at the project's later stages. With this design framework, the performance indicators are tested at the beginning stage of a design when the boundary conditions are still wide and open. This method encourages creativity and imaginative problem-solving, allowing for more flexible solutions to unanticipated challenges.

The research observed that the orientation of rooms is only sometimes chosen wisely within the existing dwelling dataset, potentially leading to more energy consumption and less comfortable living spaces for occupants. My framework integrates research findings for optimal room orientations into the design process. By recognising opportunities for improving visual comfort from the start of a project, the design process is led toward better performance from the beginning of the project.

What value did your approach and methodology bring to your thesis?

The method used for this research has several strengths and weaknesses. Weaknesses can be recognised by the model training's trial-and-error approach, which came together with my limited expertise in the machine learning domain. Strengths can be found in the scientific method in analysing the data and the helicopter view approach while creating the framework.

A weakness in the used method is that training an ML learning model is a trial-and-error process, resulting in a time-consuming task to fine-tune and train the models. Additionally, using deep learning models results in untransparent correlations that the model discovers during the training but are not accessible to understand fully. Because of this, the trial-and-error method is needed to train a model and reflect on the effect of the adjusted parameter. Additionally, my lack of in-depth knowledge and experience in machine learning hindered my ability to understand and address arising challenges during the model training fully.

The thorough examination of data and the ability to spot opportunities within the data while methodically removing noise are distinguishing strengths of the research technique used in this study. This careful data analysis methodology ensured that the research findings were robust and highly valuable. The investigation obtained vital information that might have remained concealed by closely going through the data. Another strength is the approach to examining the implementation of an ML model within the broader context of the built environment from a helicopter perspective. This overall perspective enabled a thorough evaluation of the ML model's effectiveness in real-world circumstances. Instead of focusing primarily on technical elements, the study included how the model may be realistically incorporated into architectural design.

What moral or ethical issues did you encounter during the process?

Ethical issues were critical in developing the research approach throughout the machine learning process. The dataset includes human-generated and human-selected data, inevitably leading to biases within the ML model. To achieve fair and equal outcomes, it was critical to address these biases before training the model.

Furthermore, the dataset's anonymity provided a difficulty, reducing the amount of information accessible for the study. Notably, the dataset did not include real environmental obstacles of the structures and natural objects, which was done to protect residents' privacy. To overcome this issue, I proposed an approach that uses simulation results to replicate real-world environmental obstructions, allowing the expression of potential obstacles while maintaining privacy. These ethical issues emphasised the importance of a balanced strategy that protects privacy while pursuing complete and fair research results.

Social impact

To what extent are the results applicable in practice?

The framework created as part of this research has potential for practical applications. The framework makes machine learning more accessible to professionals within the architectural field by streamlining its incorporation into the architectural design process. The framework's processing element generates a user-friendly structure for designers, and its simplicity of use suggests that architects might quickly adopt it as a tool to optimise building layouts for visual comfort during the early phases of a design.

To what extent is the projected innovative?

In the current built environment industry, collaboration between designers and AI for design guidance still needs to be improved. My framework makes a step further towards closing this gap. Applying my design framework can encourage designers to interact with AI and utilise its potential to improve design results.

How does the project contribute to sustainable development?

The ISO-15392 (2019) describes that standard sustainability involves three mutually interrelated aspects: environmental, economic, and social. This study can potentially contribute to sustainable development by directly or indirectly touching all three elements. Improving the daylight quality of a room tackles the environmental aspect indirectly. Applying the ML framework to design apartment layouts optimised for daylight and view quality can reduce energy consumption in buildings since good daylight performance results in lower electricity demand, which increases the sustainability of a building.

This research touches on all three aspects of sustainable design: people, planet, and profit. This research takes a crucial step toward decreasing our environmental impact by having the potential to reduce energy consumption in buildings. Additionally, incorporating excellent visual comfort and scenic views into apartment designs increases property prices, which benefits both property developers and homeowners.

Improved visual comfort in houses can significantly enhance inhabitants' well-being and general health, eventually leading to a higher quality of life. This aspect places the people at the heart of the building while designing for them. Daylight can have a significant impact on the social well-being of residents. Adequate natural light increases the comfort of the space and can improve mood, reduce stress, and promote the overall health and productivity of occupants. Natural lighting and view to the exterior can also create a sense of connection to the outdoors and promote a sense of community within a building. Furthermore, a lack of natural lighting can make a space feel cramped and uninviting and contribute to feelings of isolation and depression. Architects must consider the social impact of daylight and view when designing apartment buildings, mainly since people spend most of their time indoors.

How does the project affect architecture/the built environment?

This framework could lead to a completely different way of working for architects because they could get direct feedback on their layout design concerning visual comfort. In this way, designers can consider building performances from the beginning of the design process so that design choices will be made differently. Additionally, facilitating designers with a tool tackles the economic aspect because the designers will have fewer repetitive tasks. Designers can focus on the more creative tasks of a design when they have fewer repetitive tasks.

~ empty page ~

References

References

Anderson, S. R. (2003). *Health and design* [Texas Tech University]. http://hdl.handle.net/2346/50045

Arbab, M., Rahbar, M., & Arbab, M. (2021). A Comparative Study of Artificial Intelligence Models for Predicting Interior Illuminance. *Applied Artificial Intelligence*, *35*(5), 373–392. https://doi.org/10.1080/08839514.2021.1882794

Aries, M., Aarts, M., & van Hoof, J. (2015). Daylight and health: A review of the evidence and consequences for the built environment. *Lighting Research & Technology*, *47*(1), 6–27. https://doi.org/10.1177/1477153513509258

Ayoub, M. (2019). 100 Years of daylighting: A chronological review of daylight prediction and calculation methods. *Solar Energy*, *194*, 360–390. https://doi.org/10.1016/j.solener.2019.10.072

Ayoub, M. (2020). A review on machine learning algorithms to predict daylighting inside buildings. *Solar Energy*, *202*, 249–275. https://doi.org/10.1016/j.solener.2020.03.104

Baheti, P. (2021). Activation Functions in Neural Networks. *V7labs*. https://www.v7labs.com/blog/neural-networks-activation-functions

Bayoudh, K., Knani, R., Hamdaoui, F., & Mtibaa, A. (2022). A survey on deep multimodal learning for computer vision: Advances, trends, applications, and datasets. *The Visual Computer*, *38*(8), 2939–2970. https://doi.org/10.1007/s00371-021-02166-7

Bell, J. A. M. (1973). Development and practice in the daylighting of buildings. *Lighting Research & Technology*, *5*(4), 173–185. https://doi.org/10.1177/096032717300500401

Bhavsar, P. (2019). TransferLearning_Bhavsar.pdf. *Medium*. https://medium.com/modern-nlp/transfer-learning-in-nlp-f5035cc3f62f

Bishop, C. M. (2006). *Pattern recognition and machine learning* (M. Jordan, J. Kleinberg, & B. Scho¨lkopf, Eds.). Springer.

Boyce, P. R. (2003). *Human Factors in Lighting* (Second Edition). Taylor and Francis.

BREEM. (2021). *BREEAM Hea 01 Visual Comfort .pdf* (V 6.0; International New Construction). Building Research Establishment Environmental Assessment Methodology. https://files.bregroup.com/breeam/technicalmanuals/sd/international-new-construction-version-6/?utm_campaign=2241538_BREEAM%20NEW%20NC%20manual%20downloads&utm_medium=email&utm_source=BRE&dm_i=47CQ,1C1KY,860N7G,667EQ,1#05_health/hea_01_nc.htm#Daylighting_uniformity_criteria.

Brembilla, E., Azadi, S., & Nourian, P. (2021, September 1). *A computational approach for checking compliance with European view and sunlight exposure criteria*. 2021 Building Simulation Conference. https://doi.org/10.26868/25222708.2021.30353

BSI. (2019). *Daylight in buildings* (English version). British Standards Institution ; European Committee for Standardization.

Collins, B. L. (1976). Review of the psychological reaction to windows. *Lighting Research & Technology*, *8*(2), 80–88. https://doi.org/10.1177/14771535760080020601

Corrodi, M., Spechtenhauser, K., & Auer, G. (Eds.). (2008). *Illuminating: Natural Light in Residential Architecture* (1. Aufl). Birkhäuser.

Costa, C. D. (2019). The Difference between AI, ML, and Deep Learning. *Towards Data Science*. https://medium.com/@harish_6956/the-difference-between-artificial-intelligence-machine-learning-and-deep-learning-b68cdf684633

Dogan, T., & Park, Y. (2019). A critical review of daylighting metrics for residential architecture and a new metric for cold and temperate climates. *Lighting Research & Technology*, *51*(2), 206–230. https://doi.org/10.1177/1477153518755561

Edwards, L., Torcellini, P., & Laboratory, N. R. E. (2002). *A Literature Review of the Effects of Natural Light on Building Occupants*. 58. https://doi.org/10.2172/15000841

Elements of AI. (n.d.). [Educational]. Elements of AI. Retrieved January 15, 2023, from https://www.elementsofai.com/

EN 17037: Daylight in Buildings (NEN-EN 17037). (2018).

Fedak, V. (2018). Demystified: AI, Machine Learning, Deep Learning. *Towards Data Science*. https://towardsdatascience.com/demystified-ai-machine-learning-deep-learning-c5259d38678e

Figueiro, M. G., Steverson, B., Heerwagen, J., Kampschroer, K., Hunter, C. M., Gonzales, K., Plitnick, B., & Rea, M. S. (2017). The impact of daytime light exposures on sleep and mood in office workers. *Sleep Health*, *3*(3), 204–215. https://doi.org/10.1016/j.sleh.2017.03.005

Géron, A. (2019). *Hands-on machine learning with Scikit-Learn, Keras, and TensorFlow* (Second edition). O'Reilly.

Giblett, R. G. H., Lofthouse, J. C. R., & Sharp, R. W. N. (1970). *The Lighting of Buildings*. Building Research Establishment.

Gifford, R. (1995). Natural psychology: An introduction. *Journal of Environmental Psychology*, *15*(3), 167–168. https://doi.org/10.1016/0272-4944(95)90000-4

Han, J., Kamber, M., & Pei, J. (2012). *Data mining: Concepts and techniques* (3rd ed). Elsevier/Morgan Kaufmann.

Hasenmaile, F., Lohse, A., Rieder, T., & Waltert, F. (2019). *LocationLocationFloorPlan*. Credit Suisse AG, Investment Solutions & Products. https://www.credit-suisse.com/ch/en/articles/private-banking/schweizer-immobilienmarkt-2019-kaufen-ist-derzeit-guenstiger-als-mieten-201903.html

He, K., Zhang, X., Ren, S., & Sun, J. (2015). *Deep Residual Learning for Image Recognition* (arXiv:1512.03385). arXiv. http://arxiv.org/abs/1512.03385

He, Q., Li, Z., Gao, W., Chen, H., Wu, X., Cheng, X., & Lin, B. (2021). Predictive models for daylight performance of general floorplans based on CNN and GAN: A proof-of-concept study. *Building and Environment*, *206*, 108346. https://doi.org/10.1016/j.buildenv.2021.108346

Hellinga, H. Ij. (2013). *Daylight and view: The influence of windows on the visual quality of indoor spaces*. s.n.

Heschong, L. (2021). *Visual delight in architecture: Daylight, vision and view*. Routledge.

Hopkinson, R. G. (1963). *Architectural Physics: Lighting*. H.M. Stationery Off.

IES, I. E. S. (2012). *Spatial Daylight Autonomy (sDA) and Annual Sunlight Exposure (ASE)*.

ISO 15392. (2019). ISO.

Kaplan, R. (2001). The Nature of the View from Home: Psychological Benefits. *Environment and Behavior*, *33*(4), 507–542. https://doi.org/10.1177/00139160121973115

Kent, M., & Schiavon, S. (2020). Evaluation of the effect of landscape distance seen in window views on visual satisfaction. *Building and Environment*, *183*, 107160. https://doi.org/10.1016/j.buildenv.2020.107160

Kharvari, F. (2020). An empirical validation of daylighting tools: Assessing radiance parameters and simulation settings in Ladybug and Honeybee against field measurements. *Solar Energy*, *207*, 1021–1036. https://doi.org/10.1016/j.solener.2020.07.054

Klepeis, N. E., Nelson, W. C., Ott, W. R., Robinson, J. P., Tsang, A. M., Switzer, P., Behar, J. V., Hern, S. C., & Engelmann, W. H. (2001). The National Human Activity Pattern Survey (NHAPS): A resource for assessing exposure to environmental pollutants. *Journal of Exposure Science & Environmental Epidemiology*, *11*(3), 231–252. https://doi.org/10.1038/sj.jea.7500165

Ko, W. H., Kent, M. G., Schiavon, S., Levitt, B., & Betti, G. (2022). A Window View Quality Assessment Framework. *LEUKOS*, *18*(3), 268–293. https://doi.org/10.1080/15502724.2021.1965889

Kolarevic, B. (2003). *Computing the Performative in Architecture*. 457–464. https://doi.org/10.52842/conf.ecaade.2003.457

Kuhlenengel, M., Waters, C. E., & Konstantzos, I. (2019). Assessing the impact of outside view on learning: A close look to EN 17037 'view out' practices through the analysis of 220 classrooms. *Journal of Physics: Conference Series*, *1343*(1), 012159. https://doi.org/10.1088/1742-6596/1343/1/012159

Leed v4.1. (2020). U.S.Green Building Council. https://www.usgbc.org/credits/multifamily-existing-buildings/v4/eq122?view=language&return=/credits/Multifamily%20Existing%20Buildings/v4

Le-Thanh, L., Nguyen-Thi-Viet, H., Lee, J., & Nguyen-Xuan, H. (2022). Machine learning-based real-time daylight analysis in buildings. *Journal of Building Engineering*, *52*, 104374. https://doi.org/10.1016/j.jobe.2022.104374

Littlefair, P. J., King, S., Howlett, G., Ticleanu, C., & Longfield, A. (2022). Site layout planning for daylight and sunlight. *2nd*. https://doi.org/ISBN 978-1-84806-483-6

Loe, D., Watson, N., Rowlands, E., Mansfield, K., Venning, B., & Baker, J. (1999). *Lighting design for schools*. Stationery Office.

MacLeamy, P. (2004). *Collaboration Integrated Information And The Project Lifecycle*.

Mardaljevic, J., Andersen, M., Roy, N., & Christoffersen, J. (2011). Daylighting Metrics for Residential Buildings. *Proceedings of the 27th Session of the Commission International de l'Eclairage*, *CIE 197:2011*, 93–111.

McGregor, A., Roberts, C., & Cousins, F. (2013). *Two Degrees*. Taylor and Francis.

Mitchell, T. M. (1997). *Machine Learning*. McGraw-Hill.

Mohammed, M., Khan, M. B., & Bashier, E. B. M. (2016). *Machine Learning: Algorithms and Applications*. CRC Press. https://doi.org/10.1201/9781315371658

Muhammad, I., & Yan, Z. (2015). SUPERVISED MACHINE LEARNING APPROACHES: A SURVEY. *ICTACT Journal on Soft Computing*, *05*(03), 946–952. https://doi.org/10.21917/ijsc.2015.0133

Murphy, K. P. (2022). *Probabilistic machine learning: An introduction*. The MIT Press.

Nabil, A., & Mardaljevic, J. (2005). Useful daylight illuminance: A new paradigm for assessing daylight in buildings. *Lighting Research & Technology*, *37*(1), 41–57. https://doi.org/10.1191/1365782805li128oa

Neufert, E., Neufert, P., & Kister, J. (2012). *Architects' data* (4th ed). Wiley-Blackwell.

Ngarambe, J., Adilkhanova, I., Uwiragiye, B., & Yun, G. Y. (2022). A review on the current usage of machine learning tools for daylighting design and control. *Building and Environment*, *223*, 109507. https://doi.org/10.1016/j.buildenv.2022.109507

Nourkojouri, H., Shafavi, N. S., Tahsildoost, M., & Zomorodian, Z. S. (2021). Development of a Machine-Learning Framework for Overall Daylight and Visual Comfort Assessment in Early Design Stages. *Journal of Daylighting*, *8*(2), 270–283. https://doi.org/10.15627/jd.2021.21

Pearson, D. (1998). *The new natural house book: Creating a healthy, harmonious, and ecologically sound home* (1st Fireside ed., Rev. ed). Simon & Schuster.

Peña, A., Serna, I., Morales, A., & Fierrez, J. (2020). FairCVtest Demo: Understanding Bias in Multimodal Learning with a Testbed in Fair Automatic Recruitment. *Proceedings of the 2020 International Conference on Multimodal Interaction*, 760–761. https://doi.org/10.1145/3382507.3421165

Poulinakis, K. (2022). Multimodal deep learning: Definitions, Examples, Applications. *V7labs*. https://www.v7labs.com/blog/multimodal-deep-learning-guide

Reinhart, C. (2014). *Fundamentals designing with the sun* (R. Stein, Ed.). Selbstverlag.

Roy, R. (2020). AI, ML, and DL: How not to get them mixed! *Towards Data Science*. https://towardsdatascience.com/understanding-the-difference-between-ai-ml-and-dl-cceb63252a6c

Saha, S. (2018, December 15). *A Comprehensive Guide to Convolutional Neural Networks*. https://saturncloud.io/blog/a-comprehensive-guide-to-convolutional-neural-networks-the-eli5-way/

Sarker, I. H. (2021). Machine Learning: Algorithms, Real-World Applications and Research Directions. *SN Computer Science*, *2*(3), 160. https://doi.org/10.1007/s42979-021-00592-x

Schwagenscheidt, W. (1930). *Anordnung der Räume nach der Sonnenbahn*.

Sepúlveda, A., De Luca, F., Varjas, T., & Kurnitski, J. (2022). Assessing the applicability of the European standard EN 17037:2018 for office spaces in a cold climate. *Building and Environment*, *225*, 109602. https://doi.org/10.1016/j.buildenv.2022.109602

Sharma, V. (2021). ResNets: Why Do They Perform Better than Classic ConvNets? (Conceptual Analysis). *Towards Data Science*. https://towardsdatascience.com/resnets-why-do-they-perform-better-than-classic-convnets-conceptual-analysis-6a9c82e06e53

Sheng, Y., Ward, W. O., Arbabi, H., Álvarez, M., & Mayfield, M. (2022). Deep multimodal learning for residential building energy prediction. *IOP Conference Series: Earth and Environmental Science*, *1078*(1), 012038. https://doi.org/10.1088/1755-1315/1078/1/012038

SLL. (2013). *Lighting guide 9: Lighting for communal residential buildings* (New edition). Chartered Institution of Building Services Engineers.

SLL. (2014). *Lighting guide 10: Daylighting—A guide for designers* ([New edition]). Society of Light and Lighting.

Standfest, M., Franzen, M., Schröder, Y., Medina, L. G., Yarilo Villanueva Hernandez, Buck, J. H., Yen-Ling Tan, Niedzwiecka, M., & Colmegna, R. (2022). *Swiss Dwellings: A large dataset of apartment models including aggregated geolocation-based simulation results covering viewshed, natural light, traffic noise, centrality and geometric analysis* (3.0.0) [dataset]. Zenodo. https://doi.org/10.5281/ZENODO.7788422

Stevens, E., Antiga, L., & Viehmann, T. (2020). *Deep learning with PyTorch*. Manning Publications Co.

Su, Z., & Yan, W. (2015). A fast genetic algorithm for solving architectural design optimization problems. *Artificial Intelligence for Engineering Design, Analysis and Manufacturing*, *29*(4), 457–469. https://doi.org/10.1017/S089006041500044X

SwissTopo. (n.d.). *Switzerland in 3D* [Map]. https://map.geo.admin.ch/?layers=ch.swisstopo.swissnames3d&lon=8.24528&lat=46.04722&elevation=87928&heading=360.000&pitch=-44.188&lang=en&topic=ech&bgLayer=ch.swisstopo.pixelkarte-farbe

Tregenza, P., & Wilson, M. (2011). *Daylighting: Architecture and lighting design*. Routledge.

Yehoshua, R. (2023). Perceptrons: The first Neural Network Model. *Towards Data Science*. https://towardsdatascience.com/perceptrons-the-first-neural-network-model-8b3ee4513757

Zhang, X., Zhai, D., Li, T., Zhou, Y., & Lin, Y. (2023). Image inpainting based on deep learning: A review. *Information Fusion*, *90*, 74–94. https://doi.org/10.1016/j.inffus.2022.08.033

~ empty page ~

~ empty page ~

Appendix

Appendix A. Overview selected rooms for simulations

Site 138, building 137

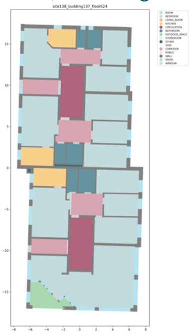

Site 172, building 354

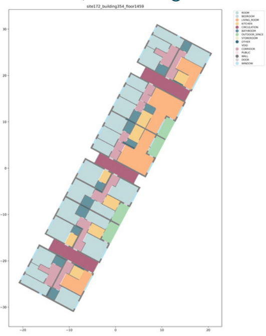

Site 389, building 931

Site 392, building 954

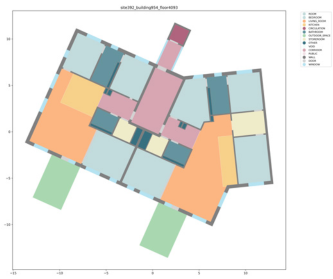

Site 456, building 1105

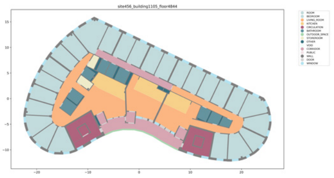

Site 788, building 1779

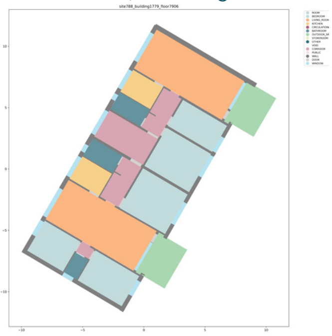

Site 999, building 2081

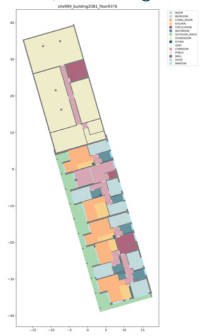

Site 1069, building 2192

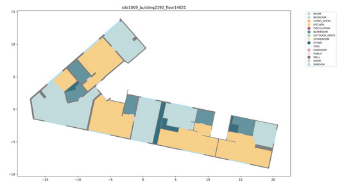

Site 1288, building 2519

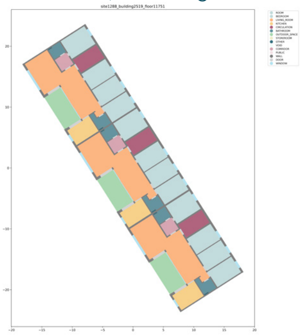

Site 2161, building 3012

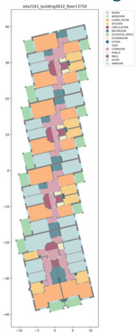

Site 2248, building 3261

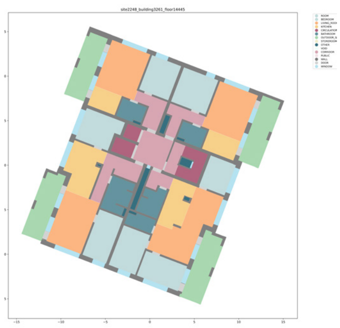

Site 3850, building 5967

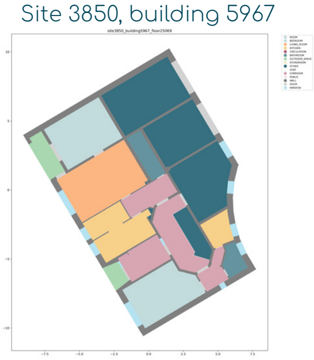

Site 4237, building 7381

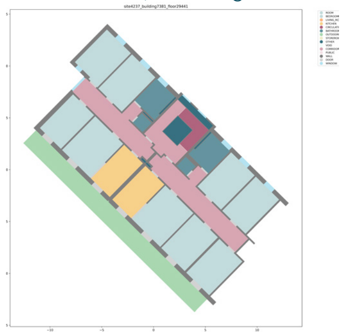

Site 10187, building 14796

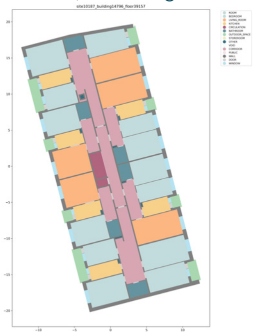

Site 11277, building 17168

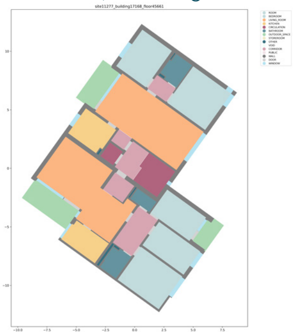

Appendix B. Colour coding of images

Colors for room type overview

Colors for room feature image

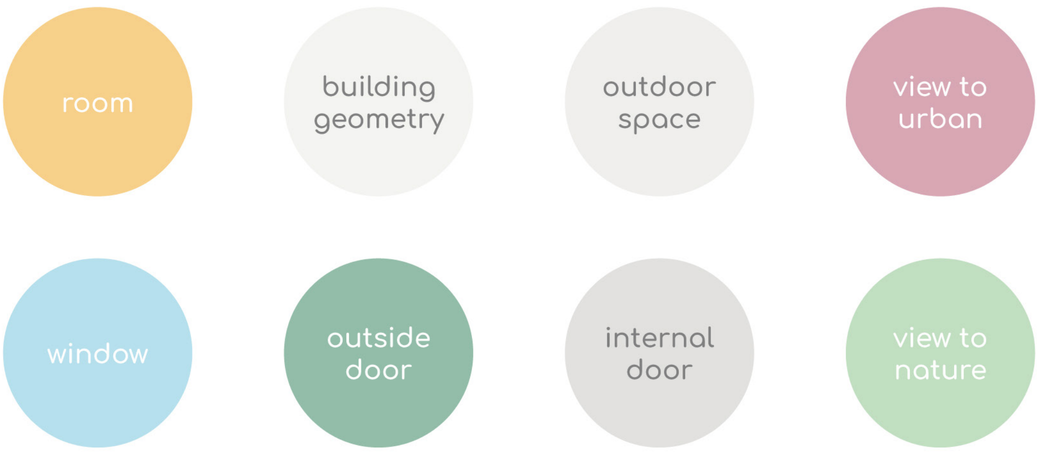

Appendix C. Detailed simulations results

room_nr		apartment_id	site_id	area_id	elevation	orientation	window_area	room_depth_ratio	window_floor_ratio	Dataset values			
										Daylight			View
										21Mar1200 Median [lx]	21Jun1200 Median [lx]	21Jun1200 Median [lx]	Sky Median
1	N1	36596017ad4f7941c88a12faf0ac4903	389	307394	2.9	['North']	2.438	1.578	0.229	365	311	337	0.499
2	N2	418e0d40fba39f6c903bfdec1fc00864	389	311254	0	['North']	5.977	1.517	0.454	876	774	796	1.009
3	N3	9bc6a41f2c75b49490bd92f27b89ee48	389	307386	0	['North']	5.973	1.545	0.431	857	741	797	1.053
4	N4	1221e19a4071debc572c5b202343ef07	138	336910	2.9	['North']	1.999	1.463	0.269	106	73	91	0.129
5	N5	dbcfc984be44586b1c7ee1ec96d2d490	2248	713845	20.3	['North']	1.942	1.006	0.115	67	66	54	0.003
6	NE1	ec40208c41d93fda40471fe821a2697e	4237	1061451	5.8	['North-East']	2.099	1.455	0.143	242	241	207	0.378
8	NE3	67a2f16595f8a10946ea807f9cfee39e	4237	1064238	5.8	['North-East']	2.119	1.456	0.144	232	238	197	0.329
9	NE4	6f2eb53992ccd6b335cadd1d651be818	1288	579291	0	['North-East']	2.34	1.385	0.168	325	371	241	0.291
10	NE5	98f768aefe735fc739fbfba6d1f3ca42	1288	578607	2.9	['North-East']	2.446	1.523	0.176	465	482	375	0.742
11	E1	19eda56a7dd7f2bbf244a0710bbd2c71	10187	1368686	2.9	['East']	3.502	1.861	0.156	188	209	139	0.003
12	E2	5084f3672df4a8da0f439e66ce2e2e90	999	402743	0	['East']	4.437	1.276	0.283	58	70	45	0.003
13	E3	63dc1eb055ecb6834ff9de2b80e336ef	999	401330	5.8	['East']	4.402	1.242	0.281	56	70	41	0.003
14	E4	15f5c22552e6261f65f05062f457488f	2161	703084	5.8	['East']	2.336	1.863	0.206	415	486	288	0.330
15	E5	15f5c22552e6261f65f05062f457488f	2161	703070	5.8	['East']	2.047	1.099	0.205	537	550	521	0.485
16	SE1	afd9e340a59c45239e0470e3e3f6de08	11277	1489797	8.7	['South-East']	3.598	1.238	0.241	715	738	512	0.321
17	SE2	afd9e340a59c45239e0470e3e3f6de08	11277	1489796	8.7	['South-East']	2.764	1.781	0.261	783	758	552	0.417
18	SE3	b98741cfe61fe7191145f340db8e42d3	392	560921	0	['South-East']	3.18	1.809	0.191	430	364	316	0.072
19	SE4	b98741cfe61fe7191145f340db8e42d3	392	919955	0	['South-East']	3.129	1.647	0.237	509	377	494	0.486
20	SE5	34590ca7b3f9983eb70fea4cd0d7d171	172	636557	8.7	['South-East']	3.386	1.248	0.24	1,073	1,022	768	1.059
21	S1	09703b6dbeaecc9da7b3d080fba05a1d	392	560664	2.9	['South']	3.19	1.447	0.185	339	175	544	0.586
22	S2	0721b690a830e964935602b2dda748f2	456	408517	17.4	['South']	2.565	1.796	0.182	324	162	520	0.742
23	S3	342969c590fa3fe1a669f7bd55567f52	456	587445	14.5	['South']	2.328	1.838	0.168	289	147	465	0.616
25	S5	93238d3f5b1af4d2d38b12e5e80fbfb0	1069	708741	14.5	['South']	6.384	3.742	0.219	336	209	285	0.298
26	SW1	09703b6dbeaecc9da7b3d080fba05a1d	392	560660	2.9	['South-West']	4.646	1.084	0.261	834	440	1,007	1.131
27	SW2	789afb678d65e82b8673cd6c31c8911a	456	408554	17.4	['South-West']	2.375	2.022	0.204	500	255	498	0.937
29	SW4	cdc2ab489daebfcb10b9435f4a14b629	1288	577913	2.9	['South-West']	2.446	1.523	0.176	432	287	372	0.624
30	SW5	9968b0f4250e2e065684b7def4313545	3850	976686	8.7	['South-West']	3.704	1.172	0.242	433	227	354	0.003
31	W1	df7f78f9d2cc8419c2326d3fb0173839	2161	703547	8.7	['West']	2.315	1.561	0.173	307	181	273	0.245
32	W2	df7f78f9d2cc8419c2326d3fb0173839	2161	703552	8.7	['West']	2.783	1.258	0.167	337	214	298	0.329
33	W3	df7f78f9d2cc8419c2326d3fb0173839	2161	703543	8.7	['West']	2.315	1.781	0.197	296	198	247	0.299
34	W4	689807445b68cafcd3f7217e52ec316b	2161	703467	8.7	['West']	2.775	1.465	0.165	309	193	264	0.257
35	W5	84b6c134ad9d47d9021d7aac3bed0d0a	138	337266	0	['West']	2.309	1.818	0.267	411	292	336	0.396
36	NW1	8e8929d2e5a2159384167854ba0b9a04	172	637130	5.8	['North-West']	3.463	1.39	0.304	445	338	358	0.367
37	NW2	8e8929d2e5a2159384167854ba0b9a04	172	637180	5.8	['North-West']	3.206	1.234	0.238	412	299	332	0.293
38	NW3	8e8929d2e5a2159384167854ba0b9a04	172	637155	5.8	['North-West']	2.161	1.726	0.235	287	225	227	0.241
39	NW4	1efb344729d812792e49f8e491ea408f	172	1547845	8.7	['North-West']	3.591	1.255	0.249	659	462	562	1.129
40	NW5	5e71168800a7543eb1e22fd626b7cc8e	788	570039	0	['North-West']	2.596	1.213	0.273	166	134	146	0.322

room_nr		apartment_id	site_id	area_id	elevation	orientation	window_area	room_depth_ratio	window_floor_ratio	Dataset values			
										Daylight			View
										21Mar1200 Median [lx]	21Jun1200 Median [lx]	21Jun1200 Median [lx]	Sky Median
1	N1	36596017ad4f7941c88a12faf0ac4903	389	307394	2.9	['North']	2.438	1.578	0.229	365	311	337	0.499
2	N2	418e0d40fba39f6c903bfdec1fc00864	389	311254	0	['North']	5.977	1.517	0.454	876	774	796	1.009
3	N3	9bc6a41f2c75b49490bd92f27b89ee48	389	307386	0	['North']	5.973	1.545	0.431	857	741	797	1.053
4	N4	1221e19a4071debc572c5b202343ef07	138	336910	2.9	['North']	1.999	1.463	0.269	106	73	91	0.129
5	N5	dbcfc984be44586b1c7ee1ec96d2d490	2248	713845	20.3	['North']	1.942	1.006	0.115	67	66	54	0.003
6	NE1	ec40208c41d93fda40471fe821a2697e	4237	1061451	5.8	['North-East']	2.099	1.455	0.143	242	241	207	0.378
8	NE3	67a2f16595f8a10946ea807f9cfee39e	4237	1064238	5.8	['North-East']	2.119	1.456	0.144	232	238	197	0.329
9	NE4	6f2eb53992ccd6b335cadd1d651be818	1288	579291	0	['North-East']	2.34	1.385	0.168	325	371	241	0.291
10	NE5	98f768aefe735fc739fbfba6d1f3ca42	1288	578607	2.9	['North-East']	2.446	1.523	0.176	465	482	375	0.742
11	E1	19eda56a7dd7f2bbf244a0710bbd2c71	10187	1368686	2.9	['East']	3.502	1.861	0.156	188	209	139	0.003
12	E2	5084f3672df4a8da0f439e66ce2e2e90	999	402743	0	['East']	4.437	1.276	0.283	58	70	45	0.003
13	E3	63dc1eb055ecb6834ff9de2b80e336ef	999	401330	5.8	['East']	4.402	1.242	0.281	56	70	41	0.003
14	E4	15f5c22552e6261f65f05062f457488f	2161	703084	5.8	['East']	2.336	1.863	0.206	415	486	288	0.330
15	E5	15f5c22552e6261f65f05062f457488f	2161	703070	5.8	['East']	2.047	1.099	0.205	537	550	521	0.485
16	SE1	afd9e340a59c45239e0470e3e3f6de08	11277	1489797	8.7	['South-East']	3.598	1.238	0.241	715	738	512	0.321
17	SE2	afd9e340a59c45239e0470e3e3f6de08	11277	1489796	8.7	['South-East']	2.764	1.781	0.261	783	758	552	0.417
18	SE3	b98741cfe61fe7191145f340db8e42d3	392	560921	0	['South-East']	3.18	1.809	0.191	430	364	316	0.072
19	SE4	b98741cfe61fe7191145f340db8e42d3	392	919955	0	['South-East']	3.129	1.647	0.237	509	377	494	0.486
20	SE5	34590ca7b3f9983eb70fea4cd0d7d171	172	636557	8.7	['South-East']	3.386	1.248	0.24	1,073	1,022	768	1.059
21	S1	09703b6dbeaecc9da7b3d080fba05a1d	392	560664	2.9	['South']	3.19	1.447	0.185	339	175	544	0.586
22	S2	0721b690a830e964935602b2dda748f2	456	408517	17.4	['South']	2.565	1.796	0.182	324	162	520	0.742
23	S3	342969c590fa3fe1a669f7bd55567f52	456	587445	14.5	['South']	2.328	1.838	0.168	289	147	465	0.616
25	S5	93238d3f5b1af4d2d38b12e5e80fbfb0	1069	708741	14.5	['South']	6.384	3.742	0.219	336	209	285	0.298
26	SW1	09703b6dbeaecc9da7b3d080fba05a1d	392	560660	2.9	['South-West']	4.646	1.084	0.261	834	440	1,007	1.131
27	SW2	789afb678d65e82b8673cd6c31c8911a	456	408554	17.4	['South-West']	2.375	2.022	0.204	500	255	498	0.937
29	SW4	cdc2ab489daebfcb10b9435f4a14b629	1288	577913	2.9	['South-West']	2.446	1.523	0.176	432	287	372	0.624
30	SW5	9968b0f4250e2e065684b7def4313545	3850	976686	8.7	['South-West']	3.704	1.172	0.242	433	227	354	0.003
31	W1	df7f78f9d2cc8419c2326d3fb0173839	2161	703547	8.7	['West']	2.315	1.561	0.173	307	181	273	0.245
32	W2	df7f78f9d2cc8419c2326d3fb0173839	2161	703552	8.7	['West']	2.783	1.258	0.167	337	214	298	0.329
33	W3	df7f78f9d2cc8419c2326d3fb0173839	2161	703543	8.7	['West']	2.315	1.781	0.197	296	198	247	0.299
34	W4	689807445b68cafcd3f7217e52ec316b	2161	703467	8.7	['West']	2.775	1.465	0.165	309	193	264	0.257
35	W5	84b6c134ad9d47d9021d7aac3bed0d0a	138	337266	0	['West']	2.309	1.818	0.267	411	292	336	0.396
36	NW1	8e8929d2e5a2159384167854ba0b9a04	172	637130	5.8	['North-West']	3.463	1.39	0.304	445	338	358	0.367
37	NW2	8e8929d2e5a2159384167854ba0b9a04	172	637180	5.8	['North-West']	3.206	1.234	0.238	412	299	332	0.293
38	NW3	8e8929d2e5a2159384167854ba0b9a04	172	637155	5.8	['North-West']	2.161	1.726	0.235	287	225	227	0.241
39	NW4	1efb344729d812792e49f8e491ea408f	172	1547845	8.7	['North-West']	3.591	1.255	0.249	659	462	562	1.129
40	NW5	5e71168800a7543eb1e22fd626b7cc8e	788	570039	0	['North-West']	2.596	1.213	0.273	166	134	146	0.322

1 bounce values				Daylight								View	
Daylight			View	difference lux			difference %			Average			
21Mar1200 Median [lx]	21Jun1200 Median [lx]	21Jun1200 Median [lx]	Sky Median [%]	21Mar1200 Median [lx]	21Jun1200 Median [lx]	21Jun1200 Median [lx]	21Mar1200 Median [%]	21Jun1200 Median [%]	21Jun1200 Median [%]	Of three days	Per orientation of three days	Sky	SkyView_ mean
78	103	83	2.231	287	208	254	79%	67%	75%	74%		1.731	347%
271	279	241	6.695	605	495	555	69%	64%	70%	68%		5.686	564%
177	209	165	8.008	680	532	632	79%	72%	79%	77%	57%	6.955	660%
141	139	125	3.742	35	66	34	33%	91%	37%	54%		3.612	2792%
58	52	52	1.040	9	14	2	13%	22%	5%	13%		1.037	34642%
66	75	52	1.716	176	166	155	73%	69%	75%	72%		1.337	354%
65	77	51	1.723	167	161	146	72%	68%	74%	71%	76%	1.394	423%
74	74	51	1.386	251	297	190	77%	80%	79%	79%		1.095	376%
92	101	64	1.555	373	381	311	80%	79%	83%	81%		0.812	109%
69	80	54	1.733	119	129	85	63%	62%	61%	62%		1.730	57851%
128	112	98	3.783	70	42	53	120%	60%	117%	99%		3.780	126442%
111	135	85	3.931	55	65	44	98%	93%	107%	99%	85%	3.928	131398%
101	109	73	2.070	314	377	215	76%	78%	75%	76%		1.740	528%
86	74	62	2.575	451	476	459	84%	86%	88%	86%		2.090	431%
248	176	173	2.327	467	562	339	65%	76%	66%	69%		2.006	625%
200	166	179	2.491	583	592	373	74%	78%	68%	73%		2.074	497%
227	186	159	1.733	203	178	157	47%	49%	50%	49%	61%	1.661	2310%
316	227	222	2.922	193	150	272	38%	40%	55%	44%		2.436	501%
350	257	273	3.077	723	765	495	67%	75%	64%	69%		2.018	191%
310	189	501	2.070	29	14	43	9%	8%	8%	8%		1.483	253%
253	185	545	2.238	71	23	25	22%	14%	5%	14%	13%	1.497	202%
318	151	434	2.060	29	4	31	10%	2%	7%	6%		1.444	235%
339	284	172	3.446	3	75	113	1%	36%	40%	25%		3.148	1056%
400	331	614	3.783	434	109	393	52%	25%	39%	39%		2.653	235%
335	197	283	9.808	165	58	215	33%	23%	43%	33%	47%	8.871	947%
133	100	128	1.555	299	187	244	69%	65%	66%	67%		0.930	149%
155	164	144	3.268	278	63	210	64%	28%	59%	50%		3.265	109302%
126	115	100	1.892	181	66	173	59%	37%	63%	53%		1.647	672%
114	107	99	2.070	223	107	199	66%	50%	67%	61%		1.741	529%
70	87	67	2.060	226	111	180	76%	56%	73%	68%	66%	1.761	589%
62	77	59	1.733	247	116	205	80%	60%	78%	73%		1.475	573%
86	94	83	2.575	325	198	253	79%	68%	75%	74%		2.179	551%
152	157	129	3.605	293	181	229	66%	54%	64%	61%		3.238	882%
127	151	114	3.087	285	148	218	69%	50%	66%	61%		2.794	953%
87	99	82	2.575	200	126	145	70%	56%	64%	63%	61%	2.334	970%
126	138	106	4.120	533	324	456	81%	70%	81%	77%		2.991	265%
93	92	83	3.090	73	42	63	44%	32%	43%	39%		2.769	861%

Multibounce values				Daylight								View	
Daylight			View	difference lux			difference %			Average			
21Mar1200 Median [lx]	21Jun1200 Median [lx]	21Jun1200 Median [lx]	Sky Median [%]	21Mar1200 Median [lx]	21Jun1200 Median [lx]	21Jun1200 Median [lx]	21Mar1200 Median [%]	21Jun1200 Median [%]	21Jun1200 Median [%]	Of three days	Per orientation of three days	Sky	SkyView_ mean
343	386	134	3.106	22	75	203	6%	24%	60%	30%		2.606	522%
682	835	366	8.912	194	61	430	22%	8%	54%	28%		7.903	783%
619	833	285	10.189	238	92	512	28%	12%	64%	35%	122%	9.136	867%
408	629	245	4.845	302	556	154	285%	762%	169%	405%		4.715	3644%
127	199	79	1.545	60	133	25	89%	202%	46%	112%		1.542	51536%
237	237	125	2.428	5	4	82	2%	2%	40%	15%		2.050	542%
170	250	130	2.549	62	12	67	27%	5%	34%	22%	31%	2.219	674%
220	194	135	2.060	105	177	106	32%	48%	44%	41%		1.769	607%
279	306	123	2.307	186	176	252	40%	36%	67%	48%		1.565	211%
263	260	117	2.575	75	51	22	40%	24%	16%	27%		2.572	86032%
372	459	221	5.097	314	389	176	541%	556%	391%	496%		5.094	170400%
372	550	246	5.260	316	480	205	564%	686%	501%	584%	243%	5.257	175882%
169	351	111	3.082	246	135	177	59%	28%	62%	50%		2.752	835%
264	272	135	3.660	273	278	386	51%	51%	74%	59%		3.175	655%
811	563	707	3.189	96	175	195	13%	24%	38%	25%		2.868	894%
853	427	722	3.389	70	331	170	9%	44%	31%	28%		2.972	713%
449	442	465	2.575	19	78	149	5%	21%	47%	24%	32%	2.503	3482%
845	487	953	3.986	336	110	459	66%	29%	93%	63%		3.500	720%
880	744	631	4.067	193	278	137	18%	27%	18%	21%		3.008	284%
765	458	823	3.064	426	283	279	126%	161%	51%	113%		2.477	423%
605	596	808	3.227	281	434	288	87%	268%	55%	137%	169%	2.485	335%
756	603	708	2.712	467	456	243	161%	310%	52%	175%		2.096	340%
1,022	770	1,079	4.670	686	561	794	204%	268%	279%	250%		4.372	1466%
815	778	1,196	5.131	19	338	189	2%	77%	19%	33%		4.001	354%
577	500	753	12.908	77	245	255	15%	96%	51%	54%	43%	11.971	1278%
416	318	235	2.307	16	31	137	4%	11%	37%	17%		1.682	269%
668	539	413	4.498	235	312	59	54%	137%	17%	69%		4.495	150453%
298	236	185	2.712	9	55	88	3%	30%	32%	22%		2.467	1007%
322	286	205	3.064	15	72	93	5%	33%	31%	23%		2.735	832%
255	323	190	2.840	41	125	57	14%	63%	23%	33%	31%	2.541	850%
247	370	171	2.575	62	177	93	20%	92%	35%	49%		2.318	900%
355	368	189	3.972	56	76	147	14%	26%	44%	28%		3.577	904%
346	501	239	4.833	99	163	119	22%	48%	33%	35%		4.466	1217%
301	470	244	4.083	111	171	88	27%	57%	27%	37%		3.790	1292%
345	321	177	3.389	58	96	50	20%	43%	22%	28%	46%	3.149	1308%
469	523	300	5.467	190	61	262	29%	13%	47%	30%		4.338	384%
263	435	182	4.067	97	301	36	58%	225%	24%	103%		3.746	1165%

Appendix D. Python codes feature extraction

This appendix includes all the Python codes used for this research. The main path of the created GitHub page is:

https://github.com/lottekat/VisualComfortLayouts/blob/14ace23d7ca7c1d2cd73b74b6667fa7b7d9ac2fa/README.md

Part I. Code feature extraction

This code include connecting windows to rooms & finding the window and orientation area per room. The code can be found at the following GitHub page:

https://github.com/lottekat/VisualComfortLayouts/tree/14ace23d7ca7c1d2cd73b74b6667fa7b7d9ac2fa/01_FeatureExtraction

Part II. Code data preparation

This code includes the cleaning of the 'Swiss dwellings' dataset and creating all the needed features and labels. The code can be found at the following GitHub page:

https://github.com/lottekat/VisualComfortLayouts/tree/14ace23d7ca7c1d2cd73b74b6667fa7b7d9ac2fa/02_DataPreperation

Part III. Code ML training

This code includes the code for the best ML model training, model 7.5A and 7.5B. The code can be found at the following GitHub page:

https://github.com/lottekat/VisualComfortLayouts/tree/14ace23d7ca7c1d2cd73b74b6667fa7b7d9ac2fa/03_MLtraining

Appendix E. Detailed model architecture

Model	Model 0	Model 1	Model 2	Model 3	Model 3.2	Model 7.5
Parameter	Only image feature ImageNet	pre-trained ResNet	Pre-trained trainable ResNet	Weights from scratch	Split-up model 3	Fine-tuned split-up model
Image input size	224x224x3 (RGB)	224x224x3 (RGB)			224x224x3 (RGB)	224x224x3 (RGB)
Numerical input	-	2 num. features			2 num. features	2 num. features
Base ResNet50 model	no weights, layers trainable	ImgeNet weight, layers frozen	ImgeNet weight, layers trainable	no weights, layers trainable	no weights, layers trainable	no weights, layers trainable
	Batch norm., leakyReLu(0.1)	Batch norm., leakyReLu(0.1)			Batch norm., leakyReLu(0.1)	Batch norm., leakyReLu(0.1)
	Global Avg. Pooling, Dense(256, ReLU kernel(0.01)), Dropout(0.5)	Global Avg. Pooling, Dropout(0.5), Dense(256, ReLU, kernel(0.01))			Global Avg. Pooling, Dense(256, ReLU kernel(0.01)), Dropout(0.5)	Global Avg. Pooling, Dense(256, ReLU kernel(0.0001)), Dropout(0.3)
	-	Concatenate: Dense and numerical input			Concatenate: Dropout and numerical input	Concatenate: Dropout and numerical input
	-	Batch norm., leakyReLu(0.1)			Batch norm., leakyReLu(0.1)	Batch norm., leakyReLu(0.1)
	-	Dense(128, ReLU, kernel(0.01)), Dropout(0.5)			Dense(128, ReLU, kernel(0.01)), Dropout(0.5)	Dense(128, ReLU, kernel(0.0001)), Dropout(0.3)
Output layer	5 labels, linear Act.	2 labels, linear Act.			4A(daylight) 3 labels, linear Act. 4B(view) 2 labels, linear Act.	4A(daylight) 3 labels, linear Act. 4B(view) 2 labels, linear Act.
Compilation	optimizer: Adam(lr = 0.0001), loss: MSE, metric: MAE	optimizer: Adam(lr=0.001), loss: MSE, metric: MAE			optimizer: Adam(lr=0.001), loss: MSE, metric: MAE	optimizer: Adam(lr=0.001), loss: MSE, metric: MAE
Max epoch, batch size	200 epoch, 64	200 epoch, 64			200 epoch, 64	100 epoch, 64
Callbacks	*early stopping(10)*	*early stopping(25)*			*early stopping(25), lr schedule(5.000 iterations, factor=0.5)*	*early stopping(25), lr schedule(5.000 iterations, factor=0.5)*

Appendix F. 12 general apartments ML evaluation

Part I. Overview selected apartments with their site and building ID

Apartment 1
Site 66, building 112

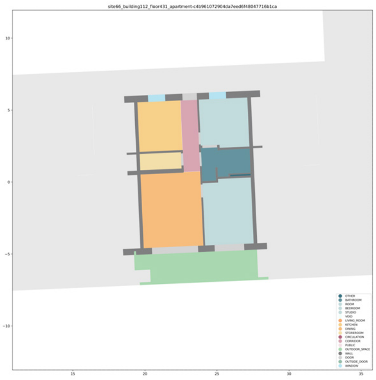

Apartment 2
Site 401, building 1010

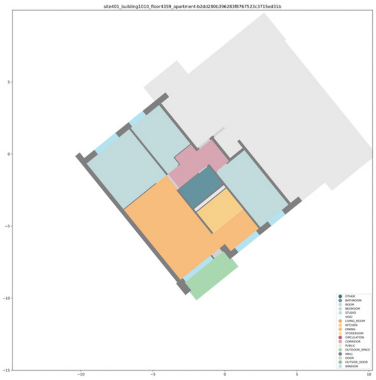

Apartment 3
Site 401, building 1017

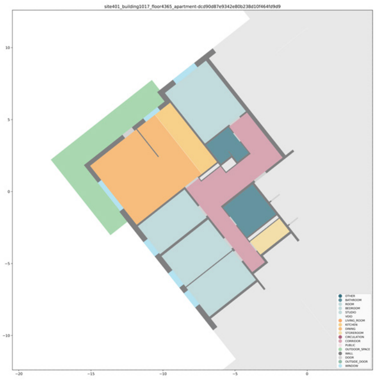

Apartment 4
Site 789, building 1727

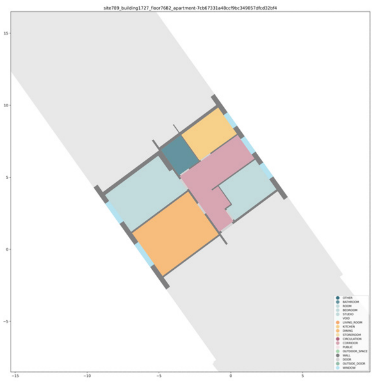

Apartment 5
Site 789, building 1729

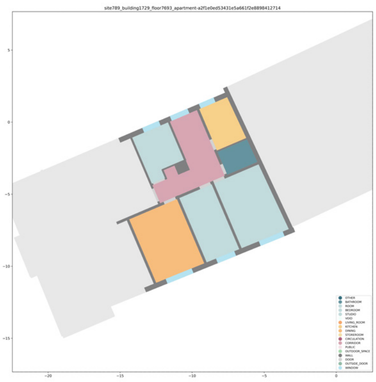

Apartment 6
Site 1067, building 2189

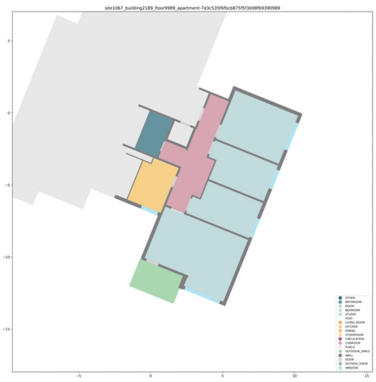

Apartment 7
Site 1105, building 2245

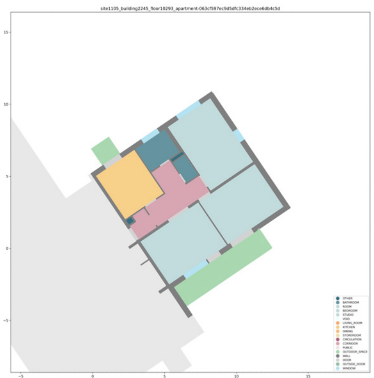

Apartment 8
Site 2161, building 3012

Apartment 9
Site 3641, building 5604

Apartment 10
Site 3958, building 6192

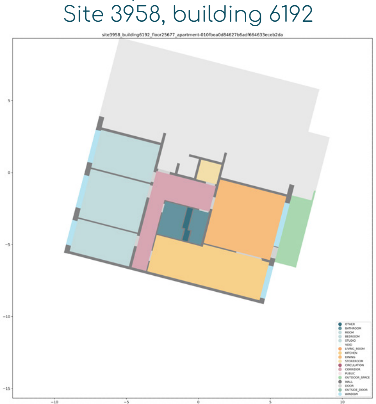

Apartment 11
Site 11726, building 18299

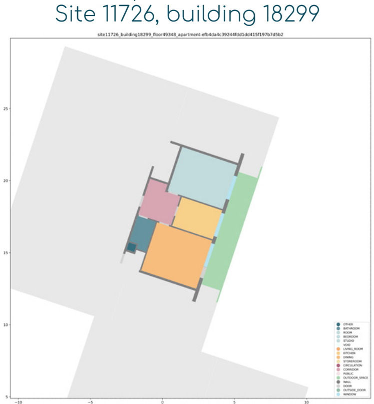

Apartment 12
Site 11726, building 18299

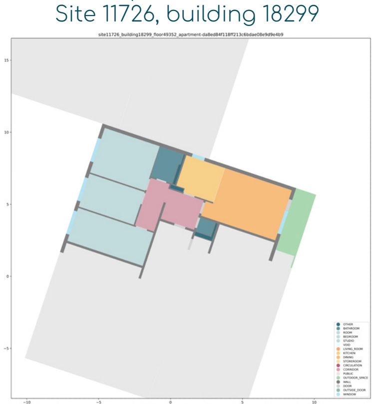

Part II. Comparison of 3 models daylight predictions on 21st of March at 12:00

Part III. Comparison of 3 models sky view predictions

Appendix G. Case study prediction code

Part I. Case study Grasshopper script

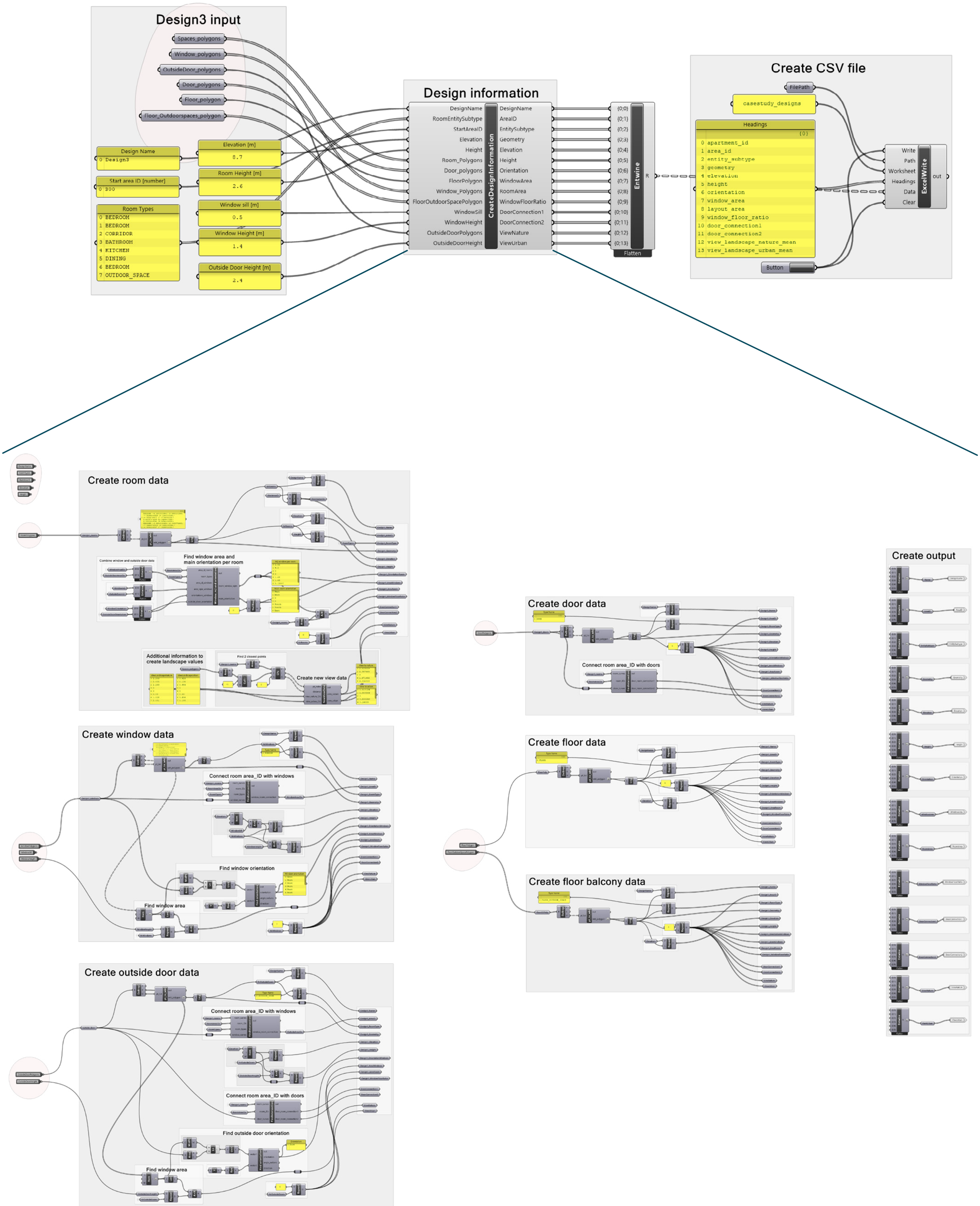

Part II. Code ML predictions

This code includes a automated version of the ML design framework. The code comes together with a Rhino Grasshopper script.

https://github.com/lottekat/VisualComfortLayouts/tree/14ace23d7ca7c1d2cd73b74b6667fa7b7d9ac2fa/04_CasestudyPredictions